



# **Characterization of ABCG30 and ABCG1 from *Arabidopsis thaliana***

Inaugural-Dissertation

zur Erlangung des Doktorgrades  
der Mathematisch-Naturwissenschaftlichen Fakultät  
der Heinrich-Heine-Universität Düsseldorf

vorgelegt von

**Kalpana Shanmugarajah**  
aus Berlin

Düsseldorf, November 2018

aus dem Institut für Biochemie  
der Heinrich-Heine-Universität Düsseldorf

Gedruckt mit der Genehmigung der  
Mathematisch-Naturwissenschaftlichen Fakultät der  
Heinrich-Heine-Universität Düsseldorf

Berichterstatter:

1. Prof. Dr. Lutz Schmitt

2. Prof. Dr. Karl-Erich Jaeger

Tag der mündlichen Prüfung: 16.01.2019



*“An experiment is a question which science poses to Nature  
and a measurement is the recording of Nature's answer. “*

*Max Planck*

## Abstract

Compared to other organisms, ABC transporters are particularly abundant in plants with for instance, 130 ABC proteins in *Arabidopsis thaliana*. Various studies emphasized the contribution of plant ABC transporters to its fitness and growth. However, most plant ABC transporters were analyzed by transgenic or mutant plant studies and unambiguous identification of transported substrates by direct functional assays are still rare. Suitable *in vitro* systems would enable to gain more insight into the plant physiology and analysis on molecular level.

In this thesis, cloning and expression studies of selected *Arabidopsis ABCG* genes resulted in introduction of the methylotrophic yeast *Pichia pastoris* as expression system for plant ABC transporters. The correct subcellular localization of the successfully expressed full size transporters AtABCG36, AtABCG30 and the half-size transporter AtABCG1 indicated that the proteins were properly folded and processed.

The second and main part of this thesis comprised the optimization of purification protocols and functional assays for characterization of AtABCG30 and AtABCG1. Initial solubilization studies and a first purification attempt of AtABCG30 provide a proper foundation for future studies. Moreover, optimization of expression and purification conditions enabled the attainment of AtABCG1 in functional, active state. It was analyzed whether AtABCG1 is involved in root suberin formation, as it originates from the same phylogenetic tree like potential suberin precursor transporters AtABCG2, AtABCG6 and AtABCG20. Additionally, AtABCG1 and another potential suberin transporter, ABCG1 from *Solanum tuberosum*, share a sequence identity of 74 %. Functional assays with purified AtABCG1 as well as phenotypic analyses of *atabcg1* mutant plants indicated an involvement in suberin barrier formation in the roots. Thereby, C<sub>20</sub>-C<sub>24</sub>  $\alpha$ ,  $\omega$ - dicarboxylic acids and C<sub>24</sub> fatty alcohols were identified by mutant plant studies as putative substrates, whereas C<sub>26</sub> fatty alcohols, C<sub>24</sub> and C<sub>26</sub> fatty acids were identified unambiguously by both, direct functional and mutant plant studies, as the AtABCG1 substrate.

The last part of this thesis comprised of a proof-of-principle for a vesicular transport assay. As reported in previous studies, AtABCG30 as well as AtABCG1 were found to be expressed in the roots and in particular *atabcg30* mutant studies indicated an involvement in root exudation. Vesicular transport assays form an alternative option for identification of transported substrates from a mixture of potential substrates, such as root exudates. The *Saccharomyces cerevisiae* ABC transporter Pdr5 was successfully used to establish a mass-spectrometry based vesicular transport. Hence, this assay can be transferred to future functional studies of heterologously expressed plant ABC transporter in yeast.

## Zusammenfassung

Im Vergleich zu anderen Organismen besitzen Pflanzen, mit zum Beispiel 130 ABC Proteinen in *Arabidopsis thaliana*, eine besonders hohe Anzahl an ABC Transportern. Durch bisherige Studien wurde verdeutlicht, dass ABC Transporter wesentlich zur Fitness und dem Wachstum von Pflanzen beitragen. Jedoch wurden die meisten Studien an transgenen oder Mutanten Pflanzen durchgeführt, wohingegen direkte funktionelle Assays zur eindeutigen Substratidentifizierung noch relativ selten sind. Dabei könnten geeignete *in vitro* Systeme einen weiteren Einblick in die Pflanzenphysiologie und die Analyse auf molekularer Ebene ermöglichen.

In dieser Dissertation wurden zunächst Studien zur Klonierung und heterologen Expression von ausgewählten ABCG Genen aus *Arabidopsis thaliana* durchgeführt. Dabei konnte die methylo troph e Hefe *Pichia pastoris* als alternatives Expressionssystem für pflanzliche ABC Transporter eingeführt werden. Die korrekte subzelluläre Lokalisierung von den erfolgreich in *Pichia pastoris* exprimierten sogenannten „full-size“ Transportern AtABCG36, AtABCG30 und dem „half-size“ Transporter AtABCG1 deutete auf eine korrekte Faltung und Prozessierung dieser Membranproteine hin.

Im zweiten und wesentlichen Teil dieser Arbeit wurden Reinigungsprotokolle und funktionelle Untersuchungen für die Charakterisierung von AtABCG30 und AtABCG1 etabliert. Erste Solubilisierungs- und Reinigungsversuche von AtABCG30 wurden durchgeführt und lieferten eine geeignete Basis für weitere Studien. Darüber hinaus wurde AtABCG1 durch die Optimierung von Expression- und Reinigungsbedingungen in einem funktionell und aktivem Zustand aufgereinigt. Es wurde untersucht ob AtABCG1 an der Suberin Formation beteiligt ist, da es zum einen von derselben phylogenetischen Unterklasse wie die potentiellen Suberin-Vorstufen Transporter AtABCG2, AtABCG6 und AtABCG20 stammt. Zum anderen besitzt AtABCG1 eine hohe Sequenzidentität (74%) zu einem weiteren potentiellen Suberinmonomer Transporter, ABCG1 aus *Solanum tuberosum*. Funktionelle Untersuchungen mit gereinigtem AtABCG1 und zusätzliche phänotypische Analysen mit *atabcg1* Mutanten Pflanzen deuteten auf eine Beteiligung von AtABCG1 in der Suberinsynthese in *Arabidopsis* Wurzeln. Dabei wurden C<sub>20</sub>-C<sub>24</sub>  $\alpha$ ,  $\omega$ - Dicarbonsäuren und das C<sub>24</sub> Fettalkohol als potentielle AtABCG1 Substrate identifiziert. Das C<sub>26</sub> Fettalkohol, und die Fettsäuren C<sub>24</sub> und C<sub>26</sub> wurden über beide Assays als AtABCG1 Substrate identifiziert.

Im letzten Teil dieser Dissertation wurde ein Nachweis über die Funktion eines vesikulären Transport Assays vorgestellt. Da beide Transporter AtABCG30 und AtABCG1 unter anderem auch in den Wurzeln exprimiert sind, ist eine Funktion im Transport von Wurzelexudaten nicht auszuschließen. Vesikuläre Transport Assays stellen eine geeignete Alternative für die

Identifizierung von transportierten Substraten aus einer Substratmischung wie zum Beispiel Wurzelexudaten dar. Durch die Verwendung des ABC Transporters Pdr5 aus *Saccharomyces cerevisiae* wurde die Etablierung eines Massenspektrometrie-basierten vesikulären Transport Assays erfolgreich durchgeführt. Folglich können zukünftige Studien an Hefe exprimierten Pflanzen ABC Transportern auch auf dieser Methode zurückgreifen.

# Table of Contents

<b>Abstract .....</b>	<b>I</b>
<b>Zusammenfassung .....</b>	<b>II</b>
<b>List of figures .....</b>	<b>VI</b>
<b>List of tables.....</b>	<b>VII</b>
<b>Abbreviations .....</b>	<b>VIII</b>
<b>1. Introduction.....</b>	<b>1</b>
1.1 Biological membranes, the doormen of cells .....	1
1.2 The ATP-binding cassette transporter superfamily .....	3
1.2.1 Transmembrane domains.....	5
1.2.2 Nucleotide binding domains.....	6
1.2.3 Transport mechanism of ABC transporters.....	7
1.3 Plant ABC transporters .....	11
1.3.1 Role of ABCG half-size transporters in barrier formation.....	13
1.3.2 Suberin biosynthesis in <i>Arabidopsis</i> .....	16
1.3.3 AtABCG1, a potential suberin transporter?.....	17
1.3.4 Plant defense related full-size ABCG transporter .....	19
1.3.5 The full-size transporter AtABCG30 .....	20
<b>2. Aims .....</b>	<b>23</b>
<b>3. Chapters .....</b>	<b>24</b>
3.1 Chapter I –Heterologous expression of plant ABC transporters .....	25
3.2 Chapter II – ABCG30 from <i>Arabidopsis thaliana</i> .....	73
3.3 Chapter III – ABCG1 from <i>Arabidopsis thaliana</i> .....	95
3.4 Chapter IV – Vesicular transport assay .....	132
<b>4. Discussion.....</b>	<b>158</b>
4.1 Cloning and heterologous expression of plant ABCG transporters.....	158
4.2 Purification of <i>Arabidopsis</i> ABCG transporters .....	161
4.3 Functional characterization of AtABCG1 .....	163

4.3.1	ABC transporters in <i>Arabidopsis</i> root suberin formation.....	166
4.3.2	Phylogenetic analysis of AtABCG1.....	168
4.4	A yeast membrane based vesicular transport assay for plant ABC transporters.....	169
<b>5.</b>	<b>Literature .....</b>	<b>172</b>
<b>6.</b>	<b>Curriculum vitae.....</b>	<b>185</b>
<b>7.</b>	<b>Acknowledgments .....</b>	<b>188</b>
<b>8.</b>	<b>Declaration .....</b>	<b>192</b>

## List of figures

Figure 1: Passive and active membrane transport.....	2
Figure 2: Structures of ABC importer and exporter classes .....	4
Figure 3: TMD structure of ABC importers and exporters .....	6
Figure 4: Structure of the HlyB NBD dimer .....	8
Figure 5: Switch model for an ABC exporter.....	9
Figure 6: Reciprocating twin channel model for an ABC exporter.....	10
Figure 7: Evolutionary tree of ABC transporters.....	12
Figure 8: Contribution of ABCG transporters in diffusion barrier formation of <i>A. thaliana</i> reproductive organs.....	14
Figure 9: Hypothetical model of the suberin macromolecular structure .....	15
Figure 10: Suberin biosynthetic pathway .....	17
Figure 11: Contribution of ABCG transporters in suberin formation in <i>A. thaliana</i> seeds and roots.....	19
Figure 12: Cooperation of <i>Arabidopsis</i> ABCG transporters to control seed germination by ABA transport.....	21
Figure 13: AtABCG1 involvement in root suberin formation.....	165
Figure 14: Hypothetical model of suberin biosynthesis in <i>Arabidopsis</i> .....	167
Figure 15: Neighbor-Joining phylogenetic tree of half-size ABCG transporters involved in suberin formation.....	169

## List of tables

Table 1: Cloning attempts of ABCG genes into bacterial and yeast vectors .....	160
--	-----



## Abbreviations

Å	Ångstrom
ABA	Abscisic acid
ABC	ATP-binding cassette
ACT2	Actin gene
ADP	Adenosine-5'-diphosphate
ASFT	Aliphatic suberin feruloyl transferase
AtABCG	ATP binding cassette subfamily G from <i>Arabidopsis thaliana</i>
<i>A. thaliana</i>	<i>Arabidopsis thaliana</i>
ATP	Adenosine-5'-triphosphate
BN-PAGE	Blue native polyacrylamide gel electrophoresis
bp	Base pair
BSEP	Bile salt export pump
BSTFA	<i>N</i> , <i>O</i> -Bis (trimethylsilyl) trifluoroacetamide
CBP	Calmodulin-binding peptide
CBB	Colloidal Coomassie Brilliant Blue
cDNA	Complementary DNA
CFTR	Cystic fibrosis transmembrane regulator
CH	Cycloheximide
CoA	Coenzyme A
Col-0	Ecotype Columbia-0
cmc	critical micellar concentration
CW	Cell wall
Da	Dalton
DNA	Deoxyribonucleic acid
DMSO	Dimethyl sulfoxide
DTT	Dithiothreitol
ECF	Energy coupling factor
<i>E. coli</i>	<i>Escherichia coli</i>
EDTA	Ethylenediaminetetraacetic acid
eGFP	Enhanced green fluorescence protein
EGTA	Ethyleneglycoltetraacetic Acid
ER	Endoplasmatic reticulum
FACT	Fatty alcohol:caffeoyl-CoA caffeoyl transferase
FAE	Fatty acid elongase

FAR	Fatty acyl reductase
FCZ	Fluconazole
g	gram
GA	Gibberellin
GC-MS	Gas Chromatography- Mass spectrometry
<i>G. hirsutum</i>	<i>Gossypium hirsutum</i>
GPAT	Glycerol 3-phosphate acyltransferase
HeLa cells	Henrietta Lacks cells
His <sub>6</sub> -tag	Hexa-histidine tag
IBA	Indole-3-butyric acid
kb	Kilo base pair
KCS	$\beta$ -ketoacyl-CoA synthase
KCZ	Ketoconazole
kDa	Kilo dalton
kg	Kilogram
K <sub>m</sub>	Michaelis-Menten constant
<i>L. lactis</i>	<i>Lactococcus lactis</i>
MDR	Multidrug resistance
mg	milligram
min	minute
ml	millilitre
mM	milimolar
mRNA	messenger Ribonucleic Acid
MS	Mass spectrometry
$\mu$ g	microgram
$\mu$ l	microlitre
$\mu$ M	mircomolar
NBD	Nucleotide binding domain
nM	nanomolar
nm	nanometre
<i>N. plumbaginifolia</i>	<i>Nicotiana plumbaginifolia</i>
OsABCG	ATP binding cassette subfamily G from <i>Oryza sativa</i>
<i>O. sativa</i>	<i>Oryza sativa</i>
PAGE	Polyacrylamide gel electrophoresis
PCR	Polymerase chain reaction
PDB	Protein data bank
PDR	Pleiotropic drug resistant

PEN 2	Penetration 2
Pgp	Permeability glycoprotein 1
<i>P. hybrida</i>	<i>Petunia hybrida</i>
PhABCG	ATP-binding cassette subfamily G from <i>Petunia hybrida</i>
Pi	Inorganic phosphate
PM	Plasma membrane
<i>P. pastoris</i>	<i>Pichia pastoris</i>
qRT-PCR	Quantitative reverse transcriptase polymerase chain reaction
R6G	Rhodamine 6 G
rbs	ribosome binding site
RNA	Ribonucleic acid
RT-PCR	Reverse transcriptase polymerase chain reaction
SBP	Substrate-binding protein
<i>S. cerevisiae</i>	<i>Saccharomyces cerevisiae</i>
SD	Standard deviation
SDS	Sodium dodecyl sulphate
SEC	Size exclusion chromatography
StABCG	ATP-binding cassette subfamily G from <i>Solanum tuberosum</i>
<i>S. tuberosum</i>	<i>Solanum tuberosum</i>
SUR	Sulfonylurea receptors
TAP	Transporter associated with antigen processing
T-DNA	Transfer-deoxyribonucleic acid
TM	Transmembrane $\alpha$ -helices
TMD	Transmembrane domain
VLCFA	Very long chain fatty acids
$V_{\max}$	maximal ATPase activity
WBC	White-brown complex
wcw	Wet cell weights

<b>Amino acid</b>	<b>Three / One letter code</b>	<b>Amino acid</b>	<b>Three / One letter code</b>
Alanine	Ala / A	Leucine	Leu / L
Arginine	Arg / R	Lysine	Lys / K
Asparagine	Asn / N	Methionine	Met / M
Aspartic acid	Asp / D	Phenylalanine	Phe / F
Cysteine	Cys / C	Proline	Pro / P
Glutamic acid	Glu / E	Serine	Ser / S
Glutamine	Gln / Q	Threonine	Thr / T
Glycine	Gly / G	Tryptophan	Trp / W
Histidine	His / H	Tyrosine	Tyr / Y
Isoleucine	Ile / I	Valine	Val / V

# 1. Introduction

## 1.1 Biological membranes, the doormen of cells

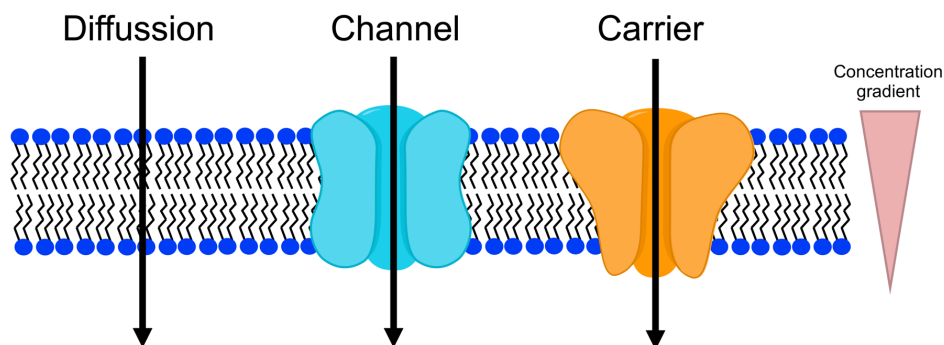
Biological membranes are lipid bilayers, which surround cells and in eukaryotes also subcellular compartments to margin the interior from the environment [1]. They are essential for the function and vitality of cells as they regulate communication, molecule transport, energy conversion and signal transduction between the cell and the environment and within cells [2-4].

Biological membranes are composed of various lipids, membrane proteins and carbohydrates. Besides glycolipids and sterols, phospholipids are the main constituents of membranes and they cause the formation of the lipid bilayer due to their amphipathic character. Thereby, their hydrophilic heads interact with the surrounding aqueous environment and the hydrophobic tails face inwards, towards each other. Singer and Nicolson ascribed biological membranes a dynamic and fluid nature due to lateral diffusion of proteins and lipids [1].

A selective permeability for the transversal movement of substrates across the lipid bilayer is dependent on the membrane composition [5]. In general, small and uncharged molecules can diffuse freely, while polar and charged molecules pass the membrane only through membrane-embedded proteins [6] (Figure 1). Consequently, membrane proteins are indispensable key players for passive as well as active transport of substrates across the biomembrane [7, 8]. Channel and carrier proteins conduct the passive transport of ions or molecules down their electrochemical gradients. Thereby carrier proteins undergo different conformations and channel proteins form water-filled pores to transport the solute across the lipid bilayer [9-11]. The active transport of substrates against a concentration gradient requires energy as for instance ATP or light and is referred to as primary active transport [12, 13]. In contrast, the secondary active transport is based on energy from the downhill movement of a second molecule [14]. Substrate transport of both molecules in the same direction is referred to as symport, while antiport describes the transport in the opposite direction.

Finally, membrane proteins can also contribute to the symmetric or asymmetric distribution of the lipid bilayer. Thereby, distribution can be affected by lateral movement of lipids and membrane proteins (lateral diffusion), while so-called lipid translocators catalyze the vertical movement of lipids from one leaflet to another [1, 15, 16].

### Passive transport



### Active transport

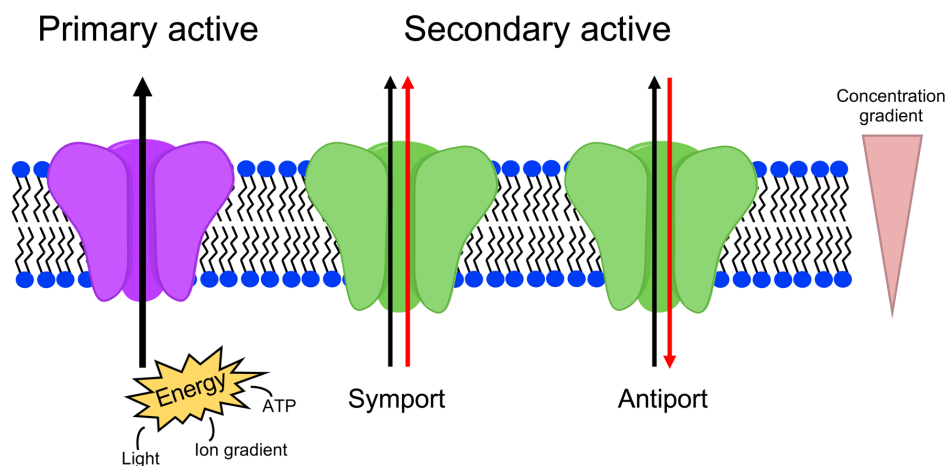


**Figure 1: Passive and active membrane transport.** Passive transport: Small and uncharged molecules can diffuse freely, while channels and pores facilitate the transport of ions and molecules along the concentration gradient across the membrane. Active transport: The primary transport of molecules against a concentration gradient is depended on energy in form of ATP or light. The secondary transport against a concentration gradient is based on energy from the downhill movement of another molecule (Ion gradient). While the transport of the substrate (black arrow) and the second molecule (red arrow) in the same direction is described as symport, is the transport in opposite direction referred to as antiport. The depicted figure is adapted from [7].

## 1.2 The ATP-binding cassette transporter superfamily

The primary active ATP-binding cassette (ABC) transporters are ubiquitous in all kingdoms of life and constitute one of the largest membrane protein superfamilies [17]. The first ABC transporter, the histidine permease from *Salmonella typhimurium*, has been cloned and sequenced almost 40 years ago and since then various reports elucidated their involvement in diverse biochemical and physiological processes [18, 19]. For instance in bacteria, ABC transporters are involved in nutrient uptake [20, 21], cell wall assembly [22-24] or drug resistance [25, 26]. Many human ABC transporters are medically important, since mutations in these proteins are associated with various disorders, for instance cystic fibrosis [27], hypercholesterolaemia [28] or diabetes [29, 30]. Similarly, plant ABC transporters contribute to overall vitality and fitness by transport of various substrates such as secondary metabolites [31], plant hormones [32-34] or coating materials [35, 36].

The general blueprint of ABC transporters is composed of two nucleotide binding domains (NBDs) and two transmembrane domains (TMDs), which are responsible for substrate binding and ATP-hydrolysis driven substrate translocation across a lipid bilayer [37]. Depending on the direction of substrate translocation an ABC transporter can function as importer or exporter (Figure 2). Both importers and exporters are found in prokaryotes, while eukaryotes harbor almost exclusively exporters [20, 38]. Few exceptional eukaryotic importers are for instance the retinal importer ABCA4, the sulfonyleurea receptors SUR1 and SUR2, the chloride channel CFTR, and *Arabidopsis* ABCG30 and ABCG40 [39, 40].

Importers mediate the uptake of diverse nutrients, including metal ions, sugar and amino acids and can be further classified into three distinct classes, I- III. The requirement of a periplasmatic substrate-binding protein (SBP) for substrate binding and delivery differentiates class I and II importers from other transporters. Moreover, class I importers translocate substrates with an alternative access mechanism, where the transporter undergoes conformational changes. Class II importers transport larger and more hydrophobic substrates and in contrast to class I, they can interact with the substrate in both nucleotide-free and ATP-bound state, while the ATP-hydrolysis facilitates an inward-facing conformation. The third class is constituted by energy coupling factor (ECF) transporters, which mediate the uptake of micronutrients. Class III importers use a membrane-embedded substrate-binding protein (EcfS) instead of a

SBP [41, 42].

ABC exporters translocate diverse compounds including toxins, drugs, metabolites and peptides. Wang *et al.* introduced a classification of ABC exporters based on the separate evolution of their TMDs: ABC1, ABC2 and ABC3 [43]. Apart from that, Thomas and Tampè presented recently a further classification into four distinct classes depending on their sequence and structural homology: class IV-V exporters, class VI extractors, class VII efflux pumps [39].

Finally, ABC transporters can be distinguished based on the number of domains, which are encoded on a single gene as full-size (TMD-NBD)<sub>2</sub> and half-size (TMD-NBD) transporters. Half-size transporters have to homo-or heterodimerize in order to form a functional translocation unit [44, 45].

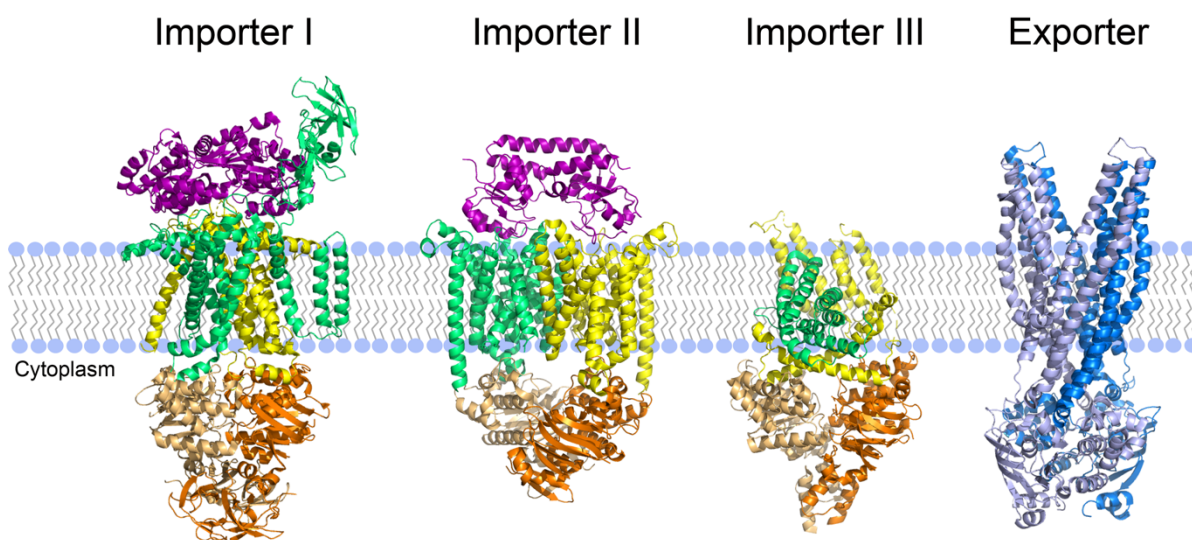


**Figure 2: Structures of ABC importer and exporter classes.** Crystal structures of ABC importer classes I-III and an ABC exporter are depicted. Class I ABC importer: Maltose transporter MalEFGK<sub>2</sub> (PBD code: 2R6G) with NBDs (MalK) highlighted in light orange and orange, TMDs (MalF and MalG) highlighted in green and yellow; and the SBP (MalE) in purple [46]. The class II ABC importer BtuCDF (PBD code: 2QI9) is depicted with NBDs (BtuD) in light orange and orange, the TMDs in green and yellow, and the SBP BtuF in purple [47]. Class III ABC importer: energy-coupling factor transporter from *Lactobacillus brevis* (PBD code: 4HZU) is depicted with NBDs (EcfA and EcfA') in light orange and orange, and TMDs (EcfT and EcfS) in green and yellow [48]. The ABC exporter Sav1866 (PBD code: 2HYD) is a homodimeric half-size transporter. Each fused NBD and TMD subunit is shown in light blue and blue, respectively [49].



### 1.2.1 Transmembrane domains

The TMDs of ABC transporters traverse the phospholipid bilayer, thus providing a translocation pathway which is on either side accessible for substrate transport. Compared to the NBDs, TMDs display little to no sequence conservation, rather a distinct topology depending on the transporter classes is present [49-51].

Type I importer contain up to eight transmembrane  $\alpha$ -helices (TM) per TMD with four  $\alpha$ -helices (TM2-5) lining the translocation pathway and one (TM1) wrapping around the outer membrane-facing surface [46, 52, 53] (Figure 3). Type II importers are comprised of ten tightly packed  $\alpha$ -helices per TMD, with an  $\alpha$ -helix (TM2) going through the center of all other helices and TM2-5 and TM7-10 packed with opposite orientation through the membrane [54, 55]. The ECF-transporters (type III importer) harbor instead of TMDs two structural as well as functional unrelated subunits: the EcfT subunit (T-component) and the EcfS subunit (S-component). The EcfT subunit has up to eight transmembrane helices, while the EcfS-component, which is responsible for substrate binding, has predominantly six  $\alpha$ -helices. In contrast to the other importer types, is the translocation pathway of Ecf transporters likely not located between the interface of the two transmembrane subunits, but restricted to the S-component [56-58]. ABC exporters consist of 6 transmembrane helices per TMD, whereby in the middle of the membrane two “wings” formed by  $\alpha$ -helices TM1-TM2 and TM3-TM6 facilitate an outward-facing conformation by pointing away from another. Due to this so-called domain-swapped arrangement, are TM1-TM3 and TM4-TM6 adjoined by a two-fold rotation around a symmetry axis in the membrane plane [49, 51, 59, 60].

A common feature to all the TMDs is the presence of coupling helices (or intracellular loops), short  $\alpha$ -helices, which are oriented nearly parallel to the membrane and form the transmission interface. Coupling helices transfer ATP binding and hydrolysis depended conformational changes of NBDs to the TMDs [49, 54]. Importers contain only one coupling helix per TMD, which interacts with the NBD on the opposite site [46, 50]. Coupling helices of importers contain a highly conserved signature motif, a so-called EAA-motif (L-loop), that interacts with a Q-loop containing groove within the NBD [49, 54, 61]. Ecf transporter harbor two long  $\alpha$ -helices in the EcfT subunit that interact with both NBDs [48, 50]. The Coupling helix in exporters extends the  $\alpha$ -helices from the membrane approximately 25-40 Å into the cytoplasm [49]. In the exporter Sav1866 the first coupling helix interacts with the NBD that is linked to the own subunit,

while the second coupling helix interacts due to domain swapping with the NBD from the other subunit [50, 62]. The transmission surface of exporters is formed by interaction between coupling helices and the X-loops (TEVGERG), a consensus motif within the NBDs. The proximity of the X-loops to the ABC signature (C-loop) is presumed to allow the transmission of conformational changes to the TMDs in exporters [49].

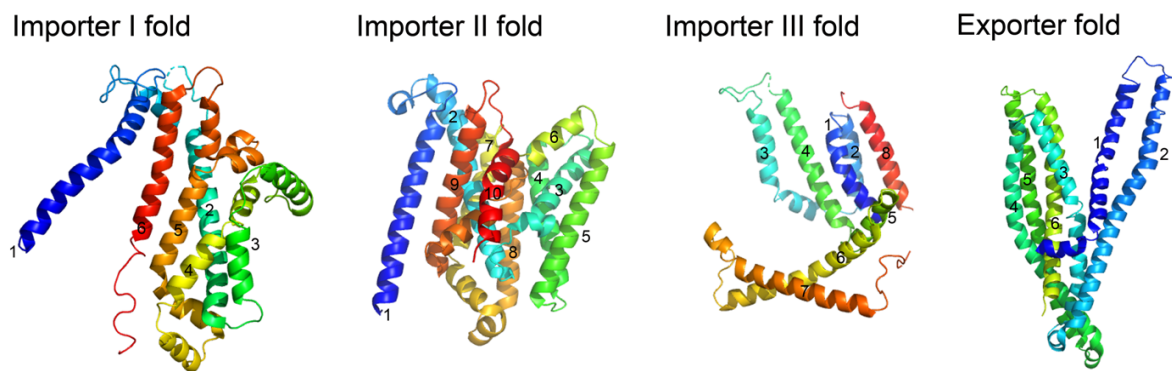


**Figure 3: TMD structure of ABC importers and exporters.** The helical folds within a TMD subunit of an ABC importer I: MalF (PBD code: 2R6G), an ABC importer II: BtuC (PBD code: 2QI9), an ABC importer III: EcfT (PBD code: 4HZU) and an ABC exporter: Sav1866 (PBD code: 2HYD) are indicated by numbers and different colors.

### 1.2.2 Nucleotide binding domains

The cytosolic NBD can be considered as the power plant of an ABC transporter, as it provides the energy for the substrate translocation by  $Mg^{2+}$ -dependent ATP binding and hydrolysis [63]. NBDs are pervaded by several conserved motifs and genome analysis revealed the NBDs as one of the most conserved phylogenetic DNA sequences among all kingdoms of life [64]. The first NBD was described in 1998 for RbsA from *Escherichia coli* (*E. coli*) and thereafter several studies have contributed to get more insight into the function and composition of NBDs [65-68].

In general, NBDs are composed by two domains: a RecA-like catalytic subdomain and a helical subdomain (Figure 4). The catalytical subdomain contains conserved motifs or residues for ATP binding and hydrolysis: the Walker A, Walker B, H-loop, D-loop, A-loop and Q-loop. The Walker A motif (P-loop; GxxGxGKS/T, where x represents any

amino acid) interacts via a conserved lysine residue and the backbone amid moieties with the  $\beta$ - and  $\gamma$ -phosphate of ATP [69]. The Walker B motif ( $\phi\phi\phi\phi$ DE, where  $\phi$  is a hydrophobic amino acid) contains a conserved aspartate residue, which contributes to the coordination of the magnesium ion and a conserved glutamate, which is presumed to polarize the water during nucleophilic attack on ATP [70]. The H-loop (switch region) contains a conserved histidine, that interacts with the conserved aspartate from the D-loop, with the  $\gamma$ -phosphate of the ATP; and acts as base for the water molecule during nucleophilic attack [66]. The D-loops (consensus motif SALD) of both NBD domains are able to affect the geometry of the catalytic side and facilitate the formation of the ATP hydrolysis site, while the A-loop (conserved aromatic residue) facilitates to position ATP by stacking with the adenine ring [71]. The Q-loop (conserved glutamine) connects together with a Pro-loop (conserved proline) the catalytic and the helical subdomains and is also the major TMD interaction side [72]. In contrast to the catalytic subdomain is the helical subdomain structurally more diverse. However, it contains the ABC signature motif (C-loop, consensus motif), a characteristic feature of the ABC superfamily, that is involved in nucleotide binding and interaction with  $\gamma$ -phosphate [44]. In absence of ATP are the NBDs of an ABC transporter separated and they dimerize upon ATP binding. Thereby the ATP molecule is 'sandwiched' in the dimer interface by the Walker A and Walker B motif from one subunit and the ABC signature sequence of the second subunit and vice versa for a further ATP ('head-to-tail' conformation). Subsequent ATP-hydrolysis leads to NBD separation and release of ADP and inorganic phosphate [49, 66, 68, 73]. Current models of the ABC transport mechanism, will be described in the next chapter.

### 1.2.3 Transport mechanism of ABC transporters

Biochemical and structural studies allowed the proposal of several ABC transport mechanism models, particularly the alternating access [74, 75], the switch [37, 76-78], the constant contact [79, 80] and the reciprocating twin channel model [81]. The alternating access model is fundamental to the other models and proposes the conformational switching of the TMDs into an outward facing conformation with low substrate affinity or the inward facing conformation with high substrate affinity for importers and reversed for exporters [54, 82, 83].

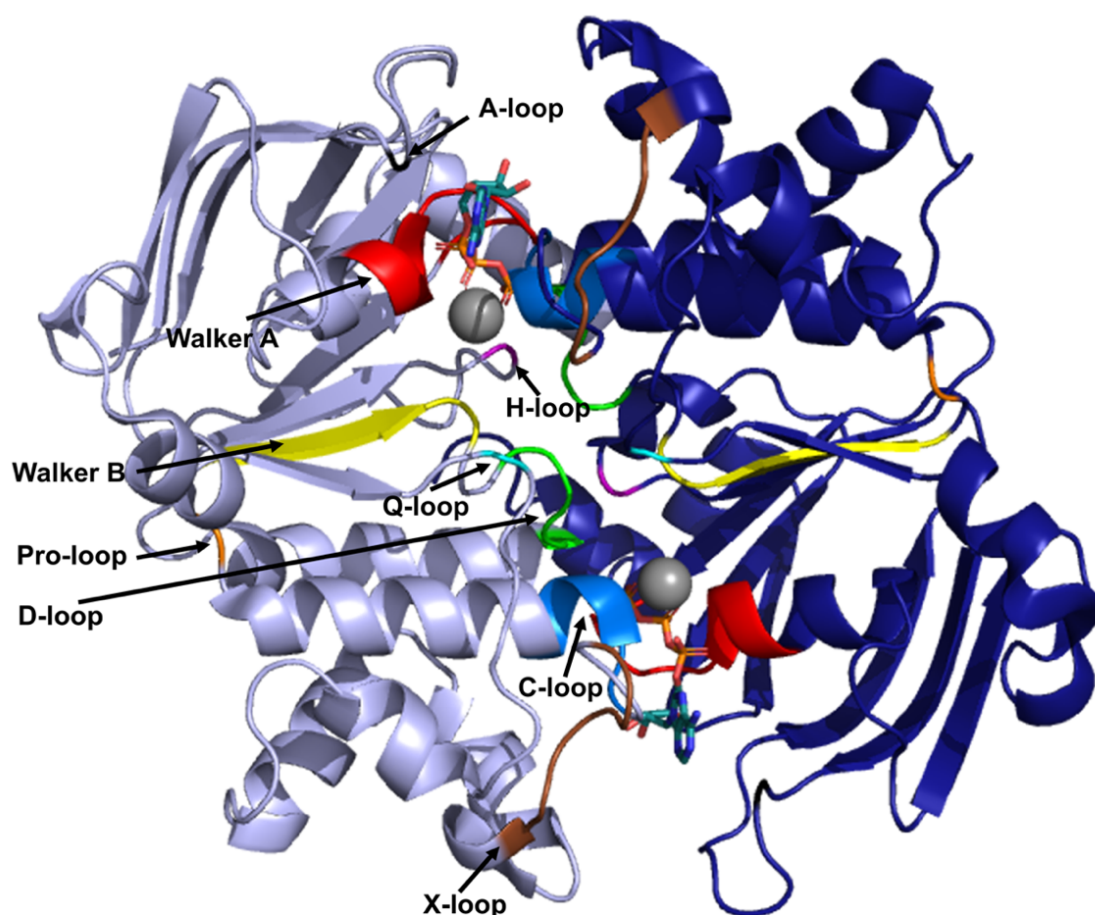


**Figure 4: Structure of the HlyB NBD dimer.** The crystal structure of the HlyB NBD dimer is depicted with the monomers highlighted in light blue and deep purple (PDB code: 1XEF). Within the catalytic subdomain is the A-loop shown in black, the Walker A motif in red, the Walker B motif in yellow, the H-loop in purple, the Q-loop in cyan, the Pro-loop in orange and the D-loop in green. The helical subdomain contains the C-loop and the X-loop, which are highlighted in blue and brown. Two ATP molecules (sticks) and  $Mg^{2+}$  (spheres) are located at the NBD interface [49, 63].

The generally accepted switch model proposes the switching of the NBDs between the dimerized state upon binding of two ATP molecules and the separated and unliganded state upon ATP hydrolysis [80] (Figure 5). Thereby the binding of two ATP molecules at the separated NBD monomers leads to the closed dimerized state with the ATPs sandwiched at the dimer interface. Subsequent hydrolysis of both ATP molecules induces the dissociation of the NBD monomers with a gap of 20-30 Å and the release of ADP/Pi. The Q-loop, coupling helices and additionally the X-loop in ABC exporters transfer the conformational changes to the TMDs, which switch either from the inward

to outward facing conformation or vice versa (importers or exporters) and enable substrate translocation.

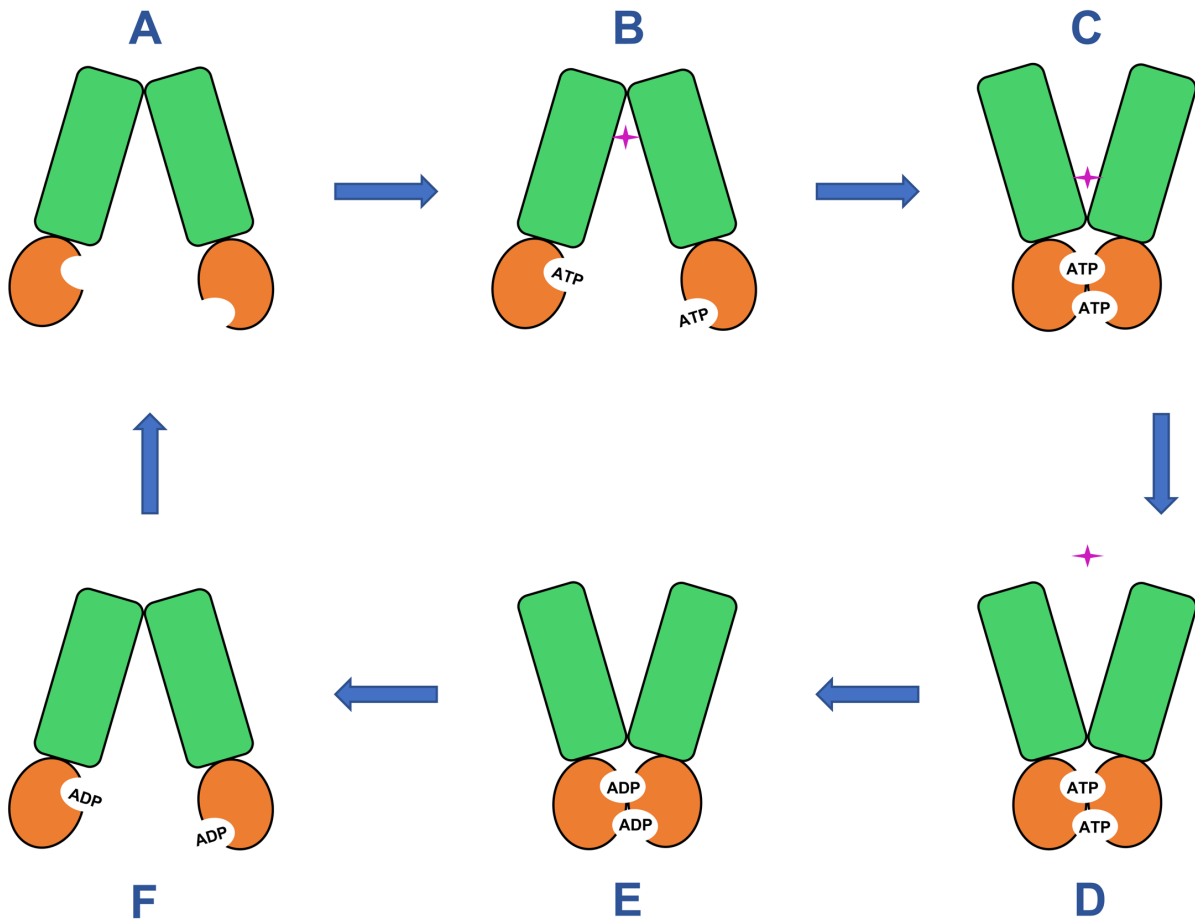


**Figure 5: Switch model for an ABC exporter.** The cartoon summarizes the conformational changes of an ABC exporter (TMDs in green and NBDs in orange) during substrate (purple) transport. (A) The ABC exporter possess an inward-facing conformation during nucleotide-free state. (B) Binding of two ATP molecules at the NBDs and substrate at the TMDs leads to (C) NBD dimerization and outward-facing conformation. (D) ATP hydrolysis leads to substrate and ADP/Pi release. (E, F) ADP-bound state induces inward-facing conformation and subsequent ADP-dissociation enables a new transport cycle. The depicted cartoon was adapted from [81].

The key feature of the constant contact model is the alternate ATP hydrolysis at each active site and that the NBDs do not completely dissociate during the catalytic cycle [80]. The recently proposed reciprocating twin channel model comprises also the constant contact model [81]. The reciprocating twin channel model proposes the existence of two separate substrate translocation pathways, which act in a

reciprocating manner in the TMDs and is coupled to the alternating cycle of ATP hydrolysis in the NBDs (Figure 6).

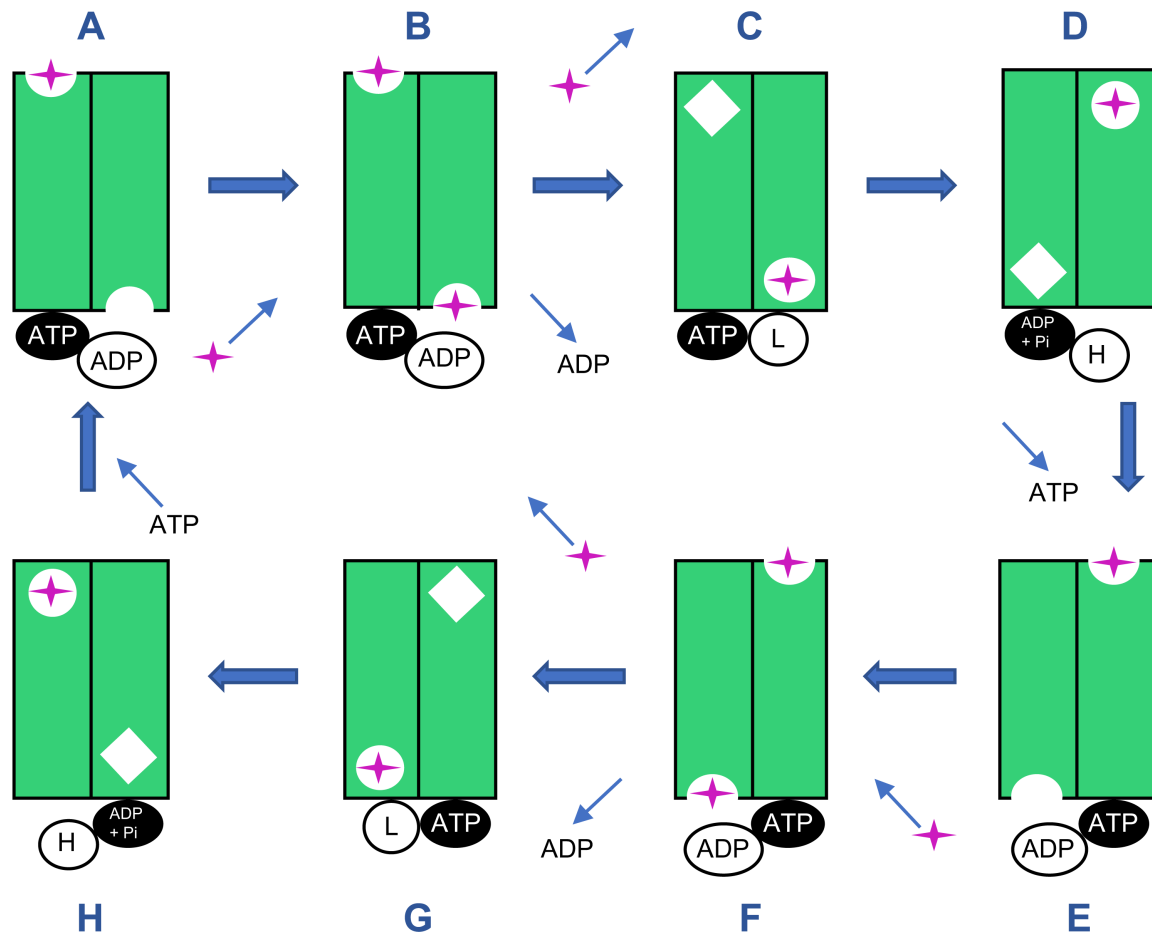


**Figure 6: Reciprocating twin channel model for an ABC exporter.** The cartoon illustrates substrate (purple) transport at two functionally separated substrate translocation pathways in the TMDs of an ABC exporter (green, channels separated by vertical line in black), which is coupled to an alternating cycle of ATP hydrolysis in the NBDs. (A) Transported substrate from prior cycle is bound at the substrate binding site (semicircle) at channel 1 and an ATP molecule bound at the NBD site 1. (B) Substrate binds at channel 2 and the transported substrate is released from channel 1. The unbound and sequestered state is shown as diamond. (C) Substrate is sequestered in channel 2 (circle) and the substrate binding site exhibits low-affinity due to ADP release (L, low affinity and H, high affinity). (D) ATP hydrolysis induces the substrate transport in channel 2 to the extracellular side of the membrane. (E) ATP binds at NBD site 2 and the ADP-bound substrate binding site 1 is open (F, G) for substrate binding. Transported substrate is released at channel 2 and ADP release leads to low affinity binding site at the NBD. (H) ATP is hydrolyzed and allows the transport of the occluded substrate in channel 1 to the extracellular membrane side. Steps (A)-(D) and (E)-(H) are reciprocal phases. The depicted cartoon was adapted from [81].

Both, the switch model and the reciprocating twin channel model propose the hydrolysis of two ATP molecules per conformational cycle. However, some ABC proteins have been shown to contain two ATP binding sites and hydrolyze only one ATP molecule per transport cycle [84]. Others as for instance BmrAB hydrolyze only one ATP molecule per cycle, because they contain a functional and a degenerated ATPase site [85, 86]. This exemplifies that the assignment of one model to all ABC transporters is not possible. The combined analysis of structural, biochemical and biophysical properties of every ABC system is necessary in order to gain insight into the specific transport mechanism [86].

### 1.3 Plant ABC transporters

ABC transporters are ubiquitously found in all kingdoms of life (Figure 7) [17]. Remarkably, constitute plants with for instance 130 ABC proteins in *Arabidopsis thaliana* (*A. thaliana*) the highest source for ABC proteins among all living organism. Compared to plants, other organism contain much lesser ABC proteins, for instance humans with 49, *E. coli* have 79 and *Saccharomyces cerevisiae* (*S. cerevisiae*) have 30 ABC proteins [36, 87]. The particularly enlarged number of ABC proteins in plants is presumably the result of evolution from microalgae to terrestrial plants. It is conceivable that multiplication and functional diversification of ABC transporter genes was needed to adapt to the autotroph and sessile lifestyle [36, 88].

The first plant ABC transporter was identified in 1993 by Martinoia and co-workers [89] and since then various studies emphasized the involvement of ABC transporters in essential physiological processes including nutrition uptake, growth and development (such as phytohormone transport, seed development or organ formation, detoxification), and biotic and abiotic stress response (such as pathogen response, transport of phenolics for UV light protection or protective layer formation) [36, 90, 91]. Most ABC proteins were localized to the plasma membrane, the tonoplast, and mitochondrial, plastidal and peroxisomal membranes [92].

Plant ABC transporters were classified in accordance with the nomenclature system for animal ABC proteins, which is based on the phylogenetic relationship and domain organization, into 8 subfamilies ABCA-ABCG. Unlike their animal counterparts, plants are lacking the ABCH subfamily [93]. ABC proteins from the A, B, C, and D subfamily



feature a forward domain (TMD-NBD) organization, while members of the subfamily ABCG have a reverse domain (NBD-TMD) organization. The ABCE and ABCF subfamily is formed by soluble ABC proteins with only two NBDs, unlike the ABCI subfamily which contains diverse genes that encode for one NBD, TMD or accessory domain [93]. So far, only 45 out of 130 *Arabidopsis* ABC transporters have been characterized, whereby identities of transported substrates were unambiguously identified by direct assays for 23 ABC transporters [91].

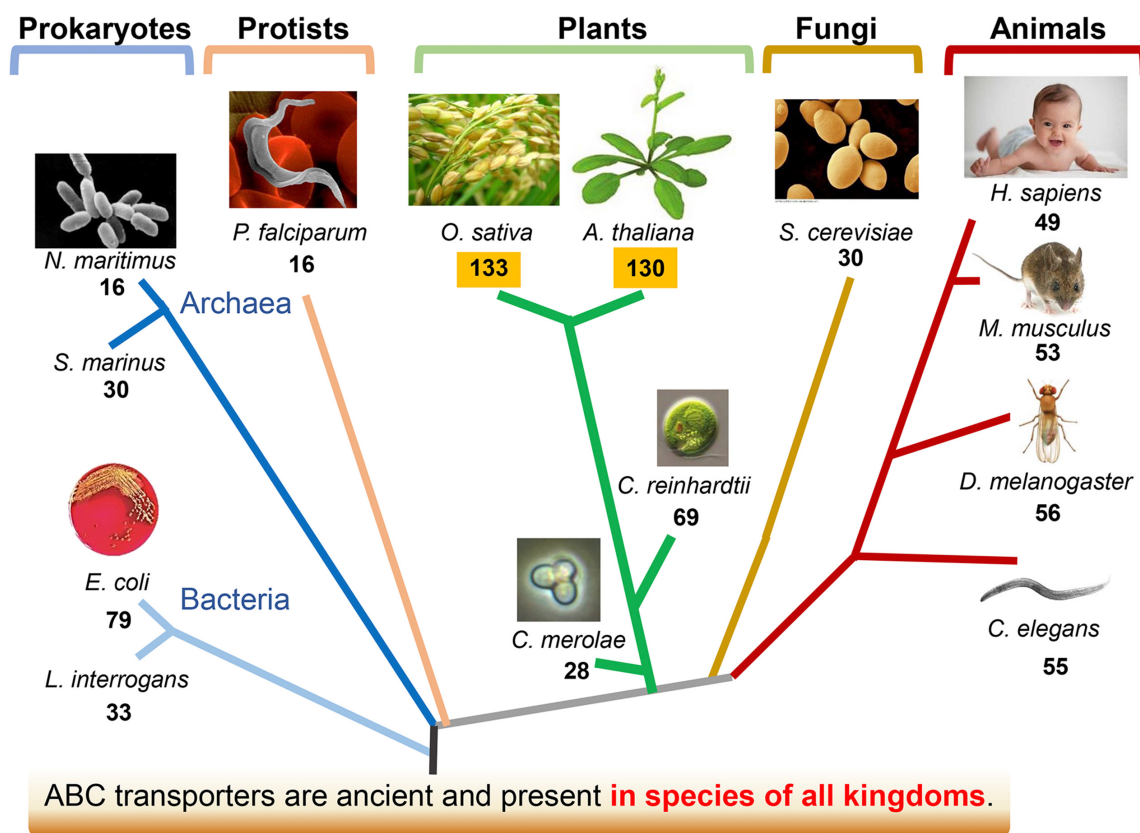


**Figure 7: Evolutionary tree of ABC transporters.** The depicted figure demonstrates that ABC transporters originate from a common ancestor and are currently found in all kingdoms of life. Numbers of ABC proteins found are given and as highlighted in yellow form plants the largest source. Depicted picture was taken from [36].

The main focus of this thesis will lie in on the ABCG subfamily. For instance, 43 members of *Arabidopsis* make the G subfamily the largest amongst all ABC subfamilies and is comprised of 28 half-size (WBC, white-brown complex) and 15 full-size (PDR, pleiotropic drug resistant) transporters.



### 1.3.1 Role of ABCG half-size transporters in barrier formation

*Arabidopsis* half-size ABCG transporters were found to be involved in diverse functions, such as antibiotic resistance [94, 95], ABA- and cytokinin transport [40, 96-100] or stomatal regulation in guard cells [101, 102]. Interestingly, most of the analyzed half-size AtABCG transporters are considered to be involved in diffusion barrier formation. Diffusion barriers, such as cutin, suberin or lignin protect plants from water loss, many environmental stress factors including drought or pathogen attack, separate different tissues and are part of nutrient uptake [103, 104].

So far, a subset of half-size AtABCG transporters, including AtABCG1, AtABCG16, AtABCG26, AtABCG9 and the full-size transporter AtABCG31 have been ascribed to be part of pollen protection (Figure 8). The pollen surface is composed of the inner intine and the outer exine layer. The intine is synthesized gametophytically, while the exine is formed by sporopollenins and can be further divided into the nexine and sexine layer [105, 106]. AtABCG1 and AtABCG16 were shown by double mutant analysis to be involved in pollen nexine and intine formation, while AtABCG26 was found to be involved in exine formation [107-113]. Yim *et al.* also showed that microspores of an *atabcg1 atabcg16* double mutant plant contained defects in pollen mitosis during postmeiotic stages of male gametophyte development [112]. Furthermore, AtABCG9 and AtABCG31 have been shown to be part of pollen coat maturation [114].

Cutin and wax are the major components of the cuticle, that covers the areal plant surface and is found since the embryonic state in *Arabidopsis* [115-117]. The cutin layer is formed by ester bound C<sub>16</sub>-C<sub>18</sub> dicarboxylic acids and is embedded and overlaid by cuticular waxes. Abundantly found wax compounds are primary and secondary alcohols, alkanes, aldehydes, ketones, fatty acids and wax esters [118, 119]. The precursors of the cuticula are synthesized in the epidermis and need to be transported through the cell wall and the plasma membrane to the extracellular space [120]. In *Arabidopsis* ABCG11, ABCG12 and ABCG13 and the full-size transporter AtABCG32 were found to be involved in wax and cutin transport (Figure 8). Both, AtABCG11 and AtABCG12 are co-expressed in the stem epidermis and are involved in wax/cutin transport from the epidermis to the extracellular matrix and the export of waxes to the cuticle, respectively [35, 121-126]. Further protein trafficking and interaction studies revealed that AtABCG11 and AtABCG12 cooperate in cuticular wax export. Thereby, AtABCG12 is retarded in the endoplasmic reticulum without heterodimerization with AtABCG11, while AtABCG11 is able to form functional

homodimers [127]. AtABCG13 was also found to be involved in cutin transport, but in flowers and especially petals [128, 129].

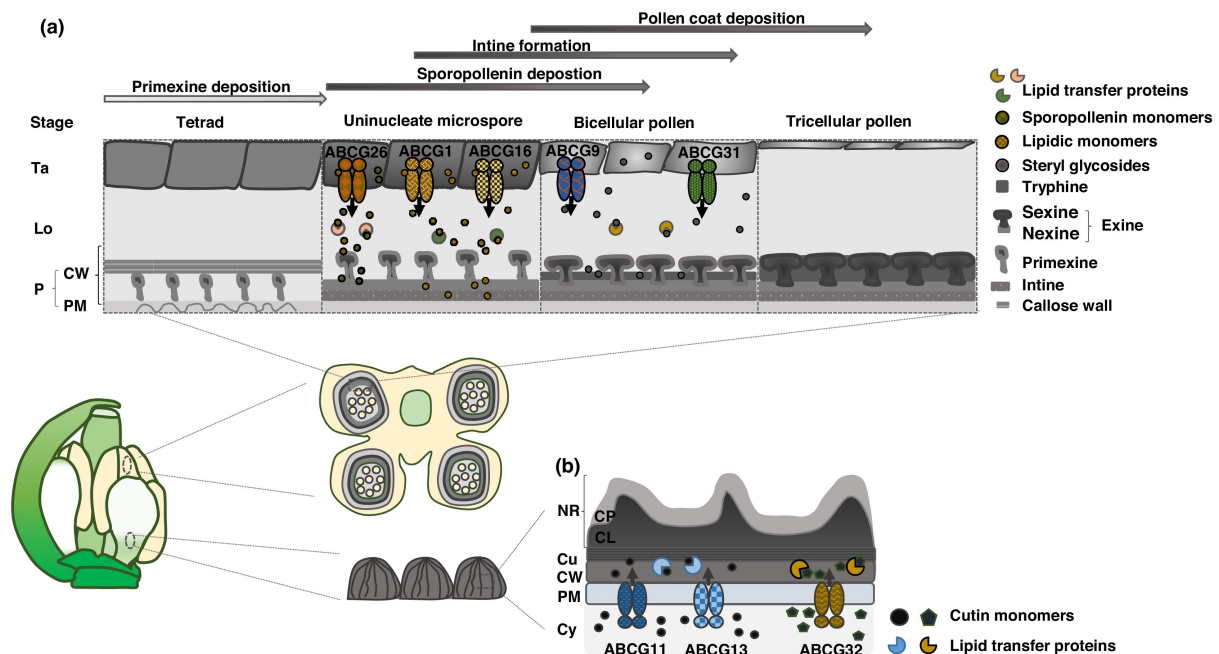


**Figure 8: Contribution of ABCG transporters in diffusion barrier formation of *A. thaliana* reproductive organs.** (a) Picture displays function of AtABCG transporter in the tapetum of the anther during pollen development. Primexine is formed during the initial stage of exine formation between the callose wall and the plasma membrane (PM) of the microspore [130]. AtABCG26 mediates sporopollenin deposition in primexine, AtABCG1 and AtABCG16 transport lipidic monomers for nexine layer formation, and AtABCG9 and AtABCG32 transport sterol glycosides for the tryphine layer formation. Lipid transfer proteins are supposed to transfer the lipidic compounds to their final destination. Lo, locule, P. pollen; CW, cell wall. (b) Picture shows the function of AtABCG transporters in the development of epicuticular ridges (nanoridge, NR) on conical cell surfaces. Cutin monomers are transported by AtABCG11, AtABCG13 and AtABCG32 to the surface of the epidermal cells at the petal. CP, cuticular proper; CL, cuticular layer; CW, cell wall; Cu, cuticle; Cy, cytosol. Figure is taken and adapted from [90].

Moreover, several *Arabidopsis* half-size transporters were described to be involved in suberin barrier formation [113, 124, 131]. The chemically complex suberin heteropolymer is mainly found in tissue-tissue or plant-environmental interfaces (such as root endodermal and peridermal cell walls) and occurs at the inner cell wall, adjacent to the plasma membrane [132]. Suberin serves particularly in liaison with the casparian strips, that consist mainly of lignin- or a lignin like polymer as the initial barrier

for the movement of water and apoplastic solutes, but further suberization can be additionally induced by abiotic or biotic stress [103, 133, 134]. Just like cutin, suberin is a glycerolipid polymer, though consisting of a polyaliphatic polyester linked with phenolic components and embedded waxes (Figure 9). The aliphatic part of suberin is formed in principal by  $\omega$ -hydroxy acids,  $\alpha,\omega$ -dicarboxylic acids, fatty acids and alcohols. Thereby, glycerol is esterified to the  $\omega$ -hydroxy and  $\alpha,\omega$ -dicarboxylic acids and the phenylpropanoid pathway derived phenolic compounds that are mainly hydroxycinnamates (commonly ferulic acid, coumaric acid and monolignols) [120, 135]. The suberin biosynthesis and the role of half-size ABCGs in suberin transport will be further elucidated later.

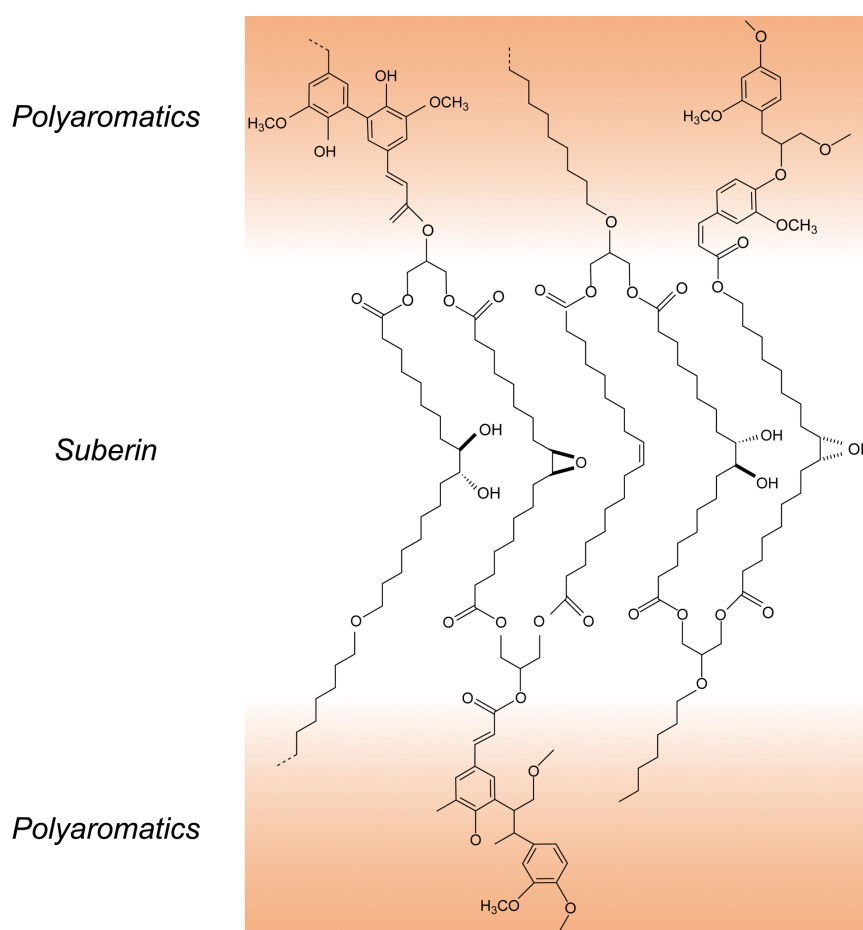


**Figure 9: Hypothetical model of the suberin macromolecular structure.** The depicted figure displays a suberized cell wall structure. The suberin polyester (translucent) in the core is covalently linked by esterification to ferulic acid to the adjacent lignin-like polyaromatics (orange). Figure is adapted from [136].

### 1.3.2 Suberin biosynthesis in *Arabidopsis*

The suberin formation can be divided into two parts, first, the biosynthesis of the aliphatic, phenolic and glycerol monomers in specific cell compartments and second, the transport through the plasma membrane for the final assembly into suberin. Depending on the plant species and tissue can the proportion of the suberin precursors differ significantly [137]. The structural formula of the main suberin monomers are depicted in Figure 10.

Vishwanath *et al.* presented, under consideration of the actual data, a detailed model on the biosynthetic pathway of suberin (Figure 10) [132]: **Acyl activation:** The first suberin biosynthesis step comprises the conversion of free fatty acids to fatty thioesters, as for instance fatty acyl-coenzyme A (CoA) thioesters. **Acyl elongation:** A fatty acid elongase complex (FAE complex) elongates the fatty acyl-CoAs to very long chain fatty acids (VLCFA-CoAs) [138].  $\beta$ -ketoacyl-CoA synthases (KCS) control the elongation process and so far, two *DA/SY/AtKCS2* and *AtKCS20* were found in *Arabidopsis* [139-141]. **Acyl oxidation:** The activated fatty acids are first  $\omega$ -hydroxylated to  $\omega$ -hydroxy fatty acids and the further oxidized by an  $\omega$ -hydroxy fatty acid dehydrogenase to  $\alpha,\omega$ -dicarboxylic acids. The  $\omega$ -hydroxylation is thereby catalyzed by two cytochrome P450-dependent, CYP86A1 and CYP86B1 fatty acid oxidases [142-144]. **Acyl reduction:** Alternatively, activated fatty acids become reduced to primary alcohols ( $C_{18}$ - $C_{22}$ ) by the fatty acyl reductases (FARs), FAR1, FAR4 and FAR5 [145-147]. **Acyl esterification:** Acyl-CoA dependent glycerol 3-phosphate acyltransferases (GPATs) catalyze the esterification of  $\omega$ -hydroxy fatty acids and  $\alpha,\omega$ -dicarboxylic acids with glycerol 3-phosphate to *sn*-2 monoacylglycerols. The phenylpropanoid pathway derived phenolic compounds are esterified by feruloyl-CoA-transferases (ASFT, aliphatic suberin feruloyl transferase; FACT, alcohol:caffeoyl-CoA caffeoyl transferase) with  $\omega$ -hydroxy fatty acids and fatty alcohols [143, 148-151].

Finally, different predictions exist for the transport mechanism of the suberin precursors for macromolecular assembly in the cell wall. On one hand are suberin precursors are presumed to be transported from the endoplasmatic reticulum (ER) to the plasma membrane through the secretory pathway as shown for the transport of cuticular waxes to the apoplast [132, 152]. Alternatively, is the precursor transport through the plasma membrane ascribed to occur by ABC transporters [132]. In *Arabidopsis* AtABCG2, AtABCG6 and AtABCG20 were found to be potential suberin

monomer transporter [113].

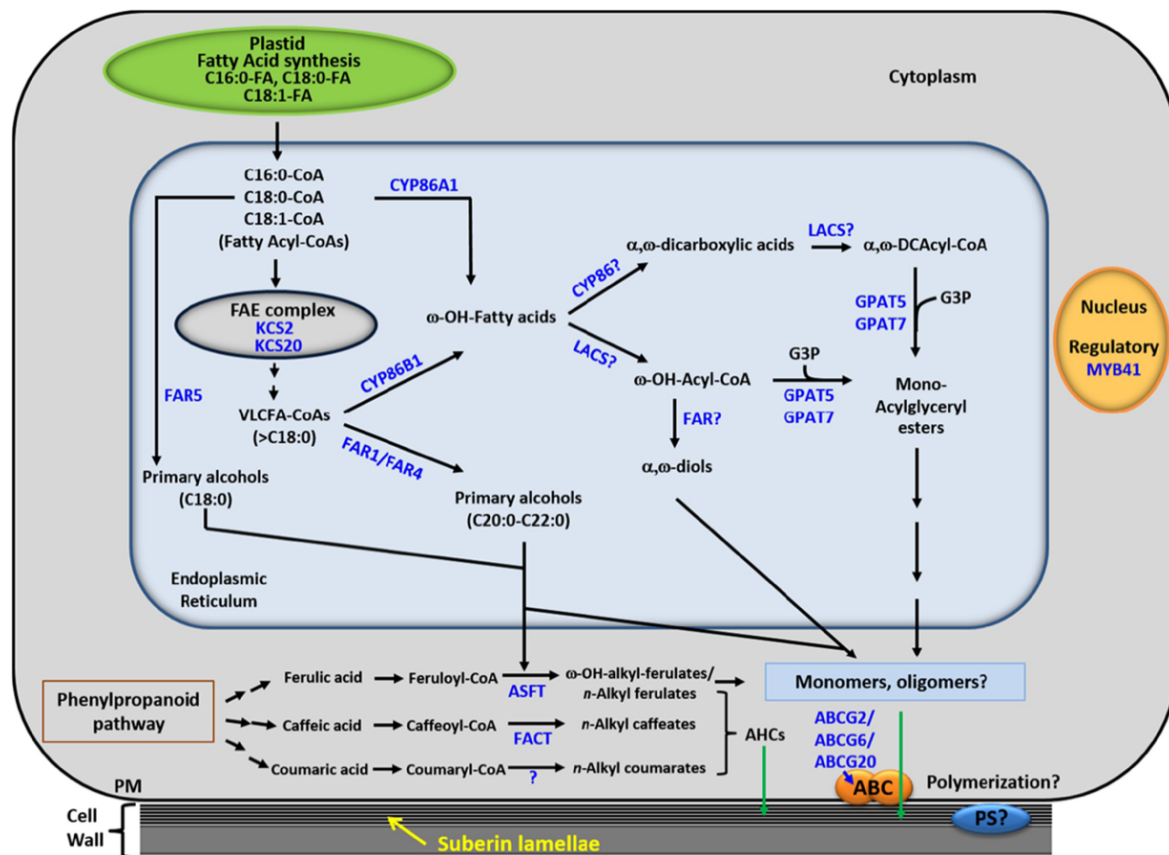


Figure 10: Suberin biosynthetic pathway. Picture is taken from [132].

### 1.3.3 AtABCG1, a potential suberin transporter?

To date, several half-size ABCG transporters across different plant species have been shown to be involved in suberin barrier formation [113, 131, 153, 154]. For instance, ABCG5 from *Oryza sativa* (*O. sativa*) has been proposed to transport ABA within guard cells, as well as very-long-chain fatty acids ( $\geq C_{28}$ ) and diacids ( $C_{16}$ ) of root suberin monomers [154, 155]. In *Arabidopsis*, AtABCG2, AtABCG6 and AtABCG20 are assumed to be involved in suberin formation, since a triple mutant plant exhibited a reduced suberin content in the root endodermis and in the seed coats. [113, 131] (Figure 11). The transporters are suspected to transport fatty acids or fatty alcohols, as an *abcg2-1 abcg6-1 abcg20-1* mutant plant contained decreased amounts of  $C_{20}$  and  $C_{22}$  fatty acids,  $C_{22}$  fatty alcohol, and  $C_{18:1}$   $\omega$ -hydroxy fatty alcohols in the root suberin. Similarly, root suberin analysis of a transgenic *AtABCG11* silenced line (*dso-*

4) revealed a 2-fold less presence of C<sub>20</sub> fatty acids, C<sub>18</sub> fatty alcohols, and C<sub>16</sub> and C<sub>18</sub> ω-OH fatty acids. However, Panikashvili *et al.* proposed that the observed effects could be the result of competition for common cutin and suberin fatty acid precursors, since AtABCG11 was already proposed to be a cutin transporter [121, 124]. Finally, ABCG1 from *Solanum tuberosum* (*S. tuberosum*) was reported to be involved in suberin precursor transport within the potato tuber. StABCG1-RNAi plants contained decreased levels of the majorly present aliphatic monomers C<sub>18:1</sub> ω-hydroxy and C<sub>18:1</sub> α, ω-dicarboxylic acids, as well as ω-hydroxy fatty acids, α, ω-dicarboxylic acids, fatty alcohols, fatty acids with a chain length of C<sub>24</sub> and longer and ferulic acid. By contrast, significantly higher amounts of saturated ω-hydroxy fatty acids, α, ω-dicarboxylic acids, and fatty acids of chain lengths of C<sub>16</sub> to C<sub>22</sub> were observed.

Notably, sequence comparison of StABCG1 with all AtABCGs, revealed that StABCG1 shares the highest similarity with AtABCG1 and AtABCG16 [153]. Both, AtABCG1 and AtABCG16 reside from the same phylogenetic clade as the potential suberin precursor transporter AtABCG2, AtABCG6 and AtABCG20. So far, *atabcg1 atabcg16* double mutant studies indicated potential roles in pollen wall formation and postmeiotic pollen development [112, 113] (Figure 11). Although all clade members displayed a spatial expression in anthers and or maturing pollen, developing seeds, vegetative shoots and roots, are studies on the suberin composition of *atabcg1* or *atabcg16* mutants are lacking [31, 113]. Furthermore, Yim *et al.* assumed due to the current knowledge on pollen wall composition, that AtABCG1 and AtABCG16 might transport lipidic and phenolic compounds [112]. Since suberin consists of similar compounds is a contribution of AtABCG1 and/or AtABCG16 to suberin barrier formation conceivable. In consistence with that, direct transport assays with heterologous in yeast expressed AtABCG16 revealed also a potential role in transport of jasmonic acid, a lipid-derived plant hormone. Similar assays are so far missing for AtABCG1, despite direct transport assays are important for unambiguous substrate identification and exposure of physiological roles. In order to further elucidate the suberin formation process in *Arabidopsis*, AtABCG1 was heterologously expressed in *Pichia pastoris* (*P. pastoris*) and characterized as shown in chapter I and III.

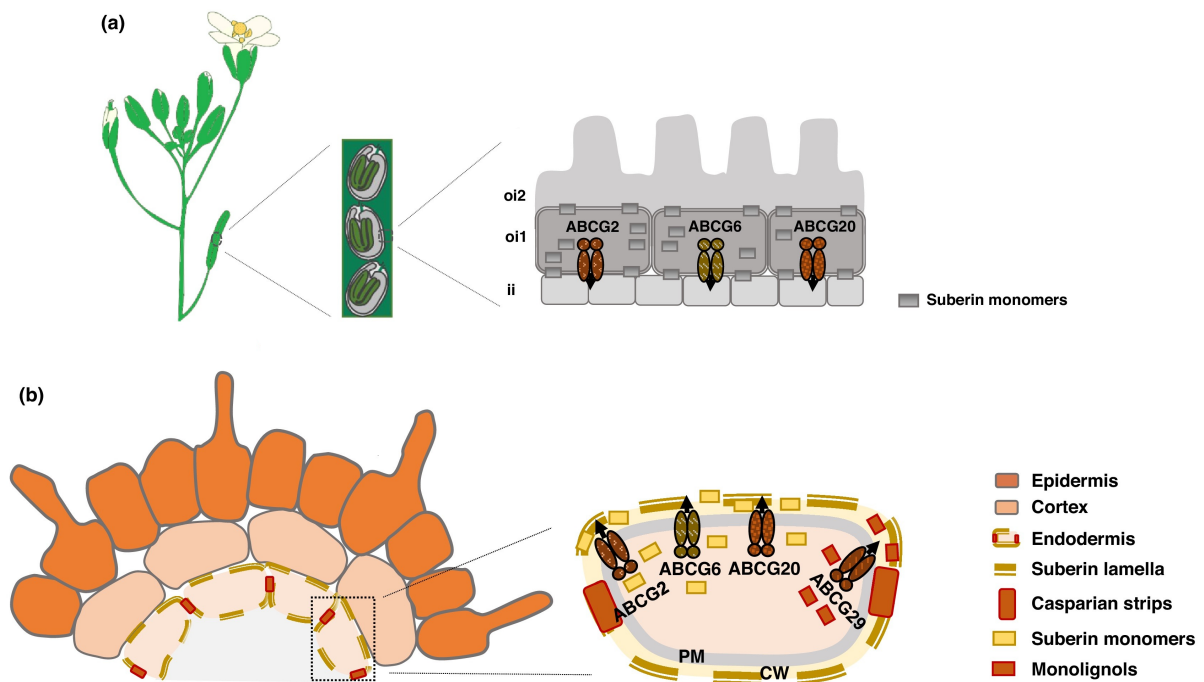


**Figure 11: Contribution of ABCG transporters in suberin formation in *A. thaliana* seeds and roots.** (a) AtABCG2, AtABCG6 and AtABCG20 are supposed to be expressed in the outer integument of the seed coat and transport suberin precursors during seed development. oi, outer integument; ii, inner integument. (b) AtABCG2, AtABCG6 and AtABCG20 transport suberin precursors from the root endodermis for the suberin lamellae formation. AtABCG29 transports monolignol for Casparian strip generation. PM, plasma membrane; CW, cell wall. Figure is taken and adapted from [90].

### 1.3.4 Plant defense related full-size ABCG transporter

Unlike half-size ABCG transporter are full-size ABCG transporters only found in plants and fungi [93]. Full-size ABCGs in plants are characterized in analog to their counterparts in human or yeast by their pleiotropic effects. Most of them are mainly expressed in roots and leaves, though only few in other tissues like flowers and stems. This emphasizes their role in transport of defense related substrates, as particularly roots and leaves are constantly exposed to various abiotic and biotic stress [156]. In concert, they have been found to be involved in various essential processes including pathogen defense [157-163], cutin precursor transport [35], resistance to heavy metals [164, 165], hormone transport [32-34, 97, 166] and transport of terpenoids [167-171]. Therefore, full-size ABCG transporter are essential for plant growth, fitness and productivity.

The *Arabidopsis* plant contains 15 full-size ABCG transporter, out of which so far for 9

transporters putative or rather unambiguous substrates were identified [91]. To the defense related transporters count for instance AtABCG34, which has been shown to be part of root exudation of organic acids as well as camalexin an *Arabidopsis* phytoalexin, that acts against necrotrophic fungi [31, 172]. AtABCG36 was shown to be involved in transport of multiple substrates and thereby enable pathogen response [163, 173-175], abiotic stress response [165, 176] and phytohormone transport [33]. Furthermore, AtABCG37 was not only found to be involved in phytohormone transport, but also in transport of coumarin from the roots [32, 34, 177-179]. Coumarin is involved in various processes such as defense against phytopathogen, abiotic stress and regulation of oxidative stress [180]. Phenolic compounds can serve as precursors of lignin synthesis, the main component of plant cell walls. AtABCG29 was shown by homologous as well as heterologous studies to mediate monolignol (p-coumaryl) transport [181]. AtABCG40 was reported to be involved besides heavy metal tolerance [182, 183] and phytohormone transport [40, 182], in sclareol transport, an antimicrobial and defense-related diterpene [164, 184]. Moreover, AtABCG32 and AtABCG31 were reported to be involved in cuticle and pollen wall formation, respectively [35, 114, 126]. The physiological role of ABCG30 in *A. thaliana* will be elucidated in the next chapter.

### 1.3.5 The full-size transporter AtABCG30

The *Arabidopsis* full-size transporter ABCG30 was reported to be involved in phytohormone and root exudation of phytochemicals [31, 40, 185].

Phytohormones allow the adaptation of plant growth and development to internal as well as external stimuli [186]. They consist of various molecule classes, such as abscisic acid (ABA), auxin, cytokinin, gibberellin (GA), jasmonic acid, ethylene, strigolactones or salicylic acid [187] and need to be transported in most cases to their site of action. Several full-size AtABCG transporters were found to be involved in phytohormone transport [33, 40, 182].

The phytohormone ABA is involved in environmental stress response and plant development [188]. For instance, seed germination is inhibited in dormant plants by ABA, while GAs promote the germination process [189-191]. In non-dormant plants are ABA and GA levels regulated by environmental factors, as for instance temperature or light quality [192-194]. Kang *et al.* showed that the ABA transport in *Arabidopsis* seeds is mediated by the cooperation of a subset of ABCG transporters, including



AtABCG30, AtABCG31, AtABCG40 and the half-size transporter AtABCG25 [40] (Figure 12). The *Arabidopsis* seeds are comprised of an embryo, which is surrounded by an endosperm layer and the testa (dead tissue layer) [195]. AtABCG25 and AtABCG31 were found to export ABA from the endosperm, while AtABCG30 and AtABCG40 import ABA into the embryo [40, 97] to prevent seed germination [40].

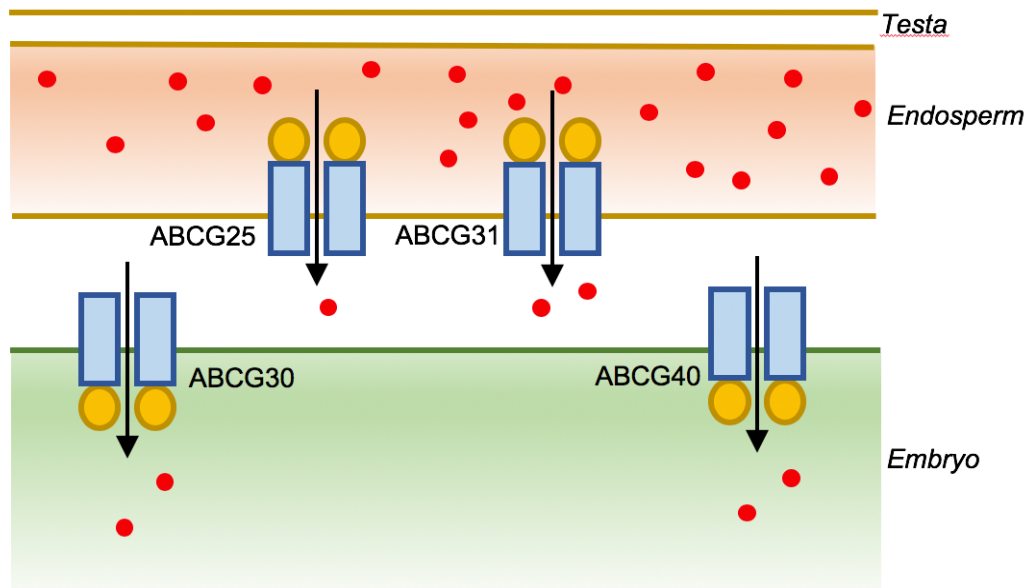


**Figure 12: Cooperation of *Arabidopsis* ABCG transporters to control seed germination by ABA transport.** AtABCG25 and AtABCG31 export ABA (red) from the endosperm, while AtABCG30 and AtABCG40 import ABA into the embryo. ABC transporters are depicted in blue (TMD) and orange (NBD). Figure is adapted from [40].

Root exudates consist of carbon-based compounds, including sugars, organic acids, complex polymers and secondary metabolites and can mediate the plant-microbiome interaction [196-198]. ABC transporters mainly contribute to the root exudation process by transporting metabolites, that are frequently found in root exudates, as for instance nucleotides [199, 200], peptides [201], fatty acids [36, 121, 202-204] or secondary metabolites [31, 166, 178, 201, 205-207]. Badri *et al.* reported that an *atabcg30* mutant exhibited significant changes in the root exudation profile and the microbial communities in the soil. Mutant plants exhibited increased abundance of phenolic compounds (benzoic acid, salicylic acid, syringic acid, tartaric acid, lactic acid,  $\alpha$ -linolenic acid, cyanidin, sinapoyl malate, Val, and indole 3-acetic acid), while the sugar

level (raffinose, glucose, fructose and mannitol) was decreased. In accordance, specific genes involved in biosynthesis and transport of secondary metabolites were upregulated [31, 185].

While ABA was unambiguously identified by flux assays as AtABCG30 substrate, are the identities of transported phytochemicals in the root not clear yet. The observed changes in the root exudation could reside from coregulation of metabolic pathways or other transporter systems [40, 185]. In order to get more insight into the role of AtABCG30 in root exudation and reveal the substrate identities are direct transport or functional assays essential.

## 2. Aims

In plants ATP-binding cassette transporters are particularly enlarged with for instance 130 ABC proteins in *Arabidopsis* [87]. Until now, only about one-third of them have been characterized, though plant ABC transporters are involved in several essential processes and contribute to plant fitness, growth and productivity [91]. Therefore, exposure of physiological roles and identity of transported substrates could contribute to better understand the plant physiology and to sustainable plant production.

Functional characterization of plant ABC transporters was so far complicated by difficulties in cloning, heterologous expression or inadequate amounts of purified protein. The first part of this thesis focuses on cloning and heterologous expression of selected AtABCG transporters. In addition, suitability of the methylotrophic yeast *Pichia pastoris* for heterologous expression of plant ABC transporters was evaluated. Successfully expressed AtABCG1 and AtABCG30 were further analyzed.

Several half-size transporters were reported to be involved in diffusion barrier formation. The half-size transporter AtABCG1 displays a spatial expression profile and has been shown to be involved in pollen wall formation and post-meiotic development. However, half-size AtABCG transporters that originate from the same phylogenetic clade were found to be involved in suberin formation [112, 113]. Studies on AtABCG1-involvement in suberin formation are lacking. In the second part of this thesis, solubilized and purified *P. pastoris* expressed AtABCG1 was biochemically characterized. After successful identification of AtABCG1 substrates by functional assays, T-DNA insertional *atabcg1* mutant plants were analyzed to verify the substrate identities.

The full-size transporter AtABCG30 was found to be involved in seed germination, by transporting the phytohormone ABA, as well as root exudation. Thereby ABA was inter alia identified by direct assays (flux experiments) as AtABCG30 substrate, whereas a changed metabolic profile and soil community in *atabcg30* mutant plants indicated an involvement in root exudation [40, 185]. Therefore, another aim of this thesis was to optimize heterologous expression and purification of AtABCG30 for subsequent biochemical studies. Moreover, identification of transported substrates from root exudates is often difficult. The final aim of this thesis was thus to establish a MS-based vesicular transport assay for plant ABC transporters.

### 3. Chapters

Chapter I	Heterologous expression of plant ABC transporters <b>Cloning and expression of selected ABC transporters from the <i>Arabidopsis thaliana</i> ABCG family in <i>Pichia pastoris</i></b> Plos One (submitted)
Chapter II	ABCG30 from <i>Arabidopsis thaliana</i> <b>Detergent screening and purification of AtABCG30 expressed in <i>Pichia pastoris</i></b> In preparation
Chapter III	ABCG1 from <i>Arabidopsis thaliana</i> <b>ABCG1 is involved in suberin barrier formation in <i>Arabidopsis thaliana</i></b> In preparation
Chapter IV	Vesicular transport assay <b>Proof-of-principle of a mass spectrometry-based vesicular transport assay for identification of plant ABCG transporter substrates</b> In preparation

### 3.1 Chapter I –Heterologous expression of plant ABC transporters

Title: Cloning and expression of selected ABC transporters from the *Arabidopsis thaliana* ABCG family in *Pichia pastoris*

Authors: Katharina Gräfe<sup>¶</sup>, Kalpana Shanmugarajah<sup>¶</sup>, Thomas Zobel, Stefanie Weidtkamp-Peters, Diana Kleinschrodt, Sander H. J. Smits and Lutz Schmitt

<sup>¶</sup> These authors contributed equally to this work.

Published in: Plos One (submitted)  
Impact factor 2.766

Own work: 40 %

Cloning and expression studies of plant ABC transporters  
Expression of AtABCG30 and AtABCG1 in *P. pastoris*  
Subcellular localization studies in *P. pastoris*  
Purification of AtABCG1 and ATPase Assay  
Writing of the manuscript

# **Cloning and expression of selected ABC transporters from the *Arabidopsis thaliana* ABCG family in *Pichia pastoris***

Katharina Gräfe<sup>1,2¶</sup>, Kalpana Shanmugarajah<sup>1,2¶</sup>, Thomas Zobel<sup>3#</sup>, Stefanie Weidtkamp-Peters<sup>3</sup>, Diana Kleinschrodt<sup>1,4</sup>, Sander H. J. Smits<sup>1</sup>, and Lutz Schmitt<sup>1,2\*</sup>

<sup>1</sup>Institute of Biochemistry, Heinrich Heine University, Düsseldorf, Germany

<sup>2</sup>Cluster of Excellence on Plant Sciences, Heinrich Heine University, Düsseldorf, Germany

<sup>3</sup>Center for Advanced Imaging, Heinrich Heine University, Düsseldorf, Germany

<sup>4</sup>Protein Production Facility, Heinrich Heine University, Düsseldorf, Germany

<sup>#</sup>Current address: Cells in Motion Interfaculty Centre, University of Münster, Münster, Germany

\* Corresponding author

lutz.schmitt@hhu.de

¶ These authors contributed equally to this work.

## Abstract

Phytohormones play a major role in plant growth and development. They are in most cases not synthesized in their target location and hence need to be transported to the site of action, by for instance ATP-binding cassette transporters. Within the ATP-binding cassette transporter family, Pleiotropic Drug Resistance transporters are known to be involved in phytohormone transport. Interestingly, PDRs are only present in plants and fungi. In contrast to fungi, biochemical studies of plant PDRs are hardly available and one major reason is that suitable overexpression systems are rarely established. In this study, we evaluate the expression system *Pichia pastoris* for heterologous overexpression of *PDR* genes of the model plant *A. thaliana*. We successfully cloned and expressed the potential phytohormone transporters PDR2 and PDR8 in *P. pastoris*. Sucrose gradient centrifugation confirmed that the overexpressed proteins were correctly targeted to the plasma membrane of *P. pastoris* and initial functional studies exhibit ATPase activity for WBC1. However, difficulties in cloning and heterologous overexpression might be particular obstacles of the PDR family, since cloning and overexpression of *White Brown Complex 1*, a half-size transporter of the same ABCG subfamily with comparable domain organization, was more easily achieved. We present strategies and highlight critical factors to successfully clone plant *PDR* genes and their heterologous overexpression in *P. pastoris*.

# Introduction

Phytohormones (plant hormones) are signal molecules which enable plants to adapt growth and development to internal and external stimuli [1]. They comprise various molecule classes like abscisic acid (ABA), auxin, cytokinin, gibberellin, jasmonic acid, ethylene, strigolactones or salicylic acid [2]. In most cases the site of action is distinct from the site of production, which requires transport mechanisms across membranes. Many ATP-binding cassette (ABC) transporters, have been shown to be involved in hormone transport in plants [3-5].

ABC transporters are ubiquitous in all kingdoms of life and facilitate the transport of a large variety of substrates across membranes using ATP hydrolysis as energy source [6, 7]. They are composed of four core domains: two nucleotide-binding domains (NBDs) and two transmembrane domains (TMDs). NBDs comprise all the sequence motifs required for ATP hydrolysis, while the TMDs are composed of 4 to 10  $\alpha$ -helices and form the substrate translocation pathway across the lipid bilayer. These four domains can be either encoded on a single gene (full-size transporter), or one NBD and one TMD are fused on one gene (half-size transporter), or all the domains are encoded by separate genes [8-12].

Compared to other organism, the ABC protein family is significantly enlarged in plants with about 130 members in *Arabidopsis thaliana* and *Oryza sativa* [11, 13, 14]. The ABC proteins are classified into eight subfamilies (ABCA – ABCG, ABCI) with ABCG subfamily being the largest [15] and showing a reverse domain orientation (NBD N-terminal to the TMD) compared to the other subfamilies. In *Arabidopsis*, the ABCG subfamily comprises 28 half-size transporters (White Brown Complex (WBC)) and 15 plant- and fungi-specific Pleiotropic Drug Resistance (PDR) full-size transporters [11]. Potential roles include heavy metal detoxification [16, 17], pathogen response [18-23] and formation of physical barriers [24-26].



Interestingly, members of the ABCG-subfamily and especially the full-size transporters were also shown to be involved in phytohormone transport [27-31]. The phytohormone ABA is involved in environmental stress response and plant development [32]. In Arabidopsis, the ABCG full-size transporters AtPDR2, AtPDR3, AtPDR12 and the half-size transporter AtWBC25 were reported to mediate ABA transport from the endosperm to the seeds [33]. It was postulated that AtPDR2 and AtPDR12 function as importers [30, 33], which is unusual for eukaryotic ABC transporters. Cytokinin and auxin regulate the overall growth and development in plants [2]. AtWBC14 was shown to be essential for cytokinin root-to-shoot translocation [34, 35], while AtPDR8 and AtPDR9 mediate the transport of the auxin precursor indole-3-butyric acid. It was hypothesized that the transporters function in hormone homeostasis [27, 29]. Another phytohormone potentially transported by a PDR is strigolactone. In *Petunia hybrida* PhPDR1 mediates the export of strigolactone, which regulates the axillary branching and the cultivation of arbuscular mycorrhizae [31]. However, identification of transported substrates by reverse genetics and knock-out analysis in plants is complicated since most *PDR* mutants exhibit pleiotropic phenotypes. For instance, AtPDR8 confers, besides a potential role in indole-3-butyric acid transport, resistance to heavy metals as well as salt and drought stress [16, 36]. In addition to that, Lu *et al.* reported that AtPDR8 transports a product of the PENETRATION 2 myrosinase pathway and contributes thereby to pathogen defense [37]. Likewise, AtPDR2 was, apart from ABA transport, reported to be involved in root exudation of secondary metabolites and thereby shape the rhizosphere microbiome [38].

Based on these studies, it is often difficult to conclusively demonstrate whether a single or various substrates are transported. Furthermore, the new emerging role of ABC transporters in plants as importers requires clarification about the transport mechanisms. However, biochemical studies, helping to better understand the proteins and the transport process are rather limited. One reason is the necessity for purified protein in adequate quantities for biochemical and/or structural studies. Hence, it is imperative to have a suitable overexpression

system that provides sufficient amounts of the protein in reasonable time. This is still a main issue concerning eukaryotic membrane proteins. Heterologous overexpression of membrane proteins is often challenging due to the size and hydrophobic nature of membrane proteins, toxicity of the protein to the host, misfolding, localization within another then the plasma membrane or lack of the proper post-translational modification(s) [19, 39-41]. Other studies also demonstrated that not only expression, but also cloning of membrane proteins, especially ABC transporters, may cause difficulties because the sequences are unstable in *Escherichia coli* [19, 42-46]. Despite these challenges, heterologous overexpression is for some subsequent applications indispensable. Homologous expression has the advantage that the protein is in its native environment, including the lipid environment, proper post-translational modification(s) and correct subcellular localization. Plant expression systems, however, often exhibit slow growth and low expression yields of the desired protein, which is unfavorable for *in vitro* studies. Heterologous expression systems, like bacterial or yeast based systems, in contrast have the advantage of fast protein production with higher yields as well as established initial purification protocols [41]. For heterologous expression of eukaryotic membrane proteins eukaryotic expression systems are in many cases more suitable over bacterial systems regarding toxicity to the host cell, posttranslational modifications, codon usage and proper folding [39, 47-51]. Insect cell as well as plant cell based systems were successfully used for the expression of several plant membrane proteins [52-54], although their major drawbacks are time consumption and/or costs and sophisticated handling. Compared to that, yeast expression systems are a good alternative, they exhibit a eukaryotic protein processing machinery and thereby combine the advantages of both prokaryotic as well as eukaryotic systems [55]. The bakers yeast *Saccharomyces cerevisiae* is an often-used system for heterologous overexpression of eukaryotic membrane proteins [56-59]. Recently, various protein structures of membrane proteins were determined in which the yeast expression system *Pichia pastoris* (reclassified as *Komagataella pastoris*) was used for heterologous expression of membrane

proteins [55], indicating its ability to produce correctly folded and processed proteins in substantial amounts. Furthermore, the same system was used to express 25 human ABC transporters [60]. Coherent major advantages are the ability (1) to grow to very high biomass concentrations, which are (2) accomplished in a reasonable time, (3) the possibility to use bioreactors, which allow control about the fermentation process by monitoring cultivation parameters, (4) the methylotrophic lifestyle, including the very strong and tightly regulated AOX1 promoter [61] and (5) its positive record in expression of affinity-tagged membrane proteins for subsequent purification and biochemical applications [60, 62, 63].

Members of the PDR family were expressed in eukaryotic systems [27, 33, 64], however, other studies also demonstrated that expression of PDRs is not always easily achieved. For example *AtABCG37/PDR9* did not localize to the correct membranes when expressed in *S. cerevisiae*. It was subsequently expressed in HeLa cells and in *Schizosaccharomyces pombe* [27]. *Nicotiana plumbaginifolia* PDR5 could neither be expressed in *S. cerevisiae* nor in *S. pombe* [65]. Expression of *NtPDR1* in the heterologous system *S. cerevisiae* was weak and unstable and the protein was not correctly localized. It was finally expressed in the homologous system. For *N. plumbaginifolia* PDR1, even cloning was not successful [19].

Here, we demonstrate the successful heterologous overexpression of *AtABCG30/PDR2*, *AtABCG36/PDR8* and the half-size transporter *AtABCG1/WBC1* using the expression system *P. pastoris*. The accomplishment of cloning and expression of large plant membrane proteins with high numbers of transmembrane helices is not always easily achieved. As described above, problems are consistently occurring, but detailed reports how to realize cloning and expression are still rare. In this study, we evaluate the expression system *P. pastoris* for heterologous expression of plant ABC transporters belonging to the PDR subfamily and employed *P. pastoris* as a host for this protein family.

## Materials and methods

### Accession numbers and cDNA

Sequence data in this article can be found in The Arabidopsis Information Resource (TAIR) database under accession numbers AT4G15230 (*AtABCG30/PDR2*), AT2G26910 (*AtABCG32/PDR4*), AT2G37280 (*AtABCG33/PDR5*), AT2G36380 (*AtABCG34/PDR6*), AT1G15210 (*AtABCG35/PDR7*), AT1G59870 (*AtABCG36/PDR8*), and AT2G39350 (WBC1) [66]. The copy DNA (cDNA) of *A. thaliana* ecotype Columbia-0 was kindly provided by Prof. Andreas Weber, Institute for Plant Biochemistry and Prof. Peter Westhoff, Institute of Developmental and Molecular Biology of Plants, Heinrich Heine University Düsseldorf.

### Growth conditions and strains

*E. coli* strains were grown on LB medium (0.5 % (w/v) yeast extract, 1 % tryptone (w/v), 1 % NaCl, 1.5 % (w/v) agar for plates) supplemented with zeocin (25 µg/ml), kanamycin (50 µg/ml) or ampicillin (100 µg/ml), depending on the resistance gene encoded on the plasmid used for transformation, and incubated at 37 °C. Liquid cultures were shaken at 180 rpm. The *E. coli* strains DH5α (Thermo Fisher Scientific), XL1-Blue, XL10-Gold, SURE 2 (all from Agilent Technologies) NEB Turbo (New England Biolabs, NEB) and CopyCutter EPI400 (epicentre) were used in this work. *P. pastoris* strain X33 (Invitrogen) and *S. cerevisiae* strain YPH500 [67] were grown on yeast peptone dextrose (YPD) medium (1 % yeast extract (w/v), 2 % tryptone (w/v), 2 % glucose (w/v), 2 % (w/v) agar for plates) at 30 °C. *P. pastoris* liquid cultures were grown in minimal glycerol medium (1.34 % yeast nitrogen base (w/v), 1 % glycerol (w/v), 4 x 10<sup>-5</sup> % (w/v) biotin) at 30 °C and 200 rpm. The buffered glycerol complex medium was composed of 100 mM potassium phosphate, 1 % (w/v) yeast extract, 2 % (w/v) peptone, 1.34 % yeast nitrogen base, 4 x 10<sup>-5</sup> % (w/v) biotin, and 1 % glycerol (v/v). For

induction of protein expression, glycerol was substituted by 0.5 % (v/v) methanol in minimal as well as in complex media.

## **Primer design and polymerase chain reaction**

The Clone Manager Suite (Sci-ED Software) was used for primer design. If required for cloning, overhangs were fused to the primers adding, for example, restriction sites to the sequence. All oligonucleotides were synthesized by MWG Eurofins. The polymerase chain reaction (PCR) was performed in a Biometra TGradient cycler using standard protocols. The optimal annealing temperatures were determined by temperature screening. All PCR products were extracted from agarose gels (Gel purification kit, Macherey-Nagel). DNA was sequenced by GATC Biotech.

## **Cloning**

The enzymes used for restriction digestion of the respective constructs were all obtained from NEB. T4 DNA ligase (NEB) was used for ligation of digested fragments. The reactions were set up according to the manufacturer's protocols except that ligation was performed overnight at 4 °C. In-Fusion cloning (Clontech) was performed according to the manufacturer's protocols with the modification that the reaction was incubated for 30 min and transformed bacteria was grown at 30 °C. The respective cloning reaction was transformed into *E. coli* XL-10Gold competent cells or into CopyCutter EPI400 cells with heat shock using standard protocols. CopyCutter EPI400 cells were grown overnight, the induction solution (epicentre) was added and cells were grown for another 4-5 h. Constructs were isolated with a plasmid isolation kit (Macharey and Nagel) and confirmed by sequencing.

Homologous recombination in *E. coli* was performed according to [68]. Briefly, electro competent Bw25113 cells were transformed with the helper plasmid pKD46. Positive clones were selected on ampicillin-containing agar plates and were made electro competent again. These cells were transformed with the expression vector and with PCR fragments that contained the *PDR* coding sequence flanked by sequences that were homologous to the expression vector. Positive clones were selected on plates containing the respective antibiotic. For removing pKD46 plasmid, cells were incubated at 43 °C. Success of transformation was confirmed by colony PCR. Homologous recombination in *S. cerevisiae* was performed similarly as described in Schiestl *et al.* (1989) . Briefly, a 3 ml YPH500 overnight culture was harvested (5,000 x g, 1 min) and the following was added to the pellet: 10 µL carrier DNA (Clontech), 500 ng insert, 100 ng linearized expression vector, 500 µL LP-mix (40 % polyethylene glycol 4000, 100 mM lithium acetate, 10 mM Tris-HCl pH 7.5 1 mM ethylenediaminetetraacetic acid (EDTA)), and 55 µL dimethyl sulfoxide. The mixture was incubated at 25 °C for 30 min followed by a heat shock at 42 °C for 15 min. 500 µL TE-buffer pH 7.5 were added and the cells were pelleted (5,000 x g, 1 min). The cells were washed with 1 ml TE-buffer (10,000 x g, 30 sec.), re-suspended in 500 µL YPD medium and regenerated for 1 h at 30 °C, 180 rpm. The culture was plated on SC minus uracil medium and incubated at 30 °C until colonies formed (2-3 days).

## **Transformation of *P. pastoris***

The expression vectors were transformed into *P. pastoris* according to the guidelines of Invitrogen. Briefly, 20 µg of the respective plasmids were linearized with *MssI* (Thermo Fisher Scientific) and transformed into 80 µL electro-competent *P. pastoris* cells. Clones were selected on YPD-agar supplemented with 500 µg/ml zeocin. Single clones were re-stroked on separate YPD plates.

## Colony PCR

One transformed *P. pastoris* colony was mixed with 25  $\mu\text{L}$  water and 5  $\mu\text{L}$  lysing enzyme solution (10 mg/ml lysing enzymes (Sigma Aldrich) in 100 mM  $\text{Na}_3\text{PO}_4$  pH 7.4, 1 mM dithiothreitol) and incubated at 30 °C for 30 min. The mix was flash-frozen in liquid nitrogen twice. For the PCR reaction, 3  $\mu\text{L}$  of the mix were added to the PCR-mix. The PCR was performed using standard protocols and the products were analyzed by agarose gel electrophoresis.

## Expression screening of transformed *P. pastoris* clones

Expression screenings were performed similarly as described in Ellinger *et al.* (2013) . 50 ml minimal glycerol medium was inoculated with  $\frac{1}{4}$  fully grown plate and shaken at 220 rpm and 30 °C for 24 h. Expression was induced by changing to minimal methanol medium. After another 24 h, 10 ml of cells were harvested by centrifugation (3,000 x g, 10 min, 4 °C) and re-suspended in 4 ml ice-cold extraction buffer (50 mM Tris-HCL pH 7.5, 200 mM NaCl, 330 mM sucrose, 1 mM EDTA, 1 mM ethylene glycol-bis( $\beta$ -aminoethyl ether)-N,N,N',N'-tetraacetic acid). The cells were centrifuged again and re-suspended in 0.5 ml extraction buffer. Zirconia beads (Roth) according to  $\frac{1}{3}$  of the total volume were added. Cells were disrupted by vortexing 6 times for 1 min and chilling on ice between the disruption cycles. Cell debris was removed by centrifugation (12,000 x g, 5 min, 4 °C) and  $\text{MgCl}_2$  was added to the supernatant to a final concentration of 10 mM. After incubation for 15 min on ice, the membranes were pelleted by centrifugation (90 min at 20,000 x g, 4 °C). The supernatant was removed and the membranes were re-suspended in extraction buffer. Expression was analyzed by SDS-PAGE and Western Blotting.

## **Fermentation**

Cells were fermented in a 15 L table-top glass fermenter (Applikon Biotechnology) according to the Invitrogen Pichia Fermentation Process Guidelines. Cells were grown overnight in 1 L minimal glycerol medium and used to inoculate 6 L basal salt medium. The fermentation was performed at 30 °C and aeration was kept larger than 20 % oxygen saturation. After a glycerol fed-batch of 50 % glycerol for 5 h, protein expression was induced by addition of methanol (3.6 ml/h/L of culture). After 48 h, cells were harvested by centrifugation (5,000 x g, 10 min, 4 °C), frozen in liquid nitrogen and stored at -80 °C for subsequent use.

## **Isolation of crude membrane vesicles from *P. pastoris***

100 g of wet cells of *P. pastoris* expressing PDR8, PDR2, WBC1 or MDR3 were thawed on ice and re-suspended with extraction buffer (50 mM Tris-HCL pH 7.5, 200 mM NaCl, 330 mM sucrose, 1 mM EDTA, 1 mM ethylene glycol-bis(β-aminoethyl ether)-N,N,N',N'-tetraacetic acid, supplemented with protease inhibitor cocktail (Roche)) to a final concentration of 0.5 g cells/ml. The cells were passed two times through a pre-cooled TS Series Cell Disruptor (Constant System) at 2.5 kbar. The disrupted cells were centrifuged twice (15,000 x g, 30 min, 4 °C). Subsequently, the membranes were centrifuged for 1 h at 125,000 x g, 4 °C. The membranes were re-suspended in buffer A (50 mM Tris-HCl pH 8, 150 mM NaCl, 15 % glycerol), frozen in liquid nitrogen and stored at -80 °C.

## **Isolation of crude membranes from *S. cerevisiae***

*S. cerevisiae* cells were grown in YPD medium at 30 °C. When the OD had reached 1.5 the nitrogen source was replenished by addition of 10 % of 5 x YP (50 g/L yeast extract;



100 g/L tryptone/peptone). Cells were harvested at an OD of approximately 3.5. The isolation of crude membranes was adapted to Ernst *et al.* (2008) and Kolaczkowski *et al.* (1996) . All steps were performed on ice or in cold rooms. Centrifuges were pre-cooled to 4 °C. Briefly, 30 g wet cells were resuspended in extraction buffer supplemented with protease inhibitor cocktail (Roche). The cells were disrupted 5 times for 1 min in a bead mill homogenizer (BioSpec) and incubated on ice between the disruptions steps. Unbroken cells were removed by 3 centrifugation steps (1,000 x g, 2 x 5 min; 3,000 x g, 5 min). Subsequently, the supernatant was centrifuged for 1 h at 21,000 x g. The resulting pellet was re-suspended in 5 ml buffer A, frozen in liquid nitrogen and stored at -80 °C.

## **Subcellular fractionation of crude membranes**

To determine the localization of PDR2, PDR8 and WBC1 in *P. pastoris*, crude membranes were diluted to 2 mg/ml in 1 ml ice-cold hypo-osmotic buffer (50 mM Tris-HCl pH 7.5, 200 mM sorbitol, 1 mM EDTA, protease inhibitor cocktail (Roche)) and layered on the top of a continuous sucrose gradient. MDR3 and PDR5 crude membranes were used as plasma membrane markers [44, 73]. The gradients were created using an ÄKTAprime plus pump system (GE Healthcare Life Sciences) generating a linear gradient ranging from 22 to 60 % sucrose in 10 mM Tris-HCl, pH 7.5, 1 mM EDTA, 800 mM sorbitol. The different membrane species were separated by ultracentrifugation (130,000 x g, 22 h, 4 °C) in a swing-out rotor. The gradients were split into 500 µL aliquots and analyzed by SDS-PAGE and Western Blotting.

## Cloning and expression of eGFP fusion proteins in *P. pastoris*

The Green Fluorescent Protein (eGFP) was fused to the N-terminus of PDR2, PDR8 and WBC1. Therefore, the *eGFP* coding sequence was cloned into the pSGP18 expression vector upstream of the respective genes. The *eGFP* gene was synthesized as a codon optimized version for *P. pastoris* and cloned into pSGP18-PDR2-Ntag and pSGP18-PDR8-Ntag by Genscript. In order to generate the construct for expression of free eGFP a stop codon was integrated downstream of the eGFP coding sequence by site directed mutagenesis PCR. All eGFP constructs were transformed into *P. pastoris* as described above. For expression, one fully-grown plate of the respective clone was used to inoculate 500 ml minimal glycerol medium in a 2 L baffled flask. After 24 h incubation the medium was exchanged to minimal methanol medium and thereby expression of the eGFP fusion proteins was induced. After 24 h, samples of the different cultures were taken and diluted to equal optical densities. Samples were immediately subjected to confocal fluorescence microscopy.

## Confocal fluorescence microscopy

20  $\mu$ L of *P. pastoris* culture expressing the respective eGFP fusion protein were mixed with 0.1 % (v/v) of the fluorescence stain SCRI Renaissance 2200 (SR2200) [74] and pipetted onto a poly-L-lysine coated slide (Thermo Scientific) and covered with a coverslip. Images were taken on a Zeiss LSM880 microscope with Airyscan and a 63 x NA 1.4 objective. For image acquisition the SR-Airyscan mode (pixel size of 40 nm) was used and the resulting images were automatically processed using the ZEN software. Figures were created using OERO.figure [75]. eGFP excitation was performed at 488 nm and SR2200 at 404 nm.

## **ATPase activity measurement of WBC1**

Heterologously expressed WBC1 and WBC1-EQ/HA was purified by calmodulin binding peptide (CBP) affinity chromatography as described elsewhere. Subsequently, ATPase activity of WBC1 was determined with the malachite green assay [76]. Reactions were performed in a total volume of 25  $\mu$ l in reaction buffer containing 10 mM  $\text{MgCl}_2$  and 1  $\mu$ g purified WBC1. The reaction was started after adding 5 mM ATP and stopped after 40 min at 25 °C by transfer into 175  $\mu$ l of 20 mM  $\text{H}_2\text{SO}_4$ . Afterwards, 50  $\mu$ l dye solution was added to quantify the amount of free phosphate spectroscopically at 595 nm. A  $\text{Na}_2\text{HPO}_4$  standard curve was used for the calibration of free phosphate.

## **Polyacrylamide gel electrophoresis and Western Blotting**

Protein expression was analyzed by SDS-PAGE using 7 % gels. Proteins were visualized by Colloidal Coomassie Brilliant Blue staining or Western Blotting. Western Blotting was performed using a tank blot system (BioRad) and proteins were detected with a primary anti-His antibody (Qiagen), anti-PDR5 antibody (Davids Biotechnologie) or a C219-antibody (Abcam) in combination with a secondary anti-mouse antibody or anti-rabbit antibody, respectively, labeled with horseradish peroxidase (Jackson Immuno Research). Protocols followed the manufacturer's instructions.

## Results

### Cloning of ABC transporters of the PDR family

For expression studies in *P. pastoris* the full-size ABC transporters *AtABCG30/PDR2*, *AtABCG32/PDR4*, *AtABCG33/PDR5*, *AtABCG34/PDR6*, *AtABCG35/PDR7* and *AtABCG36/PDR8* were chosen, all of which belong to the *A. thaliana* PDR family. These proteins are 157 to 165 kDa in size and contain 10 to 14 predicted transmembrane helices [66]. The coding sequences from *A. thaliana* cDNA were amplified in order to clone the genes into pJET1.2 for sequencing and subsequent cloning into the expression vector. Likely due to the large gene sizes (4.2 – 4.7 kbp), PCR protocols had to be optimized for each individual gene, including a screening for the correct annealing temperature combined with testing different polymerases and various buffer conditions. *PDR6* was successfully amplified using Phusion DNA polymerase (NEB), however concentrations of the resulting PCR product was so low that additional PCRs of the first product were performed. Alternatively, *PDR5* and *PDR8* were amplified with PrimeStar GXL DNA polymerase (Clontech). Despite various efforts, the complete coding sequences of *PDR2*, *PDR4* and *PDR7* could not be amplified in one step from the cDNA. Therefore, these three genes were amplified using GXL DNA polymerase in two fragments subsequently and cloned separately. All the resulting PCR products were blunt-end ligated into pJET1.2, thereafter amplified in *E. coli* and subsequently sequenced prior to subcloning into the expression vectors.

## Subcloning into pSGP18-2μ *P. pastoris* expression vector

In order to clone constructs for expression in *P. pastoris* different cloning strategies were employed. Since the complete coding sequences of PDR5, PDR6 and PDR8 were present as a single fragment, restriction digestion and ligation cloning was used for these genes. Using this, PDR6 and PDR8 were successfully cloned into pSGP18-2μ vector with a CBP tag followed by a hexa-histidine (His<sub>6</sub>) tag at the C-terminus of the protein sequence. However, in order to find the correct positive clone, at least 30 colonies were screened per transformation. In addition, the number of colonies on plates was very low, of which most contained just a fragment of the gene or were false positives. In the case of PDR5, restriction digestion and ligation cloning was unsuccessful.

Alternatively, In-Fusion cloning was used for the genes that existed in two separate fragments in pJET1.2, so that both parts are combined in the pSGP18-2μ expression vector. Using standard protocols, either none or very few colonies were obtained, which did not grow in liquid culture medium or did not contain the full plasmids as extensive parts of the gene were missing. The subsequent step was to either try alternative cloning strategies or optimize the In-Fusion cloning protocol.

Thus, homologous recombination was employed as an alternative cloning strategy. In addition to the 2μ ori present in the *P. pastoris expression* vector pSGP18 [44], which allows homologous recombination in *S. cerevisiae*, λ-Red homologous recombination in *E. coli* [68] was also used. Both homologous recombinations resulted mostly in the absence of positive clones. In the case of pSGP18-2μ-*PDR7*, some positive clones were however obtained. The isolated plasmids could not be re-transformed into *E. coli* despite testing different strains (DH5α, XL1-Blue, XL10-Gold NEB Turbo, SURE 2), incubation temperatures (37 °C, 30 °C,

RT) and media for regeneration. In addition, the yield of plasmid was low and not sufficient for direct transformation into *P. pastoris*. The  $\lambda$ -Red homologous recombination of the two fragments of *PDR4* in *E. coli* resulted in a few positive clones, however, inoculation of these clones in liquid cultures led to very poor or no cell growth at all. Since this approach was not promising, it was not used further for the remaining constructs. Instead, the In-Fusion protocol was optimized by performing gel-extraction of the DNA fragments, doubling the incubation time and changing the incubation temperature of transformed bacteria to 30 °C in comparison to the previously used temperature of 37 °C. Despite the above-mentioned strategies, numerous colonies had to be screened in order to observe positive clones. After these extensive efforts, the constructs PDR2 and PDR7 in pSGP18 were successfully obtained. However, it is worth mentioning here that, throughout the cloning process, frequent point mutations occurred in the sequences that were rectified by site-directed mutagenesis PCR.

## **Expression of PDR transporters in *P. pastoris***

The successfully cloned constructs pSGP18-2 $\mu$ -PDR8, pSGP18-PDR6, pSGP18-PDR2 and pSGP18-PDR7, respectively, were tested for small-scale expression in *P. pastoris* by selecting cells carrying the transformed genes from their respective antibiotic containing agar plates. The transformation was verified by colony PCR or sequencing the DNA obtained after plasmid isolation.

First, constructs were tested for expression using the standard protocols (Invitrogen). Since protein expression could not be detected, culture conditions were optimized. Buffered complex media were used instead of minimal media. Different incubation temperatures were tested ranging from 25 to 30 °C. Additional pre-cultures were made to obtain higher cell density before the main culture was set up. In order to increase the oxygen level in the flasks, the

cultivation volume of 50 ml was also reduced to 25 ml. Additionally, to obtain a better mRNA-ribosome interaction, the codon usage for arginine residues of the first 100 amino acids were optimized for expression in *P. pastoris*. This stabilizes the initiation complex and leads to an improved protein expression [77]. However, all these extensive efforts did not result in expression in *P. pastoris*.

## **Subcloning: change of tag position**

Since no expression was detected for C-terminally tagged PDR transporters in *P. pastoris*, the localization of the tag might be crucial for expression in *P. pastoris*. In order to check this hypothesis, N-terminally tagged constructs for expression in *P. pastoris* were generated. For this purpose, the affinity tags were synthetically produced containing a deca-Histidine (His<sub>10</sub>) and a CBP sequence, respectively (GeneArt Gene Synthesis, Invitrogen). Via In-Fusion reaction, the N-terminal tag sequence was added to the pSGP18 vector, which was previously amplified without the C-terminal tag. A codon-optimized sequence of PDR2 was synthetically produced and cloned into pSGP18-Ntag by Genscript, USA. Remarkably, during the cloning process, the company reported various instances of gene instability and re-occurring mutations. Apart from screening numerous clones, we like to stress that the problems were solved by using CopyCutter™ EPI400™ *E. coli* cells for the cloning process, which were consequently integrated into our subsequent cloning protocols. Using the above-mentioned strategy pSGP18-PDR8-Ntag was successfully obtained using In-Fusion cloning.

## **Expression of N-terminally tagged PDR transporters in *P. pastoris***

Initial expression trials of N-terminally tagged PDR2 and PDR8 in *P. pastoris* resulted in expression of truncated proteins as confirmed via Western Blot analysis (not shown).

Additional sequencing of the constructs revealed that during propagation in *E. coli*, a stop codon was created in both protein sequences, although the sequences of the constructs were correct after cloning. In another instance, the re-transformed *E. coli* clone lacked the start codon. Therefore, it is necessary to verify the sequence after every re-transformation step. After sequence rectification, the N-terminally tagged constructs pSGP18-PDR2 and pSGP18-PDR8 were successfully expressed in *P. pastoris* using standard protocols. Protein expression was obtained for all tested PDR8 clones while 2 out of 4 tested PDR2 clones showed expression as confirmed by Western Blot analysis (Figs 1 and 2). For the PDR2 and PDR8 constructs, the position of the tag was crucial for successful overexpression.

## **Cloning and expression of WBC1: half-size meaning half-problems?**

Bernaumat *et al* (2011) screened for expression of different membrane proteins using different expression systems. They reported that successful overexpression highly depends on the size of the protein and the number of transmembrane helices. This raised the possibility that vector construction and expression was only challenging and extremely time consuming for the full-size PDR transporters of the ABCG family. Therefore, we cloned *WBC1*, a half-size transporter of the ABCG family. In these transporters, only a single NBD and a single TMD are encoded on the gene and the protein has to dimerize to form a functional transporter. Subsequently, the protein, with a molecular weight of 82 kDa, is smaller than the full-size PDR transporters mentioned above. The gene was produced synthetically and codon-optimized for expression in *P. pastoris* (Invitrogen) and afterwards cloned via In-Fusion into pSGP18-Ntag vector. In addition, *WBC1* was also amplified from cDNA without any problems. The cloning of the half-size transporter *WBC1* was easily performed compared to the problematic cloning



of the PDRs, clearly indicating that the large gene size was one reason of the complicated cloning of the full-size transporters. Furthermore, none of the problems mentioned above were observed. As shown in Fig 3, small-scale expression studies of pSGP18-WBC1-Ntag resulted in three positive clones out of seven clones tested. The bands of approximately 80 and 160 kDa, respectively, clearly indicate that WBC1 was detected in the monomeric, as well as the dimeric state.

## **Subcellular localization of PDR2, PDR8 and WBC1**

In order to determine the localization of the two PDRs and WBC1 overexpressed in *P. pastoris* a continuous sucrose gradient centrifugation was performed. As shown by Western Blot analysis (Fig 4), the three proteins were detected in the gradient in the same fractions as the plasma membrane protein Pdr5 from *S. cerevisiae* [73] and as human MDR3, which was successfully expressed in *P. pastoris* before and localized to the plasma membrane [44, 73]. In addition to this, the fusion proteins eGFP-PDR2, eGFP-PDR8 and eGFP-WBC1 were expressed in *P. pastoris*. The additional eGFP tag at the N-terminus reduced the expression levels of all three proteins so that detection by immunoblotting was not possible (data not shown). However, confocal fluorescence microscopy could proof that the three fusion proteins were expressed (Fig 5). To mark the cell wall the *P. pastoris* cell walls were stained with the marker SCRI Renaissance 2200 (SR2200). The eGFP signal of the eGFP-WBC1 fusion protein clearly shows a ring-like signal that almost overlaps with the SR2200 signal indicating that the eGFP-WBC1 fusion protein localized to the plasma membrane (Fig 5, row A). However, such clear result was not obtained for the PDR fusion proteins. The eGFP signal was found for the majority of the cells in membrane structures inside the cells, while only in few cells PDR2 (Fig 5, row B) and PDR8 (Fig 5, row C) seem to localize in the plasma membrane with very faint eGFP-signals that formed rings around the cells. This indicates that in most cells the eGFP-

PDR fusion proteins were still located in endomembrane compartments. As a control free eGFP was expressed as well, which resided in the cytoplasm of *P. pastoris* cells. The GFP signal can be clearly distinguished from the SR2200 signal (Fig 5, row D). Compared to these results, *P. pastoris* cells without heterologously expressed protein did not fluoresce (data not shown). Taken together, WBC1 was the only transporter which was shown by sucrose gradient as well as confocal microscopy to be correctly targeted in the plasma membrane. Hence, WBC1 and an ATPase hydrolysis deficient mutant WBC1-EQ/HA were purified by calmodulin binding peptide affinity chromatography from *P. pastoris* crude membranes. Subsequent ATPase assays exhibited a basal activity  $13.26 \pm 0.32$  nmol/min per mg purified WBC1 (Fig 6).

## Discussion

Compared to other organisms, plants exhibit, with over 100 genes encoding for plant ABC proteins, a large variety of membrane transporters. We are focusing on the ABCG subfamily of which many have been analyzed regarding their function and expression [8, 11, 78-80]. However, identification of transported substrates is often complicated by their pleiotropic effects and reports on purified and biochemically analyzed proteins are still rare. We selected eight PDR transporters for heterologous expression. Until now, plant PDR transporters have been successfully expressed for example in yeast systems *S. cerevisiae*, *S.pombe* [81], insect cells [82] or in BY2 plant suspension cultures [65, 83].

Here, we evaluate the methylotrophic yeast *P. pastoris* as an alternative expression system for plant PDR transporters. As shown in previous studies, *P. pastoris* is a suitable host for heterologous expression of membrane proteins [44, 60, 84]. Thereby major advantages include tightly regulated promoters such as the alcohol oxidase (*AOX1*) promoter [85] and fermentable cells, which can reach high cell densities. Fed batch fermentation of successfully cloned plant PDR transporters lead up to 150 g wet cells per liter. Thus, even proteins with limited cell expression per single cell, can be produced in substantial amounts.

First cloning attempts were complicated for instance by difficulties in cDNA amplification or re-occurring mutations. To rule out that these difficulties derived from the used expression vector, additional vectors for expression in different host systems, including the yeast *S. cerevisiae* and bacterial systems *E. coli* and *L. lactis*, were selected. When we compared cloning results for the different expression vectors, cloning into *P. pastoris* vectors seemed more achievable (data only shown for *P. pastoris*). Hence it was decided to focus on optimization of cloning into *P. pastoris* vectors. So far, detailed reports about difficulties encountered while cloning of unstable or toxic DNA are rare. Therefore, critical factors which

affected the cloning and various solution approaches will be highlighted in the following section.

## Cloning of plant PDR transporters

One basic step in cloning is the amplification of the DNA. In our case, the amplification of the selected *PDR* genes from the cDNA of *A. thaliana* emerged as the first hurdle. Out of 8 *PDR* genes only *PDR8* and *PDR6* were fully amplified in one step, while the remaining genes could only be amplified in two fragments. The subsequent step included a two-step cloning. At first, the genes were cloned into a cloning vector and subsequently sequenced and amplified into the respective expression vectors. The first step of the cloning process often resulted in empty vectors or wrong inserts, although the size of the PCR product was always verified by gel electrophoresis. Hence, successful cloning of the gene into the cloning vector not only required the usual gene-specific optimization of the PCR reaction, but also screening of many clones. In the second step of cloning, the genes or gene fragments were cloned from the cloning vector into the vectors for heterologous expression. Different techniques, such as homologous recombination in *E. coli* and *S. cerevisiae* [68, 69], classical cloning via restriction sites or In-Fusion cloning were used for this purpose. Similar to the initially performed cloning reactions using cDNA, most reactions resulted either in empty vectors, mutations or significantly reduced number of clones. In addition to that, poor cell growth was observed after retransformation. One important aspect to consider here is that cloning depends on many factors, such as for example vector properties or gene toxicity. In the case of gene toxicity, a leaky promoter could be lethal for the cells [86] Every promoter has basal activity, which in combination with a high copy plasmid can lead to the accumulation of toxic proteins within the cell [87], resulting in poor cell growth and / or plasmid instability. Additionally, the cells could be more inclined to mutate the genes in order to circumvent gene toxicity. Hence, toxic genes can affect the cloning,

plasmid stability and protein expression.

In this study, cloning into the expression vector was mainly performed using *E. coli* and our attempts to express PDR8 heterologously in *E. coli* failed due to reoccurring stop codons resulting in truncated proteins (data not shown). After mutating these stop codons to the proper coding sequence, another stop codon appeared at a different position of the gene. It was also observed that after transformation of *E. coli*, the start codon of the *PDR* sequence was deleted, though sequencing results confirmed that the PCR products used in the transformation steps were correct. However, similar results had been obtained for NpPDR1 overexpression in *Nicotiana tabacum*. The cloning process had failed because the gene was always mutated during cloning in *E. coli* [19]. Thus, it is very likely that *E. coli* cannot propagate the construct of the full-size PDR genes due to toxicity. Poor cell growth could be ascribed to the fact that maintenance of a eukaryotic, and probably toxic gene, could require more metabolic energy. Thus, in order to counteract this phenomenon, various competent cell strains were used besides the standard strains such as XL1-Blue, XL10-Gold or DH5 $\alpha$ . Strains such as CopyCutter EPI400, NEB Turbo and SURE 2 were also used, which are specifically designed for cloning of unstable or toxic DNA. SURE 2 cells lack genes, which are involved in rearrangement and deletion of unstable DNA structures in *E. coli*, while CopyCutter cells are able to lower the number of many popular high-copy number plasmids. Since using low copy number plasmids can lower the basal activity, and thereby the expression of likely toxic gene products can be limited [88]. As seen from our results, CopyCutter cells seemed to be a better choice for this purpose. This indicates that the selected PDR genes were difficult to clone into *E. coli* due to toxicity. Furthermore, we experienced that cell cultivation at lower temperatures and prolonged incubation times improved very often the chances for positive clones.

After extensive screening of clones and optimization of every cloning step, it was finally possible to clone a number of genes successfully for expression. While the *P. pastoris*

expression constructs pSGP18-PDR2-Ctag, pSGP18-PDR6-Ctag, pSGP18-PDR7-Ctag and pSGP18-PDR8 with tag at both the terminus were cloned in our labs, pSGP18-PDR2-Ntag and pSGP18-WBC1-Ntag were synthesized. On the contrary, an attempt to clone the half-size transporter *WBC1* from cDNA worked straightforward. This clearly indicates that cloning of full-size PDR plant ABC transporters is quite challenging, and many factors such as gene size, cDNA quality, vector properties and gene toxicity for the host cell play an important role in the success of cloning.

## Heterologous expression of plant PDR transporters

To date, only a few *A. thaliana* PDR transporters such as PDR1, PDR2 [25], PDR3 [64], PDR6 [83] PDR9 [27] and PDR12 [33] have been heterologously expressed. Hence, it is from great importance to analyze if *PDR* gene expression can be complicated due to the nature of the gene, the expression host or tagging site.

As already described above, cloning of plant *PDR* genes can be quite difficult and time consuming. However, a subset of the intended expression constructs were successfully cloned in *P. pastoris* and expression studies were subsequently performed. Although most of the N-terminally tagged constructs (PDR2, PDR8, WBC1) were expressed, all C-terminally tagged proteins did not express. Additionally, the codon usage for arginine within the first 100 amino acids of the protein sequence was also optimised for PDR8, PDR7 and PDR2 (C-tagged constructs) to improve the stabilisation of the initiation complex as shown previously by Chen and Inouye [77]. Neither by using a His-antibody nor a CBP-antibody was it possible to detect any protein expression for the C-terminal tagged constructs. In accordance with that, it has been shown that the tag position can affect the yield of protein [89]. Thus the question arises if the protein was expressed at all or if the tag was inaccessible for immunoblot verification.

A possible reason for the lack of detectable expression could be the secondary structure of the mRNA. It has been previously shown that mutations within the ribosome binding site (rbs) lead to hairpin stability change and thereby affect the translation efficiency in *E. coli* [90]. Specific structures, such as stem-loops, can even lead to a blockage of the rbs, thus, inhibiting translation [91-93]. Notably there are studies indicating that positioning the tag at the amino-terminus can destabilise secondary structures, such as hairpin loops at the rbs, and hence, facilitate translation [94, 95]. In summary, our results indicate that codon optimization and N-terminal tagging lead to protein expression of plant ABC transporters of the PDR family.

## **Localization of heterologously expressed proteins in *P. pastoris***

For subsequent functional studies, the proper cellular localization of the overexpressed ABC transporters is of great importance in the heterologous system. *In planta* PDR8 is localized to the plasma membrane of leaf epidermal cells, as well as to the periphery of epidermal and lateral root cap cells [96, 97]. PDR2 was shown to be located in the plasma membrane of mesophyll protoplasts [33] and WBC1 localizes to the plasma membrane when transiently expressed in *N. benthamiana* [98].

In our first attempt for subcellular protein localization in *P. pastoris*, it was evident that WBC1, PDR2 and PDR8 localize in the plasma membrane. The proteins were mainly detected in the same fractions as the two membrane proteins that were known to localize to the plasma membrane, Pdr5 and MDR3 (Fig 4). Nevertheless, further faint protein bands were detected almost in the entire gradient and therefore we decided to verify the plasma membrane localization by confocal microscopy with eGFP-fusion proteins of PDR2, PDR8 and WBC1.

The fluorescence microscopy of the eGFP fusion proteins in *P. pastoris* cells showed a distinct plasma membrane localization for WBC1. In contrast to that, PDR2 and PDR8 were only partially located in the plasma membrane and mainly seen in other compartments (Fig 5). This could correlate with the protein size and / or the number of transmembrane helices. WBC1 is a half-size transporter and therefore it is possible that it passes the protein control faster than the full-size transporters. PDR2 and PDR8 get probably stucked during the protein processing and hence are not completely targeted to the plasma membrane. In support of this, the overall protein expression level of WBC1 in *P. pastoris* has been even after fermentation experiments (data not shown) higher in comparison to PDR2 and PDR8. Similar observations, have been previously made by Bernaudaut *et al.*, who postulated that increasing numbers of amino acids or transmembrane helices impede the heterologous expression of membrane proteins [39].

Another possible reason for that could be, that eGFP-fusion site can lead to mistargeting as already shown for the full-size human ABC transporter ABCC2 [99]. Drew et al. showed that C-terminal tagging facilitates the correct localization [100], while others reported mistargeting [99]. It is therefore generally recommended to test both C-terminal and N-terminal eGFP-fusion constructs. But in our case it is not applicable, because C-terminal His-tagging exhibited no protein expression and hence a C-terminal GFP-tag would lead most probably to the same result. Taken together, the plasma membrane localization of WBC1, PDR2 and PDR8 in *P. pastoris* was proven via sucrose gradient centrifugation, while a verification via confocal microscopy was only possible for WBC1. However, we believe that partial mistrafficking of PDR2 and PDR8 in the later part was likely a consequence of decreased protein expression due to size and GFP-fusioning. Subsequent functional studies with WBC1 exhibited a basal activity  $13.26 \pm 0.32$  nmol/min per mg purified WBC1. This indicates the suitability of *P. pastoris* as alternative expression system for plant half-size transporters. Similar studies need to be performed in order to analyze the functionality of *P. pastoris* expressed PDR2 and PDR8.



## Conclusions

Although cloning of plant PDR transporters can be quite laborious and seems unattainable, it is feasible provided the following points are taken into account. Our results clearly indicate that the amplification from cDNA is the first critical and crucial step. Therefore, it is important to localise the parts of the plants and conditions wherein the respective genes are highly expressed, and then subsequently obtain the cDNA.

In case the usual optimisation of the PCR does not work, the gene should be amplified in two or more fragments, although it complicates the subsequent cloning steps. Furthermore, it is worth spending more time on method optimisation and extensive screening for positive clones. In the present study, optimisation of In-Fusion and/or classical cloning lead to successful cloning of some of the selected *PDR* genes (*PDR2*, *PDR6*, *PDR7* and *PDR8*). Thus, spending more time on method optimisation and extensive screening for positive clones should facilitate cloning of any *PDR* gene into any vector. In addition, using CopyCutter cells or comparable strains that suppress plasmid replication as cloning host should be highly advantageous. Even after successful insertion of the *PDR* gene into the expression vector, frequent mutations in the coding sequence occurred, which led to insertion of stop codons or deletions of start codons. In such cases, it is worthwhile to perform a site-directed mutagenesis PCR as it is easier to re-mutate the sequence than restarting the entire cloning process.

The present study demonstrates the possible difficulties and the corresponding solutions to successful cloning of plant PDR genes. Beyond that, the methylotropic yeast *P. pastoris* is introduced and evaluated here for the first time as heterologous expression host for plant PDR transporters. It has the advantage that fermentation processes can lead to large biomasses of even poorly produced membrane proteins. As our results indicate, cloning and expression of

plant PDR transporters can emerge to be a delicate process. It is therefore advisable to keep the options broad with for example different fusion proteins and tagging sites.

We were able to express constructs of up to 170 kDa in sufficient amounts for subsequent biochemical studies. Hence, we introduce here *P. pastoris* as an alternative option for heterologous expression of plant ABC transporters. Initial functional studies with WBC1 showed basal activity, which can be analyzed for instance in future studies for substrate-stimulation. Moreover, until now *atpdr2* and *atpdr8* mutant studies exhibited pleiotropic effects in plants [16, 30, 33, 36-38]. As shown by sucrose gradient centrifugation PDR2 and PDR8 are correctly targeted in the plasma membrane of *P. pastoris*. Hence, this study provides a proper foundation for further functional studies, which could help to clarify the roles of this potential phytohormone transporters.

## Acknowledgments

We thank Iris Fey and Gereon Poschmann for technical assistance and Sakshi Khosa for valuable discussions. We are also thankful to Andreas Weber and Peter Westhoff (Heinrich Heine University Düsseldorf) for providing *A. thaliana* cDNA. We would like to thank Lauren Kotsull for critically reading the manuscript.

## References

1. Wolters H, Jurgens G. Survival of the flexible: hormonal growth control and adaptation in plant development. *Nat Rev Genet.* 2009;10(5):305-17. Epub 2009/04/11. doi: 10.1038/nrg2558. PubMed PMID: 19360022.
2. Santner A, Estelle M. Recent advances and emerging trends in plant hormone signalling. *Nature.* 2009;459(7250):1071-8. doi: 10.1038/nature08122. PubMed PMID: WOS:000267636700032.
3. Borghi L, Kang J, Ko D, Lee Y, Martinoia E. The role of ABCG-type ABC transporters in phytohormone transport. *Biochemical Society transactions.* 2015;43(5):924-30. Epub 2015/11/01. doi: 10.1042/BST20150106. PubMed PMID: 26517905; PubMed Central PMCID: PMC4613532.
4. Hellsberg E, Montanari F, Ecker GF. The ABC of Phytohormone Translocation. *Planta Med.* 2015;81(6):474-87. Epub 2015/04/24. doi: 10.1055/s-0035-1545880. PubMed PMID: 25905596.
5. Kang J, Lee Y, Sakakibara H, Martinoia E. Cytokinin Transporters: GO and STOP in Signaling. *Trends in plant science.* 2017;22(6):455-61. Epub 2017/04/05. doi: 10.1016/j.tplants.2017.03.003. PubMed PMID: 28372884.
6. Higgins CF, Hiles ID, Whalley K, Jamieson DJ. Nucleotide Binding by Membrane-Components of Bacterial Periplasmic Binding Protein-Dependent Transport-Systems. *Embo Journal.* 1985;4(4):1033-9. PubMed PMID: WOS:A1985AGX3400027.
7. Theodoulou FL. Plant ABC transporters. *Biochimica et biophysica acta.* 2000;1465(1-2):79-103. PubMed PMID: 10748248.
8. Rea PA. Plant ATP-binding cassette transporters. *Annual review of plant biology.* 2007;58:347-75. doi: 10.1146/annurev.arplant.57.032905.105406. PubMed PMID: 17263663.
9. Oswald C, Holland IB, Schmitt L. The motor domains of ABC-transporters. What can structures tell us? *Naunyn-Schmiedeberg's archives of pharmacology.* 2006;372(6):385-99. doi: 10.1007/s00210-005-0031-4. PubMed PMID: 16541253.
10. Schmitt L, Tampe R. Structure and mechanism of ABC transporters. *Curr Opin Struc Biol.* 2002;12(6):754-60. doi: Doi 10.1016/S0959-440x(02)00399-8. PubMed PMID: WOS:000179777100010.
11. Verrier PJ, Bird D, Burla B, Dassa E, Forestier C, Geisler M, et al. Plant ABC proteins--a unified nomenclature and updated inventory. *Trends in plant science.* 2008;13(4):151-9. doi: 10.1016/j.tplants.2008.02.001. PubMed PMID: 18299247.
12. Sanchez-Fernandez R, Davies TG, Coleman JO, Rea PA. The *Arabidopsis thaliana* ABC protein superfamily, a complete inventory. *The Journal of biological chemistry.* 2001;276(32):30231-44. doi: 10.1074/jbc.M103104200. PubMed PMID: 11346655.
13. Dean M, Rzhetsky A, Allikmets R. The human ATP-binding cassette (ABC) transporter superfamily. *Genome Res.* 2001;11(7):1156-66. doi: Doi 10.1101/Gr.Gr-1649r. PubMed PMID: WOS:000169650100004.
14. Sheps JA, Ralph S, Zhao ZY, Baillie DL, Ling V. The ABC transporter gene family of *Caenorhabditis elegans* has implications for the evolutionary dynamics of multidrug resistance in eukaryotes. *Genome Biol.* 2004;5(3). doi: Artn R15  
Doi 10.1186/Gb-2004-5-3-R15. PubMed PMID: WOS:000189345300009.
15. Kang J, Park J, Choi H, Burla B, Kretschmar T, Lee Y, et al. Plant ABC Transporters. *The Arabidopsis book / American Society of Plant Biologists.* 2011;9:e0153. doi: 10.1199/tab.0153. PubMed PMID: 22303277; PubMed Central PMCID: PMC3268509.
16. Kim DY, Bovet L, Maeshima M, Martinoia E, Lee Y. The ABC transporter AtPDR8 is a cadmium extrusion pump conferring heavy metal resistance. *The Plant journal : for cell and molecular biology.* 2007;50(2):207-18. Epub 2007/03/16. doi: 10.1111/j.1365-313X.2007.03044.x. PubMed PMID: 17355438.

17. Lee M, Lee K, Lee J, Noh EW, Lee Y. AtPDR12 contributes to lead resistance in *Arabidopsis*. *Plant physiology*. 2005;138(2):827-36. Epub 2005/06/01. doi: 10.1104/pp.104.058107. PubMed PMID: 15923333; PubMed Central PMCID: PMC150400.
18. Bultreys A, Trombik T, Drozak A, Boutry M. *Nicotiana plumbaginifolia* plants silenced for the ATP-binding cassette transporter gene NpPDR1 show increased susceptibility to a group of fungal and oomycete pathogens. *Molecular plant pathology*. 2009;10(5):651-63. Epub 2009/08/22. doi: 10.1111/j.1364-3703.2009.00562.x. PubMed PMID: 19694955.
19. Crouzet J, Roland J, Peeters E, Trombik T, Ducos E, Nader J, et al. NtPDR1, a plasma membrane ABC transporter from *Nicotiana tabacum*, is involved in diterpene transport. *Plant molecular biology*. 2013;82(1-2):181-92. doi: 10.1007/s11103-013-0053-0. PubMed PMID: 23564360.
20. Banasiak J, Biala W, Staszko A, Swarczewicz B, Kepczynska E, Figlerowicz M, et al. A *Medicago truncatula* ABC transporter belonging to subfamily G modulates the level of isoflavonoids. *Journal of experimental botany*. 2013;64(4):1005-15. Epub 2013/01/15. doi: 10.1093/jxb/ers380. PubMed PMID: 23314816.
21. Bienert MD, Siegmund SE, Drozak A, Trombik T, Bultreys A, Baldwin IT, et al. A pleiotropic drug resistance transporter in *Nicotiana tabacum* is involved in defense against the herbivore *Manduca sexta*. *The Plant journal : for cell and molecular biology*. 2012;72(5):745-57. doi: 10.1111/j.1365-3113.2012.05108.x. PubMed PMID: 22804955.
22. Shibata Y, Ojika M, Sugiyama A, Yazaki K, Jones DA, Kawakita K, et al. The Full-Size ABCG Transporters Nb-ABCG1 and Nb-ABCG2 Function in Pre- and Postinvasion Defense against *Phytophthora infestans* in *Nicotiana benthamiana*. *The Plant cell*. 2016;28(5):1163-81. doi: 10.1105/tpc.15.00721. PubMed PMID: 27102667; PubMed Central PMCID: PMC4904666.
23. Sasse J, Schlegel M, Borghi L, Ullrich F, Lee M, Liu GW, et al. *Petunia hybrida* PDR2 is involved in herbivore defense by controlling steroidal contents in trichomes. *Plant, cell & environment*. 2016;39(12):2725-39. Epub 2016/10/25. doi: 10.1111/pce.12828. PubMed PMID: 27628025.
24. Bessire M, Borel S, Fabre G, Carraca L, Efremova N, Yephremov A, et al. A member of the PLEIOTROPIC DRUG RESISTANCE family of ATP binding cassette transporters is required for the formation of a functional cuticle in *Arabidopsis*. *The Plant cell*. 2011;23(5):1958-70. Epub 2011/06/02. doi: 10.1105/tpc.111.083121. PubMed PMID: 21628525; PubMed Central PMCID: PMC3123938.
25. Alejandro S, Lee Y, Tohge T, Sudre D, Osorio S, Park J, et al. AtABCG29 is a monolignol transporter involved in lignin biosynthesis. *Current biology : CB*. 2012;22(13):1207-12. doi: 10.1016/j.cub.2012.04.064. PubMed PMID: 22704988.
26. Takeuchi M, Kegasa T, Watanabe A, Tamura M, Tsutsumi Y. Expression analysis of transporter genes for screening candidate monolignol transporters using *Arabidopsis thaliana* cell suspensions during tracheary element differentiation. *Journal of plant research*. 2018;131(2):297-305. doi: 10.1007/s10265-017-0979-4. PubMed PMID: WOS:000426284300010.
27. Ruzicka K, Strader LC, Bailly A, Yang H, Blakeslee J, Langowski L, et al. *Arabidopsis* PIS1 encodes the ABCG37 transporter of auxinic compounds including the auxin precursor indole-3-butyric acid. *Proceedings of the National Academy of Sciences of the United States of America*. 2010;107(23):10749-53. doi: 10.1073/pnas.1005878107. PubMed PMID: 20498067; PubMed Central PMCID: PMC2890796.
28. Ito H, Gray WM. A gain-of-function mutation in the *Arabidopsis* pleiotropic drug resistance transporter PDR9 confers resistance to auxinic herbicides. *Plant physiology*. 2006;142(1):63-74. Epub 2006/08/01. doi: 10.1104/pp.106.084533. PubMed PMID: 16877699; PubMed Central PMCID: PMC1557603.

29. Strader LC, Bartel B. The Arabidopsis PLEIOTROPIC DRUG RESISTANCE8/ABCG36 ATP binding cassette transporter modulates sensitivity to the auxin precursor indole-3-butyric acid. *The Plant cell*. 2009;21(7):1992-2007. doi: 10.1105/tpc.109.065821. PubMed PMID: 19648296; PubMed Central PMCID: PMC2729616.
30. Kang J, Hwang JU, Lee M, Kim YY, Assmann SM, Martinoia E, et al. PDR-type ABC transporter mediates cellular uptake of the phytohormone abscisic acid. *Proceedings of the National Academy of Sciences of the United States of America*. 2010;107(5):2355-60. doi: 10.1073/pnas.0909222107. PubMed PMID: 20133880; PubMed Central PMCID: PMC2836657.
31. Kretzschmar T, Kohlen W, Sasse J, Borghi L, Schlegel M, Bachelier JB, et al. A petunia ABC protein controls strigolactone-dependent symbiotic signalling and branching. *Nature*. 2012;483(7389):341-4. Epub 2012/03/09. doi: 10.1038/nature10873. PubMed PMID: 22398443.
32. Zeevart JAD, Creelman RA. Metabolism and Physiology of Absciscic-Acid. *Annu Rev Plant Phys*. 1988;39:439-73. doi: DOI 10.1146/annurev.pp.39.060188.002255. PubMed PMID: WOS:A1988N995300016.
33. Kang J, Yim S, Choi H, Kim A, Lee KP, Lopez-Molina L, et al. Absciscic acid transporters cooperate to control seed germination. *Nature communications*. 2015;6:8113. doi: 10.1038/ncomms9113. PubMed PMID: 26334616; PubMed Central PMCID: PMC4569717.
34. Zhang K, Novak O, Wei Z, Gou M, Zhang X, Yu Y, et al. Arabidopsis ABCG14 protein controls the acropetal translocation of root-synthesized cytokinins. *Nature communications*. 2014;5:3274. Epub 2014/02/12. doi: 10.1038/ncomms4274. PubMed PMID: 24513716.
35. Ko D, Kang J, Kiba T, Park J, Kojima M, Do J, et al. Arabidopsis ABCG14 is essential for the root-to-shoot translocation of cytokinin. *Proceedings of the National Academy of Sciences of the United States of America*. 2014;111(19):7150-5. Epub 2014/04/30. doi: 10.1073/pnas.1321519111. PubMed PMID: 24778257; PubMed Central PMCID: PMCPMC4024864.
36. Kim DY, Jin JY, Alejandro S, Martinoia E, Lee Y. Overexpression of AtABCG36 improves drought and salt stress resistance in Arabidopsis. *Physiol Plantarum*. 2010;139(2):170-80. doi: 10.1111/j.1399-3054.2010.01353.x. PubMed PMID: WOS:000277713200004.
37. Lu X, Dittgen J, Pislewska-Bednarek M, Molina A, Schneider B, Svatos A, et al. Mutant Allele-Specific Uncoupling of PENETRATION3 Functions Reveals Engagement of the ATP-Binding Cassette Transporter in Distinct Tryptophan Metabolic Pathways. *Plant physiology*. 2015;168(3):814-27. Epub 2015/05/30. doi: 10.1104/pp.15.00182. PubMed PMID: 26023163; PubMed Central PMCID: PMCPMC4741342.
38. Badri DV, Loyola-Vargas VM, Broeckling CD, De-la-Pena C, Jasinski M, Santelia D, et al. Altered profile of secondary metabolites in the root exudates of Arabidopsis ATP-binding cassette transporter mutants. *Plant physiology*. 2008;146(2):762-71. doi: 10.1104/pp.107.109587. PubMed PMID: 18065561; PubMed Central PMCID: PMC2245854.
39. Bernaudat F, Frelet-Barrand A, Pochon N, Dementin S, Hivin P, Boutigny S, et al. Heterologous Expression of Membrane Proteins: Choosing the Appropriate Host. *PloS one*. 2011;6(12). doi: ARTN e29191. 10.1371/journal.pone.0029191. PubMed PMID: WOS:000299113600065.
40. Gul N, Linares DM, Ho FY, Poolman B. Evolved *Escherichia coli* Strains for Amplified, Functional Expression of Membrane Proteins. *Journal of molecular biology*. 2014;426(1):136-49. doi: 10.1016/j.jmb.2013.09.009. PubMed PMID: WOS:000330681300015.

41. Lefevre F, Baijot A, Boutry M. Plant ABC transporters: time for biochemistry? Biochemical Society transactions. 2015;43:931-6. PubMed PMID: WOS:000363759700026.
42. Sami M, Yamashita H, Hirono T, Kadokura H, Kitamoto K, Yoda K, et al. Hop-resistant *Lactobacillus brevis* contains a novel plasmid harboring a multidrug resistance-like gene. J Ferment Bioeng. 1997;84(1):1-6. doi: Doi 10.1016/S0922-338x(97)82778-X. PubMed PMID: WOS:A1997XW47500001.
43. Stindt J, Ellinger P, Stross C, Keitel V, Haussinger D, Smits SHJ, et al. Heterologous Overexpression and Mutagenesis of the Human Bile Salt Export Pump (ABCB11) Using DREAM (Directed REcombination-Assisted Mutagenesis). PloS one. 2011;6(5). doi: ARTN e20562  
10.1371/journal.pone.0020562. PubMed PMID: WOS:000291097600098.
44. Ellinger P, Kluth M, Stindt J, Smits SH, Schmitt L. Detergent screening and purification of the human liver ABC transporters BSEP (ABCB11) and MDR3 (ABCB4) expressed in the yeast *Pichia pastoris*. PloS one. 2013;8(4):e60620. doi: 10.1371/journal.pone.0060620. PubMed PMID: 23593265; PubMed Central PMCID: PMC3617136.
45. Byrne JA, Strautnieks SS, Ihrke G, Pagani F, Knisely AS, Linton KJ, et al. Missense mutations and single nucleotide polymorphisms in ABCB11 impair bile salt export pump processing and function or disrupt pre-messenger RNA splicing. Hepatology. 2009;49(2):553-67. Epub 2008/12/23. doi: 10.1002/hep.22683. PubMed PMID: 19101985.
46. Noe J, Stieger B, Meier PJ. Functional expression of the canalicular bile salt export pump of human liver. Gastroenterology. 2002;123(5):1659-66. Epub 2002/10/31. PubMed PMID: 12404240.
47. Schmidt FR. Recombinant expression systems in the pharmaceutical industry. Appl Microbiol Biot. 2004;65(4):363-72. doi: 10.1007/s00253-004-1656-9. PubMed PMID: WOS:000224302000001.
48. Macauley-Patrick S, Fazenda ML, McNeil B, Harvey LM. Heterologous protein production using the *Pichia pastoris* expression system. Yeast. 2005;22(4):249-70. doi: 10.1002/yea.1208. PubMed PMID: WOS:000228218500001.
49. Georgiou G, Valax P. Expression of correctly folded proteins in *Escherichia coli*. Curr Opin Biotech. 1996;7(2):190-7. doi: Doi 10.1016/S0958-1669(96)80012-7. PubMed PMID: WOS:A1996UE90500012.
50. Grisshammer R. Understanding recombinant expression of membrane proteins. Curr Opin Biotech. 2006;17(4):337-40. doi: 10.1016/j.copbio.2006.06.001. PubMed PMID: WOS:000240023300002.
51. Midgett CR, Madden DR. Breaking the bottleneck: Eukaryotic membrane protein expression for high-resolution structural studies. J Struct Biol. 2007;160(3):265-74. doi: 10.1016/j.jsb.2007.07.001. PubMed PMID: WOS:000251473500002.
52. Kuromori T, Sugimoto E, Shinozaki K. Intertissue Signal Transfer of Abscissic Acid from Vascular Cells to Guard Cells. Plant physiology. 2014;164(4):1587-92. doi: 10.1104/pp.114.235556. PubMed PMID: WOS:000334342800005.
53. Biala W, Banasiak J, Jarzyniak K, Pawela A, Jasinski M. *Medicago truncatula* ABCG10 is a transporter of 4-coumarate and liquiritigenin in the medicarpin biosynthetic pathway. Journal of experimental botany. 2017;68(12):3231-41. doi: 10.1093/jxb/erx059. PubMed PMID: WOS:000407488500017.
54. Liepman AH, Wilkerson CG, Keegstra K. Expression of cellulose synthase-like (Csl) genes in insect cells reveals that CslA family members encode mannan synthases. Proceedings of the National Academy of Sciences of the United States of America. 2005;102(6):2221-6. doi: 10.1073/pnas.0409179102. PubMed PMID: WOS:000227072900075.

55. Byrne B. *Pichia pastoris* as an expression host for membrane protein structural biology. *Curr Opin Struc Biol*. 2015;32:9-17. doi: 10.1016/j.sbi.2015.01.005. PubMed PMID: WOS:000359032300004.
56. Demessie Z, Woolfson KN, Yu F, Qu Y, De Luca V. The ATP binding cassette transporter, VmTPT2/VmABCG1, is involved in export of the monoterpenoid indole alkaloid, vincamine in *Vinca minor* leaves. *Phytochemistry*. 2017;140:118-24. doi: 10.1016/j.phytochem.2017.04.019. PubMed PMID: WOS:000403993200011.
57. Lu YP, Li ZS, Rea PA. AtMRP1 gene of Arabidopsis encodes a glutathione S-conjugate pump: Isolation and functional definition of a plant ATP-binding cassette transporter gene. *Proceedings of the National Academy of Sciences of the United States of America*. 1997;94(15):8243-8. doi: DOI 10.1073/pnas.94.15.8243. PubMed PMID: WOS:A1997XM42800097.
58. Shitan N, Bazin I, Dan K, Obata K, Kigawa K, Ueda K, et al. Involvement of CjMDR1, a plant multidrug-resistance-type ATP-binding cassette protein, in alkaloid transport in *Coptis japonica*. *Proceedings of the National Academy of Sciences of the United States of America*. 2003;100(2):751-6. doi: 10.1073/pnas.0134257100. PubMed PMID: WOS:000180589000067.
59. Park J, Song WY, Ko D, Eom Y, Hansen TH, Schiller M, et al. The phytochelatin transporters AtABCC1 and AtABCC2 mediate tolerance to cadmium and mercury. *Plant Journal*. 2012;69(2):278-88. doi: 10.1111/j.1365-313X.2011.04789.x. PubMed PMID: WOS:000298874300008.
60. Chloupkova M, Pickert A, Lee JY, Souza S, Trinh YT, Connelly SM, et al. Expression of 25 human ABC transporters in the yeast *Pichia pastoris* and characterization of the purified ABCC3 ATPase activity. *Biochemistry*. 2007;46(27):7992-8003. doi: 10.1021/bi700020m. PubMed PMID: WOS:000247677700007.
61. Cereghino JL, Cregg JM. Heterologous protein expression in the methylotrophic yeast *Pichia pastoris*. *FEMS Microbiol Rev*. 2000;24(1):45-66. PubMed PMID: 10640598.
62. Haviv H, Cohen E, Lifshitz Y, Tal DM, Goldshleger R, Karlsh SJ. Stabilization of Na(+),K(+)-ATPase purified from *Pichia pastoris* membranes by specific interactions with lipids. *Biochemistry*. 2007;46(44):12855-67. doi: 10.1021/bi701248y. PubMed PMID: 17939686.
63. Cohen E, Goldshleger R, Shainskaya A, Tal DM, Ebel C, le Maire M, et al. Purification of Na<sup>+</sup>,K<sup>+</sup>-ATPase expressed in *Pichia pastoris* reveals an essential role of phospholipid-protein interactions. *Journal of Biological Chemistry*. 2005;280(17):16610-8. doi: 10.1074/jbc.M414290200. PubMed PMID: WOS:000228615500011.
64. Choi H, Ohyama K, Kim YY, Jin JY, Lee SB, Yamaoka Y, et al. The role of Arabidopsis ABCG9 and ABCG31 ATP binding cassette transporters in pollen fitness and the deposition of sterol glycosides on the pollen coat. *The Plant cell*. 2014;26(1):310-24. doi: 10.1105/tpc.113.118935. PubMed PMID: 24474628; PubMed Central PMCID: PMC3963578.
65. Toussaint F, Pierman B, Bertin A, Levy D, Boutry M. Purification and biochemical characterization of NpABCG5/NpPDR5, a plant pleiotropic drug resistance transporter expressed in *Nicotiana tabacum* BY-2 suspension cells. *The Biochemical journal*. 2017;474(10):1689-703. doi: 10.1042/BCJ20170108. PubMed PMID: 28298475.
66. Huala E, Dickerman AW, Garcia-Hernandez M, Weems D, Reiser L, LaFond F, et al. The Arabidopsis Information Resource (TAIR): a comprehensive database and web-based information retrieval, analysis, and visualization system for a model plant. *Nucleic acids research*. 2001;29(1):102-5. PubMed PMID: 11125061; PubMed Central PMCID: PMC29827.

67. Sikorski RS, Hieter P. A System of Shuttle Vectors and Yeast Host Strains Designed for Efficient Manipulation of DNA in *Saccharomyces cerevisiae*. *Genetics*. 1989;122(1):19-27. PubMed PMID: WOS:A1989U362600003.
68. Datsenko KA, Wanner BL. One-step inactivation of chromosomal genes in *Escherichia coli* K-12 using PCR products. *Proceedings of the National Academy of Sciences of the United States of America*. 2000;97(12):6640-5. doi: 10.1073/pnas.120163297. PubMed PMID: 10829079; PubMed Central PMCID: PMC18686.
69. Schiestl RH, Gietz RD. High-Efficiency Transformation of Intact Yeast-Cells Using Single Stranded Nucleic-Acids as a Carrier. *Current genetics*. 1989;16(5-6):339-46. doi: Doi 10.1007/Bf00340712. PubMed PMID: WOS:A1989CG90600004.
70. Reiser L, Berardini TZ, Li D, Muller R, Strait EM, Li Q, et al. Sustainable funding for biocuration: The Arabidopsis Information Resource (TAIR) as a case study of a subscription-based funding model. *Database : the journal of biological databases and curation*. 2016;2016. doi: 10.1093/database/baw018. PubMed PMID: 26989150; PubMed Central PMCID: PMC4795935.
71. Ernst R, Kueppers P, Klein CM, Schwarzmüller T, Kuchler K, Schmitt L. A mutation of the H-loop selectively affects rhodamine transport by the yeast multidrug ABC transporter Pdr5. *Proceedings of the National Academy of Sciences of the United States of America*. 2008;105(13):5069-74. doi: 10.1073/pnas.0800191105. PubMed PMID: 18356296; PubMed Central PMCID: PMC2278221.
72. Kolaczowski M, van der Rest M, Cybularz-Kolaczowska A, Soumilion JP, Konings WN, Goffeau A. Anticancer drugs, ionophoric peptides, and steroids as substrates of the yeast multidrug transporter Pdr5p. *The Journal of biological chemistry*. 1996;271(49):31543-8. PubMed PMID: 8940170.
73. Egner R, Mahe Y, Pandjaitan R, Kuchler K. Endocytosis and vacuolar degradation of the plasma membrane-localized Pdr5 ATP-binding cassette multidrug transporter in *Saccharomyces cerevisiae*. *Mol Cell Biol*. 1995;15(11):5879-87. PubMed PMID: 7565740; PubMed Central PMCID: PMCPMC230839.
74. Musielak TJ, Schenkel L, Kolb M, Henschen A, Bayer M. A simple and versatile cell wall staining protocol to study plant reproduction. *Plant Reprod*. 2015;28(3-4):161-9. Epub 2015/10/12. doi: 10.1007/s00497-015-0267-1. PubMed PMID: 26454832; PubMed Central PMCID: PMCPMC4623088.
75. Allan C, Burel JM, Moore J, Blackburn C, Linkert M, Loynton S, et al. OMERO: flexible, model-driven data management for experimental biology. *Nat Methods*. 2012;9(3):245-53. Epub 2012/03/01. doi: 10.1038/nmeth.1896. PubMed PMID: 22373911; PubMed Central PMCID: PMCPMC3437820.
76. Baykov AA, Evtushenko OA, Avaeva SM. A malachite green procedure for orthophosphate determination and its use in alkaline phosphatase-based enzyme immunoassay. *Analytical biochemistry*. 1988;171(2):266-70. Epub 1988/06/01. PubMed PMID: 3044186.
77. Chen GF, Inouye M. Suppression of the negative effect of minor arginine codons on gene expression; preferential usage of minor codons within the first 25 codons of the *Escherichia coli* genes. *Nucleic acids research*. 1990;18(6):1465-73. PubMed PMID: 2109307; PubMed Central PMCID: PMC330513.
78. Hwang JU, Song WY, Hong D, Ko D, Yamaoka Y, Jang S, et al. Plant ABC Transporters Enable Many Unique Aspects of a Terrestrial Plant's Lifestyle. *Molecular plant*. 2016;9(3):338-55. doi: 10.1016/j.molp.2016.02.003. PubMed PMID: 26902186.
79. Yazaki K, Shitan N, Sugiyama A, Takanashi K. Cell and molecular biology of ATP-binding cassette proteins in plants. *International review of cell and molecular biology*. 2009;276:263-99. doi: 10.1016/S1937-6448(09)76006-X. PubMed PMID: 19584015.



80. Kretschmar T, Burla B, Lee Y, Martinoia E, Nagy R. Functions of ABC transporters in plants. *Essays in biochemistry*. 2011;50(1):145-60. doi: 10.1042/bse0500145. PubMed PMID: 21967056.
81. Fu X, Shi P, He Q, Shen Q, Tang Y, Pan Q, et al. AaPDR3, a PDR Transporter 3, Is Involved in Sesquiterpene beta-Caryophyllene Transport in *Artemisia annua*. *Frontiers in plant science*. 2017;8:723. doi: 10.3389/fpls.2017.00723. PubMed PMID: 28533790; PubMed Central PMCID: PMC5420590.
82. Kuromori T, Miyaji T, Yabuuchi H, Shimizu H, Sugimoto E, Kamiya A, et al. ABC transporter AtABCG25 is involved in abscisic acid transport and responses. *Proceedings of the National Academy of Sciences of the United States of America*. 2010;107(5):2361-6. doi: 10.1073/pnas.0912516107. PubMed PMID: 20133881; PubMed Central PMCID: PMC2836683.
83. Khare D, Choi H, Huh SU, Bassin B, Kim J, Martinoia E, et al. Arabidopsis ABCG34 contributes to defense against necrotrophic pathogens by mediating the secretion of camalexin. *Proceedings of the National Academy of Sciences of the United States of America*. 2017;114(28):E5712-E20. doi: 10.1073/pnas.1702259114. PubMed PMID: 28652324; PubMed Central PMCID: PMC5514727.
84. Beaudet L, Urbatsch IL, Gros P. High-level expression of mouse Mdr3 P-glycoprotein in yeast *Pichia pastoris* and characterization of ATPase activity. *Method Enzymol*. 1998;292:397-413. PubMed PMID: WOS:000075571200029.
85. Tschopp JF, Brust PF, Cregg JM, Stillman CA, Gingeras TR. Expression of the lacZ gene from two methanol-regulated promoters in *Pichia pastoris*. *Nucleic acids research*. 1987;15(9):3859-76. PubMed PMID: 3108861; PubMed Central PMCID: PMC340787.
86. Ringquist S, Shinedling S, Barrick D, Green L, Binkley J, Stormo GD, et al. Translation initiation in *Escherichia coli*: sequences within the ribosome-binding site. *Molecular microbiology*. 1992;6(9):1219-29. Epub 1992/05/01. PubMed PMID: 1375310.
87. Hannig G, Makrides SC. Strategies for optimizing heterologous protein expression in *Escherichia coli*. *Trends in biotechnology*. 1998;16(2):54-60. Epub 1998/03/06. PubMed PMID: 9487731.
88. Terpe K. Overview of bacterial expression systems for heterologous protein production: from molecular and biochemical fundamentals to commercial systems. *Applied microbiology and biotechnology*. 2006;72(2):211-22. doi: 10.1007/s00253-006-0465-8. PubMed PMID: 16791589.
89. Sachdev D, Chirgwin JM. Order of fusions between bacterial and mammalian proteins can determine solubility in *Escherichia coli*. *Biochem Bioph Res Co*. 1998;244(3):933-7. doi: DOI 10.1006/bbrc.1998.8365. PubMed PMID: WOS:000072919100059.
90. de Smit MH, van Duin J. Secondary structure of the ribosome binding site determines translational efficiency: a quantitative analysis. *Proceedings of the National Academy of Sciences of the United States of America*. 1990;87(19):7668-72. PubMed PMID: 2217199; PubMed Central PMCID: PMC54809.
91. Ramesh V, De A, Nagaraja V. Engineering hyperexpression of bacteriophage Mu C protein by removal of secondary structure at the translation initiation region. *Protein engineering*. 1994;7(8):1053-7. PubMed PMID: 7809032.
92. Coleman J, Inouye M, Nakamura K. Mutations upstream of the ribosome-binding site affect translational efficiency. *Journal of molecular biology*. 1985;181(1):139-43. PubMed PMID: 3884820.
93. Griswold KE, Mahmood NA, Iverson BL, Georgiou G. Effects of codon usage versus putative 5'-mRNA structure on the expression of *Fusarium solani* cutinase in the *Escherichia coli* cytoplasm. *Protein expression and purification*. 2003;27(1):134-42. PubMed PMID: 12509995.

94. Busso D, Kim R, Kim SH. Expression of soluble recombinant proteins in a cell-free system using a 96-well format. *Journal of biochemical and biophysical methods*. 2003;55(3):233-40. PubMed PMID: 12706907.
95. Svensson J, Andersson C, Reseland JE, Lyngstadaas P, Bulow L. Histidine tag fusion increases expression levels of active recombinant amelogenin in *Escherichia coli*. *Protein expression and purification*. 2006;48(1):134-41. doi: 10.1016/j.pep.2006.01.005. PubMed PMID: WOS:000238459900019.
96. Underwood W, Somerville SC. Perception of conserved pathogen elicitors at the plasma membrane leads to relocalization of the Arabidopsis PEN3 transporter. *Proceedings of the National Academy of Sciences of the United States of America*. 2013;110(30):12492-7. doi: 10.1073/pnas.1218701110. PubMed PMID: 23836668; PubMed Central PMCID: PMC3725069.
97. Stein M, Dittgen J, Sanchez-Rodriguez C, Hou BH, Molina A, Schulze-Lefert P, et al. Arabidopsis PEN3/PDR8, an ATP binding cassette transporter, contributes to nonhost resistance to inappropriate pathogens that enter by direct penetration. *The Plant cell*. 2006;18(3):731-46. doi: 10.1105/tpc.105.038372. PubMed PMID: 16473969; PubMed Central PMCID: PMC1383646.
98. Yadav V, Molina I, Ranathunge K, Castillo IQ, Rothstein SJ, Reed JW. ABCG Transporters Are Required for Suberin and Pollen Wall Extracellular Barriers in Arabidopsis. *The Plant cell*. 2014;26(9):3569-88. doi: 10.1105/tpc.114.129049. PubMed PMID: WOS:000345919700010.
99. Nies AT, Konig J, Cui Y, Brom M, Spring H, Keppler D. Structural requirements for the apical sorting of human multidrug resistance protein 2 (ABCC2). *European journal of biochemistry / FEBS*. 2002;269(7):1866-76. Epub 2002/04/16. PubMed PMID: 11952788.
100. Drew DE, von Heijne G, Nordlund P, de Gier JW. Green fluorescent protein as an indicator to monitor membrane protein overexpression in *Escherichia coli*. *FEBS letters*. 2001;507(2):220-4. Epub 2001/10/31. PubMed PMID: 11684102.

## Figure Legends

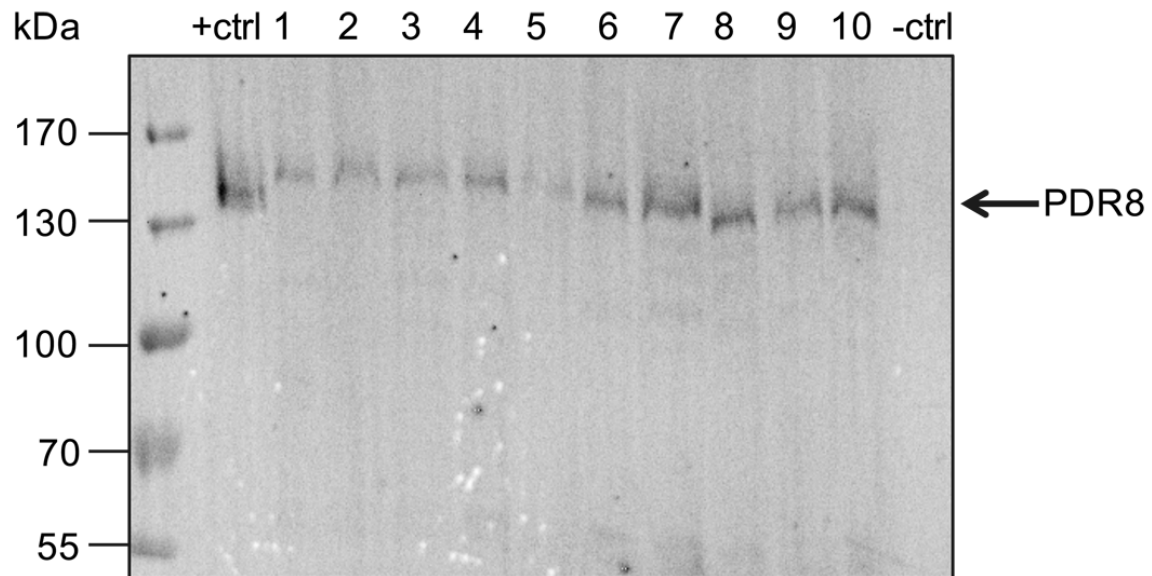


**Fig 1. Heterologous expression of PDR8 in *P. pastoris*.** Crude membranes derived from *P. pastoris* cells carrying pSGP18 (- ctrl: empty vector), BSEP [44] (+ ctrl: positive control) and pSGP18-PDR8-Ntag clones (1-10) were analyzed via SDS-PAGE and immunoblotting (anti-His-tag antibody).

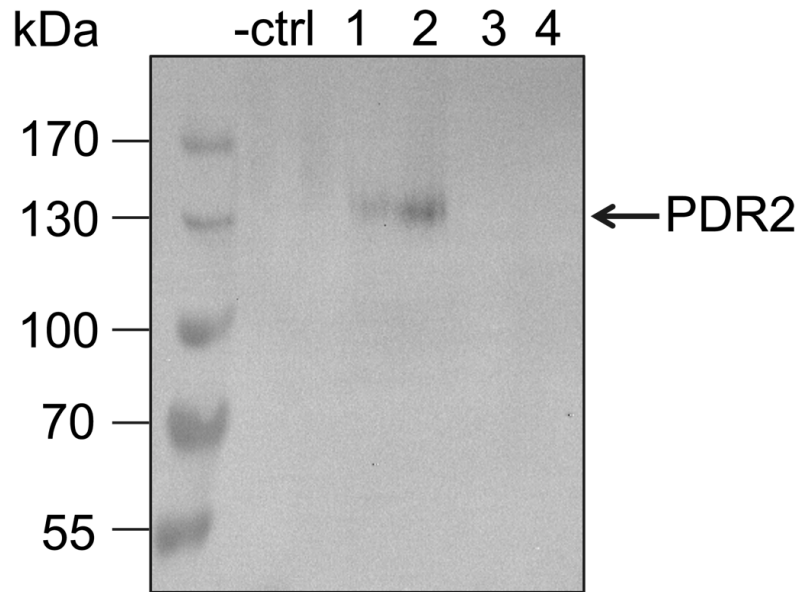


**Fig 2. Heterologous expression of PDR2 in *P. pastoris*.** Crude membranes derived from *P. pastoris* cells carrying pSGP18 (-ctrl: empty vector), and pSGP18-PDR2-Ntag clones (1-4) were analyzed via SDS-PAGE and immunoblotting (anti-His-tag antibody).

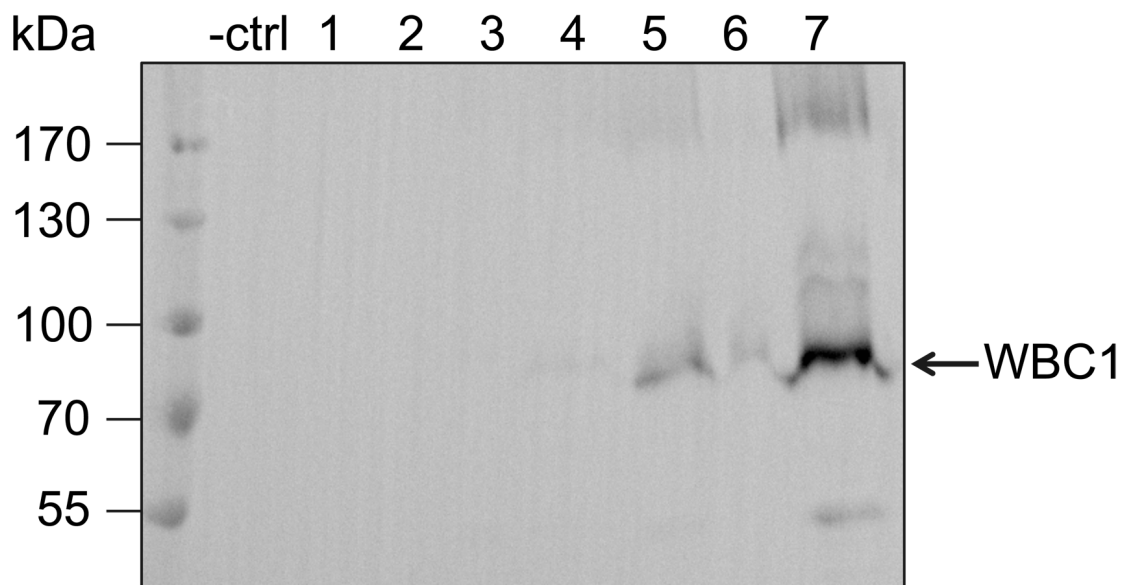


**Fig 3. Heterologous expression of WBC1 in *P. pastoris*.** Crude membranes derived from *P. pastoris* cells carrying pSGP18 (- ctrl: empty vector), and pSGP18-WBC1-Ntag clones (1-7) were analyzed via SDS-PAGE and immunoblotting (anti-His-tag antibody).

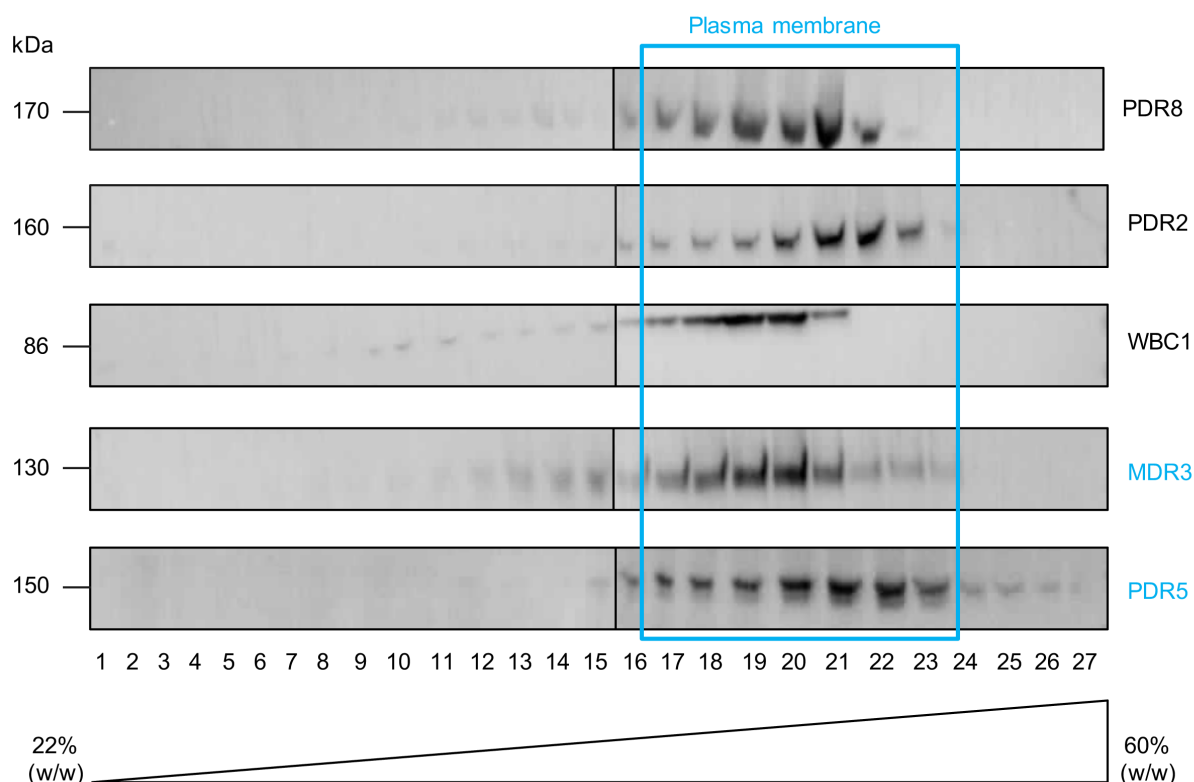


**Fig 4. Sucrose gradient centrifugation of PDR8, PDR2 and WBC1 in *P. pastoris*.** *P. pastoris* crude membranes expressing WBC1, PDR8, PDR2 and MDR3 and *S. cerevisiae* crude membranes expressing PDR5 were separated via ultracentrifugation through a continuous sucrose gradient. Samples were analyzed by SDS-PAGE and immunoblotting (anti-His-tag antibody, anti-PDR5 antibody, C219 antibody). The analyzed proteins are co-localized with the plasma membrane proteins MDR3 and PDR5. The displayed results were assembled from different Western Blots. Entire blots can be found in the supplemental material (S1-S10 Figs).

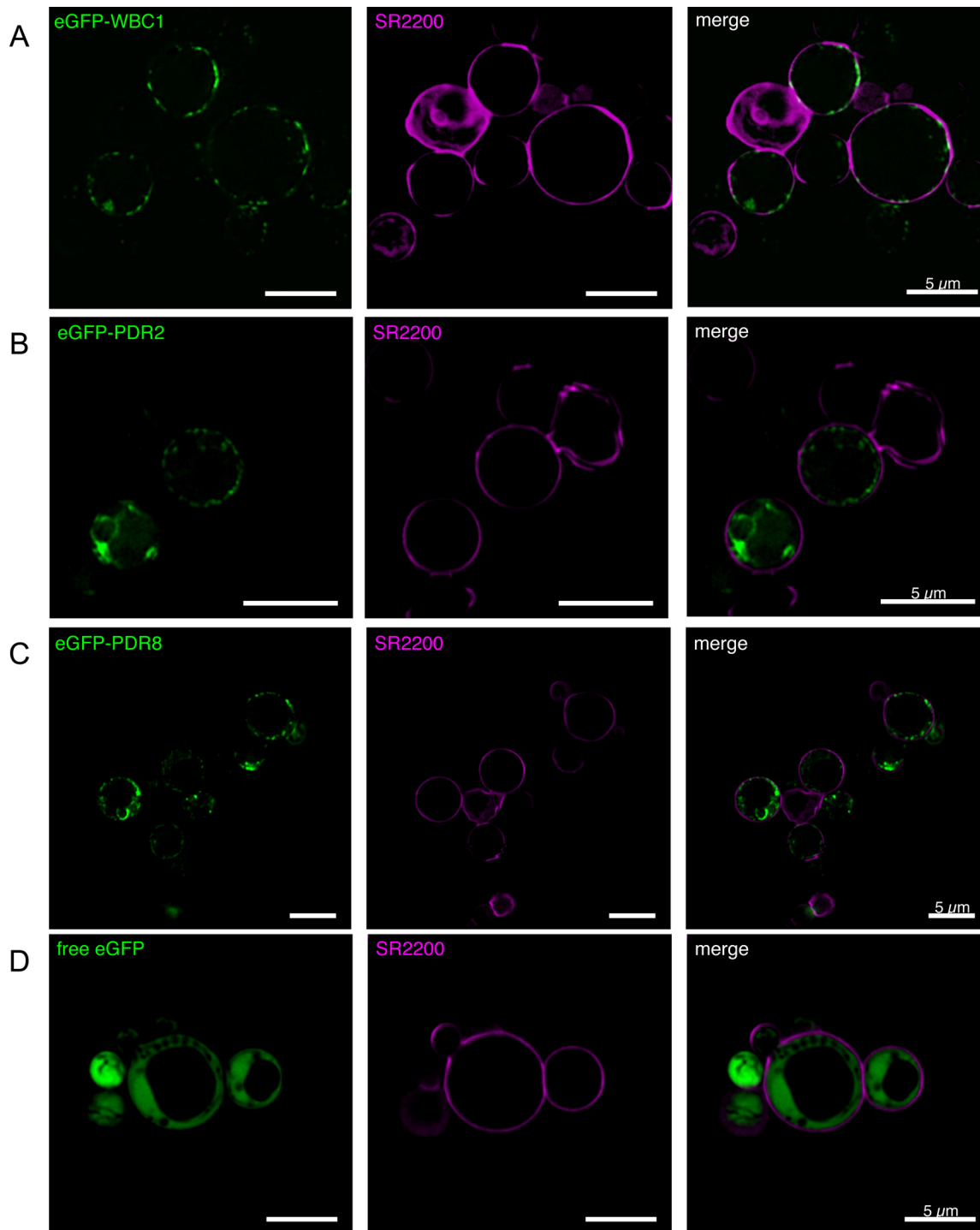


**Fig 5. Confocal fluorescence microscopy of eGFP-PDR8, eGFP-PDR2 and eGFP-WBC1 in *P. pastoris*.** *P. pastoris* cells expressing either the fusion proteins eGFP-WBC1 (row A), eGFP-PDR2 (row B), or eGFP-PDR8 (row C) were analyzed by confocal fluorescence microscopy. As a control cells expressing free eGFP (row D) were analyzed as well. The left lane shows the eGFP fluorescence signal of the respective fusion protein, the middle lane the SR220 signal and the right lane the merged signals.

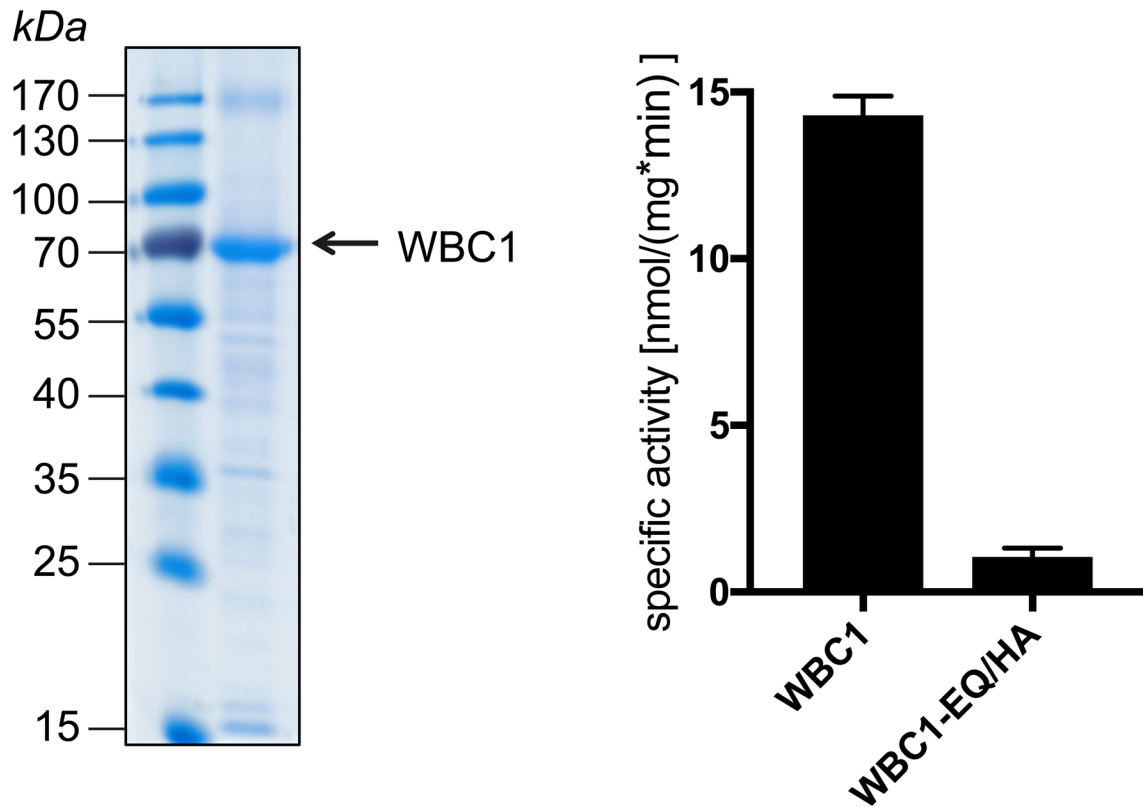
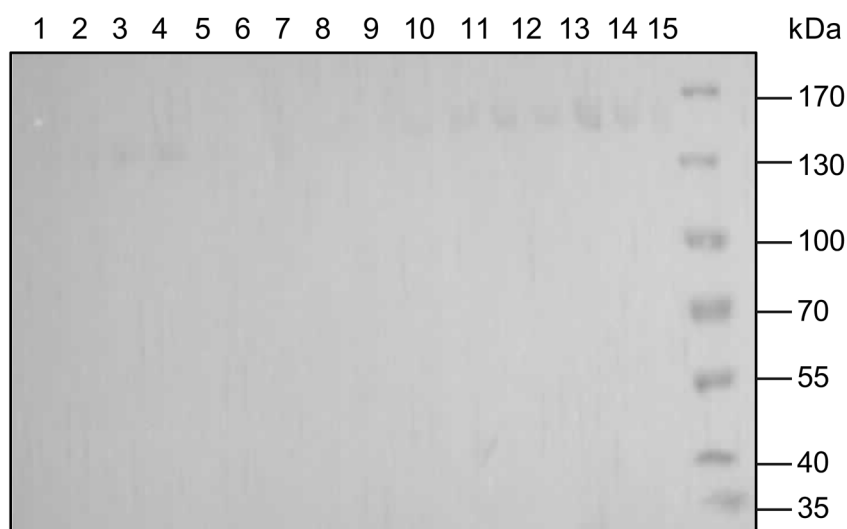
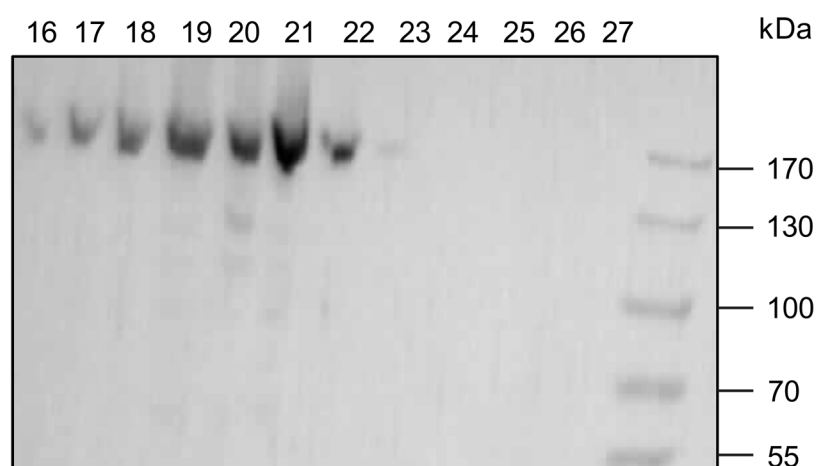


**Fig 6. Basal activity of purified WBC1.** WBC1 was purified via CBP-purification and analyzed subsequently by SDS-PAGE and Colloidal Coomassie Brilliant Blue staining. Basal activity of purified WBC1 was determined by measuring the specific activity of WBC1 against the ATPase deficient mutant WBC1-EQ/HA. Data represents mean and  $\pm$  SD of at least three independent replicates.

## Supporting Information



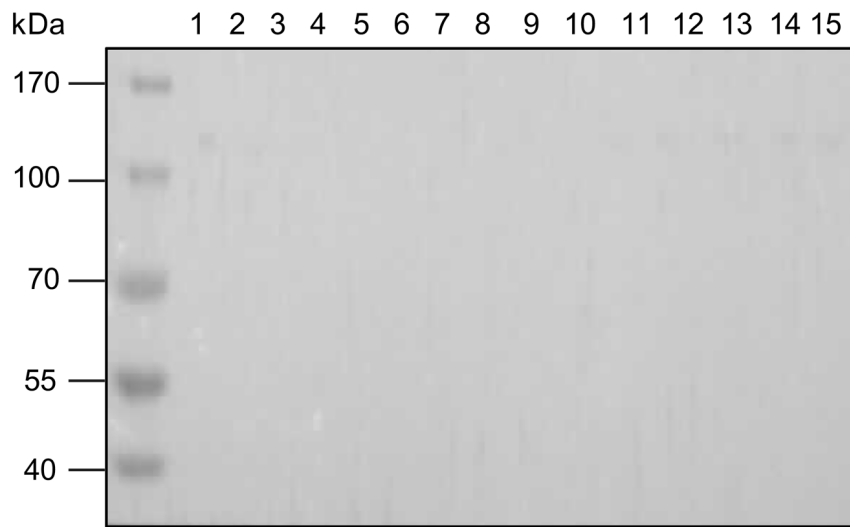
**S1 Fig. Sucrose gradient fractions 1 to 15 of PDR8 containing *P. pastoris* crude membranes.** Crude membranes were separated via ultracentrifugation through a multistep sucrose gradient. The samples were analyzed by SDS-PAGE and immunoblotting (anti-His-tag antibody).



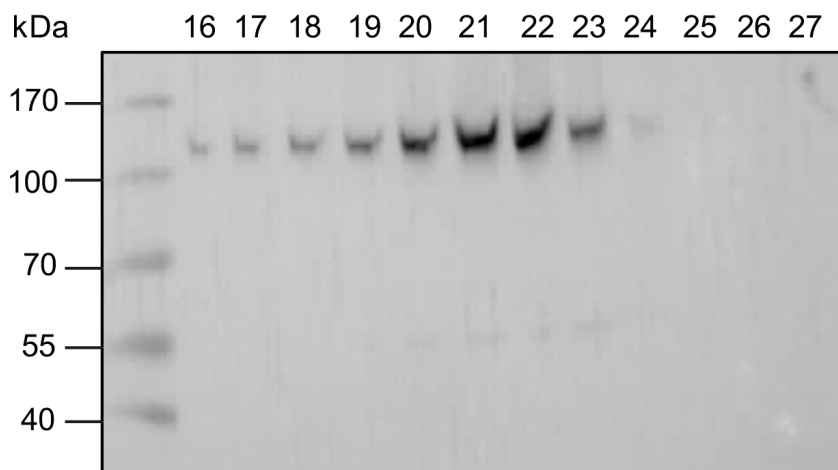
**S2 Fig. Sucrose gradient fractions 16 to 27 of PDR8 containing *P. pastoris* crude membranes.** Crude membranes were separated via ultracentrifugation through a multistep sucrose gradient. The samples were analyzed by SDS-PAGE and immunoblotting (anti-His-tag



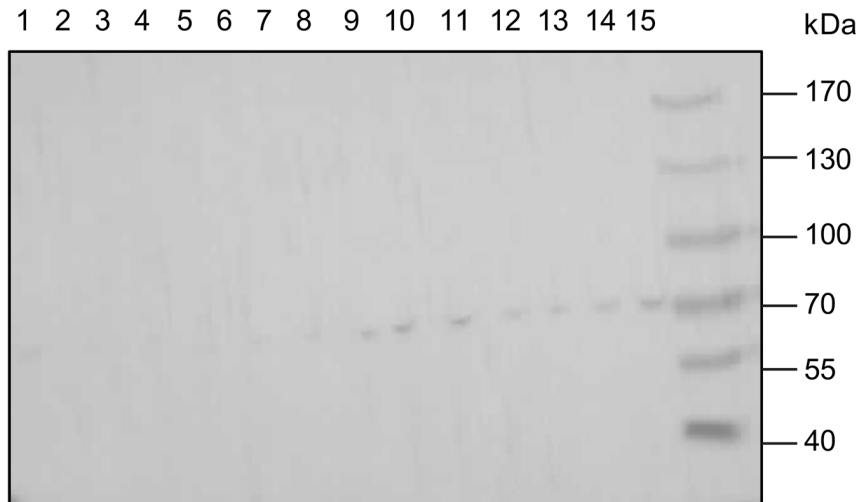
antibody).



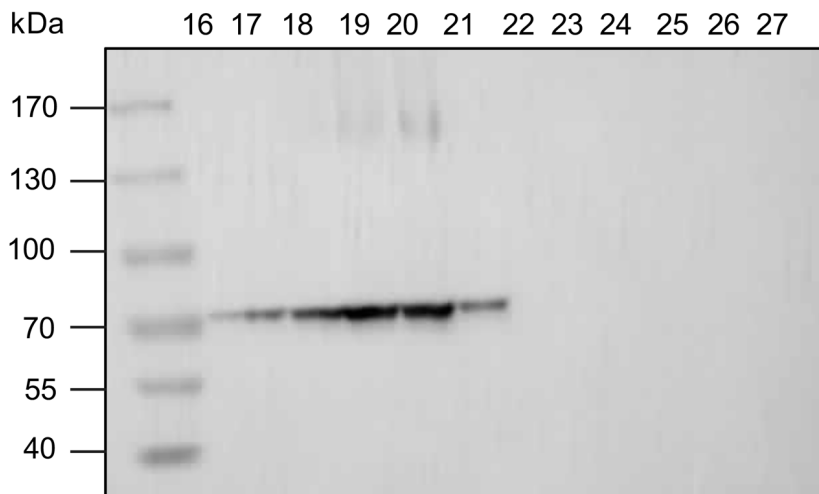
**S3 Fig. Sucrose gradient fractions 1 to 15 of PDR2 containing *P. pastoris* crude membranes.** Crude membranes were separated via ultracentrifugation through a multistep sucrose gradient. The samples were analyzed by SDS-PAGE and immunoblotting (anti-His-tag antibody).



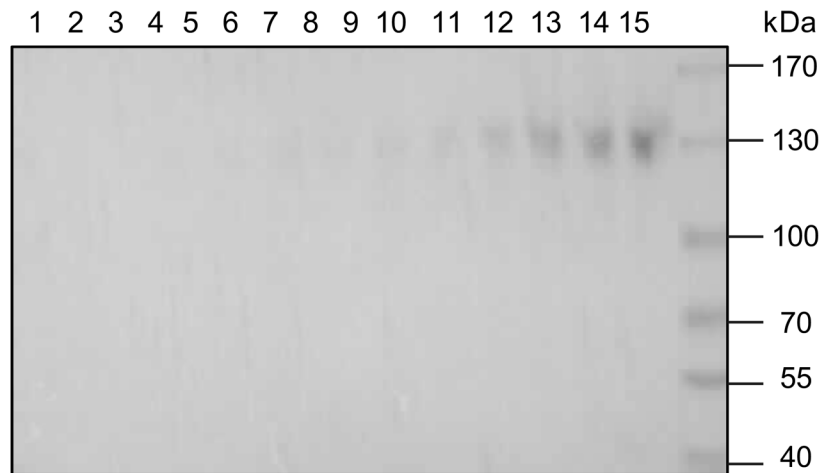
**S4 Fig. Sucrose gradient fractions 16 to 27 of PDR2 containing *P. pastoris* crude membranes.** Crude membranes were separated via ultracentrifugation through a multistep sucrose gradient. The samples were analyzed by SDS-PAGE and immunoblotting (anti-His-tag antibody).



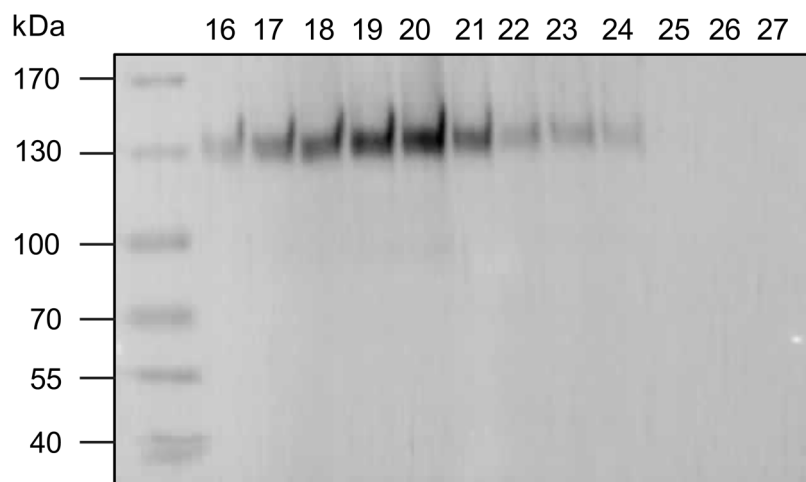
**S5 Fig. Sucrose gradient fractions 1 to 15 of WBC1 containing *P. pastoris* crude membranes.** Crude membranes were separated via ultracentrifugation through a multistep sucrose gradient. The samples were analyzed by SDS-PAGE and immunoblotting (anti-His-tag antibody).



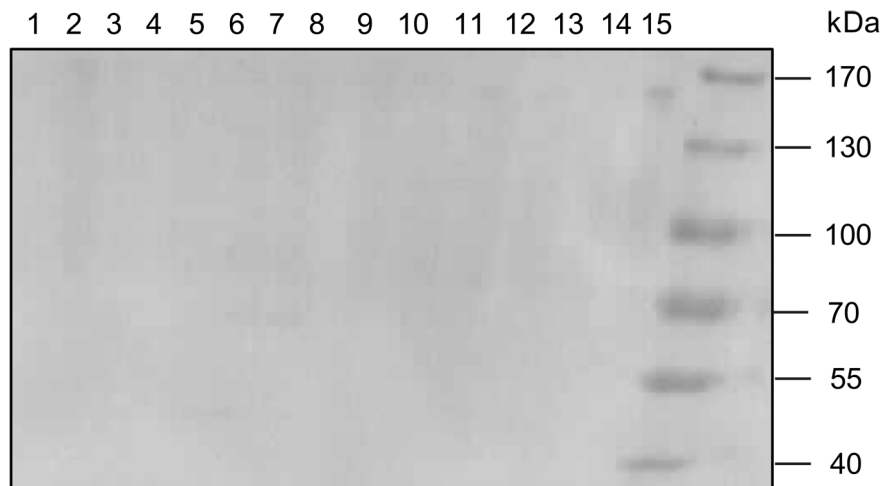
**S6 Fig. Sucrose gradient fractions 16 to 27 of WBC1 containing *P. pastoris* crude membranes.** Crude membranes were separated via ultracentrifugation through a multistep sucrose gradient. The samples were analyzed by SDS-PAGE and immunoblotting (anti-His-tag antibody).



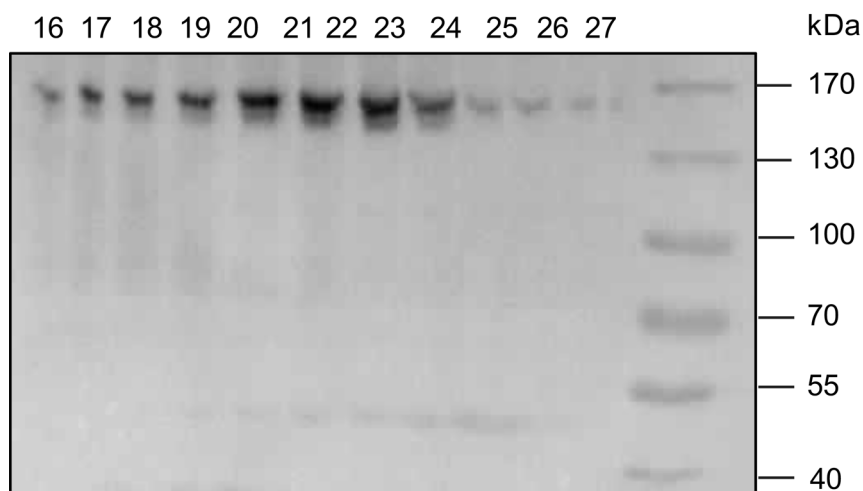
**S7 Fig. Sucrose gradient fractions 1 to 15 of MDR3 containing *P. pastoris* crude membranes.** Crude membranes were separated via ultracentrifugation through a multistep sucrose gradient. The samples were analyzed by SDS-PAGE and immunoblotting (C219 antibody).



**S8 Fig. Sucrose gradient fractions 16 to 27 of MDR3 containing *P. pastoris* crude membranes.** Crude membranes were separated via ultracentrifugation through a multistep sucrose gradient. The samples were analyzed by SDS-PAGE and immunoblotting (C219 antibody).



**S9 Fig. Sucrose gradient fractions 1 to 15 of PDR5 containing *S. cerevisiae* crude membranes.** Crude membranes were separated via ultracentrifugation through a multistep sucrose gradient. The samples were analyzed by SDS-PAGE and immunoblotting (anti-PDR5 antibody).



**S10 Fig. Sucrose gradient fractions 16 to 27 of PDR5 containing *S. cerevisiae* crude membranes.** Crude membranes were separated via ultracentrifugation through a multistep sucrose gradient. The samples were analyzed by SDS-PAGE and immunoblotting (anti-PDR5 antibody).

### **3.2 Chapter II – ABCG30 from *Arabidopsis thaliana***

Title: Detergent screening and purification of AtABCG30 expressed in *Pichia pastoris*

Authors: Kalpana Shanmugarajah, Diana Kleinschrodt, Sander H. J. Smits  
and Lutz Schmitt

Published in: In preparation

Own work: 85 %

- Fermentation of AtABCG30

- Isolation of plasma and crude membranes

- Detergent screen via dot blot and solubilization studies

- Purification of AtABCG30 and ATPase Assay

- Writing of the manuscript

## **Detergent screening and purification of AtABCG30 expressed in *Pichia pastoris***

***Kalpana Shanmugarajah<sup>1,2</sup>, Diana Kleinschrodt<sup>1,3</sup>, Sander H. J. Smits<sup>1</sup> and Lutz Schmitt<sup>1,2\*</sup>***

<sup>1</sup>Institute of Biochemistry, Heinrich-Heine-University, Düsseldorf, Germany

<sup>2</sup>Cluster of Excellence on Plant Sciences (CEPLAS), Heinrich-Heine-University, Düsseldorf, Germany

<sup>3</sup>Protein Production Facility, Heinrich-Heine-University, Düsseldorf, Germany

For correspondence

[lutz.schmitt@hhu.de](mailto:lutz.schmitt@hhu.de)

## Abstract

Plants release diverse secondary metabolites and exudates with detrimental and/ or beneficial effects into the soil. The ATP-binding cassette (ABC) transporter AtABCG30 has been reported to be involved in root-microbiome interaction by exudation of phytochemicals. Substrate identities of the transported phytochemicals in the roots have not been clarified yet, but further studies revealed a potential role of AtABCG30 in seed germination via abscisic acid transport. Hence, *in vitro* characterization with purified AtABCG30 could reveal substrate identities and kinetic parameters. Here, we present a detailed report about the cloning and expression of AtABCG30 in methylotrophic yeast *Pichia pastoris*. Initial solubilization and purification studies contribute to the evaluation of *Pichia pastoris* as an expression host for plant ABC transporters.

## Introduction

ATP-binding cassette (ABC) transporters are membrane-embedded proteins, which use ATP hydrolysis as driving force to translocate a large spectrum of substrates across the lipid bilayer [1]. They are defined by two transmembrane domains (TMD) and two nucleotide binding domains (NBD), which are responsible for substrate binding and ATP-driven substrate translocation. The TMDs contain 6-12  $\alpha$ -helices while the NBDs are characterized by conserved Walker A and B motifs, the H-, D- and the Q-loop and an ABC signature motif [2]. Plants exhibit the largest source for ABC proteins with more than 100 members in *Arabidopsis thaliana* and *Oryza sativa* [3, 4]. Plant ABC proteins are subdivided into different subfamilies, depending on their phylogenetic relationship and domain organization [5]. Based on the number of domains, which are encoded on a single gene can ABC transporters be differentiated as full-size (TMD-NBD)<sub>2</sub> or half-size transporters (TMD-NBD). Half-size transporters have to homo- or heterodimerize in order to form the functional transport unit [6].

The fungi and plant specific full-size ABCG transporters (PDR, pleiotropic drug resistance) display a reverse domain organization [5, 7]. Full-size ABCG transporters have been reported to be involved in various vital biological processes, including pathogen defense [8-14], cutin precursor transport [15], resistance to heavy metals [16, 17], hormone transport [18-22] and terpenoid transport [23-27]. However, most results are based on plant knock-out studies and biochemical analysis using purified full-size ABCGs are still rare [27, 28].

The full-size ABCG transporter AtABCG30 (AtPDR2) from *Arabidopsis thaliana* has been reported to be involved in exudation of phytochemicals in the root. The *atabcg30* mutant exhibited a significant change in the root exudate profile and the fungal and bacterial community in the soil [29]. Besides that, AtABCG30 has been shown to control seed germination by mediating abscisic acid (ABA) transport in cooperation with other ABCG transporters. Thereby, AtABCG25 and AtABCG31 export ABA from the endosperm, while AtABCG30 and AtABCG40 import ABA into the embryo [20, 30]. Thus, AtABCG30 displays pleiotropic phenotypes and transports probably multiple substrates. Identification of transported substrates in the roots could give further insight into the role of AtABCG30. Although, heterologous expression and protein purification could provide sufficient protein amounts for biochemical and structural analysis, data regarding enzymatic properties are still lacking.



As previously showed, a subset of *A. thaliana* full-size ABCG transporters, including AtABCG30, have been analyzed for heterologous expression in *Pichia pastoris* using numerous cloning strategies (Gräfe et al. (2018) *submitted*). It turned out, that many factors such as gene size, cDNA quality, vector properties, tag-positions, re-occurring mutations and gene toxicity for the host cell hampered the success of cloning. However, we were able to show succesful heterologous expression and correct targetting in *P. pastoris* for AtABCG36, AtABCG30 and AtABCG1. Here, we present a detailed report about the cloning and heterologous expression of AtABCG30 in *P. pastoris*. Initial solubilization screens with AtABCG30 membranes and subsequent purification with a calmodulin-binding protein (CBP) tag were performed and provide a proper foundation for future studies.

## Methods

### Cloning and expression of AtABCG30 in *P. pastoris*

The *AtABCG30* gene (Accession number At4g15230) was synthesized as codon optimized for expression in *P. pastoris* and cloned into the expression vector pSGP18-Ntag (GenScript®). The obtained expression construct pSGP18-AtABCG30-Ntag was transformed as previously described in Gräfe *et al.* (2018) (submitted) in electrocompetent *P. pastoris* X33 cells (Invitrogen) and analyzed for expression. Chromosomal integrated *AtABCG30* DNA was isolated (innuSPEED Bacteria/Fungi DNA Kit) and the *AtABCG30* gene was amplified by PCR using primer pairs PDR2-1 to PDR2-4 (Table 1). The amplified sequences were verified by sequencing (GATC Biotech).

**Table 1: Primers used in this study.**

Primer	Sequence 5' → 3'
PDR2-1-fw	ATGCACCATCATCACCATCATCATC
PDR2-1-rev	GGCCAACTGTTGAAGGCAAG
PDR2-2-fw	CTTGCCTTCAACAGTTGGCCC
PDR2-2-rev	CTCTGCGTAAGACAAAGGACTAAGC
PDR2-3-fw	GCTTAGTCCTTTGTCTTACGCAGAG
PDR2-3-rev	TCAAGATAAGTTCGTCGAATGTCTCAA
PDR2-4-fw	TATCTTGATGAAGAACGGTGGAC
PDR2-4-rev	AAGGACAACCTTAGCATGAAAAAGGC

### Fermentation of AtABCG30

Large-scale expression of AtABCG30 containing clones was performed in a 15 L table-top glass fermenter (Applikon Biotechnology) according to the Invitrogen *Pichia* fermentation guidelines. Cells were harvested 48 hours after methanol induction (5,000 x g, 10 min, 4 °C), flash-frozen with liquid nitrogen and stored at -80 °C until further use.

### **Isolation of AtABCG30 containing crude membranes**

100 g of AtABCG30 containing *P. pastoris* wet cells were thawed on ice, re-suspended with lysis buffer (50 mM Tris-HCl, pH 7.5, 150 mM NaCl, 1 mM EDTA, 1 mM EGTA, 0.3 M sucrose) to a final concentration of 0.5 g cells/ml and supplemented with protein inhibitor cocktail (Roche). Cells were passed two times through a pre-cooled TS Series Cell Disruptor (Constant System) at 2.5 kbar. Disrupted cells were centrifuged twice (15,000 x g, 30 min, 4 °C) to get rid of cell debris. After subsequent centrifugation (125,000 x g, 1 h, 4 °C) of the supernatant, crude membranes were re-suspended in buffer A (50 mM Tris-HCl pH 8, 150 mM NaCl, 15 % (v/v) Glycerol) and either stored at -80 °C after flash-freezing in liquid nitrogen or used directly for plasma membrane isolation.

### **Isolation of AtABCG30 containing plasma membranes**

Crude membranes obtained from 50 g of AtABCG30 containing *P. pastoris* wet cells, were used for plasma membrane isolation by a two-layer sucrose gradient (adapted from R. Serrano and Grillitsch *et al.* [31, 32]). A 53 % sucrose solution (w/w) was layered on top of a 43 % sucrose (w/w) solution and crude membranes pipetted on the top of the gradient. After ultracentrifugation in a swing-out rotor (130,000 x g, 16 h, 4 °C), plasma membranes were harvested from the interphase, re-suspended in 4 volumes of buffer A and centrifuged again (125,000 x g, 1 h, 4 °C). The pellet was resuspended in 5 ml buffer A, flash-frozen in liquid nitrogen and stored at -80 °C until further use.

### **Solubilization screen via dot blot technique**

AtABCG30 containing membranes were thawed on ice, adjusted to 5 mg/ml and solubilized in 200 µl buffer A. The solubilization was performed via gentle agitation for 1 hour at 4 °C. Subsequently, 95 different detergents (Affymetrix, Anatrace detergent kit) were tested and depending on their critical micellar concentration (cmc) used at 1 % (w/v) or higher (Supplementary Table 1). Solubilized samples were centrifuged (100,000 x g, 30 min, 4 °C) and SDS sample buffer was added to the supernatant. Afterwards, samples were heated at 65 °C for 10 min and 3 µl of each was spotted on a nitrocellulose membrane. The membrane was extensively dried and afterwards blocked for 1 hour in TBS-T with 5 % (w/v) milk powder. The solubilization efficiency of AtABCG30 was analyzed by immunoblotting with an anti-His-antibody (Qiagen). The

immunoblotting was performed using a tank blot system (Bio-Rad) following standard procedures.

### **Optimization of AtABCG30 solubilization efficiency**

The solubilization efficiency can be optimized by using different detergent to protein ratios and incubation conditions. Membranes were adjusted to 5 mg/ml, 10 mg/ml or 15 mg/ml protein concentration and detergents were used at 0.5 to 2 % final concentration (f.c.). The solubilization was performed at 4 °C or at 18 °C and incubated for one or two hours. The samples were then centrifuged (100,000 x g, 30 min, 4°C) and the pellets and supernatants were analyzed after addition of SDS sample buffer by SDS-PAGE (7 % gels) and subsequently visualized by colloidal Coomassie Brilliant Blue G-250 (CBB) staining and immunoblotting.

### **Protein Purification of AtABCG1**

The purification of AtABCG30 was conducted by calmodulin-binding protein affinity (CBP) chromatography. The crude or rather plasma membrane concentration, equivalent to 15 g wet cells, was adjusted with buffer A to 5 mg/ml. Subsequently, membranes were solubilized with 1 % Fos Choline-14 (Anatrace) for 1 hour at 4 °C and centrifuged (125,000 x g, 1 h, 4 °C). The supernatant was mixed with 2 x cmc Fos-Choline 14 and 2 ml CBP resin (Agilent Technologies, Santa Clara, CA). Samples were transferred to a gravity flow column (Bio-Rad) after overnight incubation at 4 °C on a rotator. The resin was washed with CBP binding buffer (50 mM Tris-HCl, pH 8, 10 mM CaCl<sub>2</sub> 150 mM NaCl, 1 mM MgCl<sub>2</sub>, 10 % Glycerin) and eluted with CBP elution buffer (50 mM Tris-HCl, pH 8, 150 mM NaCl, 2 mM EGTA, 10 % Glycerin) added with 2 cmc Fos-Choline-14. Purified AtABCG30 was concentrated with a 100 kDa cut-off centricon (Millipore) and directly used for ATPase assays or snap frozen in liquid nitrogen and stored at -80 °C until further use. Samples were analyzed by SDS-PAGE and immunoblotting.

## Results

As previously reported, AtABCG30 was successfully cloned into pSGP18-Ctag via In-Fusion reaction (Gräfe et al., (2018), *submitted*). The whole cloning step was complicated because of difficulties in cloning from cDNA, mutagenesis and low *E. coli* viability due to gene toxicity. Despite extensive screening, it was not possible to determine protein expression for pSGP18-AtABCG30-Ctag. In contrast, a codon optimized and synthetically produced *AtABCG30* gene (pSGP18-AtABCG30-Ntag) was successfully overexpressed and correctly targeted in the *P. pastoris* plasma membrane. Here, we report in detail about initial purification attempts of the *P. pastoris* expressed pSGP18-AtABCG30-Ntag.

### Cloning and heterologous expression of AtABCG30

The *Arabidopsis thaliana* full-size PDR transporter AtABCG30 was successfully expressed in *P. pastoris*. In order to achieve heterologous expression in *P. pastoris*, several steps including cloning, retransformation in *E. coli* for propagation, plasmid isolation and transformation in *P. pastoris* have to be successfully performed. In an initial attempt, the pSGP18-AtABCG30-Ntag plasmid was only sequence verified after cloning. As shown in Figure 1, termination products around 115 kDa were observed, whereas the molecular weight of AtABCG30 was approximately 158 kDa. Subsequently, sequencing of the propagated plasmid revealed a mutagenized nucleotide, which lead to a stop codon. Hence, the plasmid was sequenced again after propagation in *E. coli*. Although the resequencing results revealed that a majority of the plasmids tested (approximately 50 clones) were with either missing some portions of the gene or mutated, several positive clones were identified as previously shown. The sequence verified plasmid was transformed in *P. pastoris*, where the AtABCG30 gene sequence gets integrated into the chromosome. Subsequently, the chromosomal DNA was isolated and the AtABCG30 gene was amplified and verified by sequencing. In contrast to *E. coli*, no reorganization of the *AtABCG30* sequence was observed. Thus, in accordance with our previous studies, cloning or plasmid propagation steps in *E. coli* are the main reason behind *PDR* gene mutation.

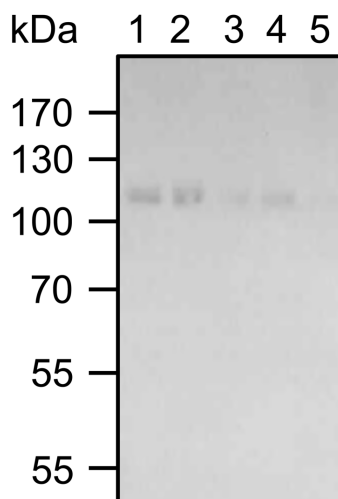


**Figure 1: Heterologous expression of AtABCG30 in *P. pastoris*.** Crude membranes derived from *P. pastoris* cells carrying pSGP18-AtABCG30-Ntag (clones 1-5) were analyzed by SDS-PAGE and immunoblotting (anti-His-tag antibody). kDa, molecular weight marker.

## Purification of AtABCG30

### ***Solubilization screen with AtABCG30 containing crude membrane***

One major advantage of *P. pastoris* is that even low expressed proteins, can be obtained in sufficient amounts for subsequent biochemical studies via fermentation [33]. The initial fermentation attempt resulted in 1.5 kg AtABCG30 containing *P. pastoris* cells. After membrane preparation, AtABCG30 was detected via immunoblotting and tested for different sample preparation conditions (Figure 2). Subsequent detergent screening via dot-blot technique resulted in higher solubilization efficiencies for zwitterionic and anionic detergents. Fos-Choline 12,14,15 and 16 were selected for further optimization screens (Figure 4, left blot). Different solubilization screens with variations in buffer, temperature, detergent and membrane concentrations were used, but a complete solubilization could not be achieved with any of the tested detergents. Thus, AtABCG30 solubilization from crude membranes needed further optimization. Since AtABCG30 is a plasma membrane transporter [34], solubilization of plasma membranes could possibly lead to a higher efficiency. Subsequent experiments were performed with AtABCG30 containing plasma membranes.

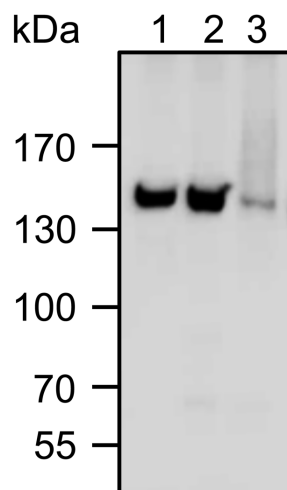


**Figure 2: Sample preparation screen of AtABCG30 containing *P. pastoris* crude membranes.** 5 µg AtABCG30 containing crude membranes were incubated prior to loading on SDS-PAGE for 10 min at (1) room temperature, (2) 65 °C or (3) 95 °C. Samples were analyzed via SDS-PAGE and immunoblotting (anti-His-tag antibody). kDa, molecular weight marker.

### ***Solubilization screen with AtABCG30 containing plasma membrane***

Isolation of highly enriched plasma membrane preparations yielded 85 mg of total membrane protein per 100 g wet cells. As shown in Figure 3, AtABCG30 represented a major proportion of the total plasma membrane proteins.

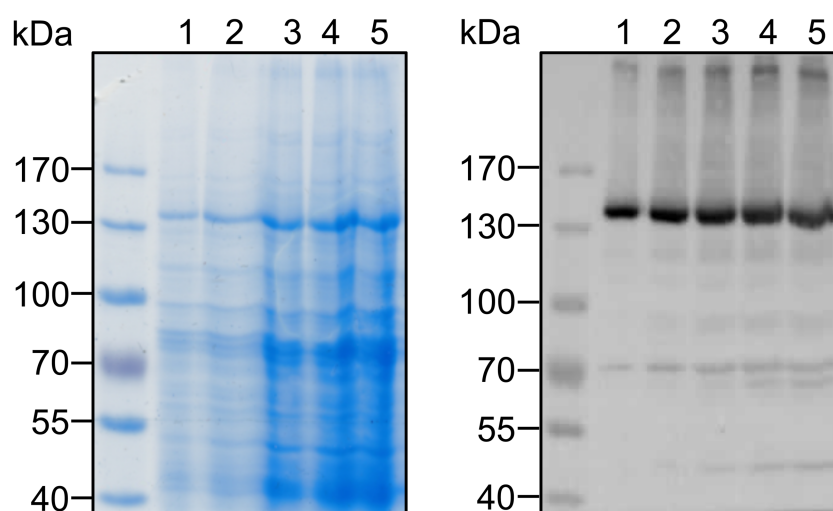


**Figure 3: Overexpression of AtABCG30 in *P. pastoris*.** AtABCG30 containing *P. pastoris* plasma membrane was isolated and subjected to SDS-PAGE/CBB and immunoblotting (anti-His-tag antibody). Lane 1: 5 µg; Lane 2: 10 µg; Lane 3: 20 µg; Lane 4: 30 µg; Lane 5: 50 µg plasma membrane; kDa, molecular weight marker.

In order to identify AtABCG30 solubilizing detergents, a detergent screen via dot blot technique was performed. Similar to the above reported dot blot with crude membranes, predominantly zwitterionic detergents were identified to efficiently solubilize AtABCG30 (Figure 4). Based on that, further solubilization experiments with different conditions were conducted, but a quantitative solubilization was not observed. The immunoblot in Figure 5 shows the supernatant and pellet fractions after solubilization of 10 mg/ml AtABCG30 containing plasma membranes in 0.5 to 2 % Fos-Choline 14, 15 and 16. AtABCG30 remains in most of the cases in the pellet and a faint protein band is only detected in the supernatant fraction of 2 % Fos-Choline 14 solubilized plasma membranes. The solubilized AtABCG30 and around 50 % of the non-solubilized proteins in the pellet fraction are stuck between the separating and stacking gel, indicating protein aggregation due to pH incompatibility. Initial solubilization tests with different buffers exhibited no improvement. Although, the buffer conditions need further optimizations, 10 mg/ml plasma membrane concentration and solubilization with 2 % Fos-Choline 14 were chosen for subsequent purification attempts.

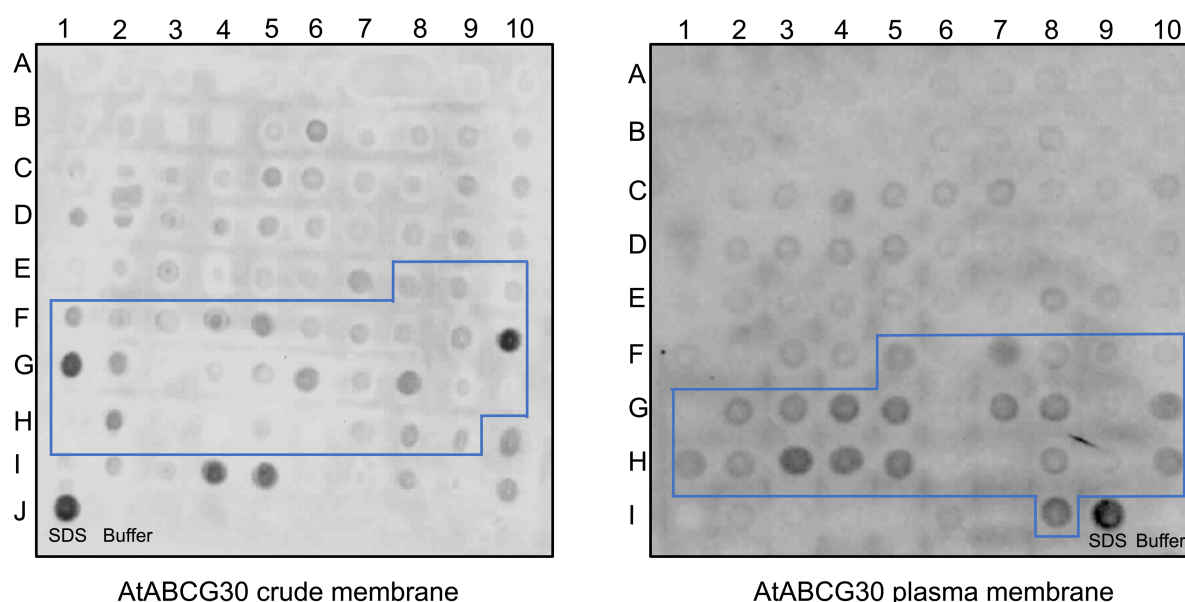


**Figure 4: Detergent screen of AtABCG30 containing *P. pastoris* crude and plasma membrane.** AtABCG30 containing membranes were adjusted to 5 mg/ml and tested for solubilization with non-ionic, anionic, cationic and zwitterionic (marked in blue) detergents. Solubilized samples were spotted on a nitrocellulose membrane and visualized by immunoblotting (anti-His-tag antibody). List of used detergents and a legend to this figure can be found in Supplementary Table 1.



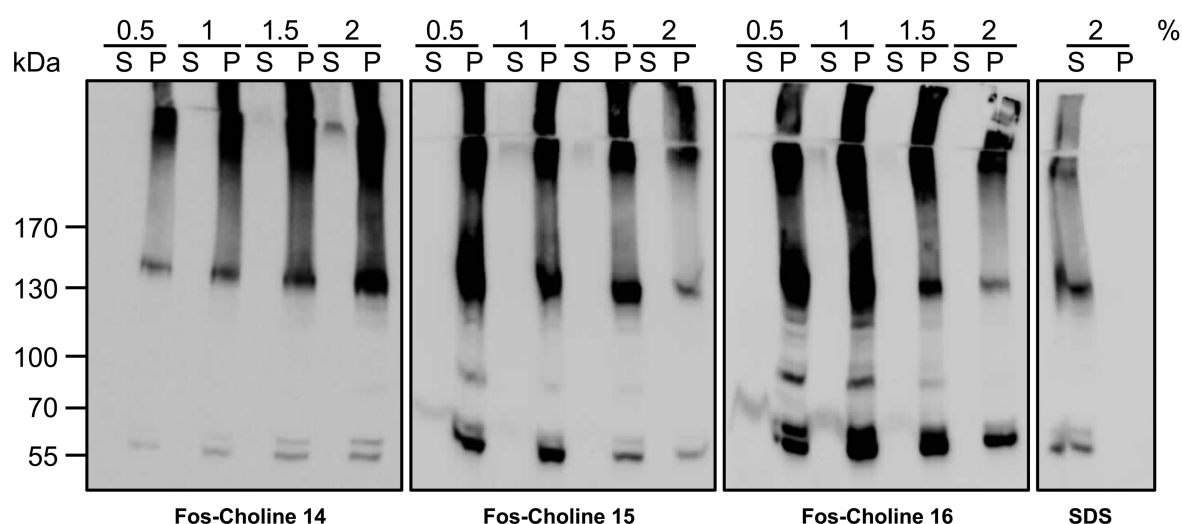


**Figure 5: Solubilization screen of AtABCG30.** 10 mg/ml of AtABCG30 containing crude membranes were solubilized for 1 hr at 4 °C using 0.5 % - 2 % Fos-Choline 14, Fos-Choline 15, Fos-Choline 16 and 2 % SDS (positive control). After centrifugation supernatant (S) and pellet (P) fractions were analyzed by SDS-PAGE and immunoblotting (anti-His-tag antibody).

### ***Calmodulin binding peptide affinity chromatography of AtABCG30***

In order to obtain purified AtABCG30 for further functional studies, a calmodulin binding protein affinity (CBP) chromatography was performed. Based on previous solubilization experiments, AtABCG30 plasma membranes were first solubilized with 2 % Fos-Choline 14 and then purified via CBP-purification. Collected fractions were subsequently analyzed by SDS-PAGE and immunoblotting. Lane E in Figure 6 refers to the concentrated elution fraction. In contrast to the above reported solubilization experiments, purified proteins were not partially aggregated and migrate around their calculated molecular weight of 158 kDa in the SDS-PAGE. The protein yield per 100 g wet cells was around 0.4 mg. In contrast to that, AtABCG30 purification from crude membranes yielded in up to 4 times more purified protein with a yield of 2 mg per 100 g wet cells (Figure 6). Simultaneously, crude membrane purified AtABCG30 contains severe protein degradation. Subsequent ATPase assays of detergent solubilized AtABCG30 exhibited no specific activity.

In conclusion, AtABCG30 was successfully purified from *P. pastoris* membranes, but the high amount of degradation products, especially observed in crude membrane purification, indicates that AtABCG30 is not stable under the used conditions. Furthermore, the high detergent to protein ratio with 2 % Fos-Choline 14 and 10 mg/ml AtABCG30 membranes could lead to protein denaturation. Hence, solubilization and

purification conditions have to be further optimized in order to obtain ATPase active and stable AtABCG30 for functional studies.

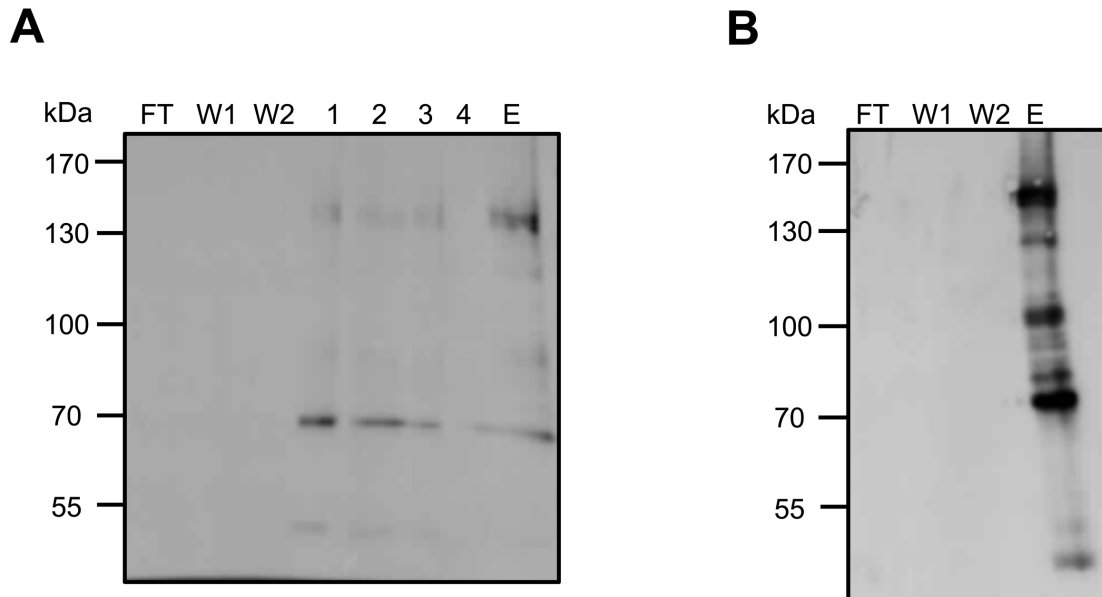


**Figure 6: CBP-purification of AtABCG30 from *P. pastoris* membranes.** AtABCG30 was purified from (A) AtABCG30 containing plasma membranes and (B) AtABCG30 containing crude membranes. Samples were analyzed by 7% SDS-PAGE and immunoblotting (anti-His-antibody). FT, flow through; W1-W2, wash fractions; 1-4, eluted fractions; E, concentrated elution fraction; kDa, molecular weight marker.

## Discussion

Plants exhibit the largest number of ABC transporters amongst all living organisms [4]. Nevertheless *in vitro* data on plant ABC transporters are still underrepresented in the literature and hence efficient overexpression systems need to be established. Heterologous expression of plant ABC transporters could not only provide purified proteins for biochemical or structural studies, but also provide further insight to the existing data based on knock-out studies or reverse genetics. Here, we report the successful heterologous expression of the full-size ABCG transporter AtABCG30 in *P. pastoris* and initial purification trials.

As reported earlier, cloning of *Arabidopsis* full-size ABCG transporters is hampered by gene size, vector properties, reoccurring mutations and significantly reduced viability while sub-cloning in *E. coli* (Gräfe et al. (2018) *submitted*). Sequencing after chromosomal AtABCG30 integration in *P. pastoris*, indicates that gene reorganization of full-size *AtABCG* sequences are only restricted to *E. coli*. In accordance with this, Noe *et al.* and Vu *et al.* report about similar observations for other membrane proteins [35, 36]. Hence every sub-cloning step in *E. coli* needs to be verified via sequencing of the gene. In contrast, *P. pastoris* is able to propagate plant ABC membrane proteins, but it has been shown that protein expression requires optimization of the expression conditions. Besides standard procedures such as varied expression time, oxygen level, cell densities at the expression start and protein-tag positions, codon optimization for expression on *P. pastoris* and; extensive screening for positive clones resulted in successful overexpression of AtABCG30.

In order to purify AtABCG30, an initial detergent screening via dot blot technique was performed. The identification of a suitable detergent depends on the solubilization efficiency and the capacity to maintain the structure and function of the solubilized protein. Dot blot experiments with AtABCG30 containing crude and plasma membranes showed that solubilization occurred mainly in the presence of zwitterionic detergents. Until now, several ABC-transporters have been successfully solubilized and purified with zwitterionic detergents [37-41]. Hence, solubilization experiments with different detergent to protein ratio or solubilization conditions were performed but failed to result in quantitative solubilization. A faint AtABCG30 band was only detected by immunoblotting of a 2 % Fos-Choline 14 set-up. The subsequent CBP-purification with crude membranes in comparison to plasma membranes resulted in protein

amounts with 2 mg per 100 g wet cells. However, crude membrane purified AtABCG30 exhibited a large degradation level. Taken together, these results indicate that although it is possible to isolate AtABCG30 protein, the current expression and/or solubilization conditions of AtABCG30 were not optimal. Moreover, deficiency of ATPase activity of the CBP-purified AtABCG30 strongly indicates the need for further optimization of the solubilization conditions including buffer composition.

*P. pastoris* has been shown to be a suitable host for membrane protein expression [39, 42, 43]. The recombinant protein expression in *P. pastoris* is based on the methanol-inducible *AOX1* promotor ( $P_{AOX1}$ ). Known advantages include simple culture conditions, eukaryote-specific modifications like glycosylation and the possibility to reach high cell densities by fermentation. By using these, even poorly expressed proteins can be purified in sufficient amounts for biochemical or structural studies [44]. Nevertheless, the methanol metabolism by-product hydrogen peroxide ( $H_2O_2$ ) can lead to oxidative stress, which can result in degradation of the recombinant protein [45, 46]. The used cells from this study descent from a single fermentation round. Further studies with reduced methanol-feeding rates in order to avoid methanol overdose or sample analysis after different induction times, could contribute to reduce protein instability. Alternatively, methanol induction can be completely avoided by replacing the  $P_{AOX1}$  promotor by a constitutive promotor like the  $P_{GAP}$  promotor [47, 48].

In summary, the present study lays a foundation for future *in vitro* studies with AtABCG30 by providing the means to obtain sufficient amount of AtABCG30 protein. Although, successful heterologous expression of AtABCG30 in *P. pastoris* and purification was obtained in this study, further optimization is required in order to obtain functionally active protein. Additionally, we were also able to isolate AtABCG30 containing plasma membranes, which can be used for identification of kinetic parameters and substrate identities.

## Acknowledgments

The authors would like to thank Iris Fey for technical assistance. This work was funded by DFG through Cluster of Excellence on Plant Sciences CEPLAS (EXC 1028) to L.S.

## References

1. Higgins, C.F., *ABC transporters: physiology, structure and mechanism--an overview*. Res Microbiol, 2001. **152**(3-4): p. 205-10.
2. Higgins, C.F. and K.J. Linton, *The ATP switch model for ABC transporters*. Nat Struct Mol Biol, 2004. **11**(10): p. 918-26.
3. Sanchez-Fernandez, R., et al., *The Arabidopsis thaliana ABC protein superfamily, a complete inventory*. J Biol Chem, 2001. **276**(32): p. 30231-44.
4. Hwang, J.U., et al., *Plant ABC Transporters Enable Many Unique Aspects of a Terrestrial Plant's Lifestyle*. Mol Plant, 2016. **9**(3): p. 338-55.
5. Verrier, P.J., et al., *Plant ABC proteins--a unified nomenclature and updated inventory*. Trends Plant Sci, 2008. **13**(4): p. 151-9.
6. Linton, K.J. and C.F. Higgins, *The Escherichia coli ATP-binding cassette (ABC) proteins*. Mol Microbiol, 1998. **28**(1): p. 5-13.
7. Crouzet, J., et al., *Organization and function of the plant pleiotropic drug resistance ABC transporter family*. FEBS Lett, 2006. **580**(4): p. 1123-30.
8. Bultreys, A., et al., *Nicotiana plumbaginifolia plants silenced for the ATP-binding cassette transporter gene NpPDR1 show increased susceptibility to a group of fungal and oomycete pathogens*. Mol Plant Pathol, 2009. **10**(5): p. 651-63.
9. Bienert, M.D., et al., *A pleiotropic drug resistance transporter in Nicotiana tabacum is involved in defense against the herbivore Manduca sexta*. Plant J, 2012. **72**(5): p. 745-57.
10. Banasiak, J., et al., *A Medicago truncatula ABC transporter belonging to subfamily G modulates the level of isoflavonoids*. J Exp Bot, 2013. **64**(4): p. 1005-15.
11. Crouzet, J., et al., *NtPDR1, a plasma membrane ABC transporter from Nicotiana tabacum, is involved in diterpene transport*. Plant Mol Biol, 2013. **82**(1-2): p. 181-92.
12. Sasse, J., et al., *Petunia hybrida PDR2 is involved in herbivore defense by controlling steroidal contents in trichomes*. Plant Cell Environ, 2016. **39**(12): p. 2725-2739.
13. Shibata, Y., et al., *The Full-Size ABCG Transporters Nb-ABCG1 and Nb-ABCG2 Function in Pre- and Postinvasion Defense against Phytophthora infestans in Nicotiana benthamiana*. Plant Cell, 2016. **28**(5): p. 1163-81.
14. Kobae, Y., et al., *Loss of AtPDR8, a plasma membrane ABC transporter of Arabidopsis thaliana, causes hypersensitive cell death upon pathogen infection*. Plant Cell Physiol, 2006. **47**(3): p. 309-18.
15. Bessire, M., et al., *A member of the PLEIOTROPIC DRUG RESISTANCE family of ATP binding cassette transporters is required for the formation of a functional cuticle in Arabidopsis*. Plant Cell, 2011. **23**(5): p. 1958-70.
16. Lee, M., et al., *AtPDR12 contributes to lead resistance in Arabidopsis*. Plant Physiol, 2005. **138**(2): p. 827-36.
17. Kim, D.Y., et al., *The ABC transporter AtPDR8 is a cadmium extrusion pump conferring heavy metal resistance*. Plant J, 2007. **50**(2): p. 207-18.
18. Ito, H. and W.M. Gray, *A gain-of-function mutation in the Arabidopsis pleiotropic drug resistance transporter PDR9 confers resistance to auxinic herbicides*. Plant Physiol, 2006. **142**(1): p. 63-74.
19. Strader, L.C. and B. Bartel, *The Arabidopsis PLEIOTROPIC DRUG RESISTANCE8/ABCG36 ATP binding cassette transporter modulates*

- sensitivity to the auxin precursor indole-3-butyric acid. *Plant Cell*, 2009. **21**(7): p. 1992-2007.
20. Kang, J., et al., *PDR-type ABC transporter mediates cellular uptake of the phytohormone abscisic acid*. *Proc Natl Acad Sci U S A*, 2010. **107**(5): p. 2355-60.
  21. Ruzicka, K., et al., *Arabidopsis PIS1 encodes the ABCG37 transporter of auxinic compounds including the auxin precursor indole-3-butyric acid*. *Proc Natl Acad Sci U S A*, 2010. **107**(23): p. 10749-53.
  22. Kretschmar, T., et al., *A petunia ABC protein controls strigolactone-dependent symbiotic signalling and branching*. *Nature*, 2012. **483**(7389): p. 341-4.
  23. Jasinski, M., et al., *A plant plasma membrane ATP binding cassette-type transporter is involved in antifungal terpenoid secretion*. *Plant Cell*, 2001. **13**(5): p. 1095-107.
  24. Yu, F. and V. De Luca, *ATP-binding cassette transporter controls leaf surface secretion of anticancer drug components in Catharanthus roseus*. *Proc Natl Acad Sci U S A*, 2013. **110**(39): p. 15830-5.
  25. Demessie, Z., et al., *The ATP binding cassette transporter, VmTPT2/VmABCG1, is involved in export of the monoterpene indole alkaloid, vincamine in Vinca minor leaves*. *Phytochemistry*, 2017. **140**: p. 118-124.
  26. Fu, X., et al., *AaPDR3, a PDR Transporter 3, Is Involved in Sesquiterpene beta-Caryophyllene Transport in Artemisia annua*. *Front Plant Sci*, 2017. **8**: p. 723.
  27. Pierman, B., et al., *Activity of the purified plant ABC transporter NtPDR1 is stimulated by diterpenes and sesquiterpenes involved in constitutive and induced defenses*. *J Biol Chem*, 2017. **292**(47): p. 19491-19502.
  28. Toussaint, F., et al., *Purification and biochemical characterization of NpABCG5/NpPDR5, a plant pleiotropic drug resistance transporter expressed in Nicotiana tabacum BY-2 suspension cells*. *Biochem J*, 2017. **474**(10): p. 1689-1703.
  29. Badri, D.V., et al., *An ABC transporter mutation alters root exudation of phytochemicals that provoke an overhaul of natural soil microbiota*. *Plant Physiol*, 2009. **151**(4): p. 2006-17.
  30. Kang, J., et al., *Absciscic acid transporters cooperate to control seed germination*. *Nat Commun*, 2015. **6**: p. 8113.
  31. Grillitsch, K., et al., *Isolation and characterization of the plasma membrane from the yeast Pichia pastoris*. *Biochim Biophys Acta*, 2014. **1838**(7): p. 1889-97.
  32. Serrano, R., *H<sup>+</sup>-ATPase from plasma membranes of Saccharomyces cerevisiae and Avena sativa roots: purification and reconstitution*. *Methods Enzymol*, 1988. **157**: p. 533-44.
  33. Tschopp, J.F., et al., *Expression of the lacZ gene from two methanol-regulated promoters in Pichia pastoris*. *Nucleic Acids Res*, 1987. **15**(9): p. 3859-76.
  34. Kang, J., et al., *Absciscic acid transporters cooperate to control seed germination*. *Nature Communications*, 2015. **6**.
  35. Noe, J., B. Stieger, and P.J. Meier, *Functional expression of the canalicular bile salt export pump of human liver*. *Gastroenterology*, 2002. **123**(5): p. 1659-66.
  36. Vu, K., et al., *The functional expression of toxic genes: lessons learned from molecular cloning of CCH1, a high-affinity Ca<sup>2+</sup> channel*. *Anal Biochem*, 2009. **393**(2): p. 234-41.
  37. Infed, N., et al., *Influence of detergents on the activity of the ABC transporter LmrA*. *Biochim Biophys Acta*, 2011. **1808**(9): p. 2313-21.
  38. McDevitt, C.A., et al., *Purification and 3D structural analysis of oligomeric human multidrug transporter ABCG2*. *Structure*, 2006. **14**(11): p. 1623-32.

39. Ellinger, P., et al., *Detergent screening and purification of the human liver ABC transporters BSEP (ABCB11) and MDR3 (ABCB4) expressed in the yeast Pichia pastoris*. PLoS One, 2013. **8**(4): p. e60620.
40. Gustot, A., et al., *Lipid composition regulates the orientation of transmembrane helices in HorA, an ABC multidrug transporter*. J Biol Chem, 2010. **285**(19): p. 14144-51.
41. Reimann, S., et al., *Interdomain regulation of the ATPase activity of the ABC transporter haemolysin B from Escherichia coli*. Biochem J, 2016. **473**(16): p. 2471-83.
42. Stindt, J., et al., *Heterologous overexpression and mutagenesis of the human bile salt export pump (ABCB11) using DREAM (Directed REcombination-Assisted Mutagenesis)*. PLoS One, 2011. **6**(5): p. e20562.
43. Chloupkova, M., et al., *Expression of 25 human ABC transporters in the yeast Pichia pastoris and characterization of the purified ABCC3 ATPase activity*. Biochemistry, 2007. **46**(27): p. 7992-8003.
44. Cereghino, J.L. and J.M. Cregg, *Heterologous protein expression in the methylotrophic yeast Pichia pastoris*. FEMS Microbiol Rev, 2000. **24**(1): p. 45-66.
45. Hilt, W. and D.H. Wolf, *Stress-induced proteolysis in yeast*. Mol Microbiol, 1992. **6**(17): p. 2437-42.
46. Xiao, A., et al., *Improvement of cell viability and hirudin production by ascorbic acid in Pichia pastoris fermentation*. Appl Microbiol Biotechnol, 2006. **72**(4): p. 837-44.
47. Waterham, H.R., et al., *Isolation of the Pichia pastoris glyceraldehyde-3-phosphate dehydrogenase gene and regulation and use of its promoter*. Gene, 1997. **186**(1): p. 37-44.
48. Delroisse, J.M., et al., *Expression of a synthetic gene encoding a Tribolium castaneum carboxylesterase in Pichia pastoris*. Protein Expr Purif, 2005. **42**(2): p. 286-94.

## Supplementary Information

### Supplementary Table 1: List of used detergents.

DB1, Detergent screen with AtABCG30 crude membrane; DB2, Detergent screen with AtABCG30 plasma membrane; N, nonionic; Z, zwitterionic; A, anionic; C, cationic, cmc, critical micellar concentration.

Position DB1	Position DB2	Detergent	cmc [%]	used [%]	Nature
	A1	Anameg®-7	0.65	1 %	N
A1	A2	Anapoe®-20	0.0072	1 %	N
A2	A3	Anapoe®-35	0.001	1 %	N
A3	A4	Anapoe®-58	0.00045	1 %	N
A4	A5	Anapoe®-80	0.0016	1 %	N
A5	A6	Anapoe®-C10E6	0.025	1 %	N
A6	A7	Anapoe®-C10E9	0.053	1 %	N
A7	A8	Anapoe®-C12E8	0.0048	1 %	N
A8	A9	Anapoe®-C12E9	0.003	1 %	N
A9	A10	Anapoe®-C12E10	0.2	1 %	N
A10	B1	Anapoe®-C13E8	0.0055	1 %	N
B1	B2	Anapoe®-X-100	0.015	1 %	N
B2	B3	Anapoe®-X-114	0.011	1 %	N
B3	B4	Anapoe®-X-305	-	1 %	N
B4	B5	Anapoe®-X-405	0.16	1 %	N
B5	B6	Big CHAP	0.25	1 %	N
B6	B7	Big CHAP deoxy	0.12	1 %	N
	B8	CYGLU®-3	0.86	2 %	N
B7	B9	CYMAL®-1	15	2 %	N
B8	B10	CYMAL®-2	5.4	2 %	N
B9	C1	CYMAL®-3	0.37	1 %	N
B10	C2	2,6-Dimethyl-4-heptyl-β-D-maltose	1.2	2 %	N
C1	E7	2-propyl-1-pentyl maltose	1.9	2 %	N
C2	D6	MEGA-8	2.5	2 %	N
C3	E3	n-Octyl-β-D-glucoside	0.53	2 %	N
C4	D10	n-Nonyl-β-D-glucoside	0.2	1 %	N
C5	E5	n-Octyl-β-D-maltoside	0.89	2 %	N
C6	E1	n-Nonyl-β-D-maltoside	0.28	2 %	N
C7	C3	n-Decyl-α-D-maltoside	-	1 %	N
	C4	n-Decyl-β-D-maltopyranoside	0.087	2 %	N
C8	E9	n-Tetradecyl-β-D-maltoside	0.00054	1 %	N
C9	F2	n-Undecyl-α-D-maltoside	0.029	1 %	N
C10	F3	n-Undecyl-β-D-maltoside	0.029	1 %	N
D1	C6	n-Dodecyl-α-D-maltoside	0.0076	1 %	N
D2	C7	n-Dodecyl-β-D-maltoside	0.0087	1 %	N
	F1	n-Tridecyl-β-D-maltoside	0.0017	1 %	N
D3	C8	n-Heptyl-β-D-thioglucoside	0.85	2 %	N
	C9	n-Heptyl-β-D-Glucopyranoside	1.9	2 %	N
D4	E4	n-Octyl-β-D-thiomaltoside	0.4	2 %	N
	C10	n-Nonyl-β-D-thiomaltoside	0.15	1 %	N



D5	C5	n-Decyl-β-D-thiomaltoside	0.045	1 %	N
	F4	n-Undecyl-β-D-thiomaltoside	0.011	1 %	N
D6	D1	n-Dodecyl-β-D-thiomaltoside	0.0026	1 %	N
D7	E6	Pentaethylene glycol monodecylether(C10E5)	0.031	1 %	N
D8	E10	Tetraethylene glycol monoethylether(C8E4)	0.25	1 %	N
	E2	Octaethylene Glycol Monodecyl Ether (C12E8)	0.0048	1 %	N
D9		Sucrose monododecanoate	0.016	1 %	N
D10		Dimethyldecylphosphine oxide	0.1	1 %	N
E1		Tripglu	3.6	2 %	N
	D7	Hexaethylene Glycol Monoethyl Ether (C8E6)	0.39	1 %	N
	D8	n-Hexyl-β-D-Glucopyranoside	6.6	2 %	N
	D9	n-Hexyl-β-D-Maltopyranoside	8.9	2 %	N
	D2	CYMAL 4	0.12	2 %	N
E2		CYGLU®-4	0.058	2 %	N
E3	D3	CYMAL®-5	0.12	2 %	N
	D4	CYMAL 6	0.028	1 %	N
E4		MEGA-10	0.21	2 %	N
E6		NP40	0.05	1 %	N
E7		Cyclohexyl-n-hexyl-β-D-maltoside	-	1 %	N
	D5	CYMAL 7	0.0099	1 %	N
	E8	Sucrose Monododecanoate	0.016	1 %	N
	F6	Anzergent 3-8	10.9	2 %	Z
E8	F7	Anzergent® 3-10	1.2	2 %	Z
E9	F8	Anzergent®3-12	0.094	1 %	Z
E10	F9	Anzergent® 3-14	0.007	1 %	Z
	F10	CHAPS	0.49	2 %	Z
F1	G1	CHAPSO	0.5	2 %	Z
F2		C-DODECAFOS™	0.77	2 %	Z
F3	G2	Cyclofos™-4	0.45	2 %	Z
F4	G3	Cyclofos™-5	0.15	1 %	Z
F5	H2	Cyclofos™-6	0.094	1 %	Z
	G5	Cyclofos™-7	0.022	1 %	Z
F6	G6	Cyclofos™-2	7.5	1 %	Z
	G7	Fos-Choline®-9	1.2	2 %	Z
	G4	Fos-Choline-10	1.2	2 %	Z
F7	G9	Cyclofos™-3	1.3	2 %	Z
F8	G10	Fos-Choline®-11	0.062	1 %	Z
F9	H1	Fos-Choline®-12	0.047	1 %	Z
F9	G10	Fos-Choline®-13	0.027	1 %	Z
F10	H3	Fos-Choline®-14	0.0046	1 %	Z
G1	H4	Fos-Choline®-15	0.0027	1 %	Z
G2	H5	Fos-Choline®-16	0.00053	1 %	Z
G3	H6	Fos-Choline®-Iso-9	0.99	2 %	Z
G4	H7	Fos-Choline®-Iso-11	0.9	2 %	Z
G5		Fos-Choline®-Iso-11-6U	0.87	2 %	Z
G6	H8	Fos-Choline®-Unisat-11-10	0.21	1 %	Z
G7	H9	Fos-Choline®-8	3.4	2 %	Z
G8		Fosfen™-9	0.014	1 %	Z
G9		Nopol-Fos™	1.4	2 %	Z

G10	I7	PMAL™-C8	-	1 %	Z
H1		PMAL™-C10	-	1 %	Z
H2	F5	n-Decyl-N,N-dimethylglycine	0.46	2 %	Z
H3	H10	n-Dodecyl-N,N-dimethylglycine	0.041	1 %	Z
	I1	n-Dodecyl-N,N-dimethylamine-N-oxide (DDAO)	0.023	1 %	Z
H4	I2	n-Tetradecyl-N,N-dimethylamine-N-oxide (TDAO)	0.0075	1 %	Z
H5		n-Dodecyl-N, N-dimethylamine-N-oxide	0.023	1 %	Z
H6		Tripao	4.5	2 %	Z
H7		n-Tetradecyl-N, N-dimethylamine-N-oxide	0.0075	1 %	Z
H8		LAPAO	0.052	2 %	Z
H9		PMAL™-C-12	-	2 %	Z
H10		2-Carboxy-w-heptadecenamidopropyldimethylamine	-	1 %	Z
	I3	Cholic acid, sodium salt	0.60	1 %	A
I1	I4	Deoxycholic acid, sodium salt	0.24	1 %	A
I2		Sodium cholate	0.41	2 %	A
	I5	Fosmea®-8	0.59	1 %	A
I3	I6	Fosmea®-10	0.15	1 %	A
I4	I8	Sodium dodecanoyl sarcosine	0.42	2 %	A
I5		n-Dodecyl-beta-iminodipropionic acid, monosodium			
I6		Decyltrimethylammonium chloride	0.07	1 %	C
I7		Dodecyltrimethylammonium chloride	0.0012	1 %	C
I8		Hexadecyltrimethylammonium chloride	0.000102	1 %	C
I9		Tetradecyltrimethylammonium chloride	0.0009	1 %	C
I10		N, N-dimethyl(3-carboxy-4-dodec-5-ene)	-	1 %	C

### 3.3 Chapter III – ABCG1 from *Arabidopsis thaliana*

Title: ABCG1 is involved in suberin barrier formation in *Arabidopsis thaliana*

Authors: Kalpana Shanmugarajah, Nicole Linka, Katharina Gräfe, Sander H. J. Smits,  
Andreas P. M. Weber, Jürgen Zeier and Lutz Schmitt

Published in: In preparation

Own work: 70 %

Cloning of AtABCG1-EQ/HA

Expression and purification of AtABCG1 and AtABCG1-EQ/HA

Determination of the native oligomeric state

Alignments for identification of potential substrates

Enzymatic characterization and substrate identification by ATPase Assays

Identification of *atabcg1* mutant plant lines

Root suberin analysis of *atabcg1* mutant and wildtype plants by GC-MS

Writing of the manuscript

**ABCG1 is involved in suberin barrier formation in  
*Arabidopsis thaliana***

***Kalpana Shanmugarajah<sup>1,4</sup>, Nicole Linka<sup>2</sup>, Katharina Gräfe<sup>1,4</sup>, Sander H. J. Smits<sup>1</sup>,  
Andreas P. M. Weber<sup>2,4</sup>, Jürgen Zeier<sup>3,4</sup> and Lutz Schmitt<sup>1,4\*</sup>***

<sup>1</sup>Institute of Biochemistry, Heinrich-Heine-University, Düsseldorf, Germany

<sup>2</sup>Institute of Plant Biochemistry, Heinrich-Heine-University Düsseldorf, Germany

<sup>3</sup>Institute for Molecular Ecophysiology of Plants, Heinrich-Heine-University, Düsseldorf, Germany

<sup>4</sup>Cluster of Excellence on Plant Sciences (CEPLAS), Heinrich-Heine University, Düsseldorf, Germany

For correspondence  
lutz.schmitt@hhu.de

## Abstract

Diffusion barriers facilitate plant survival under changing environmental conditions by controlling internal water balance and protection against biotic or abiotic stress factors. A subset of *Arabidopsis* half-size transporters was found to be involved in root suberin deposition. Further clade members, AtABCG1 and AtABCG16, are part of pollen wall formation as well as postmeiotic development, but it is unknown if they are also involved in suberin deposition. Plant mutant analysis and substrate identities could give further insight into their roles.

In this study, we have established an expression and purification protocol for AtABCG1. The basal activity of purified AtABCG1 was stimulated by fatty alcohols (C<sub>26</sub>-C<sub>30</sub>) up to 90 % and fatty acids (C<sub>24</sub>-C<sub>30</sub>) up to 80% in a chain length dependent manner. In accordance, *atabcg1* mutant analysis demonstrated a changed root suberin composition. These results indicate that AtABCG1 is not only involved in pollen wall formation, but also in root suberin formation.

## Introduction

The ATP-binding cassette (ABC) transporters are ubiquitously expressed and able to transport diverse substrates across a biological membranes [1]. The core unit of a functional ABC transporter is defined by the presence of two nucleotide-binding domains (NBDs) and two transmembrane domains (TMDs). The NBDs provide the energy by ATP binding and hydrolysis while the TMDs mediate the substrate recognition and translocation. Characteristic features of the NBDs are several highly conserved motifs such as the Walker A and B sequences, the ABC signature motif, the D, H and the Q loop. In contrast, TMDs are composed of several hydrophobic  $\alpha$ -helices [2]. Based on the number of domains, which are encoded on a single gene, ABC transporters are categorized as full-size (TMD-NBD)<sub>2</sub> or half-size transporters (TMD-NBD). Half-size transporters have to homo- or heterodimerize in order to form the functional transport unit [3].

Remarkably, plants exhibit a rich source of ABC proteins with for example 130 genes in *Arabidopsis thaliana* that are classified into eight subfamilies [4, 5]. Among these, the ABCG subfamily is the largest subfamily, with 28 half-size (white brown complex, WBC) and 15 full-size (pleiotropic drug resistance, PDR) transporters. The characteristic feature of the ABCG subfamily is the inverse domain organization where the NBDs are encoded N-terminally to the TMDs [5].

Half-size ABCGs in *A. thaliana* have been found to be involved in antibiotic resistance [6, 7], ABA and cytokinin transport [8-13] or stomatal regulation in guard cells [14, 15]. Notably, the majority of the analyzed half-size AtABCGs have been shown to be part of diffusion barrier formation. Diffusion barriers, such as cutin or suberin which are deposited in the cell wall enable plants to cope with water loss or serve as protective layers against many environmental stress factors, including drought and pathogen attack [16]. Several half-size AtABCG transporters have been shown to be involved in pollen protection. Thereby, AtABCG26 has been shown to be important for exine formation, while a double mutant analysis of AtABCG1 and AtABCG16 indicated a role in pollen nexine and intine layer formation as well as postmeiotic pollen development [17-23]. Additionally, AtABCG9 acts together with the full-size transporter AtABCG31 in pollen coat maturation [24]. In some cases, ABCG half-size transporters from the same phylogenetic clade act together in order to build up specific diffusion barriers. For example, AtABCG11, AtABCG12 and AtABCG13 are involved in cutin formation

[4, 25-30]. Another clade is formed by AtABCG1, AtABCG16, AtABCG2, AtABCG6 and AtABCG20. Amongst these, all clade members except for AtABCG1 and AtABCG16 were reported to be part of suberin formation in *Arabidopsis* roots and seeds [4, 23, 31]. Recently, sequence comparison of all AtABCGs with a potential suberin precursor transporter, StABCG1 (*Solanum tuberosum*), revealed that AtABCG1 and AtABCG16 share the highest sequence identity [32]. But so far, single *atabcg1* as well as *atabcg16* mutant analysis are lacking.

This study demonstrates first, the heterologous overexpression and purification of AtABCG1. Next, ATPase assays and phenotypic analysis of *atabcg1* mutants revealed that AtABCG1 transports specific fatty acids and fatty alcohols and thus contributes to suberin barrier formation in the roots.

## Methods

### *In vitro* characterization of AtABCG1

#### Native PAGE of AtABCG1

The native oligomeric state of AtABCG1 was determined by native gel electrophoresis using a 4-16 % Native PAGE Bis-Tris Gel (Invitrogen). Protein bands were visualized by Coomassie brilliant blue staining.

#### Cloning of AtABCG1 for expression in *P. pastoris*

As previously described, a synthetic gene of *AtABCG1* (At2g39350) with codon optimization for expression in *P. pastoris* (Invitrogen) was cloned by In-Fusion into the expression vector pSGP18-Ntag (Gräfe et al. (2018), *submitted*). An ATPase hydrolysis deficient *AtABCG1* mutant was generated by site-directed mutagenesis. First Glu259 in the conserved Walker B motif was replaced by Gln with the primer pairs ABCG1-EQ fwd/rev and additionally His291 of the H-loop was replaced by Ala with the primer pairs ABCG1-HA fwd/rev (Table S 1). Sequences were verified by DNA sequencing (GATC Biotech).

#### Transformation and expression of AtABCG1 in *P. pastoris*

The entire approach is described in detail in Gräfe et al. (2018) (submitted). Briefly, the *P. pastoris* expression constructs pSGP18-AtABCG1-Ntag and pSGP18-AtABCG1-EQ/HA-Ntag were transformed into electrocompetent X33 cells (Life Technologies) and the clones analyzed for expression. Positive clones were fermented in a 15 L table-top glass fermenter (Applikon Biotechnology) according to the Invitrogen *Pichia* fermentation guidelines.

#### Isolation of AtABCG1 crude membranes

100 g wet cells of AtABCG1 expressing *P. pastoris* cells were thawed on ice and re-suspended with lysis buffer (50 mM Tris-HCl, pH 7.5, 150 mM NaCl, 1 mM EDTA, 1 mM EGTA, 0.3 M sucrose) and protein inhibitor cocktail (Roche) was added to a final concentration of 0.5 g cells/ml. The cells were disrupted by two passages through a Cell Disruptor (Constant System) at 2.5 kbar and the cell lysate was centrifuged twice (15,000 x g, 30 min, 4 °C). Subsequently, the supernatant was centrifuged for 1h at



125,000 x g, 4 °C. Crude membranes were re-suspended in buffer A (50 mM Tris-HCl, pH 8, 150 mM NaCl, 15 % glycerol), flash frozen in liquid N<sub>2</sub> and stored at -80 °C until further usage.

### **Solubilization screen via dot blot technique**

AtABCG1 containing crude membranes were thawed on ice and solubilized in 200 µl buffer A. While the membrane concentration was adjusted to 5 mg/ml, detergents were used at 1 % (w/v) or higher depending on their critical micellar concentration (cmc). A list with used detergents is provided in the Supplementary information (Table S 2). The solubilization was carried out for 1 hour at 4°C on a rotator, afterwards samples were centrifuged (100,000 x g, 30 min, 4°C) and the supernatant supplemented with SDS sample buffer. After heating (65°C, 10 min) 3 µl of the respective samples were spotted on a nitrocellulose membrane and dried completely. The membrane was blocked for 1 h in TBS-T with 5 % (w/v) milk powder and the target protein analyzed by immunoblotting (anti-His-tag antibody).

### **Purification of AtABCG1**

The purification of AtABCG1 and AtABCG1-EQ/HA was conducted by calmodulin binding peptide affinity (CBP) chromatography. The crude membrane concentration, equivalent to 50 g wet cells, was adjusted with buffer A to 5 mg/ml. Subsequently, membranes were solubilized with 1.5 % Fos Choline-14 (Anatrace) for 2 hours at 4 °C and centrifuged (125,000 x g, 1 h, 4 °C). The supernatant was diluted 3-times with CBP binding buffer (50 mM Tris-HCl, pH 8, 10 mM CaCl<sub>2</sub> 150 mM NaCl, 1 mM Magnesiumchlorid, 10 % Glycerin) and 2x cmc Fos-Choline-14 and 2 ml CBP resin (Agilent Technologies, Santa Clara, CA) were incubated and the sample was incubated over night at 4 °C on a rotator. The resin was transferred to a gravity flow column (Bio-Rad), washed with CBP binding buffer and eluted with CBP elution buffer (50 mM Tris-HCl, pH 8, 150 mM NaCl, 2 mM EGTA, 10 % Glycerin) in the presence of 2x cmc Fos-Choline-14. The purified protein was immediately used for ATPase activity assays or aliquoted, snap frozen in liquid nitrogen and stored at – 80 °C. For Blue Native PAGE (BN-PAGE), proteins were concentrated with a 100 kDa cutoff protein concentrator (Thermo Scientific™ Pierce™) to their final concentration. Samples were analyzed by Colloidal Coomassie stained SDS-PAGE and immunoblotting.

### **ATPase activity measurements of AtABCG1**

The malachite green assay was performed with the following adaptations as outlined by Baykov *et al.* [33]. Reactions were performed in a total volume of 25 µl in reaction buffer containing 10 mM MgCl<sub>2</sub>. The reaction was started after adding 0.3 -2 µg of the purified protein together with 5 mM ATP, incubated at 25 °C and quenched after 40 min by transfer into 175 µl 20 mM H<sub>2</sub>SO<sub>4</sub>. After adding 50 µl dye solution (0.096% (w/v) malachite green, 1.48% (w/v) ammonium molybdate, and 0.173% (w/v) Tween-20 in 2.36 M H<sub>2</sub> SO<sub>4</sub>) samples were incubated for 10 min at room temperature and the amount of free inorganic phosphate (P<sub>i</sub>) was quantified thereafter by measuring the absorption at 595 nm. Samples without 10 mM MgCl<sub>2</sub> were used to subtract background values and a Na<sub>2</sub>HPO<sub>4</sub> standard curve for free phosphate calibration. For substrate stimulated ATPase activity, substrates were dissolved in chloroform or chloroform/methanol (1:1; v/v) respectively. Therefore, additional control reactions were performed in the presence of the respective solvents. Kinetic parameters were determined at ATP concentrations ranging from 0 to 6 mM. The controls were subtracted for statistical analysis. Kinetic data were fitted using the GraphPad Prism 7 Software according to the Michaelis-Menten equation:

$$v = \frac{v_{max}[S]}{K_m + [S]}$$

Here, v is equivalent to the ATPase activity, v<sub>max</sub> the maximal ATPase activity, S the substrate concentration and K<sub>m</sub> the Michaelis-Menten constant.

### ***Phenotypic analysis of Arabidopsis T-DNA insertion lines***

#### **Plant material and growth conditions**

*Arabidopsis* wildtype plants (ecotype Columbia (Col-0)) and the *Arabidopsis* SAIL T-DNA line SAIL563B03 (*atabcg1-1*) were purchased from the Nottingham Arabidopsis Stock Centre (NASC) ([www.arabidopsis.info](http://www.arabidopsis.info)). The *Arabidopsis* GABI-Kat T-DNA line GK850E07 (*atabcg1-2*) was ordered via GABI-Kat ([www.gabi-kat.de](http://www.gabi-kat.de)). Wildtype and mutant seeds were surface-sterilized for 10 minutes with 70 % (v/v) ethanol and Triton-X-100, followed by 100 % (v/v) ethanol. Seeds were stratified for at least 3 days and germinated on half-strength MS medium with 0.8 % (w/v) plant agar. Plants were

transferred to soil after 14 days and grown under long day conditions (16 h light (100  $\mu\text{mol m}^{-2} \text{s}^{-1}$ ) / 8 h darkness) at 22 °C (day) / 18 °C (night) unless stated otherwise.

### **Identification of homozygote T-DNA insertion lines**

At least 4-week-old soil grown wildtype and *AtABCG1* T-DNA insertion lines were used to identify plants homozygous for the T-DNA insertion. The genomic DNA was isolated using the DNeasy Plant Mini Kit (Qiagen) and genotyped by standard PCR reactions with gene-specific and T-DNA/gene junction specific primer pairs (Table S 1). The actin gene *ACT2* (At3g18780) was amplified as positive control with primer pairs P67/P68. Independent homozygous *atabcg1* mutant plant were further propagated.

### **RT-PCR and qRT-PCR**

Total RNA was isolated from 3-weeks-old MS-agar grown wildtype and *atabcg1-1* and *atabcg1-2* mutant seedlings using the RNeasy Plant Mini Kit (Qiagen). Samples were subjected after DNase treatment (RQ1 RNase-free DNase, Promega) to cDNA synthesis via Luna Script RT-PCR (NEB Biolabs) and thereafter analyzed for presence of full-length *AtABCG1*. Subsequent relative quantification of the *AtABCG1* gene in wildtype and mutant lines was performed using SYBR green-based PCR assay Luna Universal qRT-PCR (NEB Biolab). The primer pairs QP1/QP2, QP3/QP4 and QP7/QP8 were used for gene-specific amplification. The *AtABCG1* expression levels were normalized against those of the Type 2A phosphatase interacting protein 41 (TIP41)-like reference gene (At4g34270) called Black [34]. Transcript level was calculated based on  $\Delta\text{CT}$  values compared to the wild type [35, 36].

### **GC-Analysis of *AtABCG1* T-DNA insertion lines**

Quantitative suberin analysis was performed with 10-week-old soil grown plants (adapted to [37, 38]). Roots were carefully removed from the potting mixture and washed with deionized water to remove contaminants, cut into 5 mm pieces and dried to constant mass at 60°C. 4 mg samples were first extracted with 1 ml chloroform/methanol/water (1:2.5:1; v/v), incubated for 1 h at 50 °C and washed twice with 1 ml methanol. After adding 5  $\mu\text{g}$  internal standards heptadecanoic acid, 1-pentadecanol, 15-hydroxypentadecanoic acid, the suberin molecule was depolymerized by transesterification in 1 ml borontrifluorid in methanol (10 %, Fluka) for 24 h at 70 °C. The methanol lysate was washed twice with 1.5 ml dichloromethane

and 1 ml saturated sodium chloride respectively. The fused organic phases were subjected to solvent extraction with Na<sub>2</sub>SO<sub>4</sub> and extensively dried under inert N<sub>2</sub> gas. Subsequently, 16 µl BSTFA (*N*, *O*-Bis(trimethylsilyl)trifluoroacetamide) and pyridine, respectively, and 80 µl dichloromethane were added. Samples were incubated at 70 °C for 30 min before they were analyzed by GC-MS (DB-1). Suberin compounds were quantified by integration of the resulting ion chromatograms. Thereby, quantifier ions and retention times were used from Table S 3. Heptadecanoic acid was used as internal standard for the quantification of *p*-coumaric acid, ferulic acid, α, ω-dicarboxylic acids and fatty acids, 15-hydroxypentadecanoic acid for ω-hydroxyacids and dihydroxyacids, and 1-pentadecanol for fatty alcohols.

### **Sequence Alignments**

Protein alignments of AtABCG1 (At2g39350); ACT2 (At3g18780); StABCG1, (XP\_006345915) and PhABCG1 (JQ088099) were performed using the CLUSTALW program ([www.ebi.ac.uk/Tools/clustalw](http://www.ebi.ac.uk/Tools/clustalw)) with default settings.

## Results

### Cloning, expression and purification of AtABCG1

As previously reported, *AtABCG1* was successfully cloned and overexpressed in the methylotrophic yeast *P. pastoris* (Gräfe et al. (2018) *submitted*). Next, we generated an ATP hydrolysis deficient *AtABCG1-EQ/HA* mutant by the implementation of one mutation (E259Q) in the Walker B motif and another mutation (H291A) in the H-loop of the NBD [39, 40]. Expression and purification of *AtABCG1* and *AtABCG1-EQ/HA* was performed according to identical protocol. In order to determine a suitable detergent for solubilization of AtABCG1, a detergent screen with 95 detergents (Figure S 1, Table S 1) was implemented via dot-blot technique [41]. After further solubilization tests, the membrane concentration was adjusted to 5 mg/ml and solubilized with 1.5 % (w/v) Fos-Choline-14 for 2 hours at 4 °C. Subsequently, solubilized calmodulin binding-peptide (CBP)-tagged AtABCG1 was purified by CBP chromatography, yielding approximately 2 mg AtABCG1 per 100 g wet cells. Purified fractions were analyzed with respect to purity via Colloidal Coomassie stained SDS-PAGE and identified by immunoblotting using an anti-His antibody (Figure 1).

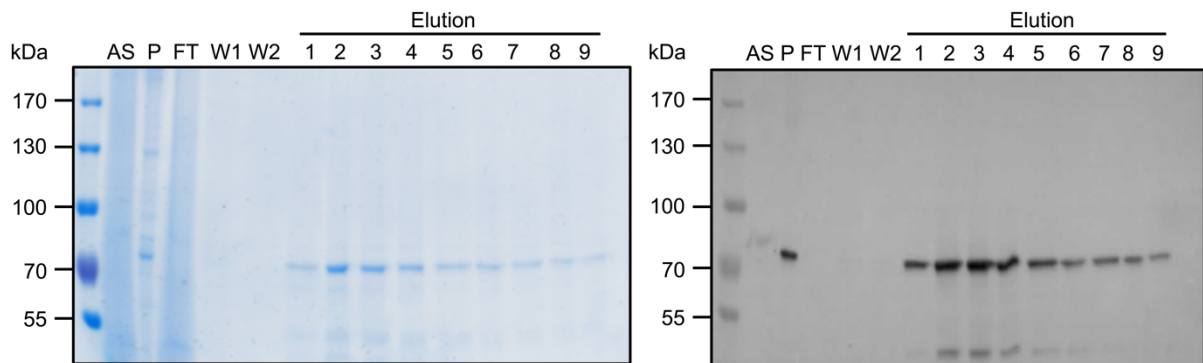


**Figure 1: Calmodulin binding peptide (CBP) purification of AtABCG1.** AtABCG1 was solubilized in Fos Choline-14 and purified by CBP resin. Fractions were analyzed via 7% SDS-PAGE (left panel) or immunoblotting (anti-His-tag antibody, right panel). AtABCG1 has a calculated molecular weight of 86 kDa. The lower 45 kDa band in the elution fractions 2-6 arises as verified by immunoblotting also from AtABCG1 and is likely a degradation product. Pre-stained molecular weight markers are shown on the left. AS, after solubilization; P, pellet; FT, flow through; W1-W2, washing fraction.

### AtABCG1 is a homodimer

Since the AtABCG1 is a half-size transporter, it consists of only a single NBD and a single TMD encoded on the gene. Half-size transporters, have to homo- or heterodimerize in order to form a functional transporter. CBP-purified AtABCG1 migrates on SDS-PAGE as monomer with an approximate molecular weight of 86 kDa (Figure 1). The corresponding BN-PAGE (Figure 2) demonstrated that the native oligomeric state of AtABCG1 was dimeric and the oligomerization was not reversed by addition of 1% SDS. A complete monomerization was not observed even in the presence of 3 % SDS, which indicates that AtABCG1 is a stable homodimer, which requires the denaturing conditions of an SDS-PAGE for quantitative monomerization. The supplementation with 2 or 5 cmc Fos Choline-14 had no impact on the protein stability. Further faint bands around 480 kDa could descend from impurities or protein aggregation (dimer/dimer). Hence AtABCG1 is mainly present as a homodimer and further protein-protein interaction studies might reveal potential interaction partners that would results in heterodimerization as described for AtABCG11 and AtABCG12 [42].

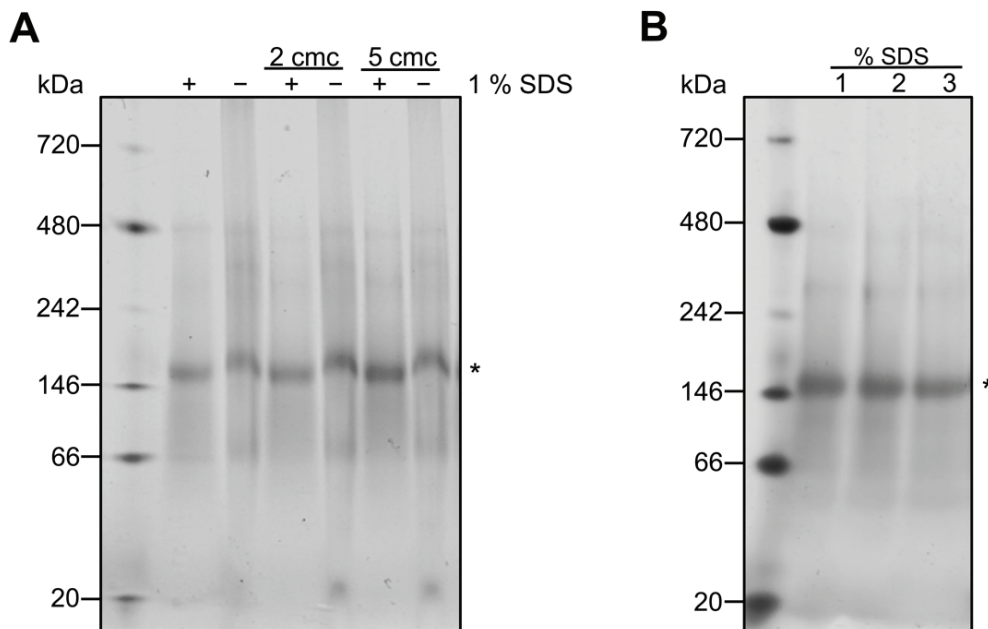


**Figure 2: Native oligomeric state of AtABCG1.** CBP purified AtABCG1 was subjected to 4-16 % Bis-Tris BN-PAGE. *A*, Samples were analyzed in different Fos Choline-14 concentration (0x cmc, 2x cmc, 5x cmc). Native AtABCG1 partially migrates under SDS substitution mainly with 172 kDa as homodimeric ( ) protein. *B*, Samples were submitted with 2x cmc Fos-Choline 14 and analyzed in different SDS-concentration (1 %, 2 %, 3 %). A molecular weight marker is shown in the left. +, samples substituted with 1 % SDS; -, samples without SDS.

### ATPase activity of purified AtABCG1

The malachite green based ATPase assay was employed to analyze the specific activity of detergent-purified AtABCG1. Background activity from impurities was determined by the ATPase hydrolysis deficient mutant AtABCG1-EQ/HA and subtracted prior to analysis. The concentration of purified AtABCG1 and AtABCG1-EQ/HA was kept constant in the assay, while ATP concentration was varied from 0 mM to 8 mM. Subsequently, data analysis was performed according to the Michaelis-Menten equation (see Materials and Methods). Wildtype AtABCG1 exhibited a maximal reaction velocity  $v_{\max}$  of  $17.1 \pm 0.1$  nmol min<sup>-1</sup> per mg purified AtABCG1 and a  $K_m$  value of  $1.8 \pm 0.1$  mM (Figure 3, Table 1). It has been often reported that solubilization in milder detergents or detergent exchange during purification can lead to higher specific activity [43, 44]. However, neither changing the detergent during CBP purification nor size exclusion chromatography with simultaneous exchange of Fos-Choline 14 to milder detergents, resulted in increased ATPase activity.

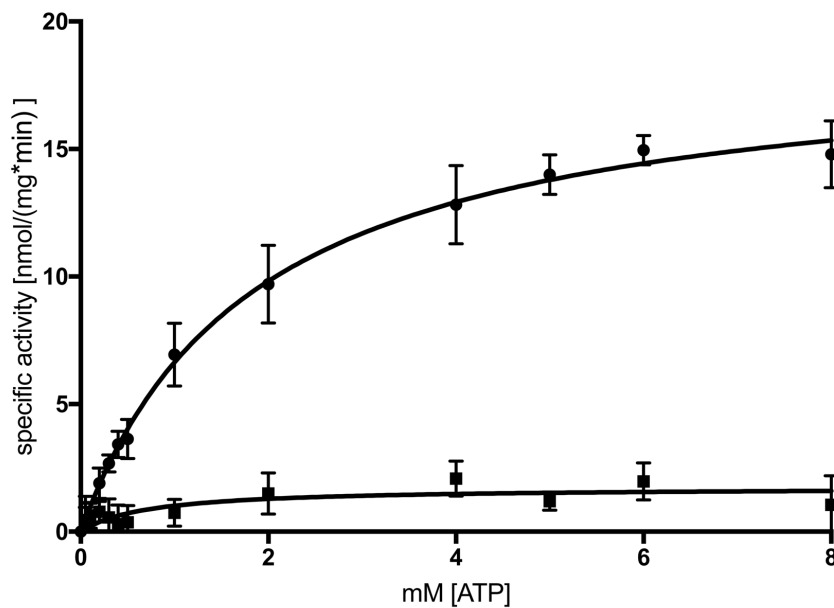


**Figure 3: ATPase activity of purified AtABCG1 and AtABCG1-EQ/HA mutant.** The ATPase activity of CBP purified AtABCG1 and the EQ/HA mutant was measured in presence of 0 to 8 mM ATP. Data was analyzed according to Michaelis-Menten equation and represents mean and  $\pm$  SD of at least three independent replicates.

**Table 1: Kinetic parameters of AtABCG1 and AtABCG1-EQ/HA.**

Protein	K <sub>m</sub> [mM]	v <sub>max</sub> [nmol/(mg*min)]
AtABCG1	1.8 ± 0.1	18.8 ± 0.4
AtABCG1-EQ/HA	0.7 ± 0.4	1.7 ± 0.3

### Substrate stimulated ATPase activity of AtABCG1

So far, detailed reports on potential AtABCG1 substrates are lacking. In order to further infer the physiological role of AtABCG1, sequence comparison with selected ABCG1 transporters from other plants was performed (Figure S 2). While StABCG1 is involved in suberin formation, PhABCG1 has been reported to mediate volatile transport [32, 45]. AtABCG1 shares with 74 %, the highest amino acid identity with StABCG1 and only 31 % with PhABCG1 (Figure S 2). Separate NBD and TMD alignments exhibited a similar result with 69 % and 81 % identity for StABCG1 and 33 % and 26 % for PhABCG1.

To analyze whether *A. thaliana* AtABCG1 is involved in suberin formation, ATPase activity measurements were performed in the presence of suberin precursor molecules (Figure S 3). Fatty alcohols and acids with chain length of C<sub>16</sub> to C<sub>30</sub> were analyzed and a significant effect was seen for C<sub>26</sub> to C<sub>30</sub> and C<sub>24</sub> to C<sub>30</sub>, respectively (Figure 4 A). The effect of 1-tetracosanol (C<sub>24</sub>) was not analyzed as it precipitated under the applied assay conditions.

As summarized in Figure 4 B and C, further assays with varying substrate concentration ranging from 0 µM to 65 µM revealed stimulatory effects according to Michael-Menten equation suggesting that these compounds represent substrates of AtABCG1. In detail, ATPase activity was stimulated by 1-hexacosanol (50.7 ± 4.0 %), 1-octacosanol (90.1 ± 4.8 %), 1-triacontanol (69.6 ± 5.1 %), tetracosanoic acid (46.1 ± 5.2 %), hexacosanoic acid (78.5 ± 3.3 %), octacosanoic acid (49.5 ± 3.2 %) and tricontanoic acid (32.3 ± 0.8 %) (Table 2). Thereby, 1-triacontanol and tetracosanoic acid displayed a K<sub>m</sub> value with 5.3 ± 1.2 µM and 5.4 ± 2.1 µM, respectively. A correlation between kinetic values and chain length was only partially observed. The stimulatory effect increased with the substrate chain length up to 1-octococanol (C<sub>28</sub>) and hexacosanoic acid (C<sub>26</sub>), respectively and decreased thereafter.



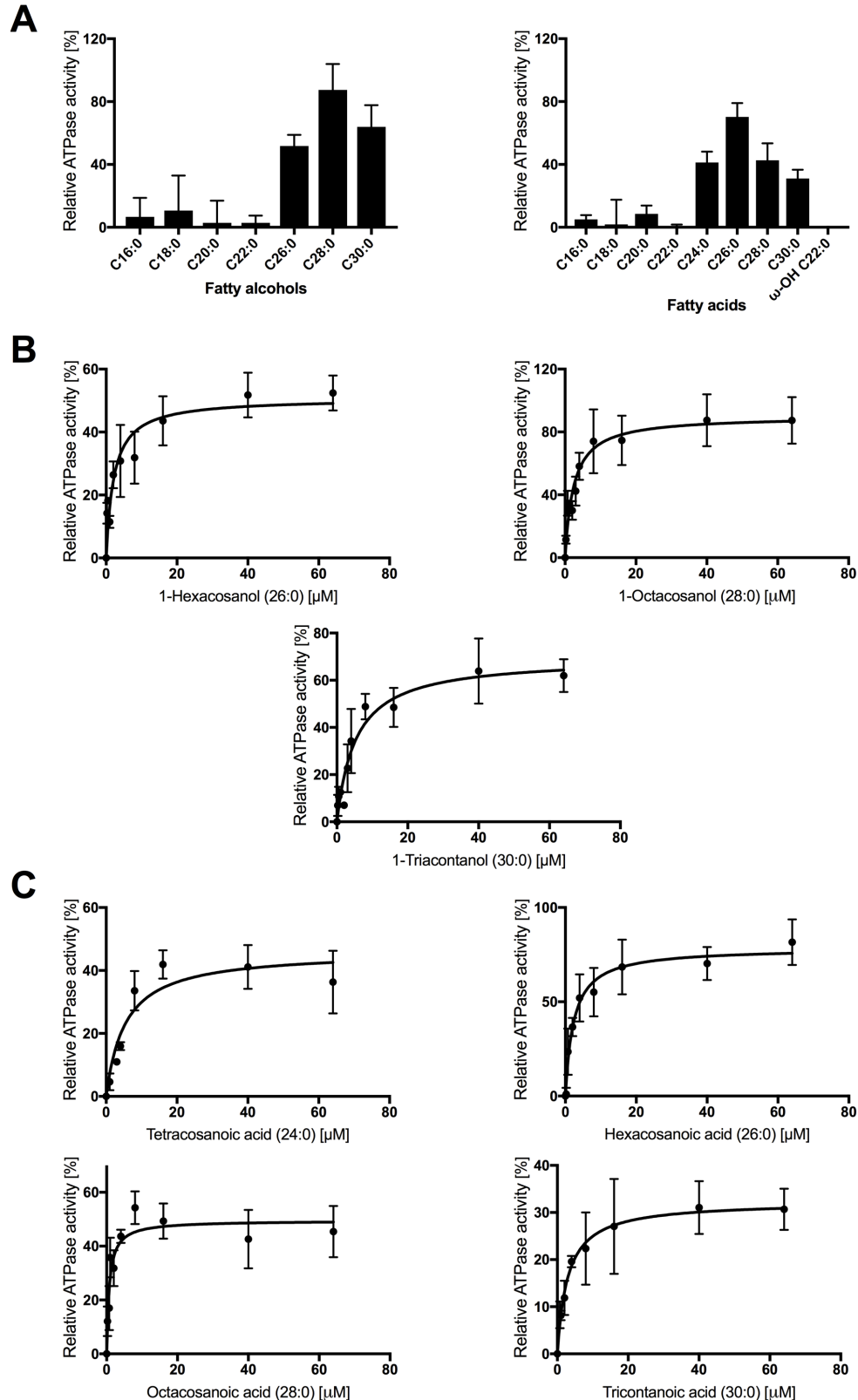


**Figure 4: Substrate stimulated AtABCG1 ATPase activity.** A, Relative ATPase activity of AtABCG1 in presence of 40 μM fatty acids and fatty alcohols (C<sub>16</sub>- C<sub>30</sub>). B-C, Concentration dependent relative AtABCG1 activity in the presence of fatty acids (C<sub>24</sub>- C<sub>30</sub>) and fatty alcohols (C<sub>26</sub>- C<sub>30</sub>). The ATPase activity of the EQ/HA mutant was subtracted and data fitted according to Michaelis-Menten kinetics. Data represent mean and ± SD of at least three independent replicates.

**Table 2: AtABCG1 stimulation in presence of fatty alcohols and fatty acids.**

Substrate	K <sub>m</sub> [μM]	v <sub>max</sub> [%]
<i>Fatty alcohols</i>		
1-Hexacosanol (26:0)	2.1 ± 0.7	50.7 ± 4.0
1-Octacosanol (28:0)	2.4 ± 0.4	90.1 ± 4.8
1-Triacontanol (30:0)	5.3 ± 1.2	69.6 ± 5.1
<i>Fatty acids</i>		
Tetracosanoic acid (24:0)	5.4 ± 2.1	46.1 ± 5.2
Hexacosanoic acid (26:0)	2.3 ± 0.4	78.5 ± 3.3
Octacosanoic acid (28:0)	0.7 ± 0.2	49.5 ± 3.2
Tricontanoic acid (30:0)	2.9 ± 0.2	32.3 ± 0.8

Based on these results, we examined whether the specific activity of AtABCG1 was affected by potential PhABCG1 substrates, since AtABCG1 is also highly expressed in the flowers [23]. AtABCG1 specific ATP hydrolysis was not changed in presence of the volatile methyl benzoate. The analysis of another potential PhABCG1 substrate, benzyl alcohol, was not possible in our assay due to its viscos character.

However, the above reported results revealed potential AtABCG1 substrates and thus our results strongly indicate an involvement of AtABCG1 in suberin or suberin-like substance formation. However, it has to be taken in account that the used substrates were not isolated from the initially analyzed plants. Consequently, *atabcg1* knock-out mutant studies were performed.

### **Effect of AtABCG1 knock-out on *Arabidopsis* root suberin composition**

To investigate the role of AtABCG1 in root suberin formation, two independent T-DNA *A. thaliana* insertional mutants in Col-0 type, *atabcg1-1* (SAIL563B03) and *atabcg1-2* (GK850E07), were obtained from Nottingham Arabidopsis Stock Center and GABI-Kat, respectively. Homozygous *atabcg1-1* and *atabcg1-2* mutant plants were identified by genomic PCR and further analyzed by qRT-PCR (Figure 5). Both homozygous mutant plants were verified as AtABCG1 knock-out lines, since the full-length *AtABCG1* transcript was absent in *atabcg1-2* and *atabcg1-2* (Figure S 4). Based on qRT-PCR analysis using primer binding downstream of the T-DNA the *AtABCG1* transcript-level in comparison to the wildtype was decreased up to 95 % in *atabcg1-1*, but *atabcg1-2* showed a 5- to 10-fold increase (Figure 5 C). Enhanced promotor located inside the T-

DNA region can cause a strong expression of the 3' end of the *AtABCG1* mRNA. However, a functional protein cannot be produced due to the interruption of the coding region by T-DNA [46].).

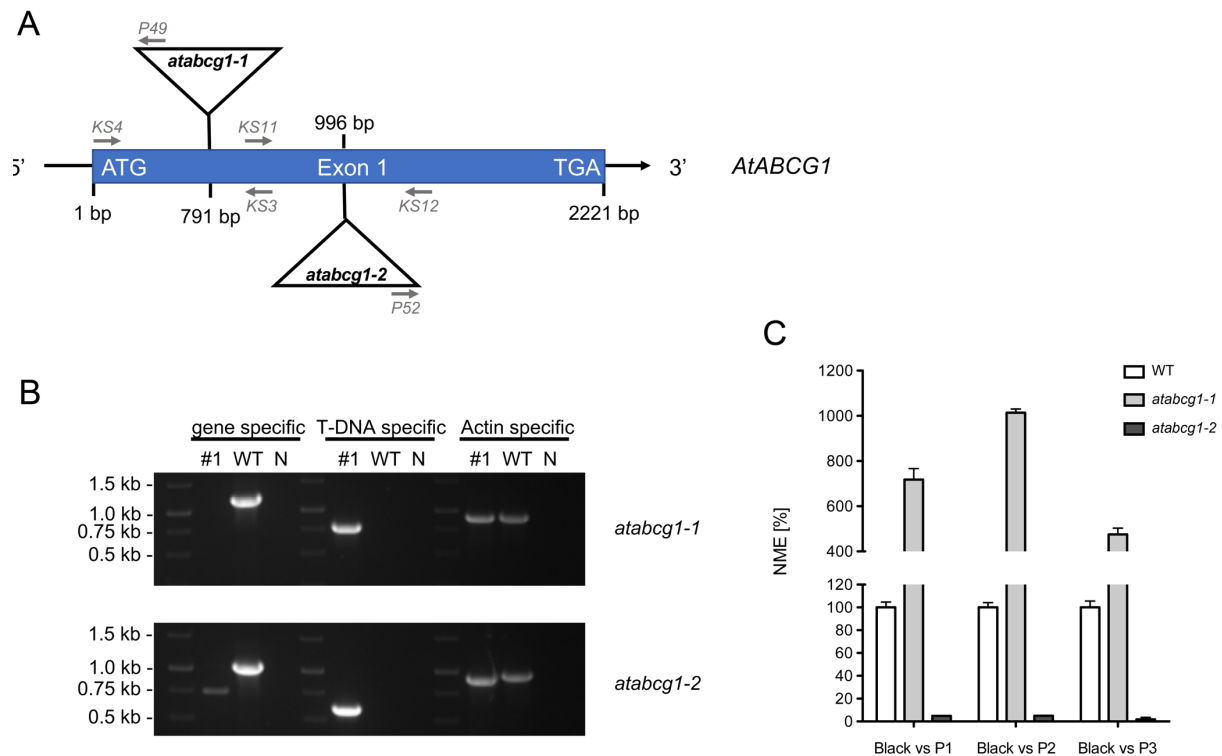


**Figure 5: Characterization of T-DNA insertional *atabcg1* mutant lines.** A: Genomic organization of the two independent T-DNA insertional *atabcg1* mutant lines *atabcg1-1* and *atabcg1-2*. The *atabcg1-1* line contains a T-DNA insertion at 791 bp and the *atabcg1-2* line one at 996 bp. Arrows indicate the primers used for the mutant characterization. B: Genetic analysis of the *atabcg1* mutant lines *atabcg1-1* and *atabcg1-2*. Genomic DNA of wildtype (WT) and mutant lines (#1) were analyzed for *AtABCG1* gene specific, T-DNA specific and actin specific amplification products. N, negative control. C: Relative mRNA transcript level of *AtABCG1* in *atabcg1-1* and *atabcg1-2* was analyzed by QRT-PCR (P1-P3, primer pairs 1-3).

Subsequently, roots from 10 week-soil grown wildtype and both *atabcg1* mutant plants were analyzed to infer the role of *AtABCG1* in *Arabidopsis* root suberin formation. Suberin monomers were extracted from the respective root sample by transesterification and their relative abundance determined by mass spectrometry. The total amount of the identified suberin monomers per dry weight was similar in both wildtype and *atabcg1* mutant lines (Figure S 5). However, comparison of the relative abundance per suberin monomer class for wildtype and both mutant plants revealed

different values for specific  $\alpha,\omega$  dicarboxylic acids, fatty acids and fatty alcohols (Figure 6). The relative abundance of the  $\alpha,\omega$  dicarboxylic acids C<sub>20</sub>, C<sub>22</sub> and C<sub>24</sub> showed in both *atabcg1-1* and *atabcg1-2* mutant lines a chain-length depending decrease from around 90 % to 50 % abundance, whereby the maximal decrease was observed for the C<sub>24</sub>  $\alpha,\omega$  dicarboxylic acid ( $38.5 \pm 9.0$  % for *atabcg1-1*;  $49.4 \pm 4.8$  % for *atabcg1-2*). As described above, we were able to identify by ATPase assays with purified AtABCG1 several suberin precursor monomers with stimulatory effects on the specific ATPase activity of AtABCG1. For instance, the C<sub>26</sub> fatty acid (hexacosanoic acid) stimulated the ATPase activity of purified AtABCG1 up to 80 % ( $78.5 \pm 3.3$  %). In consistent with this observation was the relative abundance of the C<sub>26</sub> fatty acid in *atabcg1* mutant plants of approximately 61 % ( $51.5 \pm 5.7$  % for *atabcg1-1*,  $70.6 \pm 4.7$  % for *atabcg1-2*). While the C<sub>24</sub> fatty acid (tetracosanoic acid) stimulated the ATPase activity of purified AtABCG1 up to 50 % ( $46.1 \pm 5.2$  %), the *atabcg1* mutant plants showed no significant change in its relative abundance ( $96.6 \pm 7.6$  % for *atabcg1-1*;  $86.9 \pm 6.8$  % for *atabcg1-2*). A further compliance was found for the C<sub>26</sub> fatty alcohol (1-hexacosanol), which stimulated the ATPase activity of AtABCG1 up to 50 % ( $50.7 \pm 4.0$ %) and occurs significantly reduced ( $58.6 \pm 11.0$  % for *atabcg1-1*;  $36.4 \pm 0.2$  % for *atabcg1-2*) in AtABCG1 lacking plants. The C<sub>24</sub> fatty alcohol showed a slightly reduced relative abundance ( $87.8 \pm 22.3$  % for *atabcg1-1*;  $86.1 \pm 13.6$  % for *atabcg1-2*), whereas functional assays were due to lacking substrate solubility not performed. Moreover, a remarkable difference was found among both mutant lines for the relative abundance of C<sub>18:2</sub> fatty acid and p-coumaric acid, whereby the amount was two-fold higher and 30 % decreased, respectively in the *atabcg1-1* mutant line ( $171.2 \pm 8.9$  % for C<sub>18:2</sub>;  $88.2 \pm 8.7$  % for p-coumaric acid). Hence it is not clear, if C<sub>18:2</sub> fatty acid and p-coumaric acid are potential AtABCG1 substrates.

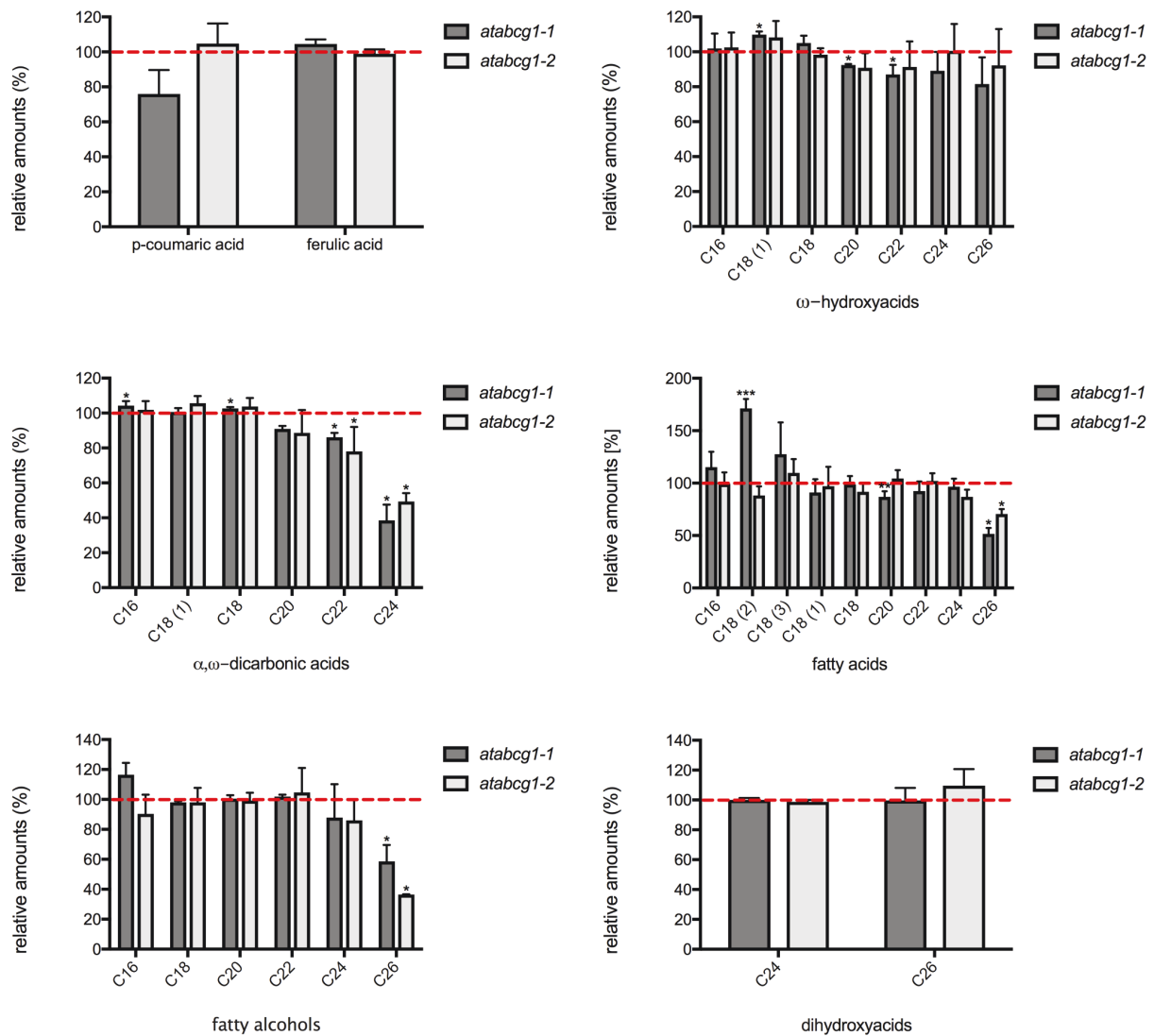


**Figure 6: Monomer composition of *Arabidopsis* wildtype and *atabcg1* mutant root suberin.** The relative abundance of suberin monomers in the independent T-DNA insertional mutant lines *atabcg1-1* (n=4) and *atabcg1-2* (n=4) per substance class is depicted in comparison to the wildtype (n=4). The suberin monomers were quantified using quantifier ions and retention times from Supplemental Table S 2. red, wildtype values set to 100 %. Data represents mean and  $\pm$  SD. Significance analysis between *atabcg1* mutants and wildtype samples were performed by t test. (two-tailed):  $P \leq 0.0001$ ,  $P \leq 0.01$ ,  $P \leq 0.05$ .

To date, several *Arabidopsis* half-size ABC transporters have been shown via mutant analysis to be involved in root suberin barrier formation, including AtABCG2, AtABCG6, AtABCG11 and AtABCG20 [23, 28]. In addition to that, the obtained data for functional assays with heterologous in *P. pastoris* expressed, detergent purified AtABCG1 as well as root suberin analysis of *atabcg1* mutants, provide the first evidence for the involvement of AtABCG1 in root suberin composition. Direct functional

assays with purified AtABCG1 revealed C<sub>26</sub>-C<sub>30</sub> fatty alcohols and C<sub>24</sub>-C<sub>30</sub> fatty acids as potential AtABCG1 substrates, whereas subsequent *atabcg1* mutant studies of both *atabcg1* mutants verified C<sub>24</sub> and C<sub>26</sub> fatty acids and C<sub>26</sub> fatty alcohol unambiguously as AtABCG1 substrates. The C<sub>24</sub> fatty alcohol and C<sub>20</sub>, C<sub>22</sub> and C<sub>24</sub>  $\alpha,\omega$  dicarboxylic acids are putative AtABCG1 substrates. However, subsequent direct functional assays were not performed as they were soluble or not commercially available, respectively. Therefore, it is not clear if the altered content of C<sub>24</sub> fatty alcohol and C<sub>20</sub>-C<sub>24</sub>  $\alpha,\omega$ -dicarboxylic acids in the *atabcg1* mutants can be ascribed to AtABCG1 or other AtABCG1 knock-out related impact on metabolic pathways or transporters.

## Discussion

Several half-size transporters across different plant species have been shown to be involved in suberin barrier formation [23, 31, 32, 47]. Suberin is a chemically complex glycerolipid polymer that is mainly found in tissue-tissue or plant-environmental interfaces (such as root endodermal and peridermal cell walls) [48]. It forms particularly in liaison with the casparian strips the initial barrier for the movement of water and apoplastic solutes in the roots [16]. The present study aimed to further elaborate the current knowledge regarding the physiological role of ABCG1 from *A. thaliana*, a half-size transporter which originates from the same phylogenetic clade like the potential suberin precursor transporters AtABCG2, AtABCG6 and AtABCG20 [23, 31]. In the first part of this study, AtABCG1 was heterologously expressed in *P. pastoris* and detergent purified. Subsequent Blue native PAGE analysis demonstrated that Fos-Choline-14 solubilized AtABCG1 is a homodimer. Consistent with this observation is the fact that another half-size transporter AtABCG11 adopts also a homodimeric state [42]. However, AtABCG11 was also able to form heterodimers with AtABCG12, AtABCG9 and AtABCG14. While AtABCG12 and AtABCG11 are found cooperate in cuticular wax transport, AtABCG11-AtABCG9 and -AtABCG14 heterodimers were involved in transport of squalene-derived metabolites [11, 42]. Based on that, protein-protein interaction studies might reveal potential interaction partners of and further physiological roles of AtABCG1. The enzymatic activity of purified AtABCG1 was confirmed, as briefly introduced before in Gräfe et al. (2018, *submitted*), by malachite green based ATPase assays. A reaction velocity  $v_{\max}$  of  $17.1 \pm 0.1$  nmol min<sup>-1</sup> per mg purified AtABCG1 and a  $K_m$  value of  $1.8 \pm 0.1$  mM in comparison to the EQ/HA mutant were obtained. Both an EQ (E259Q) as well as HA (H291A) mutation were known to cause ATPase hydrolysis deficiency [39, 40]. Thus, an EQ/HA double mutant was generated in order to avoid ATPase activity residing from contamination with other ATPases. Amino acid sequence comparison of AtABCG1 with StABCG1 and PhABCG1, homonymous half-size transporters that are supposed to transport suberin precursors and volatiles, respectively, revealed the highest identity amongst AtABCG1 and StABCG1 (with 74 % sequence, 69 % NBD sequence and 81 % TMD sequence identity). Additionally, Landgraf et al. compared the amino acid sequence of StABCG1 with all *Arabidopsis* ABCG transporters and had identified AtABCG1 amongst those with the highest similarity [32]. In consistence with that, we could demonstrate here for

the first time by a functional assay using purified protein that the ATPase activity was stimulated by certain suberin precursor molecules. The specific activity of AtABCG1 was stimulated up to 90 % by fatty alcohols and acids with chain length of  $C_{26}$ - $C_{30}$  and  $C_{24}$ - $C_{30}$ , respectively. Thereby increased the stimulatory effect with the substrate chain length up to 90 % for  $C_{28}$  fatty alcohol and 80 % for  $C_{26}$  fatty acid, respectively and decreased thereafter. A similar chain-length dependent transport was proposed for StABCG1, whereby the mutant plant contained decreased levels of  $\omega$ -hydroxy fatty acids,  $\alpha$ ,  $\omega$ - dicarboxylic acids, fatty alcohols, fatty acids with a chain length of  $C_{24}$  and longer [32].

Studies on T-DNA insertional *atabcg1* mutants confirmed results of the direct functional assays with purified AtABCG1 majorly. Mutant plants exhibited a chain-length dependent decreased relative abundance of  $C_{20}$ - $C_{24}$   $\alpha$ ,  $\omega$ - dicarboxylic acids,  $C_{24}$  and  $C_{26}$  fatty acids and alcohols. Differences amongst the results of direct functional assays and mutant studies can be ascribed to various aspects. First, measured stimulation levels were not corresponding completely with the measured relative abundance of suberin precursors in AtABCG1 lacking plants. The  $C_{24}$  fatty acid stimulated the specific activity of AtABCG1 up to 50 % ( $K_m=5.4 \pm 2.1 \mu M$ ), while the *atabcg1* mutant plants contained still about 90 % of the substrate. One possible reason could be the substitution or co-transport by other transporters, which are absent in assays with purified protein. In *Arabidopsis*, several half-size transporters were found to be part of suberin formation, but the substrate specificity is different from AtABCG1. AtABCG2, AtABCG6 and AtABCG20 were suspected to transport  $C_{20}$  and  $C_{22}$  fatty acids,  $C_{22}$  fatty alcohol, and  $C_{18:1}$   $\omega$ -hydroxy fatty alcohols. Thereby, single and double mutant plants showed weaker suberin phenotypes than a triple mutant plant [23]. Another half-size transporter, AtABCG11 had a partially similar substrate specificity with decreased abundance of  $C_{20}$  fatty acids,  $C_{18}$  fatty alcohols, and  $C_{16}$  and  $C_{18}$   $\omega$ -hydroxy fatty acids in the root suberin [25, 28]. Thus, on one hand suberin deposition may not only depend on one specific transporter, rather several half-size ABCG transporters contribute to it, possibly also by heterodimerization. On the other side, it is conceivable that transporters with overlapping substrate identities could substitute in principle the function of the other, knocked-out transporter to a certain extend. In accordance, Yadav et al. also reported that the expression level of AtABCG16 was significantly increased in *atabcg2 atabcg6 atabcg20* triple mutant plants, although AtABCG16 was so far not shown to be part of suberin formation [23]. Nevertheless, we were able to



detect commonly found monomers  $\omega$ -hydroxy fatty acids,  $\alpha$ ,  $\omega$ - dicarboxylic acids, fatty acids, fatty alcohols ( $C_{16}$ - $C_{26}$ ), dihydroxy acids and phenolic compounds coumaric acid and ferulic acid after suberin transesterification of wildtype and *atabcg1* mutant plants [49]. But fatty acids and alcohols with  $\geq C_{26}$ , which have been found to be potential StABCG1 substrates were also stimulating the specific activity of purified AtABCG1 [32]. This emphasizes that AtABCG1 and StABCG1 exhibit not only sequence similarity, but also an overlapping substrate specificity with high affinity for fatty acids and fatty alcohols composed of longer carbon chains. An almost consistent substrate specificity for lipidic compounds was found for several half-size ABCG transporters, even across different plant species. For instance, ABCG5 from *Oryza sativa* (*O. sativa*) was found to transport very-long-chain fatty acids ( $\geq C_{28}$ ) and diacids ( $C_{16}$ ) of root suberin monomers [47] and ABCG1 from *Gossypium hirsutum* (*G. hirsutum*) was found to be part of lipid transport besides cotton fiber development [50]. In *Arabidopsis*, such as ABCG2, ABCG6, ABCG20 and ABCG11 were shown to be part of suberin barrier formation [23, 28, 31], ABCG1, ABCG16, ABCG26 and ABCG9 to be part of pollen protection and development [17-24] and finally ABCG11, ABCG12 and ABCG13 were found to be part of wax and cutin transport [25-30, 51]. Therefore, transport of lipidic compounds seems to be a well conserved function amongst plant half-size ABCG transporters. In accordance with that, were we able to identify  $C_{20}$ - $C_{24}$   $\alpha$ ,  $\omega$ -dicarboxylic acids and  $C_{24}$  fatty alcohol by mutant plant studies as putative substrates. Both, direct functional and *atabcg1* mutant plant studies revealed  $C_{26}$  fatty alcohols,  $C_{24}$  and  $C_{26}$  fatty acids unambiguously as AtABCG1 substrates. Moreover, the present study introduces for first time, purification, characterization on enzymatic level and direct functional assays of a *P. pastoris* expressed plant ABC transporter.

## **Acknowledgments**

We thank Iris Fey and Patrick Lenz for technical assistance. We also thank Diana Kleinschrodt, Sakshi Khosa and Lennart Charton for valuable discussions and support. Research was supported by the DFG Cluster of Excellence on Plant Sciences CEPLAS (EXC 1028) (to A.W., J.Z. and L.S.).

## **Author Contribution**

Conceived and designed the experiments: K.S., N.L., K.G., S.S., A.W., J.Z., L.S.  
Performed the experiments: K.S., N.L., K.G., J.Z. Analyzed the data: K.S., N.L., S.S., A.W., J.Z., L.S. Wrote the manuscript: K.S., S.S., L.S.

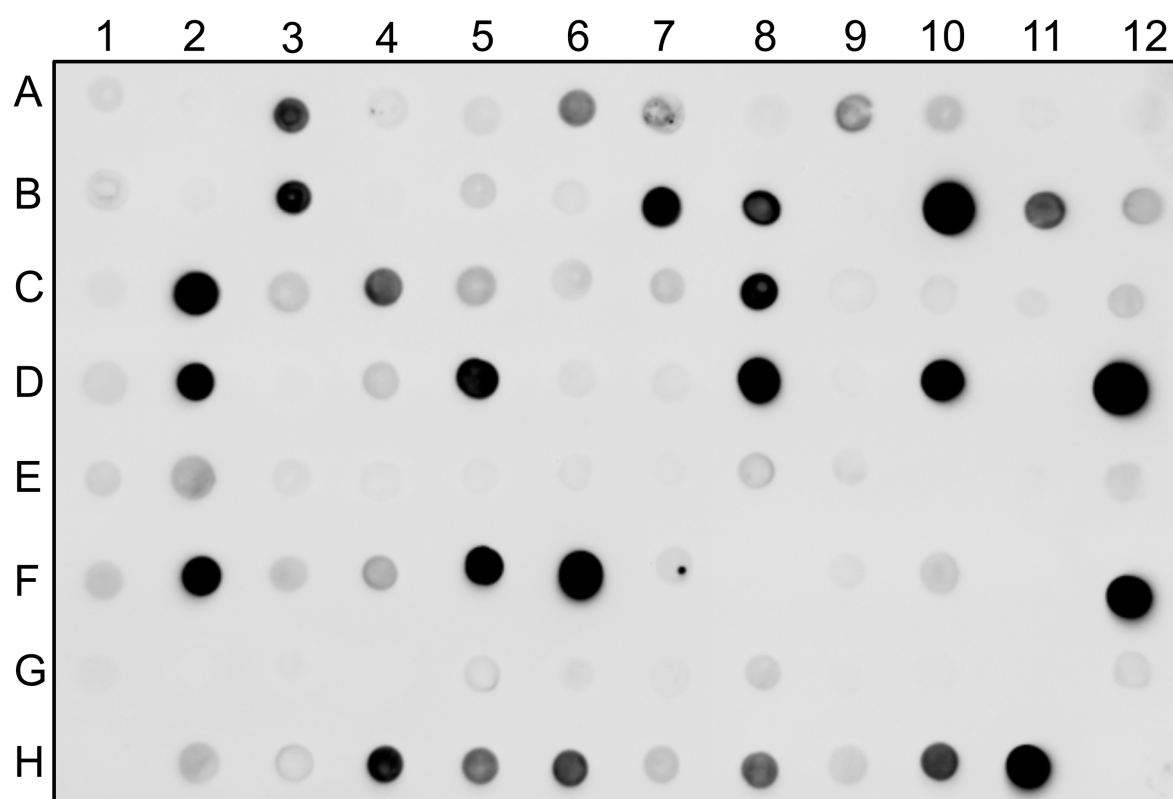
## References

1. Higgins, C.F., *ABC transporters: physiology, structure and mechanism--an overview*. Res Microbiol, 2001. **152**(3-4): p. 205-10.
2. Higgins, C.F. and K.J. Linton, *The ATP switch model for ABC transporters*. Nat Struct Mol Biol, 2004. **11**(10): p. 918-26.
3. Linton, K.J. and C.F. Higgins, *The Escherichia coli ATP-binding cassette (ABC) proteins*. Mol Microbiol, 1998. **28**(1): p. 5-13.
4. Sanchez-Fernandez, R., et al., *The Arabidopsis thaliana ABC protein superfamily, a complete inventory*. J Biol Chem, 2001. **276**(32): p. 30231-44.
5. Verrier, P.J., et al., *Plant ABC proteins--a unified nomenclature and updated inventory*. Trends Plant Sci, 2008. **13**(4): p. 151-9.
6. Mentewab, A. and C.N. Stewart, Jr., *Overexpression of an Arabidopsis thaliana ABC transporter confers kanamycin resistance to transgenic plants*. Nat Biotechnol, 2005. **23**(9): p. 1177-80.
7. Mentewab, A., et al., *RNA-seq analysis of the effect of kanamycin and the ABC transporter AtWBC19 on Arabidopsis thaliana seedlings reveals changes in metal content*. PLoS One, 2014. **9**(10): p. e109310.
8. Kuromori, T., et al., *ABC transporter AtABCG25 is involved in abscisic acid transport and responses*. Proc Natl Acad Sci U S A, 2010. **107**(5): p. 2361-6.
9. Kang, J., et al., *PDR-type ABC transporter mediates cellular uptake of the phytohormone abscisic acid*. Proc Natl Acad Sci U S A, 2010. **107**(5): p. 2355-60.
10. Kang, J., et al., *Abscisic acid transporters cooperate to control seed germination*. Nat Commun, 2015. **6**: p. 8113.
11. Le Hir, R., et al., *ABCG9, ABCG11 and ABCG14 ABC transporters are required for vascular development in Arabidopsis*. Plant J, 2013. **76**(5): p. 811-24.
12. Ko, D., et al., *Arabidopsis ABCG14 is essential for the root-to-shoot translocation of cytokinin*. Proc Natl Acad Sci U S A, 2014. **111**(19): p. 7150-5.
13. Zhang, K., et al., *Arabidopsis ABCG14 protein controls the acropetal translocation of root-synthesized cytokinins*. Nat Commun, 2014. **5**: p. 3274.
14. Kuromori, T., E. Sugimoto, and K. Shinozaki, *Arabidopsis mutants of AtABCG22, an ABC transporter gene, increase water transpiration and drought susceptibility*. Plant J, 2011. **67**(5): p. 885-94.
15. Kuromori, T., et al., *Functional relationship of AtABCG21 and AtABCG22 in stomatal regulation*. Sci Rep, 2017. **7**(1): p. 12501.
16. Nawrath, C., et al., *Apoplastic diffusion barriers in Arabidopsis*. Arabidopsis Book, 2013. **11**: p. e0167.
17. Quilichini, T.D., A.L. Samuels, and C.J. Douglas, *ABCG26-mediated polyketide trafficking and hydroxycinnamoyl spermidines contribute to pollen wall exine formation in Arabidopsis*. Plant Cell, 2014. **26**(11): p. 4483-98.
18. Choi, H., et al., *An ABCG/WBC-type ABC transporter is essential for transport of sporopollenin precursors for exine formation in developing pollen*. Plant J, 2011. **65**(2): p. 181-93.
19. Quilichini, T.D., et al., *ATP-binding cassette transporter G26 is required for male fertility and pollen exine formation in Arabidopsis*. Plant Physiol, 2010. **154**(2): p. 678-90.
20. Kuromori, T., et al., *Arabidopsis mutant of AtABCG26, an ABC transporter gene, is defective in pollen maturation*. J Plant Physiol, 2011. **168**(16): p. 2001-5.

21. Dou, X.Y., et al., *WBC27, an adenosine tri-phosphate-binding cassette protein, controls pollen wall formation and patterning in Arabidopsis*. J Integr Plant Biol, 2011. **53**(1): p. 74-88.
22. Yim, S., et al., *Postmeiotic development of pollen surface layers requires two Arabidopsis ABCG-type transporters*. Plant Cell Rep, 2016.
23. Yadav, V., et al., *ABCG transporters are required for suberin and pollen wall extracellular barriers in Arabidopsis*. Plant Cell, 2014. **26**(9): p. 3569-88.
24. Choi, H., et al., *The role of Arabidopsis ABCG9 and ABCG31 ATP binding cassette transporters in pollen fitness and the deposition of sterol glycosides on the pollen coat*. Plant Cell, 2014. **26**(1): p. 310-24.
25. Bird, D., et al., *Characterization of Arabidopsis ABCG11/WBC11, an ATP binding cassette (ABC) transporter that is required for cuticular lipid secretion*. Plant J, 2007. **52**(3): p. 485-98.
26. Ukitsu, H., et al., *Cytological and biochemical analysis of COF1, an Arabidopsis mutant of an ABC transporter gene*. Plant Cell Physiol, 2007. **48**(11): p. 1524-33.
27. Luo, B., et al., *An ABC transporter gene of Arabidopsis thaliana, AtWBC11, is involved in cuticle development and prevention of organ fusion*. Plant Cell Physiol, 2007. **48**(12): p. 1790-802.
28. Panikashvili, D., et al., *The Arabidopsis DSO/ABCG11 transporter affects cutin metabolism in reproductive organs and suberin in roots*. Mol Plant, 2010. **3**(3): p. 563-75.
29. Panikashvili, D., et al., *The Arabidopsis ABCG13 transporter is required for flower cuticle secretion and patterning of the petal epidermis*. New Phytol, 2011. **190**(1): p. 113-24.
30. Takeda, S., et al., *The Half-Size ABC Transporter FOLDED PETALS 2/ABCG13 Is Involved in Petal Elongation through Narrow Spaces in Arabidopsis thaliana Floral Buds*. Plants (Basel), 2014. **3**(3): p. 348-58.
31. Fedi, F., et al., *Awake1, an ABC-Type Transporter, Reveals an Essential Role for Suberin in the Control of Seed Dormancy*. Plant Physiol, 2017. **174**(1): p. 276-283.
32. Landgraf, R., et al., *The ABC transporter ABCG1 is required for suberin formation in potato tuber periderm*. Plant Cell, 2014. **26**(8): p. 3403-15.
33. Baykov, A.A., O.A. Evtushenko, and S.M. Awaeva, *A malachite green procedure for orthophosphate determination and its use in alkaline phosphatase-based enzyme immunoassay*. Anal Biochem, 1988. **171**(2): p. 266-70.
34. Czechowski, T., et al., *Genome-wide identification and testing of superior reference genes for transcript normalization in Arabidopsis*. Plant Physiol, 2005. **139**(1): p. 5-17.
35. Simon, P., *Q-Gene: processing quantitative real-time RT-PCR data*. Bioinformatics, 2003. **19**(11): p. 1439-40.
36. Schmittgen, T.D. and K.J. Livak, *Analyzing real-time PCR data by the comparative C(T) method*. Nat Protoc, 2008. **3**(6): p. 1101-8.
37. Zeier, J., et al., *Chemical analysis and immunolocalisation of lignin and suberin in endodermal and hypodermal/rhizodermal cell walls of developing maize (Zea mays L.) primary roots*. Planta, 1999. **209**(1): p. 1-12.
38. Zeier, J., *Pflanzliche Abschlussgewebe der Wurzel: Chemische Zusammensetzung und Feinstruktur der Endodermis in Abhängigkeit von Entwicklung und äußeren Einflüssen*. Dissertation Universität Würzburg, 1998.

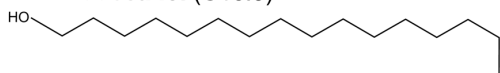
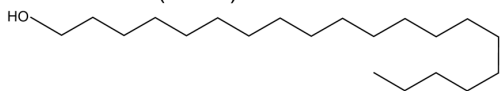
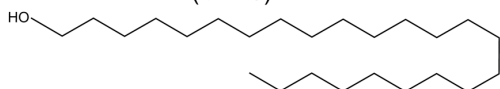
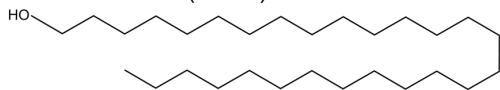
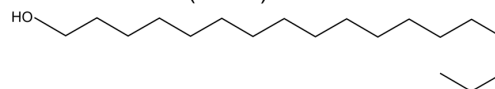
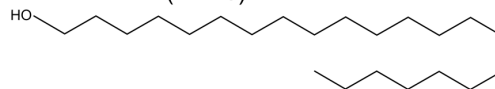
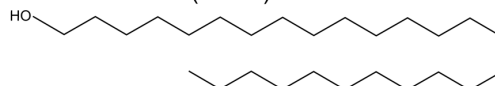
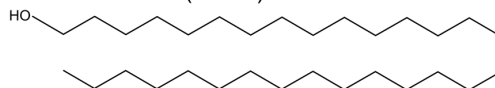
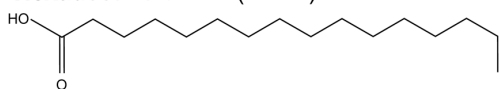
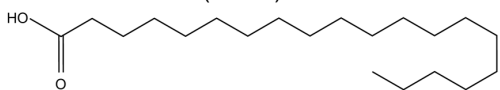
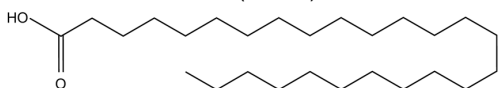
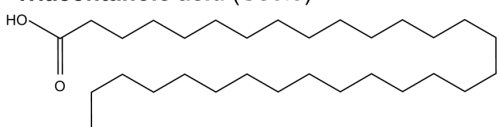
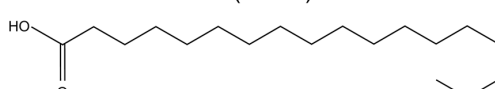
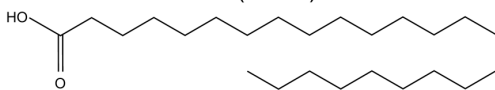
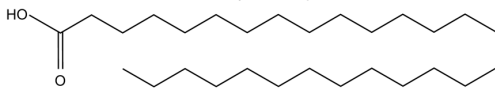
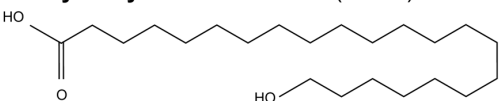
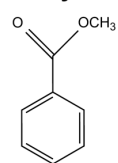
39. Smith, P.C., et al., *ATP binding to the motor domain from an ABC transporter drives formation of a nucleotide sandwich dimer*. Mol Cell, 2002. **10**(1): p. 139-49.
40. Zaitseva, J., et al., *H662 is the linchpin of ATP hydrolysis in the nucleotide-binding domain of the ABC transporter HlyB*. EMBO J, 2005. **24**(11): p. 1901-10.
41. Ellinger, P., et al., *Detergent screening and purification of the human liver ABC transporters BSEP (ABCB11) and MDR3 (ABCB4) expressed in the yeast Pichia pastoris*. PLoS One, 2013. **8**(4): p. e60620.
42. McFarlane, H.E., et al., *Arabidopsis ABCG transporters, which are required for export of diverse cuticular lipids, dimerize in different combinations*. Plant Cell, 2010. **22**(9): p. 3066-75.
43. Reimann, S., et al., *Interdomain regulation of the ATPase activity of the ABC transporter haemolysin B from Escherichia coli*. Biochem J, 2016. **473**(16): p. 2471-83.
44. Hofacker, M., et al., *Structural and functional fingerprint of the mitochondrial ATP-binding cassette transporter Mdl1 from Saccharomyces cerevisiae*. J Biol Chem, 2007. **282**(6): p. 3951-61.
45. Adebessin, F., et al., *Emission of volatile organic compounds from petunia flowers is facilitated by an ABC transporter*. Science, 2017. **356**(6345): p. 1386-1388.
46. Wang, Y.H., *How effective is T-DNA insertional mutagenesis in Arabidopsis?* Journal of Biochemical Technology, 2008. **1.1**(11-20).
47. Shiono, K., et al., *RCN1/OsABCG5, an ATP-binding cassette (ABC) transporter, is required for hypodermal suberization of roots in rice (Oryza sativa)*. Plant J, 2014. **80**(1): p. 40-51.
48. Vishwanath, S.J., et al., *Suberin: biosynthesis, regulation, and polymer assembly of a protective extracellular barrier*. Plant Cell Rep, 2015. **34**(4): p. 573-86.
49. Franke, R., et al., *Apoplastic polyesters in Arabidopsis surface tissues--a typical suberin and a particular cutin*. Phytochemistry, 2005. **66**(22): p. 2643-58.
50. Zhu, Y.Q., et al., *An ATP-binding cassette transporter GhWBC1 from elongating cotton fibers*. Plant Physiol, 2003. **133**(2): p. 580-8.
51. Panikashvili, D., et al., *The Arabidopsis DESPERADO/AtWBC11 transporter is required for cutin and wax secretion*. Plant Physiol, 2007. **145**(4): p. 1345-60.

## Supplementary Information



**Figure S 1: Solubilization screen of AtABCG1 using Dot Blot technique.** AtABCG1 containing *P. pastoris* crude membranes were solubilized with 95 different detergents. The solubilized protein was spotted on a nitrocellulose membrane and analyzed by subsequent immunoblotting (anti-His-tag antibody) for solubilization efficiency. List of used detergents and concentrations can be found in Table S 2.



**A****1-Hexadecanol (C16:0)****1-Eicosanol (C20:0)****1-Tetracosanol (C24:0)****1-Octacosanol (C28:0)****1-Octadecanol (C18:0)****1-Docosanol (C22:0)****1-Hexacosanol (C26:0)****1-Triacontanol (C30:0)****B****Hexadecanoic acid (C16:0)****Eicosanoic acid (C20:0)****Hexacosanoic acid (C26:0)****Triacontanoic acid (C30:0)****Octadecanoic acid (C18:0)****Tetracosanoic acid (C24:0)****Octacosanoic acid (C28:0)****C** **$\omega$ -Hydroxydocosanoic acid (C22:0)****Methyl benzoate**

**Figure S 3: Structures of substrates used in this study.** A, fatty alcohols with chain length of C 16:0 to C 30:0. B, fatty acids with chain length of C 16:0 to C 20:0 and C 24:0 to C 30:0. C, chemical structure of  $\omega$ -Hydroxydocosanoic acid and methyl benzoate. Created with Chemdraw 16.0.



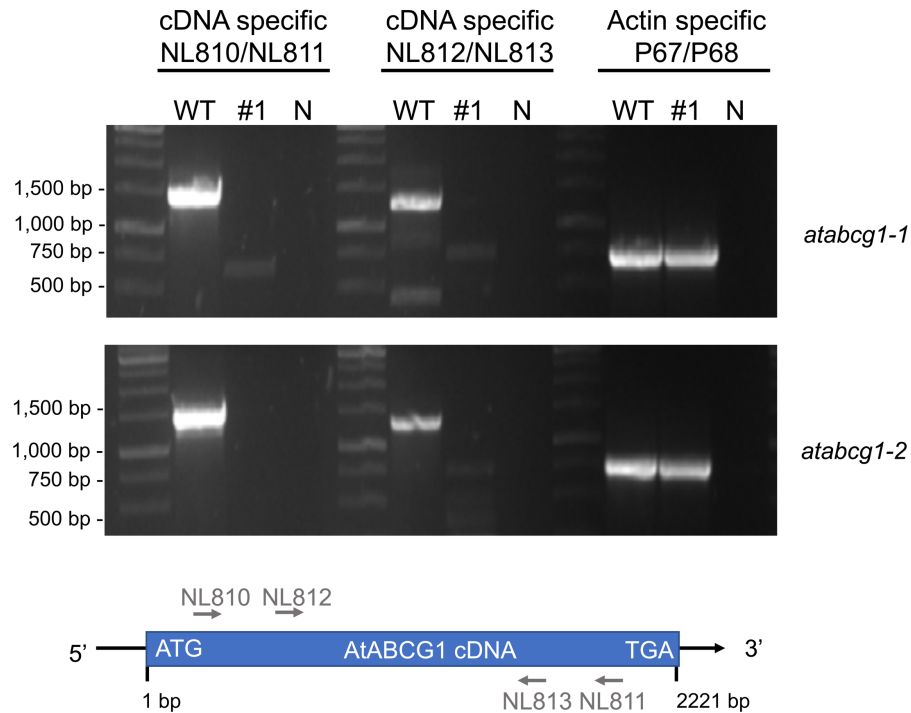


**Figure S 4: Presence of full-length *AtABCG1* in T-DNA insertional *atabcg1* mutant lines.** Amplification of full-length *AtABCG1* was performed from cDNA isolated from *atabcg1-1* and *atabcg1-2* lines and the depicted primer pairs.

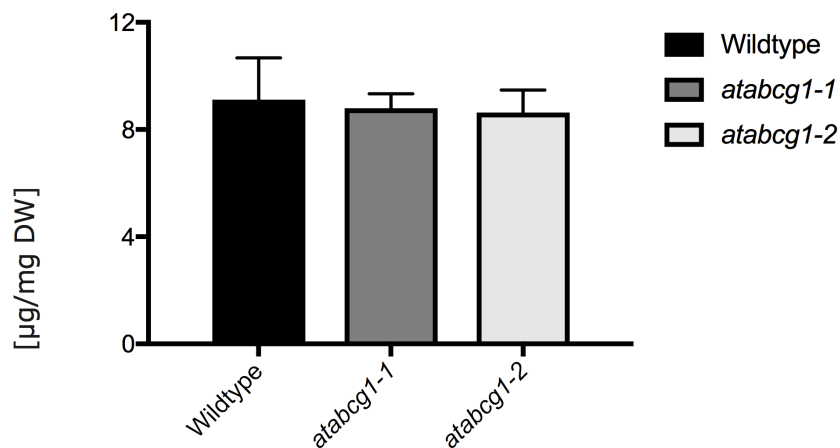


**Figure S 5: Suberin content in wildtype and *atabcg1* mutant lines.** Total amount of released suberin monomers after transesterification of wildtype and T-DNA insertional *atabcg1* mutant lines *atabcg1-1* and *atabcg1-2*. Amounts are given in μg suberin per dry weight root sample. Data represent mean ± SD of at least 4 independent experiments. Wildtype (n=7), *atabcg1-1* (n=4) and *atabcg1-2* (n=5) independent experiments.

**Table S 1: Primers used in this study.**

Primer	Application	DNA sequence (5' → 3')
ABCG1-EQ fwd	E259Q mutation	GTTGTTCTTGGACCAGCCAACTTCCGG
ABCG1-EQ rev	E259Q mutation	CCGGAAGTTGGCTGGTCCAAGAACAAC
ABCG1-HA fwd	H291A mutation	GTTATCATGTCCATTGCCCAACCATCCCACAG
ABCG1-HA-rev	H291A mutation	CTGTGGGATGGTTGGGCAATGGACATGATAAC
KS3	SAIL563B03	GCATTGATCGTTTCGAGAGAG
KS4	SAIL563B03	CGAGACTCCAGTTCACGAGTC
KS11	GK850E07	GGATCCGGAGATAGCTCAAAC
KS12	GK850E07	GCATTGATCGTTTCGAGAGAG
P49	LB SAIL line	TAGCATCTGAATTTTCATAACCAATCTCGATACAC
P52	LB GK line	CCCATTGACGTGAATGTAGACAC
P67	Actin2 fwd	TTCAATGTCCCTGCCATGTA
P68	Actin2 rev	TGAACAATCGATGGACCTGA
QP1	ABCG1_fwd1	GACAACACGCCATTAGGGGA
QP2	ABCG1_rev1	ATCGTTACCCCGAGGGACTT
QP3	ABCG1_fwd2	ACACGCCATTAGGGGAACTAC
QP4	ABCG1_rev2	GAGGGACTTGCTCACTGTACC
QP7	ABCG1_fwd3	AGGTGTGGTTCAGCTGAGTA
QP8	ABCG1_rev3	AAGAACCCTAAAGCAACTGTGA
P90	Black_fwd	GTGAAAAGTGTGGAGAGAAGCAA
P91	Black_rev	TCAACTGGATACCCTTTTCGCA
NL810	ABCG1 cDNA fwd2	TCAGAAACGCGGCTAAACT
NL811	ABCG1 cDNA rev2	ACACCTTGCTGCCTCAGAAT
NL812	ABCG1 cDNA fwd3	CATGCGTACAGTTCCATTCG
NL813	ABCG1 cDNA rev3	GAAGGCGAAGAACCCTAACC

**Table S 2: List of used detergents in solubilization screen.** A, anionic; Z, zwitterionic; N, nonionic.

Position	Detergent	cmc	used cmc (%)	nature
A1	Big CHAP	0.25	1 %	N
A2	Big CHAP deoxy	0.12	1 %	N
A3	Anzergent® 3-10	1.2	2 %	Z
A4	Anameg®-7	0.65	1 %	N
A5	Anapoe®-C10E6	0.025	1 %	N
A6	Deoxycholic acid. sodium salt	0.24	1 %	A
A7	CYGLU®-3	0.86	2 %	N
A8	Anapoe®-C13E8	0.0055	1 %	N
A9	Anapoe®-58	0.00045	1 %	N
A10	Anapoe®-80	0.0016	1 %	N
A11	2-propyl-1-pentyl maltose	1.9	2 %	N
A12	Anapoe®-X-405	0.16	1 %	N
B1	CYMAL®-1	15	2 %	N
B2	CYMAL®-2	5.4	2 %	N
B3	Fos-Choline®-12	0.047	1 %	Z
B4	Anapoe®-X-100	0.015	1 %	N
B5	Sodium cholate	0.41	2 %	A
B6	Cyclofos™-2	7.5	1 %	Z
B7	Anzergent® 3-14	0.007	1 %	Z
B8	Fos-Choline®-9	1.2	2 %	Z
B9	Fos-Choline®-Iso-11-6U	0.87	2 %	Z
B10	Fos-Choline®-16	0.00053	1 %	Z
B11	Cyclofos™-4	0.45	2 %	Z
B12	Anapoe®-C10E9	0.053	1 %	N
C1	Anapoe®-C12E8	0.0048	1 %	N
C2	Anapoe®-35	0.001	1 %	N
C3	Anapoe®-C12E9	0.003	1 %	N
C4	Cyclofos™-6	0.094	1 %	Z
C5	Anapoe®-C12E10	0.2	1 %	N
C6	Anapoe®-X-114	0.011	1 %	N
C7	n-Nonyl-β-D-thiomaltoside	0.15	1 %	N
C8	Cyclofos™-5	0.15	1 %	Z
C9	Anapoe®-X-305	-	1 %	N
C10	CYMAL®-3	0.37	1 %	N
C11	n-Tetradecyl-N,N-dimethylamine-N-oxide	0.0075	1 %	Z
C12	Cyclofos™-3	1.3	2 %	Z
D1	Fos-Choline®-8	3.4	2 %	Z
D2	Fos-Choline®-Unisat-11-10	0.21	1 %	Z
D3	2.6-Dimethyl-4-heptyl-β-D-maltose	1.2	2 %	N

<b>D4</b>	Sucrose monododecanoate	0.016	1 %	N
<b>D5</b>	n-Dodecyl- $\alpha$ -D-maltoside	0.0076	1 %	N
<b>D6</b>	CYGLU®-4	0.058	2 %	N
<b>D7</b>	Dimethyldecylphosphine oxide	0.1	1 %	N
<b>D8</b>	n-Dodecyl-N,N-dimethylglycine	0.041	1 %	Z
<b>D9</b>	Fos-Choline®-Iso-11	0.9	2 %	Z
<b>D10</b>	Fos-Choline®-14	0.0046	1 %	Z
<b>D11</b>	Fos-Choline®-Iso-9	0.99	2 %	Z
<b>D12</b>	Fos-Choline®-15	0.0027	1 %	Z
<b>E1</b>	Tripglu	3.6	2 %	N
<b>E2</b>	2-Carboxy-5-pentadecenamidopropyldimethylamine	-	1 %	Z
<b>E3</b>	Fos-Choline®-15	0.0027	1 %	Z
<b>E4</b>	CYMAL®-5	0.12	2 %	N
<b>E5</b>	n-Dodecyl-N,N-dimethylamine-N-oxide	0.023	1 %	Z
<b>E6</b>	CHAPS	0.49	2 %	Z
<b>E7</b>	MEGA-10	0.21	2 %	N
<b>E8</b>	n-Octyl- $\beta$ -D-thiomaltoside	0.4	2 %	N
<b>E9</b>	Decyl- $\beta$ -D-glucoside	0.07	1 %	N
<b>E10</b>	CYMAL®-5	0.12	2 %	N
<b>E11</b>	n-Undecyl- $\beta$ -D-thiomaltoside	0.011	1 %	N
<b>E12</b>	Anapoe®-20	0.0072	1 %	N
<b>F1</b>	Tetraethylene glycol monoethylether(C8E4)	0.25	1 %	N
<b>F2</b>	Fosfen™-9	0.014	1 %	Z
<b>F3</b>	n-Tetradecyl-N,N-dimethylamine-N-oxide	0.0075	1 %	Z
<b>F4</b>	C-DODECAFOS™	0.77	2 %	Z
<b>F5</b>	2-Carboxy-w-heptadecenamidopropyldimethylamine	-	1 %	Z
<b>F6</b>	SDS		10 %	
<b>F7</b>	n-Heptyl- $\beta$ -D-thioglucoside	0.85	2 %	N
<b>F8</b>	Negative control			
<b>F9</b>	n-Decyl- $\alpha$ -D-maltoside	-	1 %	N
<b>F10</b>	LAPAO	0.052	2 %	Z
<b>F11</b>	PMAL™-8	-	1 %	Z
<b>F12</b>	n-Dodecyl- $\beta$ -iminodipropionic acid. monosodium salt	N/A	1 %	A
<b>G1</b>	Nopol-Fos™	1.4	2 %	Z
<b>G2</b>	Tripao	4.5	2 %	Z
<b>G3</b>	MEGA-8	2.5	2 %	N
<b>G4</b>	PMAL™-C10	-	1 %	Z
<b>G5</b>	N,N dimethyl(3-carboxy-4-dodec-5-ene) aminopropylamine	0.0178	1 %	Z
<b>G6</b>	Cyclohexyl-n-hexyl- $\beta$ -D-maltoside	-	1 %	N

<b>G7</b>	Fosmea®-10	0.15	1 %	A
<b>G8</b>	n-Dodecyl- $\beta$ -D-maltoside	0.0087	1 %	N
<b>G9</b>	NP40	0.05-0.3	1 %	N
<b>G10</b>	n-Dodecyl- $\beta$ -D-maltoside	0.0087	1 %	N
<b>G11</b>	CHAPSO	0.5	2 %	Z
<b>G12</b>	n-Octyl- $\beta$ -D-glucoside	0.53	2 %	N
<b>H1</b>	Decyltrimethylammonium chloride	0.07	1 %	C
<b>H2</b>	n-Nonyl- $\beta$ -D-maltoside	0.28	2 %	N
<b>H3</b>	n-Octyl- $\beta$ -D-maltoside	0.89	2 %	N
<b>H4</b>	n-Tetradecyl- $\beta$ -D-maltoside	0.00054	1 %	N
<b>H5</b>	n-Undecyl- $\alpha$ -D-maltoside	0.029	1 %	N
<b>H6</b>	n-Undecyl- $\beta$ -D-maltoside	0.029	1 %	N
<b>H7</b>	n-Nonyl- $\beta$ -D-glucoside	0.2	1 %	N
<b>H8</b>	n-Dodecyl- $\beta$ -D-thiomaltoside	0.0026	1 %	N
<b>H9</b>	Anzergent®3-12	0.094	1 %	Z
<b>H10</b>	n-Decyl-N, N-dimethylglycine	0.46	2 %	Z
<b>H11</b>	Sodium dodecanoyl sarcosine	0.42	2 %	A
<b>H12</b>	PMAL™-C-12	-	2 %	Z
<b>I1</b>	Dodecyltrimethylammonium chloride	0.0012	1 %	C
<b>I2</b>	Hexadecyltrimethylammonium chloride	0.000102	1 %	C
<b>I3</b>	Tetradecyltrimethylammonium chloride	0.0009	1 %	C

**Table S 3: Analytical data of compounds monomers detected by GC/MS.**

compound	quantifier ion (m/z)	characteristic ions (m/z)	retention time (min)
p-coumaric acid	250	235, 219, 203	17.7
ferulic acid	250	280, 265, 219	20.5
<b>ω-hydroxyacids</b>			
C16	311	343, 159, 146, 103, 75	26.8
C18:1	337	384, 369, 353, 159, 146	29.4
C18	339	371, 159, 146, 103, 75	29.9
C20	367	399, 159, 146, 103, 75	32.9
C22	395	427, 159, 146, 103, 75	35.6
C24	423	455, 159, 146, 103, 75	38.2
C26	451	483, 159, 146, 103, 75	40.6
<b>α, ω-dicarboxylic acids</b>			
C16	98	283, 112, 84	25.9
C18:1	98	340, 308, 276	28.6
C18	98	311, 112, 84	29.4
C20	98	339, 112, 84	32.2
C22	98	367, 112, 84	35.1
C24	98	395, 112, 84	37.7
<b>fatty acid</b>			
C16	87	270, 74, 143	20.5
C18:2	87	294, 263, 109, 95, 81, 67	23.3
C18:3	87	292, 236, 108, 95, 79, 67	23.4
C18:1	87	296, 264, 222, 97, 83	23.5
C18	87	298, 74, 143	24.1
C20	87	326, 74, 143	27.4
C22	87	354, 74, 143	30.6
C24	87	382, 74, 143	33.5
C26	87	410, 74, 143	36.2
<b>fatty alcohol</b>			
C16	299	103, 75	21.5
C18	327	103, 75	25.0
C20	355	103, 75	28.2
C22	383	103, 75	31.3
C24	411	103, 75	34.1
C26	439	103, 75	36.8
<b>dihydroxyacids</b>			
C24_2OH	411	455	36.2
C26_2OH	439	483	38.7
<b>internal standard</b>			
1-pentadecanol	285	103, 75	19.7
heptadecanoic acid	87	284, 84, 143	22.3

15-hydroxypentadecanoic acid	297	329, 159, 146, 103, 75	25.1
------------------------------	-----	------------------------	------

### **3.4 Chapter IV – Vesicular transport assay**

Title: Proof-of-principle of a mass spectrometry-based vesicular transport assay for identification of plant ABCG transporter substrates

Authors: Kalpana Shanmugarajah, Katharina Gräfe, Sabine Metzger,  
Sander H. J. Smits and Lutz Schmitt

Published in: In preparation

Own work: 65 %

Expression and isolation of Pdr5 containing plasma membranes

Rhodamine 6G transport assays

Method optimization of vesicular transport assay

Writing of the manuscript



## **Proof-of-principle of a mass spectrometry-based vesicular transport assay for identification of plant ABCG transporter substrates**

***Kalpana Shanmugarajah<sup>1,2</sup>, Katharina Gräfe<sup>1,2</sup>, Sabine Metzger<sup>2,3</sup>, Sander H. J. Smits<sup>1</sup> and Lutz Schmitt<sup>1,2\*</sup>***

<sup>1</sup>Institute of Biochemistry, Heinrich-Heine-University, Düsseldorf, Germany

<sup>2</sup>Cluster of Excellence on Plant Sciences, Heinrich-Heine-University, Düsseldorf, Germany

<sup>3</sup>MS-Platform, Department of Biology, University of Cologne, Cologne, Germany

For correspondence

[lutz.schmitt@hhu.de](mailto:lutz.schmitt@hhu.de)

## Abstract

Sustainable plant production systems include efficient and resource preserving agriculture. Hence, it is important to identify controllable key elements in plants. The plant-microbe interaction in the root forms one key element in plants. Plants release root exudates into the rhizosphere, which enables them to shape the microbial communities in the soil. Thereby, beneficial microorganism can be attracted or pathogens defended. ATP-binding (ABC) transporters represent one possibility to release exudates into the soil. The identification of the transported substrates could help to better understand the plant physiology and moreover it would allow us to change the microbial communities in the soil in order to improve crop yield and growth. Here, we report about the proof-of-principle vesicular transport assay with Pdr5 from *Saccharomyces cerevisiae* based on mass spectrometry. Initial results reveal critical steps and provide a foundation for future studies with plant ABC transporters, which are expressed heterologous in yeast systems.

## Introduction

Plant growth, fitness and productivity mainly depends on its ability to adapt to environmental conditions. This includes also the interaction with microbial communities above or below ground [1-3].

The rhizosphere harbors the plant roots and the surrounding soil. Primarily root systems serve as physical support and are responsible for water and nutrient-uptake. Hence, they allow plants to deal with various abiotic stresses, as for instance drought, nutrient shortage, extreme temperatures and salinity. On the other hand, roots release exudates into the rhizosphere, which are essential for plant-microbiome interactions. Root exudates enable plants to shape the microbial community in the rhizosphere and are mainly composed of carbon-based compounds, including sugars, organic acids, complex polymers and secondary metabolites [4-6].

Several ABC (ATP-binding cassette) transporters are involved in transport of metabolites found frequently in root exudates, as for instance nucleotides [7, 8], peptides [9], fatty acids [10-14] or secondary metabolites [9, 15-20]. The ABC superfamily consists of membrane-embedded proteins, which enable the transport of various substrates across a lipid bilayer [21]. The general blueprint consists of two nucleotide-binding domains (NBDs) and two transmembrane domains (TMDs). The NBDs hydrolyze ATP and provide the driving force for substrate binding and translocation at the TMDs. While the NBDs contain several conserved motifs, like the Walker A and B motifs, the H-, D- and the Q-loop and ABC signature motif, the TMDs consist of 6-12  $\alpha$ -helices [22]. ABC transporters can be categorized by the number of domains which are encoded on a single gene. Full-size ABC transporters consist of each, two NBDs and TMDs (TMD-NBD)<sub>2</sub>, while half-size transporters consist of each one TMD and NBD (TMD-NBD). Half-size transporters form a functional transport unit by homo- or heterodimerization [23, 24].

In comparison to other organisms, plants contain the largest number of ABC proteins with for example 130 genes in *Arabidopsis thaliana* (*A. thaliana*) and 133 genes in *Oryza sativa* [14, 25]. Depending on their phylogenetic relationship and domain organization, plant ABCs are subdivided into eight subfamilies ABCA to ABCG and ABCI. The largest subfamily is constituted by the ABCG subfamily with 28 half-size (also known as white brown complex, WBC) and 15 full-size (pleiotropic drug resistance, PDR) transporters. ABCG transporters are only found in fungi and plants

and exhibit a reverse domain organization, where the NBDs are encoded N-terminally to the TMDs [26].

Badri *et al.* identified 25 ABC transporters including several ABCG subfamily members to be highly expressed in the roots [18]. They hypothesized that those transporters might be involved in root exudation processes, since root exudation of phytochemicals has been shown to occur near the root tip and elongation zone [18, 27, 28]. Subsequent analysis with selected ABC transporters, revealed changes in exudate profiles of the respective mutant plants. In accordance with that, further studies with an *atabcg30* mutant exhibited significant changes in the root exudate profile and the microbial communities in the soil [18, 29]. Thus, identification of transported substrates from root exudates could help to get further insight into the plant physiology and enable regulation of the plant-microbe interaction. A mass spectrometry (MS)-based vesicular transport assay, as previously introduced by Krumpochova, Sapthi [30], could allow the identification of the transported substrate from a mixture of potential substrates or root exudates. Krumpochova *et al.* prepared inside-out oriented vesicles from *Spodoptera frugiperda* Sf9 insect cells overproducing ABCC2, incubated them with extracts from mouse urine and identified transported compounds by MS [30]. Several human ABC transporters have been analyzed using similar approaches, as for instance ABCG2 which has been screened for substrates in plasma, bile and urine from mice [31], ABCC3 [32], ABCC5 [33, 34] or ABCC6 [35, 36]. A plant ABC transporter, that was characterized after heterologous expression in *Lactococcus lactis* by a similar approach, is for instance AtABCB25 [37].

The purpose of this study is the development of a MS-based vesicular transport assay for heterologously expressed plant ABC transporters. Previously, we could show successful heterologous expression and correct targeting of the full-size ABCG transporters AtABCG30, AtABCG36 and the half-size transporter AtABCG1 in the yeast *Pichia pastoris* (*P. pastoris*) (Gräfe *et al.* (2018) *submitted*). Therefore, the plasma membrane localized full-size ABCG transporter Pdr5 from *Saccharomyces cerevisiae* (*S. cerevisiae*) was used for method optimization and proof-of-principle [38, 39]. Pdr5 overexpression in yeast leads to resistance against various unrelated cytotoxic compounds (multidrug resistance, MDR) [40-42]. Advantages of using Pdr5 for method optimization are a similar membrane composition to *P. pastoris*, since Pdr5 is also a yeast transporter, already established transport assays, which provide a proper basis for further method development and the availability of various substrates.

Here, we present MS data of initial transport assays with Pdr5 containing plasma membrane vesicles. This study provides the basis for future MS-based transport assays with plant ABC transporters.

## Methods

### Strains and expression conditions

The yeast strain YRE1001 (*MATa ura 3-52 trp1-1 leu2-3, 112 his3-11,15 ade2-1 pdr1-3 pdr5pdr5prom::TRP1*) and the corresponding ATP hydrolysis deficient Pdr5-E1036Q strain [43] were cultured in YPD medium (10 g/l yeast extract, 20 g/l peptone, 20 g/l glucose) at 30 °C until an OD<sub>600</sub> of 1.5 was reached. The nitrogen source was replenished by addition of a 10<sup>th</sup> volume 5 x YP (50g/l yeast extract, 100 g/l tryptone/peptone) and the cells harvested (5,000 x g, 15 min, 4 °C) at an OD<sub>600</sub> of 3.5. The resulting cell pellets were directly used for isolation of plasma membranes or flash-frozen in liquid nitrogen and stored at -80 °C until further use.

### Isolation of Pdr5 containing plasma membranes

The isolation of plasma membranes was performed as described in Ernst, Kueppers [43] and Kolaczowski, van der Rest [44]. Briefly, approximately 30 g of the respective cells were resuspended in lysis buffer (50 mM Tris-acetate, 5 mM EDTA, pH 8) supplemented with protease inhibitor (EDTA-free; Roche). Cells were disintegrated by vigorous shaking with glass beads and afterwards cleared from unbroken cells and cell debris (2 x 5 min at 1,000 x g and 1 x 5 min at 3,000 x g, 4 °C). The supernatant was centrifuged (40 min 20,000 x g at 4 °C) and the pellet resuspended in 10 mM Tris-acetate (pH 7.5) and 0.2 mM EDTA. Mitochondrial membranes were removed by acetic acid precipitation at pH 5.2 and subsequent centrifugation (5 min 7,000 x g at 4 °C). Plasma membranes were obtained after adjustment to pH 7.5 and centrifugation (30 min 26,500 x g at 4 °C), resuspended in storage buffer (50 mM Hepes (pH 7)), snap-frozen in liquid nitrogen and stored at -80 °C until further usage.

### Rhodamine 6G transport assay

The rhodamine 6G (R6G) transport activity of Pdr5 containing plasma membranes was assayed according to Kolaczowski et al. (1996). Measurements were performed on a FluoroLog III fluorescence spectrometer (Horiba) with the excitation wavelength at 529 nm and the emission wavelength at 553 nm. 30 µg plasma membrane was resuspended in 1 ml transport buffer (50 mM Hepes (pH 7.0), 10 mM MgCl<sub>2</sub>, 150 nM R6G and 10 mM azide) and incubated at 35 °C. R6G molecules are transported in presence of 10 mM ATP to the inner leaflet or the vesicle lumen, where thereupon non-

fluorescent R6G eximers are formed. The maximal R6G transport activity  $v_{\max}$  of Pdr5 is defined by the final relative decrease in the fluorescence intensity. Furthermore, the R6G transport activity of Pdr5 was analyzed in presence of varying concentrations of ketoconazole, fluconazole or cycloheximide (20 nM - 800 nM). Ketoconazole, fluconazole and R6G were obtained from Sigma-Aldrich and cycloheximide was obtained from Fluka. R6G fluorescence quenching was analyzed using Prism (version 7, GraphPad). Stock solutions were prepared in dimethyl sulfoxide (DMSO, Acros Organics) and diluted with buffer.

### **Calculation of the molecular surface volume**

The molecular surface volume was calculated using the ProteinVolume 1.3 program (<http://gmlab.bio.rpi.edu/>) with default settings [45]. The respective coordinate files were taken from Ligand Expo [46] and can be found under the following PDB ID codes: R6G, RHQ; ketoconazole, KTN; cycloheximide, 3HE; fluconazole, TPF.

### **Vesicular transport assay**

Crude plasma membrane preparations are comprised of membrane sheets, right-side-out oriented vesicles with NBDs located in the vesicle lumen and inside-out oriented vesicles with NBDs in the cytosol. Therefore, only plasma membrane sheets and inside-out oriented vesicles enable the ATP-driven substrate translocation by an ABC transporter [47].

Vesicular transport assays with crude plasma membrane preparations allow the substrate identification of inside-out oriented membrane vesicles. The R6G-based transport assay was adapted from Kolaczowski, van der Rest [44]) to analyze the ketoconazole transport activity of Pdr5 containing plasma membranes, as follows: 30  $\mu$ g plasma membrane was resuspended in 1 ml transport buffer (20 mM Tris-HCl (pH 7), 200 nM ketoconazole, 10 mM  $MgCl_2$  and 10 mM azide) and incubated for 1 h at 35 °C under slight shaking. The sample was centrifuged (30 min 100,000 x g at 4 °C) and the resulting pellet washed 3 times in 1 ml transport buffer without ketoconazole. Afterwards, the pellet was resuspended in 100  $\mu$ l  $H_2O$  and incubated for 1 h on ice for vesicle disruption by osmotic pressure or disrupted for 1 h by sonification. Furthermore, samples were tested for disruption by 1 % saponin or methanol (80 %, 50 %, 20 % (v/v)). Samples were centrifuged (30 min, 270,000 x g, 4 °C) to get rid of disrupted

membranes and the resulting supernatant with the vesicle content analyzed by mass spectrometry.

### **MS analysis**

For the MS measurements, the samples were diluted 1:1 with 60 % methanol acidified with 5 % formic acid. The MS analyses were performed with an ESI Q-TOF instrument (Q-STAR XL, Applied Biosystems, Darmstadt Germany) that was equipped with an offline-nanospray source ion source (Proxeon, Odense, Denmark). The overview mass spectra were recorded across a  $m/z$  range from 200 to 1000. For the fragment spectra of ketoconazole, the mass of 531.1 Da was selected in the first quadrupole, the second quadrupole was used as a collision cell whereas the occurred fragments are analyzed in the time of flight mass analyzer.



## Results

### R6G transport assays with Pdr5

The optimization of a MS-based vesicular transport assay requires calibration and optimization of different parameters. The first step was the identification of a suitable Pdr5 substrate. The R6G based transport assay was adapted to analyze the transport of the non-fluorescent Pdr5 substrates ketoconazole, fluconazole or cycloheximide by Pdr5 [44]. It was expected that the addition of a second, non-fluorescent Pdr5 substrate in excess would lead in a competitive transport situation and therefore to a decreased R6G transport and fluorescence quenching effect. In this way, it would be possible to determine the concentration, where the non-fluorescent substrate was maximally transported by Pdr5.

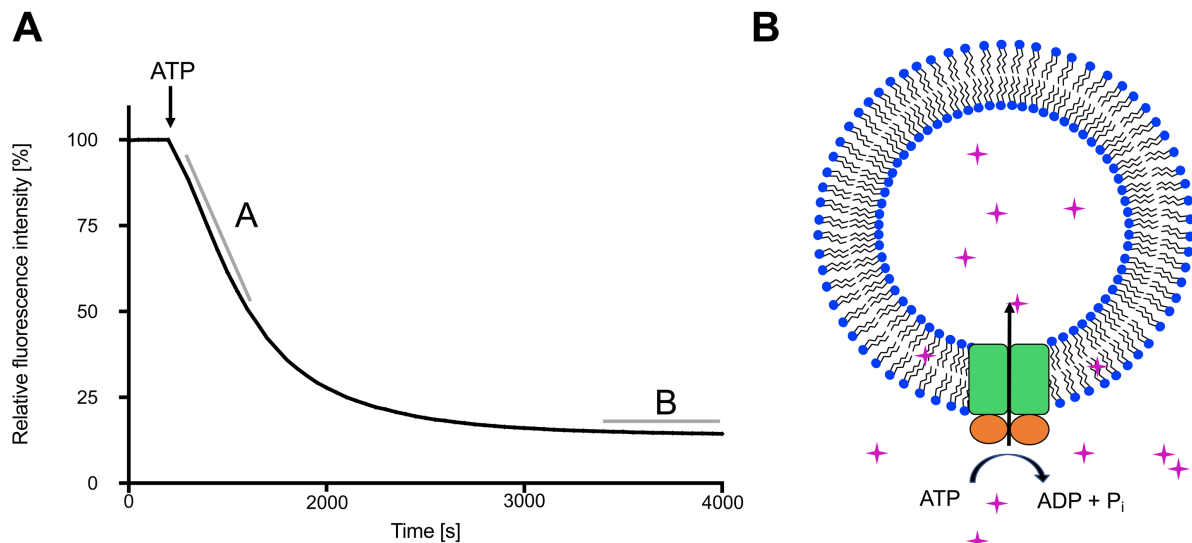
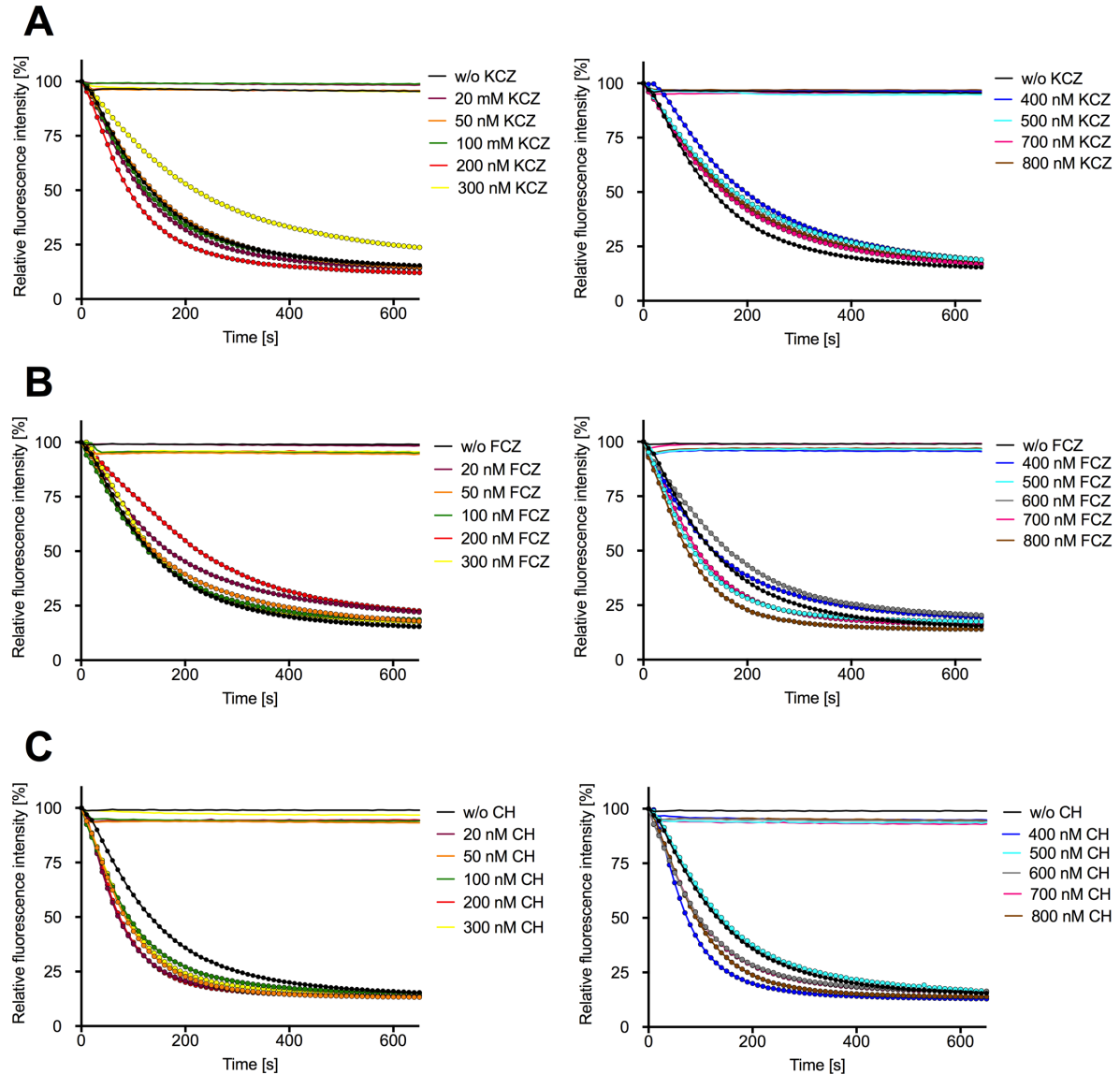


**Figure 1: R6G transport assay with inside-out oriented plasma membranes. A.** Representative graph of a R6G transport assay with Pdr5 containing plasma membranes. Addition of ATP leads to rapid decrease of the relative fluorescence intensity (A) until the maximal transport velocity is reached in the saturation phase (B). **B.** Model of an inside-out oriented plasma membrane vesicle. ATP-hydrolysis provides the energy for substrate (for instance ketoconazole) transport into the vesicle. Orange, NBDs; green, TMDs; violet, substrate.

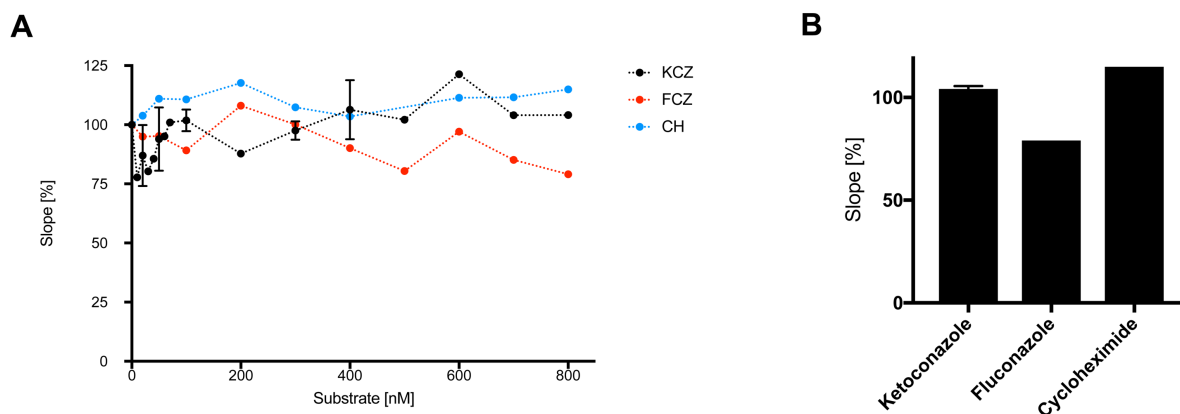
As shown in Figure 1, the presence of R6G leads upon ATP addition to a rapid decrease of the fluorescence intensity. The slope determines thereby the rate of active transport and the subsequent saturation phase displays the maximal R6G transport by

the Pdr5 containing plasma membrane vesicles. In the subsequent transport assays, the R6G concentration was kept constant at 150 nM, while 20 nM to 800 nM ketoconazole, fluconazole or cycloheximide were used. Interestingly, even the presence of ketoconazole, fluconazole or cycloheximide in excess did not exhibited an inhibition of the R6G fluorescence quenching (Figure 2). Analogous assays with the ATP hydrolysis deficient Pdr5-EQ mutant exhibited due to the absence of R6G transport, no altered fluorescence intensity. The comparison of the slope values showed that the R6G transport in presence of ketoconazole and cycloheximide remains around 100 %, while the values in presence of fluconazole show a slight decrease with up to 75 % active R6G transport at 800 nM (Figure 3).

These results clearly indicated that neither ketoconazole, fluconazole nor cycloheximide were able to inhibit the R6G fluorescence quenching reaction significantly. Thus, the analyzed non-fluorescent substrates were not able to compete with R6G for Pdr5-dependent transport.



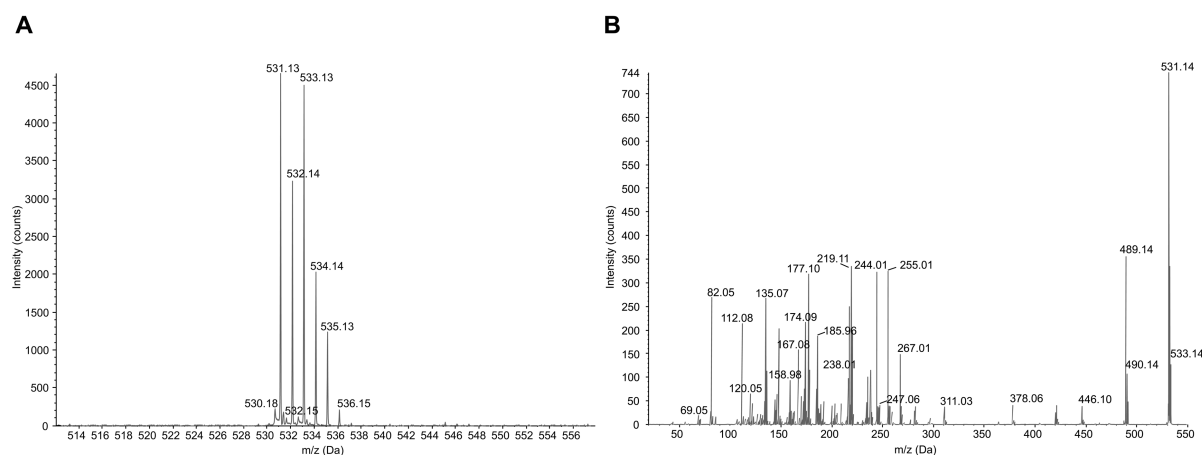
**Figure 2: R6G-based transport assays with Pdr5 containing plasma membranes.** The relative fluorescence intensity of R6G was analyzed in presence of 20 nM- 800 nM non-fluorescent Pdr5 substrates ketoconazole (A), fluconazole (B) and cycloheximide (C). Data was normalized prior to ATP addition to 100 %. KCZ, ketoconazole; FCZ, fluconazole; CH, cycloheximide; w/o, without; Pdr5 is highlighted in contrast to Pdr5-EQ with circles.



**Figure 3: Active transport rates of R6G by Pdr5 in presence of ketoconazole, fluconazole and cycloheximide.** (A) Slope values of the relative R6G fluorescence intensity in presence of ketoconazole, fluconazole and cycloheximide were determined with Prism (version 7, GraphPad) and normalized to 100%. (B) Comparison of the active R6G transport rates of Pdr5 in presence of 800 nM ketoconazole, fluconazole and cycloheximide. Data of transport assays with ketoconazole represent mean values and  $\pm$  SD of two independent experiments. KCZ, ketoconazole; FCZ, fluconazole; CH, cycloheximide.

### MS-based transport assays with Pdr5

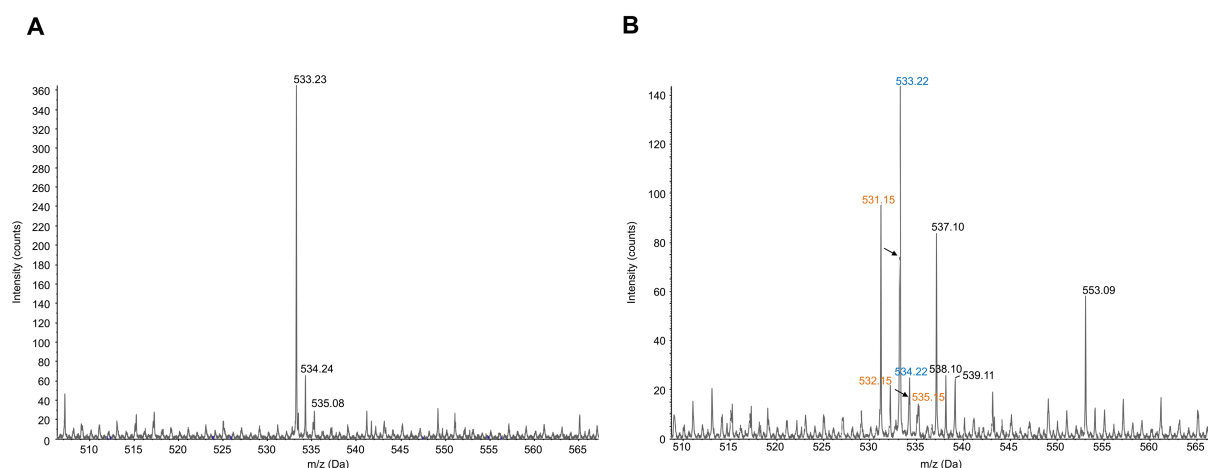
The optimization of MS-based transport assays with Pdr5 containing plasma membranes requires a substrate with distinct mass spectra and low detection limit. Ketoconazole was selected for subsequent experiments, because it was possible to identify 22,000 counts for a 20 nM (0.01 ng/ $\mu$ l) ketoconazole sample (Figure S 1). Hence, even minimal amounts of Pdr5-transported ketoconazole should be detectable by MS. The corresponding MS spectra showed a distinct distribution of the ketoconazole isotopes with most abundant masses of 531.13, 532.14, 533.13, 534.14 and 535.13 Da. The fragment spectrum of ketoconazole was created by fragmentation of the signal at 531.13 Da (Figure 4).



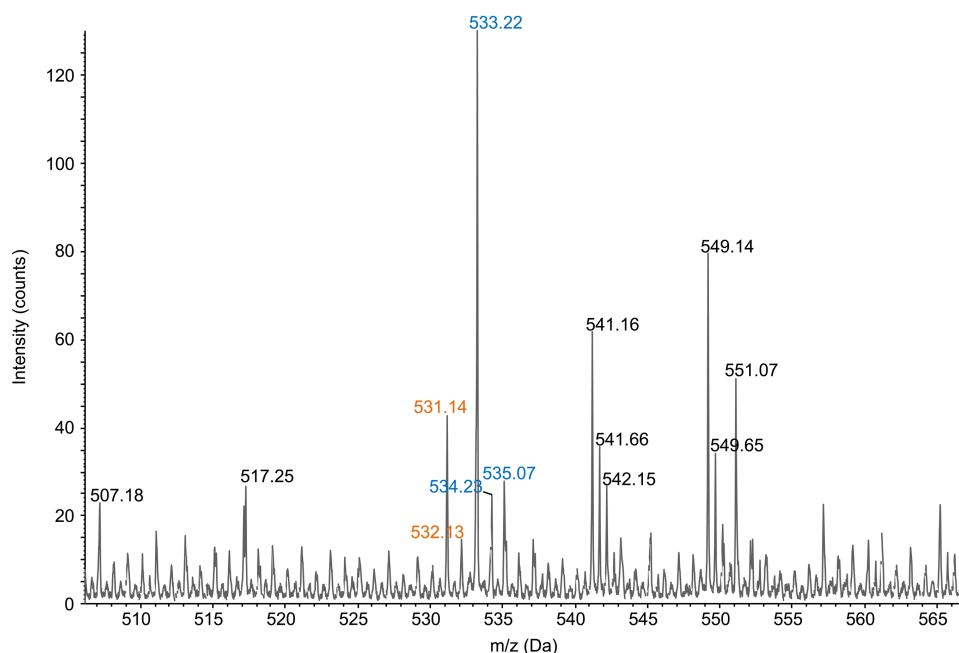
**Figure 4: MS analysis of ketoconazole.** (A) Isotopic distribution pattern of pure ketoconazole. (B) Fragment spectra of ketoconazole (531.14 Da).

So far, Hepes buffer was used for transport assays with Pdr5 plasma membranes. However, it was not possible to identify ketoconazole in Hepes buffer (Figure S 2) by MS analysis due to large amounts of impurities. Subsequent experiments were performed, after verification of the Pdr5 transport activity by R6G assays, in Tris buffer. Samples were incubated for 1 h at 30 °C to allow maximal ketoconazole transport into the vesicles. Afterwards, vesicles were washed 3 times to get rid of excess and not transported ketoconazole. Thereby, wash fractions were also analyzed by MS to determine the number of necessary washing steps.

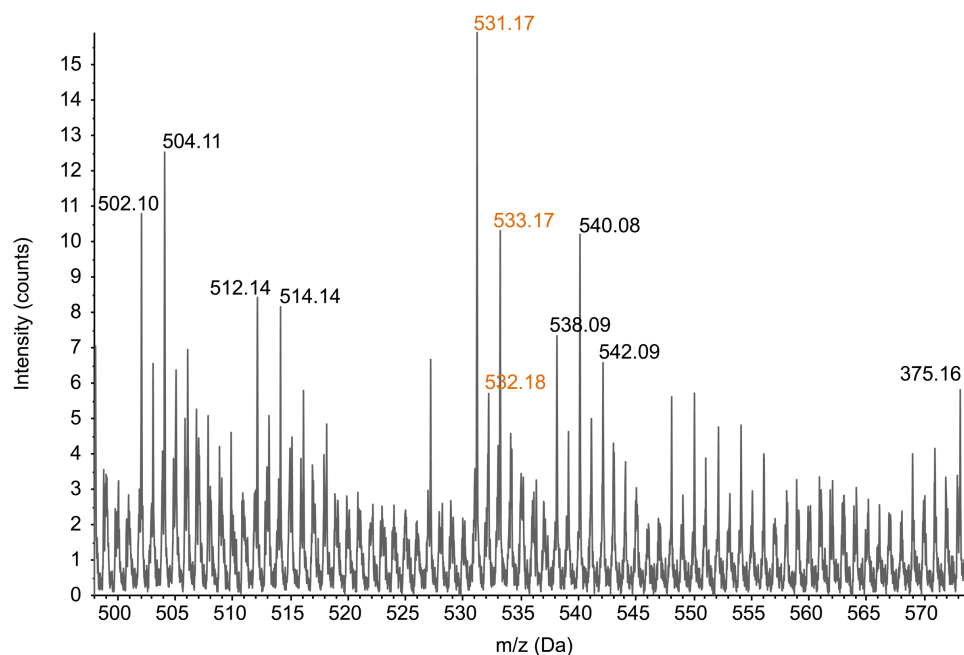
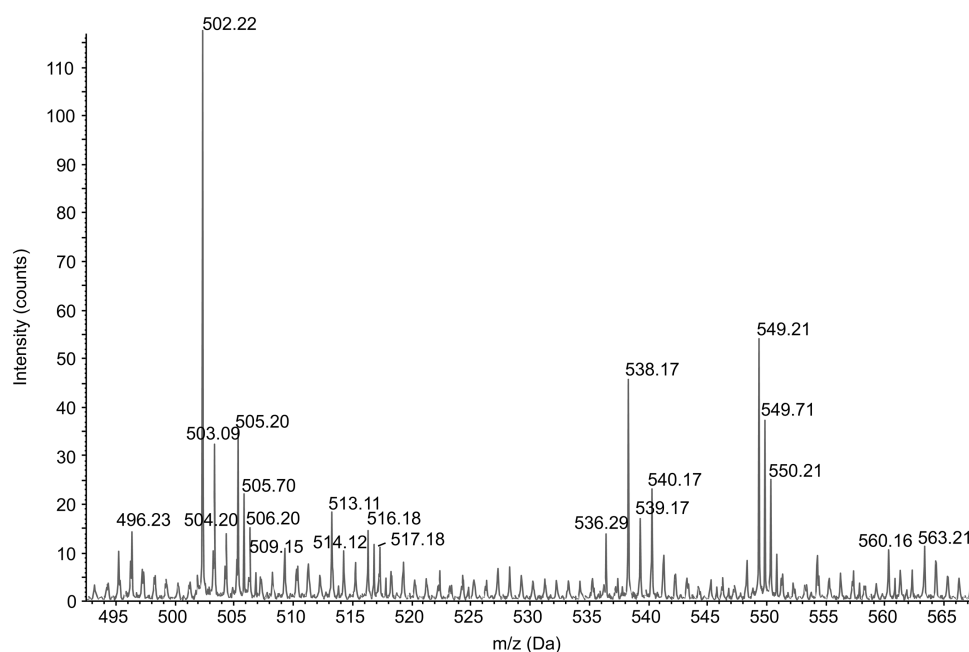
Next, different vesicle disruption methods, including saponin, sonification, osmotic pressure and methanol were tested and the vesicle content analyzed by MS. As shown in Figure 5, saponin and ketoconazole had a partially overlapping isotope distribution. Moreover, MS analysis after vesicle disruption with 1 % saponin resulted in only 45 counts for ketoconazole (Figure 6) [48]. Therefore, saponin was not used any further. Vesicle disruption by osmotic pressure showed even lower ketoconazole amounts (16 counts). In contrast to that, no ketoconazole was identified after vesicle disruption by sonification (Figure 7).



**Figure 5: MS analysis of saponin and ketoconazole.** The isotopic distribution pattern of pure saponin (A) and a saponin/ketoconazole solution is shown (B). Arrows, indicate the overlapping area of the ketoconazole and saponin isotopes; orange, most abundant ketoconazole isotopes; blue, most abundant saponin isotopes.



**Figure 6: MS analysis after ketoconazole transport into Pdr5 plasma membrane vesicles.** Inside-out oriented Pdr5 plasma membrane vesicles were tested for ketoconazole transport efficiency after vesicle disruption by 1 % saponin. Highlighted in orange are most abundant ketoconazole isotopes, while most abundant saponin isotopes are shown in blue.

**A****B**

**Figure 7: MS analysis of ketoconazole in Pdr5 containing vesicles after disruption by osmotic pressure and sonification.** Inside-out oriented Pdr5 plasma membrane vesicles were tested for ketoconazole transport efficiency after vesicle disruption by osmotic pressure (A) and sonification (B). Most abundant ketoconazole isotopes are highlighted in orange.

Finally, methanol was tested for vesicle disruption efficiency and the first attempt failed, because the pellets were instable after the final centrifugation step. A proper separation of the vesicle content and the disrupted vesicles was not possible after using 100 % methanol. Therefore, 80 %, 50 % and 20 % methanol solutions were tested and the final centrifugation step increased from 100,000 x g to 270,000 x g (Figure 8). So far, MS analysis after vesicle disruption with saponin exhibited the highest ketoconazole intensity with 45 counts. Compared to that, vesicle disruption with 80 % and 50 % methanol enabled the identification of approximately 25 times higher ketoconazole intensities. It was possible to identify 1200 counts of ketoconazole after transport assays with Pdr5, while measurements with the ATP-hydrolysis deficient mutant Pdr5-EQ resulted in 300 counts of ketoconazole after the disruption with 80 % and no counts of ketoconazole for the 50 % methanol (Figure 8). The presence of the most abundant ketoconazole fragments, is despite impurities, especially for the measurement at 50 % methanol, comparable with the fragment spectra of pure ketoconazole (Figure S 3).

Taken together, it was possible to modify the initially used R6G-based transport assay with Pdr5 plasma membranes in order to identify substrate identities via MS. The selection of ketoconazole for method optimization proved to be effective, as even low ketoconazole amounts (20 nM) could be identified. That allowed the identification of different assay parameters, including incubation time of the assay, number of necessary washing steps to get rid of excess substrate, centrifugation settings and membrane disruption methods. In principle, it was possible to disrupt Pdr5 plasma membranes by osmotic pressure, saponin and 80 % or rather 50 % methanol. However, comparison of the overview spectra and the identified ketoconazole amounts clearly demonstrated membrane disruption by 80 % and 50 % methanol as most effective for substrate identification via MS. Thus, the here determined final experimental conditions can be transferred for substrate identification on *P. pastoris* expressed AtABCG30, AtABCG36 or AtABCG1.



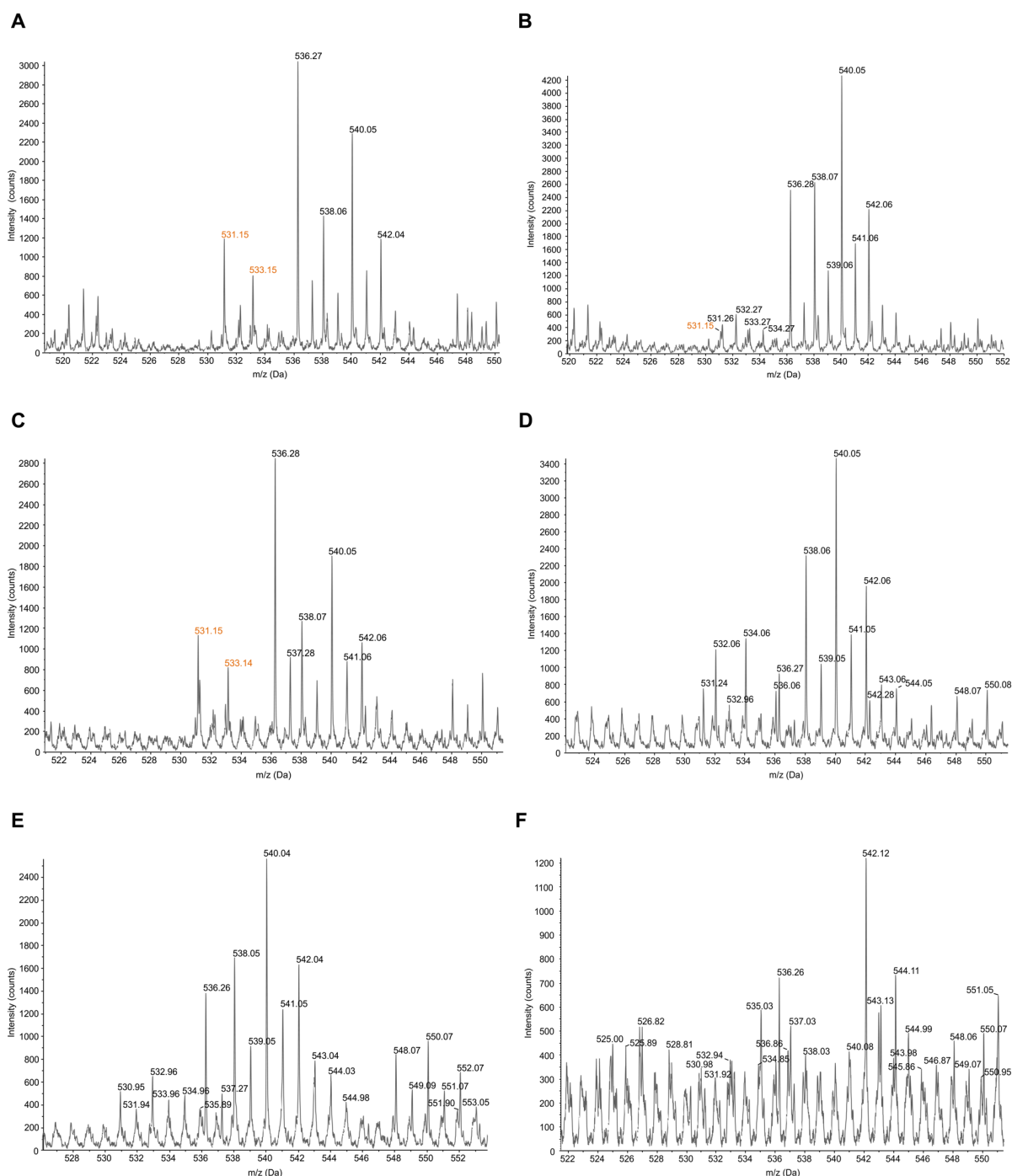


**Figure 8: MS analysis of ketoconazole in Pdr5 containing vesicles after disruption with methanol.** Inside-out oriented Pdr5 plasma membrane vesicles were tested for ketoconazole transport efficiency after vesicle disruption by 80 % methanol (A, Pdr5; B, Pdr5-EQ), 50 % methanol (C, Pdr5; D, Pdr5-EQ) and 20 % methanol (E, Pdr5; F, Pdr5-EQ). Most abundant ketoconazole isotopes are highlighted in orange. Fragment spectra of ketoconazole can be found in the supplemental (Figure S 3).

## Discussion

The identification of the transported substrates from root exudates, could contribute to deepen the current knowledge about the physiology of plant ABC transporters. In contrast to knock-out or reverse genetic studies, transport assays with inside-out oriented plasma membrane vesicles could provide a direct evidence of the identity of the substrate(s). Disadvantages of first mentioned assays are, that mainly one substrate can be analyzed at a time and isolation of specific metabolites from root exudates in sufficient amounts can be challenging. Commercially available metabolites could also behave differently than the natural ones. Hence, the number of the tested substrates have to be restricted to the most potential substrates. An elegant way to circumvent such obstacles would be the development of an MS-based transport assay, which allows the simultaneous analysis of a mixture of potential substrates as for example root exudates. A similar approach has been already introduced by Krumpochova *et al.* (2012). They have demonstrated the identification of transported substrates from body fluids by a MS-based vesicular transport assay and so far, several human ABC transporters have been successfully characterized with similar approaches [30-34, 36]. Here, we used the multidrug resistant ABC transporter Pdr5 from *S. cerevisiae* to establish a similar MS-based assay for previously in *P. pastoris* expressed AtABCG30, AtABCG36 and AtABCG1 (Gräfe *et al.* (2018) *submitted*).

### ***Transport activity of Pdr5 in presence of R6G and selected azoles***

In order to identify maximal substrate concentration for subsequent vesicular transport assays, R6G based transport assays were performed in the presence of non-fluorescent Pdr5 substrates such as ketoconazole, cycloheximide or fluconazole [44]. Contrary to our expectations, the results revealed no inhibition of R6G transport in the presence of ketoconazole, cycloheximide or fluconazole. Similar, observations have been made by Golin *et al.*, for trifluoperazine, who postulated that this could be an effect of multiple binding sites [49]. The substrate selection and transport process of Pdr5, is not completely understood, but current data indicate that the molecular volume of the substrates and specific binding sites are the basis of substrate selection by Pdr5 [41, 44, 50, 51]. It was reported that substrates with surface volumes which are smaller than 90 Å<sup>3</sup> are transported only with low efficiency [41, 44, 50, 51]. According to these criteria, none of the used substrates possess volumes smaller than this limiting value

(cycloheximide: 285 Å<sup>3</sup>, ketoconazole: 481 Å<sup>3</sup>, R6G: 480 Å<sup>3</sup>, fluconazole: 270 Å<sup>3</sup>; calculated with ProteinVolume 1.3). Interestingly, ketoconazole and R6G possess almost identical molecular volumes, which should enable them in principle to compete for Pdr5 translocation. The lack of inhibition of R6G transport in the presence of excess ketoconazole demonstrates that Pdr5 exhibits multiple substrate binding sites. So far, at least three different substrate binding sites have been postulated for Pdr5 and Jancikova *et al.* showed recently that azoles are able to bind to one or two binding sites, while R6G can only bind to one site [41, 44, 50, 51].

In conclusion, it was not possible to identify optimal substrate concentrations for subsequent experiments with Pdr5 plasma membrane vesicles. However, under consideration of the current knowledge regarding the Pdr5 substrate selection process, we conclude that the obtained results could reflect the presence of multiple substrate binding sites. Neither ketoconazole, fluconazole nor cycloheximide compete with R6G for translocation by Pdr5.

### ***Optimization of an MS-based vesicular transport assay***

Ketoconazole was chosen for the optimization of MS-based vesicular assays, because it exhibited a distinct isotope pattern and a low detection limit of at least 20 nM. Comparison of the overview spectra and/or the fragment spectra allowed to adjust different parameters as for instance vesicle concentration, incubation time of the transport assay, washing steps and vesicle disruption methods. The analyzed vesicle disruption methods included mechanical disruption (osmotic pressure, sonification) and detergent (saponin) or organic solvent (methanol) mediated disruption.

The *S. cerevisiae* plasma membrane was apparently resistant to the applied osmotic pressure and sonification conditions, while methanol and partially saponin were able to disrupt the plasma membrane efficiently. Saponin disrupts membranes by interaction with membrane cholesterol [52, 53]. One reason for the low efficiency of disruption of saponin might be the cholesterol depletion, which is replaced in yeast cells by ergosterol [54, 55]. In comparison to that, different methanol concentrations, ranging from 20 % to 100 % were tested and it was finally possible to detect approximately 25 times higher ketoconazole amounts after membrane disruption with 80 % and 50 % methanol. Hence, we were able to establish a very sensitive approach for the substrate identification of ABC transporters.

## **Summary**

In this study, we were able to use Pdr5 containing plasma membranes for the development of a vesicular transport assay. First, R6G transport assays, which were performed to identify optimal substrate concentrations for subsequent vesicular transport assays, revealed that neither ketoconazole, cycloheximide nor fluconazole compete with R6G for translocation by Pdr5. Thus, we were able to demonstrate, as previously shown for example by Golin, Ambudkar [49], that Pdr5 possesses multiple substrate binding sites.

In the second part of this study, we were able to modify the initial R6G transport assay protocol in order to establish a sensitive MS-based vesicular transport assay. Different membrane disruption methods were tested and it was possible to identify ketoconazole from initially 45 counts after saponin disruption, with finally 1200 counts after using 80 % and 50 % methanol. Therefore, the here introduced assay can be used for future studies on heterologously in yeast expressed plant ABC transporters. Thereby, a mixture of potential substrates or root exudates can be used for substrate identification, since similar approaches with body fluids, have been already successfully demonstrated for several human ABC transporters as for instance ABCC2 or ABCG2 [30, 31].

## **Acknowledgment**

We thank Manuel Wagner and Katja Döhl for important technical support and many helpful discussions. This work was funded by the DFG through Cluster of Excellence on Plant Sciences CEPLAS (EXC 1028) to L.S.

## References

1. Saleem, M., et al., *Microbial Interactions in the Phyllosphere Increase Plant Performance under Herbivore Biotic Stress*. Front Microbiol, 2017. **8**: p. 41.
2. Saleem, M. and L.A. Moe, *Multitrophic microbial interactions for eco- and agro-biotechnological processes: theory and practice*. Trends Biotechnol, 2014. **32**(10): p. 529-37.
3. Schmidt, J.E., T.M. Bowles, and A.C. Gaudin, *Using Ancient Traits to Convert Soil Health into Crop Yield: Impact of Selection on Maize Root and Rhizosphere Function*. Front Plant Sci, 2016. **7**: p. 373.
4. Badri, D.V., et al., *Influence of ATP-Binding Cassette Transporters in Root Exudation of Phytoalexins, Signals, and in Disease Resistance*. Front Plant Sci, 2012. **3**: p. 149.
5. Venturi, V. and C. Keel, *Signaling in the Rhizosphere*. Trends Plant Sci, 2016. **21**(3): p. 187-198.
6. Haichar, F.E.Z., et al., *Stable isotope probing of carbon flow in the plant holobiont*. Curr Opin Biotechnol, 2016. **41**: p. 9-13.
7. Roux, S.J. and I. Steinebrunner, *Extracellular ATP: an unexpected role as a signaler in plants*. Trends Plant Sci, 2007. **12**(11): p. 522-7.
8. Thomas, C., et al., *A role for ectophosphatase in xenobiotic resistance*. Plant Cell, 2000. **12**(4): p. 519-33.
9. Kang, J., et al., *Plant ABC Transporters*. Arabidopsis Book, 2011. **9**: p. e0153.
10. Jiang, Y., et al., *Plants transfer lipids to sustain colonization by mutualistic mycorrhizal and parasitic fungi*. Science, 2017. **356**(6343): p. 1172-1175.
11. Luginbuehl, L.H., et al., *Fatty acids in arbuscular mycorrhizal fungi are synthesized by the host plant*. Science, 2017. **356**(6343): p. 1175-1178.
12. Pighin, J.A., et al., *Plant cuticular lipid export requires an ABC transporter*. Science, 2004. **306**(5696): p. 702-4.
13. Bird, D., et al., *Characterization of Arabidopsis ABCG11/WBC11, an ATP binding cassette (ABC) transporter that is required for cuticular lipid secretion*. Plant J, 2007. **52**(3): p. 485-98.
14. Hwang, J.U., et al., *Plant ABC Transporters Enable Many Unique Aspects of a Terrestrial Plant's Lifestyle*. Mol Plant, 2016. **9**(3): p. 338-55.
15. Boursiac, Y., et al., *ABA transport and transporters*. Trends Plant Sci, 2013. **18**(6): p. 325-33.
16. Borghi, L., et al., *The role of ABCG-type ABC transporters in phytohormone transport*. Biochem Soc Trans, 2015. **43**(5): p. 924-30.
17. Kretschmar, T., et al., *A petunia ABC protein controls strigolactone-dependent symbiotic signalling and branching*. Nature, 2012. **483**(7389): p. 341-4.
18. Badri, D.V., et al., *Altered profile of secondary metabolites in the root exudates of Arabidopsis ATP-binding cassette transporter mutants*. Plant Physiol, 2008. **146**(2): p. 762-71.
19. Fourcroy, P., et al., *Involvement of the ABCG37 transporter in secretion of scopoletin and derivatives by Arabidopsis roots in response to iron deficiency*. New Phytol, 2014. **201**(1): p. 155-67.
20. Sasse, J., E. Martinoia, and T. Northen, *Feed Your Friends: Do Plant Exudates Shape the Root Microbiome?* Trends Plant Sci, 2018. **23**(1): p. 25-41.
21. Higgins, C.F., *ABC transporters: physiology, structure and mechanism--an overview*. Res Microbiol, 2001. **152**(3-4): p. 205-10.

22. Higgins, C.F. and K.J. Linton, *The ATP switch model for ABC transporters*. Nat Struct Mol Biol, 2004. **11**(10): p. 918-26.
23. Linton, K.J. and C.F. Higgins, *The Escherichia coli ATP-binding cassette (ABC) proteins*. Mol Microbiol, 1998. **28**(1): p. 5-13.
24. Schmitt, L. and R. Tampe, *Structure and mechanism of ABC transporters*. Curr Opin Struct Biol, 2002. **12**(6): p. 754-60.
25. Sanchez-Fernandez, R., et al., *The Arabidopsis thaliana ABC protein superfamily, a complete inventory*. J Biol Chem, 2001. **276**(32): p. 30231-44.
26. Verrier, P.J., et al., *Plant ABC proteins--a unified nomenclature and updated inventory*. Trends Plant Sci, 2008. **13**(4): p. 151-9.
27. Hawes, M.C., et al., *Function of root border cells in plant health: pioneers in the rhizosphere*. Annu Rev Phytopathol, 1998. **36**: p. 311-27.
28. Bais, H.P., et al., *Exudation of fluorescent beta-carbolines from Oxalis tuberosa L roots*. Phytochemistry, 2002. **61**(5): p. 539-43.
29. Badri, D.V., et al., *An ABC transporter mutation alters root exudation of phytochemicals that provoke an overhaul of natural soil microbiota*. Plant Physiol, 2009. **151**(4): p. 2006-17.
30. Krumpalova, P., et al., *Transportomics: screening for substrates of ABC transporters in body fluids using vesicular transport assays*. FASEB J, 2012. **26**(2): p. 738-47.
31. van de Wetering, K. and S. Sapth, *ABCG2 functions as a general phytoestrogen sulfate transporter in vivo*. FASEB J, 2012. **26**(10): p. 4014-24.
32. van de Wetering, K., et al., *Targeted metabolomics identifies glucuronides of dietary phytoestrogens as a major class of MRP3 substrates in vivo*. Gastroenterology, 2009. **137**(5): p. 1725-35.
33. Jansen, R.S., et al., *N-lactoyl-amino acids are ubiquitous metabolites that originate from CNDP2-mediated reverse proteolysis of lactate and amino acids*. Proc Natl Acad Sci U S A, 2015. **112**(21): p. 6601-6.
34. Jansen, R.S., et al., *ATP-binding Cassette Subfamily C Member 5 (ABCC5) Functions as an Efflux Transporter of Glutamate Conjugates and Analogs*. J Biol Chem, 2015. **290**(51): p. 30429-40.
35. Fulop, K., et al., *ABCC6 does not transport vitamin K3-glutathione conjugate from the liver: relevance to pathomechanisms of pseudoxanthoma elasticum*. Biochem Biophys Res Commun, 2011. **415**(3): p. 468-71.
36. Jansen, R.S., et al., *ABCC6 prevents ectopic mineralization seen in pseudoxanthoma elasticum by inducing cellular nucleotide release*. Proc Natl Acad Sci U S A, 2013. **110**(50): p. 20206-11.
37. Schaedler, T.A., et al., *A conserved mitochondrial ATP-binding cassette transporter exports glutathione polysulfide for cytosolic metal cofactor assembly*. J Biol Chem, 2014. **289**(34): p. 23264-74.
38. Decottignies, A., et al., *Solubilization and characterization of the overexpressed PDR5 multidrug resistance nucleotide triphosphatase of yeast*. J Biol Chem, 1994. **269**(17): p. 12797-803.
39. Egner, R., et al., *Genetic separation of FK506 susceptibility and drug transport in the yeast Pdr5 ATP-binding cassette multidrug resistance transporter*. Mol Biol Cell, 1998. **9**(2): p. 523-43.
40. Meyers, S., et al., *Interaction of the yeast pleiotropic drug resistance genes PDR1 and PDR5*. Curr Genet, 1992. **21**(6): p. 431-6.
41. Golin, J., et al., *Studies with novel Pdr5p substrates demonstrate a strong size dependence for xenobiotic efflux*. J Biol Chem, 2003. **278**(8): p. 5963-9.

42. Rogers, B., et al., *The pleiotropic drug ABC transporters from Saccharomyces cerevisiae*. J Mol Microbiol Biotechnol, 2001. **3**(2): p. 207-14.
43. Ernst, R., et al., *A mutation of the H-loop selectively affects rhodamine transport by the yeast multidrug ABC transporter Pdr5*. Proc Natl Acad Sci U S A, 2008. **105**(13): p. 5069-74.
44. Kolaczowski, M., et al., *Anticancer drugs, ionophoric peptides, and steroids as substrates of the yeast multidrug transporter Pdr5p*. J Biol Chem, 1996. **271**(49): p. 31543-8.
45. Chen, C.R. and G.I. Makhatadze, *ProteinVolume: calculating molecular van der Waals and void volumes in proteins*. BMC Bioinformatics, 2015. **16**: p. 101.
46. Feng, Z., et al., *Ligand Depot: a data warehouse for ligands bound to macromolecules*. Bioinformatics, 2004. **20**(13): p. 2153-5.
47. Galian, C., et al., *Optimized purification of a heterodimeric ABC transporter in a highly stable form amenable to 2-D crystallization*. PLoS One, 2011. **6**(5): p. e19677.
48. Jacob, M.C., M. Favre, and J.C. Bensa, *Membrane cell permeabilization with saponin and multiparametric analysis by flow cytometry*. Cytometry, 1991. **12**(6): p. 550-8.
49. Golin, J., S.V. Ambudkar, and L. May, *The yeast Pdr5p multidrug transporter: how does it recognize so many substrates?* Biochem Biophys Res Commun, 2007. **356**(1): p. 1-5.
50. Hanson, L., et al., *The role of hydrogen bond acceptor groups in the interaction of substrates with Pdr5p, a major yeast drug transporter*. Biochemistry, 2005. **44**(28): p. 9703-13.
51. Jancikova, I., et al., *Differences in the arrangement of the Pdr5p multidrug transporter binding pocket of Saccharomyces cerevisiae and Kluyveromyces lactis*. FEMS Yeast Res, 2017. **17**(7).
52. Lorent, J.H., J. Quetin-Leclercq, and M.P. Mingeot-Leclercq, *The amphiphilic nature of saponins and their effects on artificial and biological membranes and potential consequences for red blood and cancer cells*. Org Biomol Chem, 2014. **12**(44): p. 8803-22.
53. Korchowiec, B., et al., *Impact of two different saponins on the organization of model lipid membranes*. Biochim Biophys Acta, 2015. **1848**(10 Pt A): p. 1963-73.
54. Zinser, E., F. Paltauf, and G. Daum, *Sterol composition of yeast organelle membranes and subcellular distribution of enzymes involved in sterol metabolism*. J Bacteriol, 1993. **175**(10): p. 2853-8.
55. Opekarova, M. and W. Tanner, *Specific lipid requirements of membrane proteins--a putative bottleneck in heterologous expression*. Biochim Biophys Acta, 2003. **1610**(1): p. 11-22.

## Supplementary Information

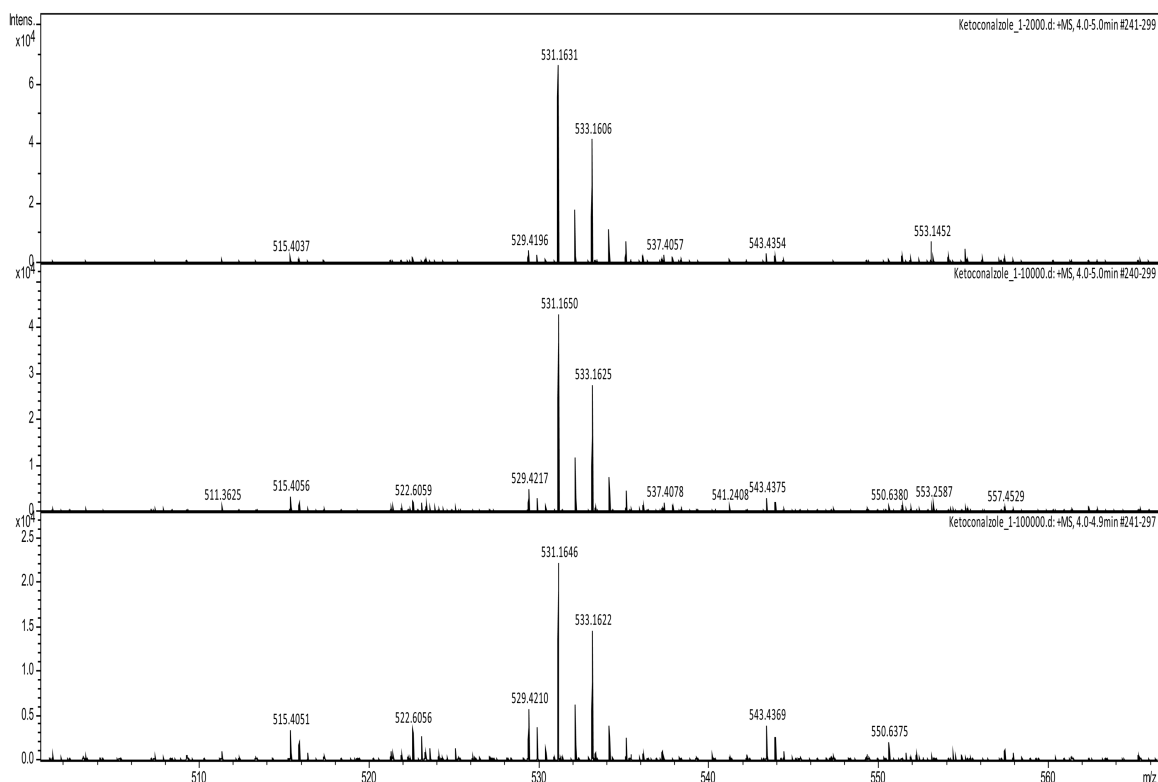


**Figure S 1: Detection limit of ketoconazole for mass spectrometry.** A 1 mg/ml ketoconazole solution was diluted 1:2000, 1:10,000 and 1:100,000 and identified by MS (531.16 Da). Intens., Intensity in counts.

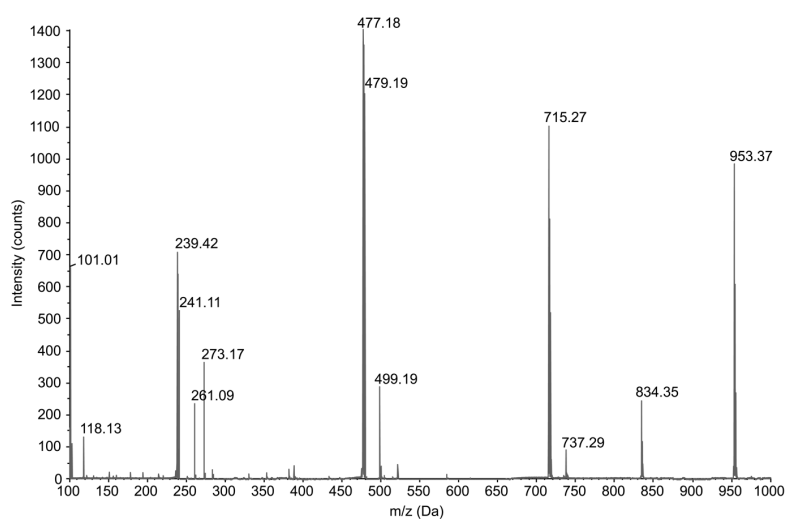


**Figure S 2: Mass spectrometry analysis of ketoconazole in Hepes buffer.** A distinct identification of ketoconazole (531.1 Da) was due to impurities not possible in Hepes buffer.



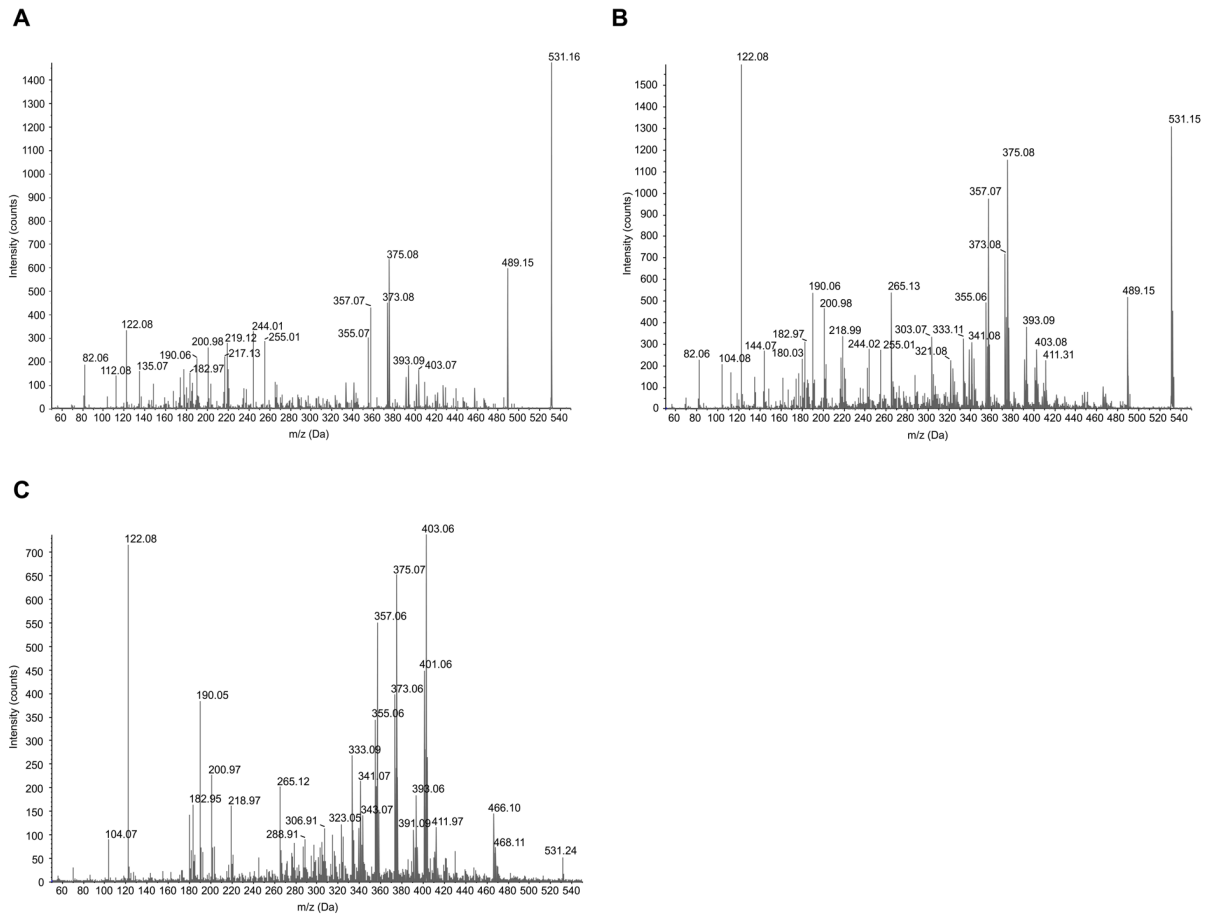


**Figure S 3: Fragment spectra of Pdr5 transported ketoconazole after plasma membrane disruption by methanol.** Inside-out oriented Pdr5 plasma membrane vesicles were analyzed by MS for ketoconazole transport efficiency after vesicle disruption by 80 % methanol (A), 50 % methanol (B) and 20 % methanol (C).

## 4. Discussion

Plants contain, probably due to their sessile and autotroph lifestyle, the largest number of ABC transporters. Despite this huge number, metabolic diversity and presence of various membrane types in eukaryotes require the participation of ABC transporters in many unrelated yet essential functions. Hence, direct transport assays are essential for the unambiguous substrate identification and exposure of their physiological roles. According to Lefevre and Boutry, substrate identities of only 23 out of 130 *Arabidopsis* ABC proteins have been resolved so far via direct transport assays [91].

In this thesis, the methylotrophic yeast *P. pastoris* was introduced as heterologous expression system for plant ABC transporters. Moreover, critical steps which need to be considered during cloning of full-size *ABCG* (PDR) genes or unstable DNA were highlighted (chapter I). The successfully overexpressed full-size transporter AtABCG30 and the half-size transporter AtABCG1 were further studied.

An initial purification protocol for the full-size ABC transporter AtABCG30 is presented (chapter II). The half-size transporter AtABCG1 was purified in a functional active state and shown to be stimulated by suberin precursor molecules. Subsequent *atabcg1* mutant plants studies were performed to verify the identity of the transported substrates (chapter III). Finally, a mass spectrometry-based vesicular transport assay was developed and is presented as an alternative method for substrate identification of ABC transporters (chapter IV).

### 4.1 Cloning and heterologous expression of plant ABCG transporters

The main prerequisite for biochemical and/or biophysical characterization(s) of membrane proteins is the identification of a heterologous expression system that is able to produce the recombinant protein in sufficient amounts. However, heterologous overexpression of membrane proteins is often hampered by gene size, the hydrophobic nature, gene toxicity, misfolding, incorrect localization and / or post-translational modifications [160, 208-210]. As summarized recently by Lefevre and Boutry, plant ABC transporters were characterized by utilizing both prokaryotic and

eukaryotic expression systems, though the optimal expression system was not ascertained yet [91]. Identification of the heterologous expression system rather depends on the protein characteristics and intended experiments.

Prokaryotic expression systems were hitherto rarely used for the characterization of plant ABC transporters and that can be mainly related to the different codon bias or lacking eukaryotic protein processing machinery [211-213]. For instance, the Gram-negative bacterium *E. coli* is the most prominent heterologous expression system for recombinant proteins, but only one full-size ABC transporter was characterized by using it [211, 214]. Similarly, the Gram-positive bacterium *Lactococcus lactis* (*L. lactis*), which is also popular for membrane protein expression, was also once utilized to characterize a plant ABC transporter [215, 216]. Therefore, prokaryotic hosts might not be ideal for heterologous expression of plant ABC transporters.

Yeast systems were the most widely used host for heterologous expression of plant ABC transporters [91]. Thereby, *S. cerevisiae* was successfully used to characterize transporters from the ABCB- and ABCC-subfamily, while characterization of ABCG-family transporters was hampered for instance by wrong subcellular localization [32, 34, 217, 218]. In contrast, characterization of some auxin transporters was achieved by using *Schizosaccharomyces pombe* [34, 219]. Moreover, few transporters have been heterologously expressed in human HeLa cells, insect cells and even *Xenopus* oocytes [34, 97, 220-223]. Finally, also plants were used to characterize plant ABC transporters. Thereby, isolated protoplasts or suspension cells such as tobacco BY-2 cells were successfully used for transport assays [97, 171].

In this thesis, the methylotrophic yeast *P. pastoris* was introduced and evaluated as heterologous expression system for plant ABCG transporters (chapter I).

The initial subcloning attempts of the full-size ABCG genes from the *Arabidopsis* cDNA were complicated due to the gene size of approximately 4-5 kilobase pairs, re-occurring mutations, empty vectors or poor cell growth after transformation into *E. coli* for propagation. Gene specific optimized In-Fusion® cloning with large overlapping regions for homologous recombination in the vector and amplification of the respective gene in two or more fragments, emerged as efficient approach to clone instable gene sequences. But the major obstacle was the gene instability or toxicity of full-size ABCG genes in *E. coli*, which prevented further propagation of successfully cloned genes. Similar observations were made also for other membrane proteins, whereby cloning was hampered due to unstable sequences in *E. coli* [160, 224-228]. Despite these

obstacles, cloning was successfully accomplished by gene sequencing after every subcloning step, extensive screening for positive clones and use of *E. coli* strains, that were specifically designed for propagation of unstable or toxic DNA. Successfully subcloned genes were first attempted to clone into expression vectors for heterologous expression in bacterial systems such as *E. coli* or *L. lactis* and yeast systems like *P. pastoris* and *S. cerevisiae*. However, initial cloning attempts were unsuccessful, except cloning into *P. pastoris*, which was hence further optimized. Finally, 4 out of 6 attempted genes were cloned successfully in *P. pastoris* expression vectors (Table 1). Importantly, only N-terminal tagged constructs of AtABCG36 and additionally codon optimized AtABCG30 and AtABCG1 were successfully overexpressed.

**Table 1: Cloning attempts of ABCG genes into bacterial and yeast vectors.** -, cloning not successful; ✓, cloning accomplished; , not attempted.

Expression Host	Vector	Tag Position	PDR2	PDR4	PDR5	PDR6	PDR7	PDR8
<i>P. pastoris</i>	pSGP18	C	✓	-	-	✓	✓	✓
		N	✓	-		-	-	✓
<i>S. cerevisiae</i>	p426GPD	C	-	-			-	-
	pESC-His	C	-				-	
<i>E. coli</i>	pET16b	C						-
		N				-		✓
	pET28b	C	-		-		-	
		N			-			
<i>L. lactis</i>	pNZ-SV-Entero-His	C	-				-	-
	pIL-SV	C	-				-	-
		N	-				-	

The cloning of the full-size *ABCG* genes as well as the identification of a *P. pastoris* clone expressing the desired protein was time consuming. The critical steps are summarized in this thesis and might help to accomplish future cloning and expression in *P. pastoris* of *ABCG* genes straight forward. The methylotrophic yeast *P. pastoris* constitutes a new expression system for plant ABC transporters, that provides many advantages as for instance the eukaryotic protein processing machinery, tightly regulated promoters and high-density fermentation [229]. Gene sequencing after transformation in *P. pastoris* indicated that gene reorganization of the full-size *ABCG* genes is only restricted to *E. coli* and hence proper expression, processing and localization are not hampered by gene toxicity to the host. The suitability of *P. pastoris* for membrane protein characterization was previously reported for several human ABC transporters [226, 230, 231]. In concert, heterologous expression of AtABCG36 and codon optimized AtABCG30 and AtABCG1 in *P. pastoris* was achieved without visual proteolytic degradation. The correct localization in the plasma membrane was shown by sucrose gradient centrifugation and indicates that the transporters were properly folded and processed. Fermentation attempts resulted in high cell densities yielding up to 1.5 kilogram quantities of wet cell weights (wcw). The purification and functional characterization of AtABCG30 and AtABCG1 were presented in chapter II and III, respectively.

## **4.2 Purification of *Arabidopsis* ABCG transporters**

The purification of membrane proteins in a functional state is essential for any further protein characterization. Detergents, amphipathic molecules with a hydrophilic head and a hydrophilic tail, are able to isolate membrane proteins from the lipid bilayer. Based on the charge of the head group can detergents be differentiated in anionic, zwitterionic, cationic and neutral classes. Up to 100 different detergents were tested using the dot blot technique for solubilization of AtABCG30 and AtABCG1 from the lipid bilayer [226]. The following section compares the purification of the full-size ABCG transporter AtABCG30 and the half-size ABCG transporter AtABCG1.

The dot-blot experiments with AtABCG30 containing crude membranes resulted in in higher solubilization efficiencies for zwitterionic and anionic detergents. Subsequent solubilization screens with variations in buffer, temperature, detergent and membrane

concentrations remained ineffective. A similar experimental approach with AtABCG30 containing plasma membranes, remained unsuccessful as well. Although different conditions were tested, a quantitative solubilization, most probably due to pH-incompatibility or not ideal buffer conditions was not obtained. Solubilized and non-solubilized proteins remained aggregated between the separating and stacking gel sections (chapter II; Figure 5). Fos-Choline 14 was chosen for a subsequent purification attempt, as it was found in both detergent screens amongst the detergents, which efficiently solubilized AtABCG30. A calmodulin-binding peptide (CBP) affinity purification from AtABCG30 containing plasma membranes yielded in approximately 0.4 mg purified AtABCG30 per 100 g wet cell, while the purification from crude membranes yielded up to 4 times more purified protein with 2 mg per 100 g wet cells. The latter one exhibited thereby severe proteolytic degradation. The enzymatic activity was subsequently analyzed and resulted, due to inappropriate purification conditions, in lack of AtABCG30 activity.

In contrast, purification of the half-size transporter AtABCG1 was more successful. A dot blot experiment, followed by optimization of solubilization and buffer conditions, resulted in efficient solubilization of AtABCG1 from crude membranes. Subsequent CBP affinity purification yielded in 2 mg purified AtABCG1 per 100 g wet cells (chapter III, Figure 1). A BN-PAGE demonstrated that the native oligomeric state of the detergent purified AtABCG1 was homodimeric. Potential interaction partners could be revealed by further protein-protein interaction studies. The protein functionality was confirmed by ATPase assays, whereby purified AtABCG1 exhibited a maximal reaction velocity  $v_{\max}$  of  $17.1 \pm 0.1 \text{ nmol min}^{-1}$  per mg purified AtABCG1 and a  $K_m$  value of  $1.8 \pm 0.1 \text{ mM}$  (chapter III; Figure 3, Table 1).

In conclusion, the full-size transporter AtABCG30, as well as the half-size transporter AtABCG1 were expressed for the first time heterologously in *P. pastoris* and shown to be correctly targeted to the plasma membrane. Subsequent purification attempts indicated that the purification of a half-size transporter was successful in comparison to the purification of the full-size transporter. A challenging factor could also be the number of alpha helices per TMD. The AtABCG1 monomer contains 6 alpha helices, while AtABCG30 contains 7 alpha helices per TMD (as predicted by TOPCONS, <http://topcons.cbr.su.se/>). A higher number could cause the need for harsher or higher amounts of detergents, which in turn can make solubilization without complete delipidation challenging. Nevertheless, it is not the first time that a purified ABC

transporter lacks ATPase activity. For instance, similarly in *P. pastoris* expressed and Fos-Choline solubilized human ABC transporter BSEP lacked ATPase activity, despite changing to milder detergents after solubilization [226]. Further examples are *P. pastoris* expressed AtABCG36 (K. Gräfe, PhD thesis, HHU Düsseldorf 2018), human ABCD1, the *L. lactis* ABC transporter LmrA [232, 233]. As shown in chapter II the applied solubilization conditions of AtABCG30 were already unfavorable, yet further optimization of the solubilization and purification conditions, including detergent exchange to milder detergents could enable retaining the ATPase activity of purified AtABCG30. However, for the first time AtABCG1, was heterologously expressed in *P. pastoris* and purified in a functional state. So far only few plant ABC transporters, for instance AtABCD1 [234], AtABCB25 [216] and ABCG1 from *Nicotiana tabacum* [171] were purified in a functional state and characterized by a ATPase assay.

### 4.3 Functional characterization of AtABCG1

Due to their sessile lifestyle plants are exposed to various abiotic and biotic stress factors including drought, UV light, atmospheric pollutants, pathogen attack or plant wounding. Diffusion barriers enable plants to counter those stress factors and provide hence a first physical defense barrier [103, 104]. Suberin is a complex glycerolipid-phenolic polymer, that mainly occurs in tissue-tissue or plant-environmental interfaces, as for instance root endodermal and peridermal cell walls [132]. It forms in concert with the Casparian strips, apoplastic barriers for water and solute movements in the roots [103, 133]. Additional suberization in the tissues can be induced by abiotic (for instance salinity, organic acids, high nutrients, drought) and biotic (for instance pathogens, plant wounding) stress factors [134, 137, 235-237]. The suberin polymer consists of a polyaliphatic polyester, which is linked with phenolic components and embedded in waxes. Typically found monomers of the aliphatic part are  $\omega$ -hydroxy acids,  $\alpha,\omega$ -dicarboxylic acids, fatty acids and alcohols. Thereby glycerol is esterified to the  $\omega$ -hydroxy and  $\alpha,\omega$ -dicarboxylic acids and the phenylpropanoid pathway derived phenolic compounds [120, 135]. In this thesis, the *Arabidopsis* half-size transporter ABCG1 was analyzed regarding its involvement in root suberin formation.

Comparative sequence analysis amongst ABCG1 from *A. thaliana*, *S. tuberosum* and

*Petunia hybrida* (*P. hybrida*) revealed the highest identity amongst AtABCG1 and the potential suberin precursor transporter StABCG1 (74 % sequence, 69 % NBD sequence, 81 % TMD sequence identity). Based on that, commercially available putative StABCG1 substrates were selected and purified AtABCG1 was analyzed by functional assays for substrate specificity. The basal activity of purified AtABCG1 was stimulated up to 90 % by fatty alcohols and acids with chain length of and C<sub>26</sub>-C<sub>30</sub> and C<sub>24</sub>-C<sub>30</sub>, respectively. Similar to StABCG1 that was assumed to be involved in transport of  $\omega$ -hydroxy fatty acids,  $\alpha$ ,  $\omega$ - dicarboxylic acids, fatty alcohols, fatty acids with a chain length of C<sub>24</sub> and longer, increased the stimulatory effect on AtABCG1 with the substrate chain length up to 90 % for C<sub>28</sub> fatty alcohol and 80 % for C<sub>26</sub> fatty acid, respectively and decreased thereafter [153]. Similarly, specific activity of several ABC transporters, as for instance Pdr5, the human TAP (transporter associated with antigen processing) or efflux transporter P-glycoprotein (P-gp/MDR1) were found to be induced by their transported substrates [238-241]. Subsequent studies on T-DNA insertional *atabcg1* mutants confirmed these results largely. In comparison to wildtype plants contained mutant plants decreased relative abundance of C<sub>20</sub>-C<sub>24</sub>  $\alpha$ ,  $\omega$ - dicarboxylic acids, C<sub>24</sub> and C<sub>26</sub> fatty acids and alcohols in the roots. Thus, C<sub>20</sub>-C<sub>24</sub>  $\alpha$ ,  $\omega$ - dicarboxylic acids were identified by mutant plant studies as putative substrates, while C<sub>26</sub> fatty alcohols, C<sub>24</sub> and C<sub>26</sub> fatty acids were identified unambiguous by both, direct functional and mutant plant studies, as AtABCG1 substrates (Figure 13).

Although, this study clearly indicated the involvement of AtABCG1 in suberin formation and revealed transported substrates unambiguously, further studies could help to better understand the physiological role of AtABCG1 in the plant and estimate its impact in suberin formation. For instance, were ABC transporters with similar substrate specificity for aliphatic suberin monomers lacking the dark suberin lamellae in the root that is normally found in wildtype plants [113, 153]. The *atabcg2 atabcg6 atabcg20* triple mutant plant displayed besides reduced abundance of suberin monomers in the roots and the seeds also increased permeability [113]. Hence similar studies with *atabcg1* mutant plants could help to further elucidate and phenotypically verify the role of AtABCG1 in suberin formation.



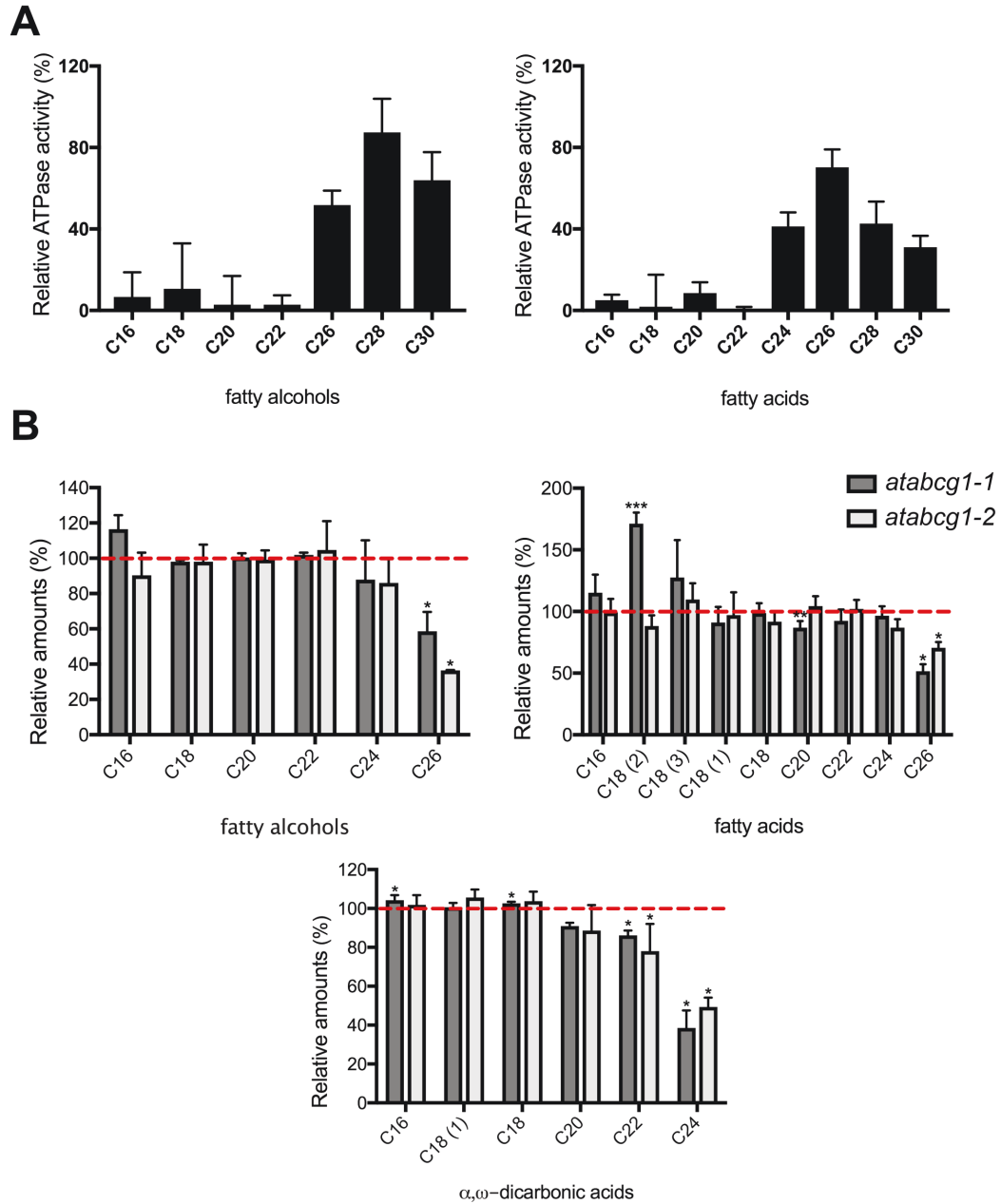


**Figure 13: AtABCG1 involvement in root suberin formation.** A, Relative ATPase activity of AtABCG1 in presence of 40  $\mu$ M fatty acids and fatty alcohols (C<sub>16</sub>- C<sub>30</sub>). B, Monomer composition of *Arabidopsis* wildtype and *atabcg1* mutant root suberin. The relative abundance of suberin monomers in the independent T-DNA insertional mutant lines *atabcg1-1* (n=4) and *atabcg1-2* (n=4) per substance class is depicted in comparison to the wildtype (n=4). red, wildtype values set to 100 %. Data represents mean and  $\pm$  SD. Significance analysis between *atabcg1* mutants and wildtype samples were performed by t test. (two-tailed):  $P \leq 0.0001$ ,  $P \leq 0.01$ ,  $P \leq 0.05$ . The Figure is assembled by from Figures 4 and 6 of chapter III.

#### 4.3.1 ABC transporters in *Arabidopsis* root suberin formation

So far, AtABCG1 was mainly considered, as shown by *atabcg1 atabcg16* double mutant studies, to be involved in pollen wall formation and postmeiotic pollen development [112, 113]. Thereby, the single *atabcg1* mutant showed no fertility defects, which might indicate a heterodimerization or overlapping substrate specificity for AtABCG1 and AtABCG16.

However, as described above AtABCG1 was also found to be involved in suberin precursor transport. The plasma membrane localized half-size transporter AtABCG1 belongs to a phylogenetic clade of half-size transporters (AtABCG2, AtABCG6, AtABCG20, AtABCG16), that are co-expressed with several suberin biosynthesis genes, including *GPAT5*, *FAR1*, *FAR4*, *FAR5*, *CYP86A1*, *CYP86B1*, and *ASFT*. The expression of these suberin biosynthesis genes can be induced by abiotic stress factors as for instance salt, wounding or the phytohormone ABA [143, 144, 146, 242, 243]. Notably, ABA and salt treatment was also found to induce gene expression of all clade members [113].

Further physiological roles within the plant, as shown here for AtABCG1, are conceivable for all clade member, since all genes displayed a spatial expression pattern, that included anthers and or maturing pollen, developing seeds, vegetative shoots and roots [113]. In concert, direct transport assays with AtABCG16, which is found on the same phylogenetic subclade as AtABCG1, revealed that its transport function is not only restricted to pollen related compounds, but also jasmonic acid [244]. The involvement of AtABCG16 in suberin formation might also be possible, as the *AtABCG16* transcript level was significantly increased in *atabcg2 atabcg6 atabcg20* triple mutant plants. Thus, the whole gene clade might be involved in suberin formation and on the other hand further physiological roles might be indicated through the spatial expression pattern.

As shown in Figure 14, suberin monomers of the aliphatic domain are synthesized in the endoplasmatic reticulum, while the components for the aliphatic polyester are derived from the phenylpropanoid pathway in the cytosol. Different predictions exist for the transport of the suberin building blocks across the plasma membrane, such as the secretory pathway, passive transport of oleophilic bodies or transport by ABC transporters [132, 152]. In *Arabidopsis* triple mutant studies revealed that AtABCG2, AtABCG6 and AtABCG20 are involved in transport of C<sub>20</sub> and C<sub>22</sub> fatty acids, C<sub>22</sub> fatty alcohol, and C<sub>18:1</sub>  $\omega$ -hydroxy fatty alcohols, while AtABCG11 is of proposed to transport

C<sub>20</sub> fatty acids, C<sub>18</sub> fatty alcohols, and C<sub>16</sub> and C<sub>18</sub> ω-OH fatty acids. However, a direct involvement of AtABCG11 is not suspected, rather competition for common cutin and suberin fatty acid precursors, since AtABCG11 was already proposed to be a cutin transporter [113, 121, 124]. The cutin layer is formed by ester bound C<sub>16</sub>-C<sub>18</sub> dicarboxylic acids, which is embedded and overlaid by cuticular waxes. [118, 119]. Thereby, abundantly found wax compounds are primary and secondary alcohols, alkanes, aldehydes, ketones, fatty acids and wax esters [118, 119]. Besides AtABCG11, were ABCG12 and ABCG13 and the full-size transporter AtABCG32 found to be involved in wax and cutin transport [35, 121-126]. Root suberin analysis of these cutin transporters might reveal a possible function in suberin formation.

Finally, we could show in this thesis that AtABCG1 is involved in transport of C<sub>20</sub>-C<sub>24</sub> α, ω- dicarboxylic acids, C<sub>26</sub> and C<sub>24</sub> fatty alcohols and acids, respectively. The transported suberin precursors are assembled in the cell wall into the suberin macromolecule. Nevertheless, the involvement of further half-size transporters, possibilities for dimerization or co-transport have to be examined. For instance, Yadav et al. proposed that the half-size transporters AtABCG10 and AtABCG23 might contribute to the suberin formation as well, as they were co-expressed with suberin biosynthesis genes [113].

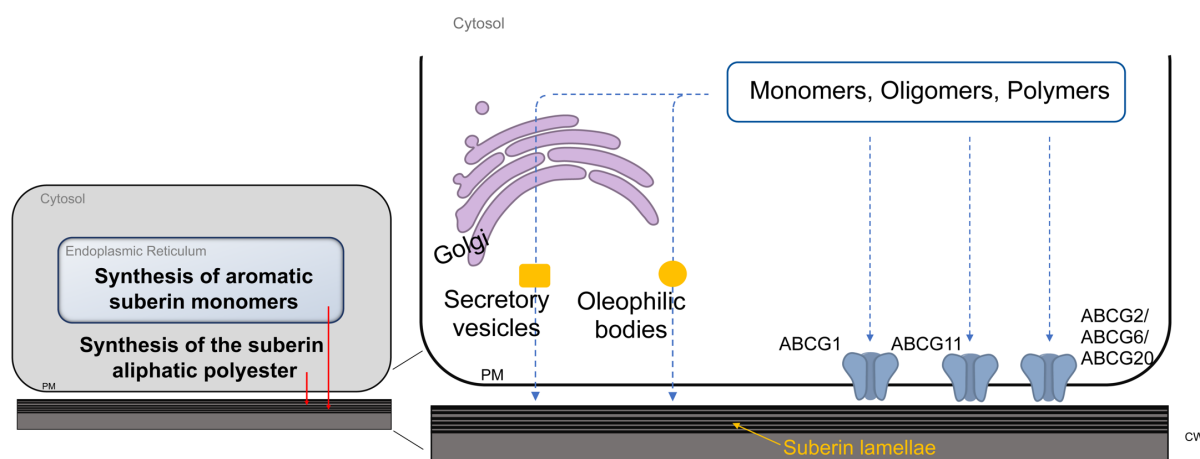


**Figure 14: Hypothetical model of suberin biosynthesis in *Arabidopsis*.** Adapted from [132] and [245].

### 4.3.2 Phylogenetic analysis of AtABCG1

Notably, half-size transporters across different plant species were found to contribute to suberin barrier formation [113, 131, 153, 154]. A phylogenetic analysis of half-size ABCG transporters that are presumed to transport suberin precursors from *A. thaliana*, *O. sativa* and *S. tuberosum* was performed (Figure 15). Potential suberin precursor transporters clustered together, whereby AtABCG1-AtABCG16 and AtABCG2-AtABCG20, respectively localized to different subclades. Thereby AtABCG16, (84 %), AtABCG6 (72 %) and StABCG1 (74 %) displayed the highest amino acid sequence identity with AtABCG1. OsABCG5, AtABCG2 and AtABCG20 had 63 % to 67 % sequence identity with AtABCG1. AtABCG11 which was presumed to be indirectly involved in suberin formation and rather in cutin formation clustered together with the other cutin transporters, AtABCG12 and AtABCG13. AtABCG10 and AtABCG23, transporters that were co-expressed with suberin biosynthesis genes clustered separately as well [113]. Hence, these transporters might be involved, similar to AtABCG11, indirectly in suberin synthesis. The final cluster is formed by the remaining transporters, whereby AtABCG9 and AtABCG14 differentiate on a subclade. AtABCG14 was found to be part of cytokinin and lipid transport, while AtABCG9 is involved in lipid transport as well and additionally in transport of steryl glycosides for pollen wall formation. AtABCG22 and AtABCG25 were found to be involved in ABA transport. Although AtABCG9 and AtABCG26 was ascribed to be part of pollen wall formation, were they located on a separate cluster than AtABCG1 and AtABCG16. In accordance the amino acid sequence identity with AtABCG1 (29 % and 25 %) and AtABCG16 (30 % and 27 %) was very low. Thus, AtABCG1 and AtABCG16 are rather closely related to potential suberin precursor transporters. Even though AtABCG16 was found to be involved together with AtABCG1 in pollen development and protection, can the involvement in suberin formation not be ruled out. As shown by Yadav et al. was the *AtABCG16* expression significantly increased in *AtABCG2*, *AtABCG6* and *AtABCG20* lacking plants, which might indicate a compensatory function [113].

In conclusion, the obtained results indicate that the suberin formation across the analyzed plant species seems to be a half-size ABCG transporter dominated function. Possible reasons could be the capacity for dimerization, that could enable to branch out the substrate specificity that is essential to transport the huge number of suberin precursor molecules.

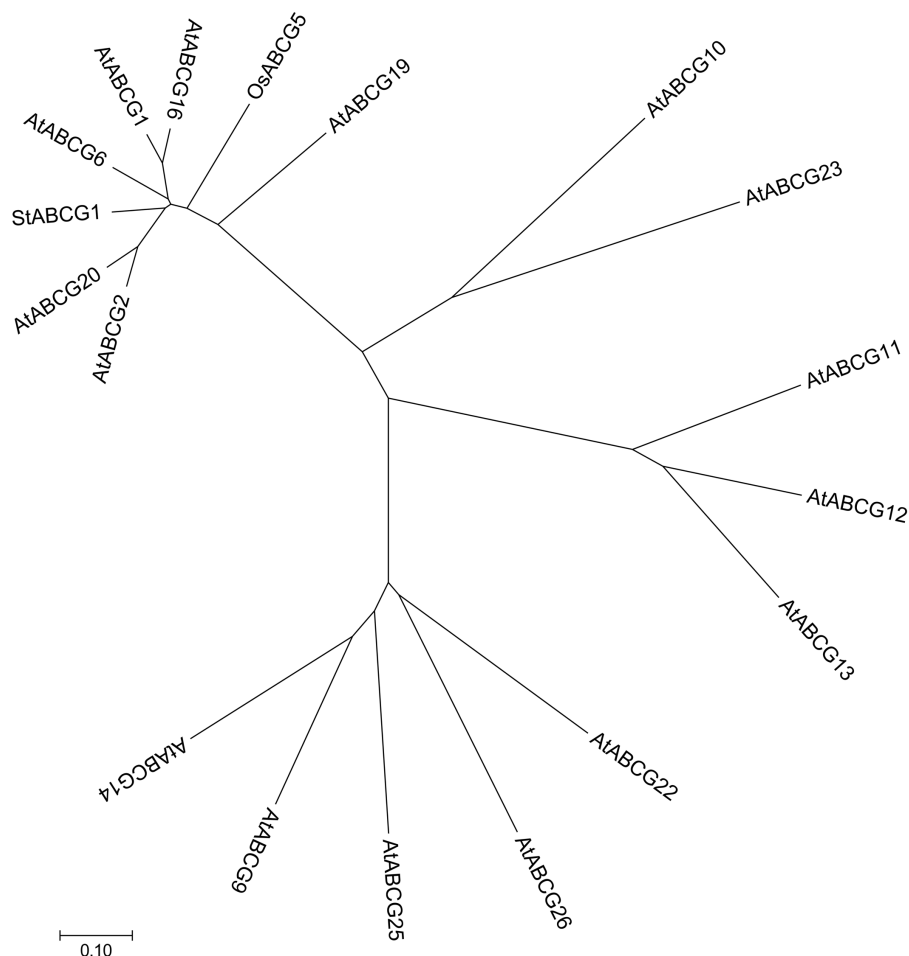


**Figure 15: Neighbor-Joining phylogenetic tree of half-size ABCG transporters involved in suberin formation.** The evolutionary history of functionally characterized half-size ABCG transporters from *A. thaliana* and potential suberin precursor transporters from *O. sativa* and *S. tuberosum* was inferred using the Neighbor-Joining method [246]. Sequence alignments were performed with ClustalOmega. The optimal tree with the sum of branch length equal to 5.155 is shown. The tree is drawn to scale, with branch lengths in the same units as those of the evolutionary distances used to infer the phylogenetic tree. The evolutionary distances were computed using the Poisson correction method [247] and are in the units of the number of amino acid substitutions per site. All positions containing gaps and missing data were removed. There were a total of 514 positions in the final dataset. Evolutionary analysis were conducted in MEGA7 [248].

#### 4.4 A yeast membrane based vesicular transport assay for plant ABC transporters

Both, AtABCG30 and AtABCG1, are inter alia highly expressed in the roots and were therefore hypothesized to be involved in root exudation [31]. Root exudates are mainly

composed of carbon-based compounds, including sugars, organic acids, complex polymers and secondary metabolites and enable plants to shape the microbial community in the rhizosphere [196-198]. In concert, an *atabcg30* mutant plant exhibited significant changes in the root exudate profile and the microbial communities in the soil [31, 185]. Hence AtABCG30 transport function is not only restricted to ABA transport in the seeds and a similar function in root exudation is conceivable for AtABCG1 as well.

In general, unambiguous substrate identification of heterologous expressed membrane proteins can be accomplished for instance by ATPase assays with purified (chapter III) or lipid-reconstituted proteins. Alternatively, vesicular transport assays with radioactive labeled or fluorescent substrates were used for substrate identification [249]. However, identification of transported substrates from a wide spectrum of potential substrates can become very laborious by using these kinds of methods. The mass spectrometry (MS) based vesicular transport assay constitutes an efficient alternative, as it enables the identification of the transported substrates from a mixture of potential substrates or root exudates. As previously introduced by Krumpochova et al., inside-out oriented membrane vesicles that contain the ABC transporter, were incubated in the presence of ATP with a mixture of potential substrates. Transported substrates can subsequently be identified via MS [250]. So far, one plant ABC transporter, AtABCB25, was characterized after heterologous expression in *L. lactis* by a similar approach [216].

The last chapter of this thesis presented the proof-of-principle of a MS-based vesicular transport assay for heterologous in yeast expressed ABC transporters. The full-size ABCG transporter Pdr5 from *S. cerevisiae* was used for method-optimization, as it is similar to AtABCG30 and AtABCG1 located in the plasma membrane and known to be resistant against various unrelated cytotoxic compounds (multidrug resistance, MDR) [239, 251-254].

The R6G transport assay protocol [255] was used to establish a sensitive MS-based vesicular transport assay. Buffer conditions, incubation conditions, and number of necessary washing steps were defined by comparison with the respective MS spectra. Subsequently, membrane disruption efficiencies of different methods, including mechanical disruption (osmotic pressure, sonification) and detergent (saponin) or organic solvent (methanol) were analyzed by MS. Finally, it was possible to identify ketoconazole from initially 45 counts after saponin disruption, with finally 1200 counts

after using 80 % and 50 % methanol (chapter IV, Figure 8). Hence the here established assay can be applied on AtABCG30 or AtABCG1 containing *P. pastoris* plasma membrane vesicles for the identification of transported substrates from a mixture of potential substances, as for instance root exudates.

This thesis laid a new foundation for future studies on plant ABC transporters. The identification of transported substances can not only help to get more insight into the plant physiology, but also contribute to improve plant growth, fitness and obtain a sustainable plant production.

## 5. Literature

1. Singer, S.J. and G.L. Nicolson, *The fluid mosaic model of the structure of cell membranes*. Science, 1972. **175**(4023): p. 720-31.
2. Kusumi, A., et al., *Membrane mechanisms for signal transduction: the coupling of the meso-scale raft domains to membrane-skeleton-induced compartments and dynamic protein complexes*. Semin Cell Dev Biol, 2012. **23**(2): p. 126-44.
3. Glancy, B. and R.S. Balaban, *Role of mitochondrial Ca<sup>2+</sup> in the regulation of cellular energetics*. Biochemistry, 2012. **51**(14): p. 2959-73.
4. Raposo, G. and W. Stoorvogel, *Extracellular vesicles: exosomes, microvesicles, and friends*. J Cell Biol, 2013. **200**(4): p. 373-83.
5. Vereb, G., et al., *Dynamic, yet structured: The cell membrane three decades after the Singer-Nicolson model*. Proc Natl Acad Sci U S A, 2003. **100**(14): p. 8053-8.
6. Gouaux, E. and R. Mackinnon, *Principles of selective ion transport in channels and pumps*. Science, 2005. **310**(5753): p. 1461-5.
7. Watson, H., *Biological membranes*. Essays Biochem, 2015. **59**: p. 43-69.
8. Alberts, B., et al., *Molecular Biology of the Cell*, 4th edition. New York: Garland Science, 2002.
9. Roux, B., et al., *Ion selectivity in channels and transporters*. J Gen Physiol, 2011. **137**(5): p. 415-26.
10. Hille, B., C.M. Armstrong, and R. MacKinnon, *Ion channels: from idea to reality*. Nat Med, 1999. **5**(10): p. 1105-9.
11. Diamond, J.M. and Y. Katz, *Interpretation of nonelectrolyte partition coefficients between dimyristoyl lecithin and water*. J Membr Biol, 1974. **17**(2): p. 121-54.
12. Boyer, P.D., *The ATP synthase--a splendid molecular machine*. Annu Rev Biochem, 1997. **66**: p. 717-49.
13. Lanyi, J.K., *Bacteriorhodopsin*. Annu Rev Physiol, 2004. **66**: p. 665-88.
14. Boudker, O., et al., *Coupling substrate and ion binding to extracellular gate of a sodium-dependent aspartate transporter*. Nature, 2007. **445**(7126): p. 387-93.
15. van Helvoort, A., et al., *MDR1 P-glycoprotein is a lipid translocase of broad specificity, while MDR3 P-glycoprotein specifically translocates phosphatidylcholine*. Cell, 1996. **87**(3): p. 507-17.
16. Devaux, P.F., et al., *How lipid flippases can modulate membrane structure*. Biochim Biophys Acta, 2008. **1778**(7-8): p. 1591-600.
17. Higgins, C.F., *ABC transporters: physiology, structure and mechanism--an overview*. Res Microbiol, 2001. **152**(3-4): p. 205-10.
18. Higgins, C.F., et al., *Complete nucleotide sequence and identification of membrane components of the histidine transport operon of S. typhimurium*. Nature, 1982. **298**(5876): p. 723-7.
19. Theodoulou, F.L. and I.D. Kerr, *ABC transporter research: going strong 40 years on*. Biochem Soc Trans, 2015. **43**(5): p. 1033-40.
20. Davidson, A.L., et al., *Structure, function, and evolution of bacterial ATP-binding cassette systems*. Microbiol Mol Biol Rev, 2008. **72**(2): p. 317-64, table of contents.
21. Cui, J. and A.L. Davidson, *ABC solute importers in bacteria*. Essays Biochem, 2011. **50**(1): p. 85-99.
22. Raetz, C.R., et al., *Lipid A modification systems in gram-negative bacteria*. Annu Rev Biochem, 2007. **76**: p. 295-329.



23. Cuthbertson, L., V. Kos, and C. Whitfield, *ABC transporters involved in export of cell surface glycoconjugates*. Microbiol Mol Biol Rev, 2010. **74**(3): p. 341-62.
24. Ruiz, N., et al., *Identification of two inner-membrane proteins required for the transport of lipopolysaccharide to the outer membrane of Escherichia coli*. Proc Natl Acad Sci U S A, 2008. **105**(14): p. 5537-42.
25. Wong, K., et al., *Towards understanding promiscuity in multidrug efflux pumps*. Trends Biochem Sci, 2014. **39**(1): p. 8-16.
26. Seeger, M.A. and H.W. van Veen, *Molecular basis of multidrug transport by ABC transporters*. Biochim Biophys Acta, 2009. **1794**(5): p. 725-37.
27. Gadsby, D.C., P. Vergani, and L. Csanady, *The ABC protein turned chloride channel whose failure causes cystic fibrosis*. Nature, 2006. **440**(7083): p. 477-83.
28. Rudkowska, I. and P.J. Jones, *Polymorphisms in ABCG5/G8 transporters linked to hypercholesterolemia and gallstone disease*. Nutr Rev, 2008. **66**(6): p. 343-8.
29. Tang, C. and J.F. Oram, *The cell cholesterol exporter ABCA1 as a protector from cardiovascular disease and diabetes*. Biochim Biophys Acta, 2009. **1791**(7): p. 563-72.
30. Tarling, E.J., T.Q. de Aguiar Vallim, and P.A. Edwards, *Role of ABC transporters in lipid transport and human disease*. Trends Endocrinol Metab, 2013. **24**(7): p. 342-50.
31. Badri, D.V., et al., *Altered profile of secondary metabolites in the root exudates of Arabidopsis ATP-binding cassette transporter mutants*. Plant Physiol, 2008. **146**(2): p. 762-71.
32. Ito, H. and W.M. Gray, *A gain-of-function mutation in the Arabidopsis pleiotropic drug resistance transporter PDR9 confers resistance to auxinic herbicides*. Plant Physiol, 2006. **142**(1): p. 63-74.
33. Strader, L.C. and B. Bartel, *The Arabidopsis PLEIOTROPIC DRUG RESISTANCE8/ABCG36 ATP binding cassette transporter modulates sensitivity to the auxin precursor indole-3-butyric acid*. Plant Cell, 2009. **21**(7): p. 1992-2007.
34. Ruzicka, K., et al., *Arabidopsis PIS1 encodes the ABCG37 transporter of auxinic compounds including the auxin precursor indole-3-butyric acid*. Proc Natl Acad Sci U S A, 2010. **107**(23): p. 10749-53.
35. Bessire, M., et al., *A member of the PLEIOTROPIC DRUG RESISTANCE family of ATP binding cassette transporters is required for the formation of a functional cuticle in Arabidopsis*. Plant Cell, 2011. **23**(5): p. 1958-70.
36. Hwang, J.U., et al., *Plant ABC Transporters Enable Many Unique Aspects of a Terrestrial Plant's Lifestyle*. Mol Plant, 2016. **9**(3): p. 338-55.
37. Higgins, C.F. and K.J. Linton, *The ATP switch model for ABC transporters*. Nat Struct Mol Biol, 2004. **11**(10): p. 918-26.
38. Bouige, P., et al., *Phylogenetic and functional classification of ATP-binding cassette (ABC) systems*. Curr Protein Pept Sci, 2002. **3**(5): p. 541-59.
39. Thomas, C. and R. Tampe, *Multifaceted structures and mechanisms of ABC transport systems in health and disease*. Curr Opin Struct Biol, 2018. **51**: p. 116-128.
40. Kang, J., et al., *Abscisic acid transporters cooperate to control seed germination*. Nat Commun, 2015. **6**: p. 8113.
41. Slotboom, D.J., *Structural and mechanistic insights into prokaryotic energy-coupling factor transporters*. Nat Rev Microbiol, 2014. **12**(2): p. 79-87.

42. Rodionov, D.A., et al., *A novel class of modular transporters for vitamins in prokaryotes*. J Bacteriol, 2009. **191**(1): p. 42-51.
43. Wang, B., et al., *Membrane porters of ATP-binding cassette transport systems are polyphyletic*. J Membr Biol, 2009. **231**(1): p. 1-10.
44. Schmitt, L. and R. Tampe, *Structure and mechanism of ABC transporters*. Curr Opin Struct Biol, 2002. **12**(6): p. 754-60.
45. Linton, K.J. and C.F. Higgins, *The Escherichia coli ATP-binding cassette (ABC) proteins*. Mol Microbiol, 1998. **28**(1): p. 5-13.
46. Oldham, M.L., et al., *Crystal structure of a catalytic intermediate of the maltose transporter*. Nature, 2007. **450**(7169): p. 515-21.
47. Hvorup, R.N., et al., *Asymmetry in the structure of the ABC transporter-binding protein complex BtuCD-BtuF*. Science, 2007. **317**(5843): p. 1387-90.
48. Wang, T., et al., *Structure of a bacterial energy-coupling factor transporter*. Nature, 2013. **497**(7448): p. 272-6.
49. Dawson, R.J. and K.P. Locher, *Structure of a bacterial multidrug ABC transporter*. Nature, 2006. **443**(7108): p. 180-5.
50. ter Beek, J., A. Guskov, and D.J. Slotboom, *Structural diversity of ABC transporters*. J Gen Physiol, 2014. **143**(4): p. 419-35.
51. Rees, D.C., E. Johnson, and O. Lewinson, *ABC transporters: the power to change*. Nat Rev Mol Cell Biol, 2009. **10**(3): p. 218-27.
52. Hollenstein, K., D.C. Frei, and K.P. Locher, *Structure of an ABC transporter in complex with its binding protein*. Nature, 2007. **446**(7132): p. 213-6.
53. Kadaba, N.S., et al., *The high-affinity E. coli methionine ABC transporter: structure and allosteric regulation*. Science, 2008. **321**(5886): p. 250-3.
54. Locher, K.P., A.T. Lee, and D.C. Rees, *The E. coli BtuCD structure: a framework for ABC transporter architecture and mechanism*. Science, 2002. **296**(5570): p. 1091-8.
55. Pinkett, H.W., et al., *An inward-facing conformation of a putative metal-chelate-type ABC transporter*. Science, 2007. **315**(5810): p. 373-7.
56. Eitinger, T., et al., *Canonical and ECF-type ATP-binding cassette importers in prokaryotes: diversity in modular organization and cellular functions*. FEMS Microbiol Rev, 2011. **35**(1): p. 3-67.
57. Yu, Y., et al., *Planar substrate-binding site dictates the specificity of ECF-type nickel/cobalt transporters*. Cell Res, 2014. **24**(3): p. 267-77.
58. Erkens, G.B., et al., *The structural basis of modularity in ECF-type ABC transporters*. Nat Struct Mol Biol, 2011. **18**(7): p. 755-60.
59. Ward, A., et al., *Flexibility in the ABC transporter MsbA: Alternating access with a twist*. Proc Natl Acad Sci U S A, 2007. **104**(48): p. 19005-10.
60. Dong, J., G. Yang, and H.S. McHaourab, *Structural basis of energy transduction in the transport cycle of MsbA*. Science, 2005. **308**(5724): p. 1023-8.
61. Mourez, M., M. Hofnung, and E. Dassa, *Subunit interactions in ABC transporters: a conserved sequence in hydrophobic membrane proteins of periplasmic permeases defines an important site of interaction with the ATPase subunits*. EMBO J, 1997. **16**(11): p. 3066-77.
62. Becker, J.P., et al., *Dynamics and structural changes induced by ATP binding in SAV1866, a bacterial ABC exporter*. J Phys Chem B, 2010. **114**(48): p. 15948-57.
63. Oswald, C., I.B. Holland, and L. Schmitt, *The motor domains of ABC-transporters. What can structures tell us?* Naunyn Schmiedeberg's Arch Pharmacol, 2006. **372**(6): p. 385-99.

64. Isenbarger, T.A., et al., *The most conserved genome segments for life detection on Earth and other planets*. Orig Life Evol Biosph, 2008. **38**(6): p. 517-33.
65. Armstrong, S.T., L.; Zhang, H.; Hermodson, M.; Stauffacher, C., *Powering the ABC transporters: the 2.5 Å crystal structure of the ABC domain of RBSA*. Pediatr. Pulmonol, 1998. **17**: p. 91-92.
66. Zaitseva, J., et al., *Functional characterization and ATP-induced dimerization of the isolated ABC-domain of the haemolysin B transporter*. Biochemistry, 2005. **44**(28): p. 9680-90.
67. Verdon, G., et al., *Crystal structures of the ATPase subunit of the glucose ABC transporter from Sulfolobus solfataricus: nucleotide-free and nucleotide-bound conformations*. J Mol Biol, 2003. **330**(2): p. 343-58.
68. Smith, P.C., et al., *ATP binding to the motor domain from an ABC transporter drives formation of a nucleotide sandwich dimer*. Mol Cell, 2002. **10**(1): p. 139-49.
69. Walker, J.E., et al., *Distantly related sequences in the alpha- and beta-subunits of ATP synthase, myosin, kinases and other ATP-requiring enzymes and a common nucleotide binding fold*. EMBO J, 1982. **1**(8): p. 945-51.
70. Oldham, M.L. and J. Chen, *Snapshots of the maltose transporter during ATP hydrolysis*. Proc Natl Acad Sci U S A, 2011. **108**(37): p. 15152-6.
71. Ambudkar, S.V., et al., *The A-loop, a novel conserved aromatic acid subdomain upstream of the Walker A motif in ABC transporters, is critical for ATP binding*. FEBS Lett, 2006. **580**(4): p. 1049-55.
72. Schmitt, L., et al., *Crystal structure of the nucleotide-binding domain of the ABC-transporter haemolysin B: identification of a variable region within ABC helical domains*. J Mol Biol, 2003. **330**(2): p. 333-42.
73. Zaitseva, J., et al., *A molecular understanding of the catalytic cycle of the nucleotide-binding domain of the ABC transporter HlyB*. Biochem Soc Trans, 2005. **33**(Pt 5): p. 990-5.
74. Senior, A.E., M.K. al-Shawi, and I.L. Urbatsch, *The catalytic cycle of P-glycoprotein*. FEBS Lett, 1995. **377**(3): p. 285-9.
75. Jardetzky, O., *Simple allosteric model for membrane pumps*. Nature, 1966. **211**(5052): p. 969-70.
76. Chen, J., et al., *A tweezers-like motion of the ATP-binding cassette dimer in an ABC transport cycle*. Mol Cell, 2003. **12**(3): p. 651-61.
77. van der Does, C. and R. Tampe, *How do ABC transporters drive transport?* Biol Chem, 2004. **385**(10): p. 927-33.
78. Zaitseva, J., et al., *A structural analysis of asymmetry required for catalytic activity of an ABC-ATPase domain dimer*. EMBO J, 2006. **25**(14): p. 3432-43.
79. Sauna, Z.E., et al., *Catalytic cycle of ATP hydrolysis by P-glycoprotein: evidence for formation of the E.S reaction intermediate with ATP-gamma-S, a nonhydrolyzable analogue of ATP*. Biochemistry, 2007. **46**(48): p. 13787-99.
80. Jones, P.M. and A.M. George, *Mechanism of the ABC transporter ATPase domains: catalytic models and the biochemical and biophysical record*. Crit Rev Biochem Mol Biol, 2013. **48**(1): p. 39-50.
81. Jones, P.M. and A.M. George, *A reciprocating twin-channel model for ABC transporters*. Q Rev Biophys, 2014. **47**(3): p. 189-220.
82. Dawson, R.J., K. Hollenstein, and K.P. Locher, *Uptake or extrusion: crystal structures of full ABC transporters suggest a common mechanism*. Mol Microbiol, 2007. **65**(2): p. 250-7.
83. Aller, S.G., et al., *Structure of P-glycoprotein reveals a molecular basis for poly-specific drug binding*. Science, 2009. **323**(5922): p. 1718-22.

84. Zutz, A., et al., *Asymmetric ATP hydrolysis cycle of the heterodimeric multidrug ABC transport complex TmrAB from Thermus thermophilus*. J Biol Chem, 2011. **286**(9): p. 7104-15.
85. Mishra, S., et al., *Conformational dynamics of the nucleotide binding domains and the power stroke of a heterodimeric ABC transporter*. Elife, 2014. **3**: p. e02740.
86. Locher, K.P., *Mechanistic diversity in ATP-binding cassette (ABC) transporters*. Nat Struct Mol Biol, 2016. **23**(6): p. 487-93.
87. Sanchez-Fernandez, R., et al., *The Arabidopsis thaliana ABC protein superfamily, a complete inventory*. J Biol Chem, 2001. **276**(32): p. 30231-44.
88. Rea, P.A., *Plant ATP-binding cassette transporters*. Annu Rev Plant Biol, 2007. **58**: p. 347-75.
89. Martinoia, E., Grill, E., Tommasini, R., Kreuz, K., Amrhein, N., *ATP-dependent glutathione S-conjugate export pump in the vacuolar membrane of plants*. Nature, 1993. **364**(6434): p. 247.
90. Do, T.H.T., E. Martinoia, and Y. Lee, *Functions of ABC transporters in plant growth and development*. Curr Opin Plant Biol, 2017. **41**: p. 32-38.
91. Lefevre, F. and M. Boutry, *Towards identification of the substrates of ATP-binding cassette transporters*. Plant Physiol, 2018.
92. Kretschmar, T., et al., *Functions of ABC transporters in plants*. Essays Biochem, 2011. **50**(1): p. 145-60.
93. Verrier, P.J., et al., *Plant ABC proteins--a unified nomenclature and updated inventory*. Trends Plant Sci, 2008. **13**(4): p. 151-9.
94. Mentewab, A. and C.N. Stewart, Jr., *Overexpression of an Arabidopsis thaliana ABC transporter confers kanamycin resistance to transgenic plants*. Nat Biotechnol, 2005. **23**(9): p. 1177-80.
95. Mentewab, A., et al., *RNA-seq analysis of the effect of kanamycin and the ABC transporter AtWBC19 on Arabidopsis thaliana seedlings reveals changes in metal content*. PLoS One, 2014. **9**(10): p. e109310.
96. Kuromori, T., et al., *ABC transporter AtABCG25 is involved in abscisic acid transport and responses*. Proc Natl Acad Sci U S A, 2010. **107**(5): p. 2361-6.
97. Kang, J., et al., *PDR-type ABC transporter mediates cellular uptake of the phytohormone abscisic acid*. Proc Natl Acad Sci U S A, 2010. **107**(5): p. 2355-60.
98. Le Hir, R., et al., *ABCG9, ABCG11 and ABCG14 ABC transporters are required for vascular development in Arabidopsis*. Plant J, 2013. **76**(5): p. 811-24.
99. Ko, D., et al., *Arabidopsis ABCG14 is essential for the root-to-shoot translocation of cytokinin*. Proc Natl Acad Sci U S A, 2014. **111**(19): p. 7150-5.
100. Zhang, K., et al., *Arabidopsis ABCG14 protein controls the acropetal translocation of root-synthesized cytokinins*. Nat Commun, 2014. **5**: p. 3274.
101. Kuromori, T., E. Sugimoto, and K. Shinozaki, *Arabidopsis mutants of AtABCG22, an ABC transporter gene, increase water transpiration and drought susceptibility*. Plant J, 2011. **67**(5): p. 885-94.
102. Kuromori, T., et al., *Functional relationship of AtABCG21 and AtABCG22 in stomatal regulation*. Sci Rep, 2017. **7**(1): p. 12501.
103. Nawrath, C., et al., *Apoplastic diffusion barriers in Arabidopsis*. Arabidopsis Book, 2013. **11**: p. e0167.
104. Schreiber, L., *Transport barriers made of cutin, suberin and associated waxes*. Trends Plant Sci, 2010. **15**(10): p. 546-53.
105. Blackmore, S., et al., *Pollen wall development in flowering plants*. New Phytol, 2007. **174**(3): p. 483-98.

106. Scott, R., *Pollen exine-the sporopollenin enigma and the physics of pattern*. In: *Seminar series society for experimental biology*. Cambridge University Press, 1994. **55**: p. 49-49.
107. Quilichini, T.D., A.L. Samuels, and C.J. Douglas, *ABCG26-mediated polyketide trafficking and hydroxycinnamoyl spermidines contribute to pollen wall exine formation in Arabidopsis*. *Plant Cell*, 2014. **26**(11): p. 4483-98.
108. Choi, H., et al., *An ABCG/WBC-type ABC transporter is essential for transport of sporopollenin precursors for exine formation in developing pollen*. *Plant J*, 2011. **65**(2): p. 181-93.
109. Quilichini, T.D., et al., *ATP-binding cassette transporter G26 is required for male fertility and pollen exine formation in Arabidopsis*. *Plant Physiol*, 2010. **154**(2): p. 678-90.
110. Kuromori, T., et al., *Arabidopsis mutant of AtABCG26, an ABC transporter gene, is defective in pollen maturation*. *J Plant Physiol*, 2011. **168**(16): p. 2001-5.
111. Dou, X.Y., et al., *WBC27, an adenosine tri-phosphate-binding cassette protein, controls pollen wall formation and patterning in Arabidopsis*. *J Integr Plant Biol*, 2011. **53**(1): p. 74-88.
112. Yim, S., et al., *Postmeiotic development of pollen surface layers requires two Arabidopsis ABCG-type transporters*. *Plant Cell Rep*, 2016.
113. Yadav, V., et al., *ABCG transporters are required for suberin and pollen wall extracellular barriers in Arabidopsis*. *Plant Cell*, 2014. **26**(9): p. 3569-88.
114. Choi, H., et al., *The role of Arabidopsis ABCG9 and ABCG31 ATP binding cassette transporters in pollen fitness and the deposition of sterol glycosides on the pollen coat*. *Plant Cell*, 2014. **26**(1): p. 310-24.
115. Shao, S., et al., *The outermost cuticle of soybean seeds: chemical composition and function during imbibition*. *J Exp Bot*, 2007. **58**(5): p. 1071-82.
116. Mintz-Oron, S., et al., *Gene expression and metabolism in tomato fruit surface tissues*. *Plant Physiol*, 2008. **147**(2): p. 823-51.
117. Tanaka, H., et al., *A subtilisin-like serine protease is required for epidermal surface formation in Arabidopsis embryos and juvenile plants*. *Development*, 2001. **128**(23): p. 4681-9.
118. Bonaventure, G., et al., *Analysis of the aliphatic monomer composition of polyesters associated with Arabidopsis epidermis: occurrence of octadeca-cis-6, cis-9-diene-1,18-dioate as the major component*. *Plant J*, 2004. **40**(6): p. 920-30.
119. Kunst, L. and A.L. Samuels, *Biosynthesis and secretion of plant cuticular wax*. *Prog Lipid Res*, 2003. **42**(1): p. 51-80.
120. Pollard, M., et al., *Building lipid barriers: biosynthesis of cutin and suberin*. *Trends Plant Sci*, 2008. **13**(5): p. 236-46.
121. Bird, D., et al., *Characterization of Arabidopsis ABCG11/WBC11, an ATP binding cassette (ABC) transporter that is required for cuticular lipid secretion*. *Plant J*, 2007. **52**(3): p. 485-98.
122. Ukitsu, H., et al., *Cytological and biochemical analysis of COF1, an Arabidopsis mutant of an ABC transporter gene*. *Plant Cell Physiol*, 2007. **48**(11): p. 1524-33.
123. Luo, B., et al., *An ABC transporter gene of Arabidopsis thaliana, AtWBC11, is involved in cuticle development and prevention of organ fusion*. *Plant Cell Physiol*, 2007. **48**(12): p. 1790-802.
124. Panikashvili, D., et al., *The Arabidopsis DSO/ABCG11 transporter affects cutin metabolism in reproductive organs and suberin in roots*. *Mol Plant*, 2010. **3**(3): p. 563-75.

125. Panikashvili, D., et al., *The Arabidopsis DESPERADO/AtWBC11 transporter is required for cutin and wax secretion*. Plant Physiol, 2007. **145**(4): p. 1345-60.
126. Fabre, G., et al., *The ABCG transporter PEC1/ABCG32 is required for the formation of the developing leaf cuticle in Arabidopsis*. New Phytol, 2016. **209**(1): p. 192-201.
127. McFarlane, H.E., et al., *Arabidopsis ABCG transporters, which are required for export of diverse cuticular lipids, dimerize in different combinations*. Plant Cell, 2010. **22**(9): p. 3066-75.
128. Panikashvili, D., et al., *The Arabidopsis ABCG13 transporter is required for flower cuticle secretion and patterning of the petal epidermis*. New Phytol, 2011. **190**(1): p. 113-24.
129. Takeda, S., et al., *The Half-Size ABC Transporter FOLDED PETALS 2/ABCG13 Is Involved in Petal Elongation through Narrow Spaces in Arabidopsis thaliana Floral Buds*. Plants (Basel), 2014. **3**(3): p. 348-58.
130. Ariizumi, T. and K. Toriyama, *Genetic regulation of sporopollenin synthesis and pollen exine development*. Annu Rev Plant Biol, 2011. **62**: p. 437-60.
131. Fedi, F., et al., *Awake1, an ABC-Type Transporter, Reveals an Essential Role for Suberin in the Control of Seed Dormancy*. Plant Physiol, 2017. **174**(1): p. 276-283.
132. Vishwanath, S.J., et al., *Suberin: biosynthesis, regulation, and polymer assembly of a protective extracellular barrier*. Plant Cell Rep, 2015. **34**(4): p. 573-86.
133. Naseer, S., et al., *Casparian strip diffusion barrier in Arabidopsis is made of a lignin polymer without suberin*. Proc Natl Acad Sci U S A, 2012. **109**(25): p. 10101-6.
134. Franke, R.B., I. Dombrink, and L. Schreiber, *Suberin goes genomics: use of a short living plant to investigate a long lasting polymer*. Front Plant Sci, 2012. **3**: p. 4.
135. Franke, R. and L. Schreiber, *Suberin--a biopolyester forming apoplastic plant interfaces*. Curr Opin Plant Biol, 2007. **10**(3): p. 252-9.
136. Graca, J., *Suberin: the biopolyester at the frontier of plants*. Front Chem, 2015. **3**: p. 62.
137. Kolattukudy, P.E., *Polyesters in higher plants*. Adv Biochem Eng Biotechnol, 2001. **71**: p. 1-49.
138. Samuels, L., L. Kunst, and R. Jetter, *Sealing plant surfaces: cuticular wax formation by epidermal cells*. Annu Rev Plant Biol, 2008. **59**: p. 683-707.
139. Millar, A.A. and L. Kunst, *Very-long-chain fatty acid biosynthesis is controlled through the expression and specificity of the condensing enzyme*. Plant J, 1997. **12**(1): p. 121-31.
140. Franke, R., et al., *The DAISY gene from Arabidopsis encodes a fatty acid elongase condensing enzyme involved in the biosynthesis of aliphatic suberin in roots and the chalaza-micropyle region of seeds*. Plant J, 2009. **57**(1): p. 80-95.
141. Lee, S.B., et al., *Two Arabidopsis 3-ketoacyl CoA synthase genes, KCS20 and KCS2/DAISY, are functionally redundant in cuticular wax and root suberin biosynthesis, but differentially controlled by osmotic stress*. Plant J, 2009. **60**(3): p. 462-75.
142. Beisson, F., Y. Li-Beisson, and M. Pollard, *Solving the puzzles of cutin and suberin polymer biosynthesis*. Curr Opin Plant Biol, 2012. **15**(3): p. 329-37.

143. Molina, I., et al., *Identification of an Arabidopsis feruloyl-coenzyme A transferase required for suberin synthesis*. Plant Physiol, 2009. **151**(3): p. 1317-28.
144. Compagnon, V., et al., *CYP86B1 is required for very long chain omega-hydroxyacid and alpha, omega -dicarboxylic acid synthesis in root and seed suberin polyester*. Plant Physiol, 2009. **150**(4): p. 1831-43.
145. Vishwanath, S.J., et al., *Suberin-associated fatty alcohols in Arabidopsis: distributions in roots and contributions to seed coat barrier properties*. Plant Physiol, 2013. **163**(3): p. 1118-32.
146. Domergue, F., et al., *Three Arabidopsis fatty acyl-coenzyme A reductases, FAR1, FAR4, and FAR5, generate primary fatty alcohols associated with suberin deposition*. Plant Physiol, 2010. **153**(4): p. 1539-54.
147. Rowland, O. and F. Domergue, *Plant fatty acyl reductases: enzymes generating fatty alcohols for protective layers with potential for industrial applications*. Plant Sci, 2012. **193-194**: p. 28-38.
148. Gou, J.Y., X.H. Yu, and C.J. Liu, *A hydroxycinnamoyltransferase responsible for synthesizing suberin aromatics in Arabidopsis*. Proc Natl Acad Sci U S A, 2009. **106**(44): p. 18855-60.
149. Kosma, D.K., et al., *Identification of an Arabidopsis fatty alcohol:caffeoyl-Coenzyme A acyltransferase required for the synthesis of alkyl hydroxycinnamates in root waxes*. Plant Physiol, 2012. **160**(1): p. 237-48.
150. Boher, P., et al., *The potato suberin feruloyl transferase FHT which accumulates in the phellogen is induced by wounding and regulated by abscisic and salicylic acids*. J Exp Bot, 2013. **64**(11): p. 3225-36.
151. Yang, W., et al., *A distinct type of glycerol-3-phosphate acyltransferase with sn-2 preference and phosphatase activity producing 2-monoacylglycerol*. Proc Natl Acad Sci U S A, 2010. **107**(26): p. 12040-5.
152. McFarlane, H.E., et al., *Golgi- and trans-Golgi network-mediated vesicle trafficking is required for wax secretion from epidermal cells*. Plant Physiol, 2014. **164**(3): p. 1250-60.
153. Landgraf, R., et al., *The ABC transporter ABCG1 is required for suberin formation in potato tuber periderm*. Plant Cell, 2014. **26**(8): p. 3403-15.
154. Shiono, K., et al., *RCN1/OsABCG5, an ATP-binding cassette (ABC) transporter, is required for hypodermal suberization of roots in rice (Oryza sativa)*. Plant J, 2014. **80**(1): p. 40-51.
155. Matsuda, S., et al., *Rice Stomatal Closure Requires Guard Cell Plasma Membrane ATP-Binding Cassette Transporter RCN1/OsABCG5*. Mol Plant, 2016. **9**(3): p. 417-427.
156. Nuruzzaman, M., et al., *Plant pleiotropic drug resistance transporters: transport mechanism, gene expression, and function*. J Integr Plant Biol, 2014. **56**(8): p. 729-40.
157. Bultreys, A., et al., *Nicotiana plumbaginifolia plants silenced for the ATP-binding cassette transporter gene NpPDR1 show increased susceptibility to a group of fungal and oomycete pathogens*. Mol Plant Pathol, 2009. **10**(5): p. 651-63.
158. Bienert, M.D., et al., *A pleiotropic drug resistance transporter in Nicotiana tabacum is involved in defense against the herbivore Manduca sexta*. Plant J, 2012. **72**(5): p. 745-57.
159. Banasiak, J., et al., *A Medicago truncatula ABC transporter belonging to subfamily G modulates the level of isoflavonoids*. J Exp Bot, 2013. **64**(4): p. 1005-15.

160. Crouzet, J., et al., *NtPDR1, a plasma membrane ABC transporter from Nicotiana tabacum, is involved in diterpene transport*. Plant Mol Biol, 2013. **82**(1-2): p. 181-92.
161. Sasse, J., et al., *Petunia hybrida PDR2 is involved in herbivore defense by controlling steroidal contents in trichomes*. Plant Cell Environ, 2016. **39**(12): p. 2725-2739.
162. Shibata, Y., et al., *The Full-Size ABCG Transporters Nb-ABCG1 and Nb-ABCG2 Function in Pre- and Postinvasion Defense against Phytophthora infestans in Nicotiana benthamiana*. Plant Cell, 2016. **28**(5): p. 1163-81.
163. Kobae, Y., et al., *Loss of AtPDR8, a plasma membrane ABC transporter of Arabidopsis thaliana, causes hypersensitive cell death upon pathogen infection*. Plant Cell Physiol, 2006. **47**(3): p. 309-18.
164. Lee, M., et al., *AtPDR12 contributes to lead resistance in Arabidopsis*. Plant Physiol, 2005. **138**(2): p. 827-36.
165. Kim, D.Y., et al., *The ABC transporter AtPDR8 is a cadmium extrusion pump conferring heavy metal resistance*. Plant J, 2007. **50**(2): p. 207-18.
166. Kretzschmar, T., et al., *A petunia ABC protein controls strigolactone-dependent symbiotic signalling and branching*. Nature, 2012. **483**(7389): p. 341-4.
167. Jasinski, M., et al., *A plant plasma membrane ATP binding cassette-type transporter is involved in antifungal terpenoid secretion*. Plant Cell, 2001. **13**(5): p. 1095-107.
168. Yu, F. and V. De Luca, *ATP-binding cassette transporter controls leaf surface secretion of anticancer drug components in Catharanthus roseus*. Proc Natl Acad Sci U S A, 2013. **110**(39): p. 15830-5.
169. Demessie, Z., et al., *The ATP binding cassette transporter, VmTPT2/VmABCG1, is involved in export of the monoterpenoid indole alkaloid, vincamine in Vinca minor leaves*. Phytochemistry, 2017. **140**: p. 118-124.
170. Fu, X., et al., *AaPDR3, a PDR Transporter 3, Is Involved in Sesquiterpene beta-Caryophyllene Transport in Artemisia annua*. Front Plant Sci, 2017. **8**: p. 723.
171. Pierman, B., et al., *Activity of the purified plant ABC transporter NtPDR1 is stimulated by diterpenes and sesquiterpenes involved in constitutive and induced defenses*. J Biol Chem, 2017. **292**(47): p. 19491-19502.
172. Khare, D., et al., *Arabidopsis ABCG34 contributes to defense against necrotrophic pathogens by mediating the secretion of camalexin*. Proc Natl Acad Sci U S A, 2017. **114**(28): p. E5712-E5720.
173. Stein, M., et al., *Arabidopsis PEN3/PDR8, an ATP binding cassette transporter, contributes to nonhost resistance to inappropriate pathogens that enter by direct penetration*. Plant Cell, 2006. **18**(3): p. 731-46.
174. Campe, R., et al., *ABC transporter PEN3/PDR8/ABCG36 interacts with calmodulin that, like PEN3, is required for Arabidopsis nonhost resistance*. New Phytol, 2016. **209**(1): p. 294-306.
175. Lu, X., et al., *Mutant Allele-Specific Uncoupling of PENETRATION3 Functions Reveals Engagement of the ATP-Binding Cassette Transporter in Distinct Tryptophan Metabolic Pathways*. Plant Physiol, 2015. **168**(3): p. 814-27.
176. Kim, D.Y., et al., *Overexpression of AtABCG36 improves drought and salt stress resistance in Arabidopsis*. Physiol Plant, 2010. **139**(2): p. 170-80.
177. Rodriguez-Celma, J., et al., *Mutually exclusive alterations in secondary metabolism are critical for the uptake of insoluble iron compounds by Arabidopsis and Medicago truncatula*. Plant Physiol, 2013. **162**(3): p. 1473-85.



178. Fourcroy, P., et al., *Involvement of the ABCG37 transporter in secretion of scopoletin and derivatives by Arabidopsis roots in response to iron deficiency*. New Phytol, 2014. **201**(1): p. 155-67.
179. Fourcroy, P., et al., *Facilitated Fe Nutrition by Phenolic Compounds Excreted by the Arabidopsis ABCG37/PDR9 Transporter Requires the IRT1/FRO2 High-Affinity Root Fe(2+) Transport System*. Mol Plant, 2016. **9**(3): p. 485-488.
180. Bourgaud, F., Hehn, A., Labat, R., Doerper, S., Gontier, E., Kellner, S., Matern, U. , *Biosynthesis of coumarins in plants: a major pathway still to be unravelled for cytochrome P450 enzymes*. Phytochemistry Reviews, 2006. **5**(2-3), : p. 293-308.
181. Alejandro, S., et al., *AtABCG29 is a monolignol transporter involved in lignin biosynthesis*. Curr Biol, 2012. **22**(13): p. 1207-12.
182. Campbell, E.J., et al., *Pathogen-responsive expression of a putative ATP-binding cassette transporter gene conferring resistance to the diterpenoid sclareol is regulated by multiple defense signaling pathways in Arabidopsis*. Plant Physiol, 2003. **133**(3): p. 1272-84.
183. Seo, S., et al., *Identification of natural diterpenes that inhibit bacterial wilt disease in tobacco, tomato and Arabidopsis*. Plant Cell Physiol, 2012. **53**(8): p. 1432-44.
184. Zhu, F.Y., et al., *Sorghum extracellular leucine-rich repeat protein SbLRR2 mediates lead tolerance in transgenic Arabidopsis*. Plant Cell Physiol, 2013. **54**(9): p. 1549-59.
185. Badri, D.V., et al., *An ABC transporter mutation alters root exudation of phytochemicals that provoke an overhaul of natural soil microbiota*. Plant Physiol, 2009. **151**(4): p. 2006-17.
186. Wolters, H. and G. Jurgens, *Survival of the flexible: hormonal growth control and adaptation in plant development*. Nat Rev Genet, 2009. **10**(5): p. 305-17.
187. Santner, A. and M. Estelle, *Recent advances and emerging trends in plant hormone signalling*. Nature, 2009. **459**(7250): p. 1071-1078.
188. Zeevaart, J.A.D. and R.A. Creelman, *Metabolism and Physiology of Absciscic-Acid*. Annual Review of Plant Physiology and Plant Molecular Biology, 1988. **39**: p. 439-473.
189. Bewley, J.D., *Seed Germination and Dormancy*. Plant Cell, 1997. **9**(7): p. 1055-1066.
190. Hilhorst, H.W.M., Karssen, C. M. , *Seed dormancy and germination: the role of abscisic acid and gibberellins and the importance of hormone mutants*. Plant growth regulation, 1992. **11**(3): p. 225-238.
191. Debeaujon, I. and M. Koornneef, *Gibberellin requirement for Arabidopsis seed germination is determined both by testa characteristics and embryonic abscisic acid*. Plant Physiol, 2000. **122**(2): p. 415-24.
192. Toh, S., et al., *High temperature-induced abscisic acid biosynthesis and its role in the inhibition of gibberellin action in Arabidopsis seeds*. Plant Physiol, 2008. **146**(3): p. 1368-85.
193. Verslues, P.E. and E.A. Bray, *Role of abscisic acid (ABA) and Arabidopsis thaliana ABA-insensitive loci in low water potential-induced ABA and proline accumulation*. J Exp Bot, 2006. **57**(1): p. 201-12.
194. Piskurewicz, U., et al., *Far-red light inhibits germination through DELLA-dependent stimulation of ABA synthesis and ABI3 activity*. EMBO J, 2009. **28**(15): p. 2259-71.
195. Muller, K., S. Tintelnot, and G. Leubner-Metzger, *Endosperm-limited Brassicaceae seed germination: abscisic acid inhibits embryo-induced*

- endosperm weakening of Lepidium sativum (cress) and endosperm rupture of cress and Arabidopsis thaliana*. Plant Cell Physiol, 2006. **47**(7): p. 864-77.
196. Badri, D.V., et al., *Influence of ATP-Binding Cassette Transporters in Root Exudation of Phytoalexins, Signals, and in Disease Resistance*. Front Plant Sci, 2012. **3**: p. 149.
  197. Venturi, V. and C. Keel, *Signaling in the Rhizosphere*. Trends Plant Sci, 2016. **21**(3): p. 187-198.
  198. Haichar, F.E.Z., et al., *Stable isotope probing of carbon flow in the plant holobiont*. Curr Opin Biotechnol, 2016. **41**: p. 9-13.
  199. Roux, S.J. and I. Steinebrunner, *Extracellular ATP: an unexpected role as a signaler in plants*. Trends Plant Sci, 2007. **12**(11): p. 522-7.
  200. Thomas, C., et al., *A role for ectophosphatase in xenobiotic resistance*. Plant Cell, 2000. **12**(4): p. 519-33.
  201. Kang, J., et al., *Plant ABC Transporters*. Arabidopsis Book, 2011. **9**: p. e0153.
  202. Jiang, Y., et al., *Plants transfer lipids to sustain colonization by mutualistic mycorrhizal and parasitic fungi*. Science, 2017. **356**(6343): p. 1172-1175.
  203. Luginbuehl, L.H., et al., *Fatty acids in arbuscular mycorrhizal fungi are synthesized by the host plant*. Science, 2017. **356**(6343): p. 1175-1178.
  204. Pighin, J.A., et al., *Plant cuticular lipid export requires an ABC transporter*. Science, 2004. **306**(5696): p. 702-4.
  205. Boursiac, Y., et al., *ABA transport and transporters*. Trends Plant Sci, 2013. **18**(6): p. 325-33.
  206. Borghi, L., et al., *The role of ABCG-type ABC transporters in phytohormone transport*. Biochem Soc Trans, 2015. **43**(5): p. 924-30.
  207. Sasse, J., E. Martinoia, and T. Northen, *Feed Your Friends: Do Plant Exudates Shape the Root Microbiome?* Trends Plant Sci, 2018. **23**(1): p. 25-41.
  208. Bernaudat, F., et al., *Heterologous Expression of Membrane Proteins: Choosing the Appropriate Host*. Plos One, 2011. **6**(12).
  209. Gul, N., et al., *Evolved Escherichia coli Strains for Amplified, Functional Expression of Membrane Proteins*. Journal of Molecular Biology, 2014. **426**(1): p. 136-149.
  210. Lefevre, F., A. Baijot, and M. Boutry, *Plant ABC transporters: time for biochemistry?* Biochemical Society Transactions, 2015. **43**: p. 931-936.
  211. Lee, M., et al., *The ABC transporter AtABCB14 is a malate importer and modulates stomatal response to CO<sub>2</sub>*. Nature Cell Biology, 2008. **10**(10): p. 1217-1223.
  212. Wagner, S., et al., *Rationalizing membrane protein overexpression*. Trends Biotechnol, 2006. **24**(8): p. 364-71.
  213. Midgett, C.R. and D.R. Madden, *Breaking the bottleneck: eukaryotic membrane protein expression for high-resolution structural studies*. J Struct Biol, 2007. **160**(3): p. 265-74.
  214. Terpe, K., *Overview of bacterial expression systems for heterologous protein production: from molecular and biochemical fundamentals to commercial systems*. Appl Microbiol Biotechnol, 2006. **72**(2): p. 211-22.
  215. Monne, M., et al., *Functional expression of eukaryotic membrane proteins in Lactococcus lactis*. Protein Sci, 2005. **14**(12): p. 3048-56.
  216. Schaedler, T.A., et al., *A conserved mitochondrial ATP-binding cassette transporter exports glutathione polysulfide for cytosolic metal cofactor assembly*. J Biol Chem, 2014. **289**(34): p. 23264-74.
  217. van den Brule, S. and C.C. Smart, *The plant PDR family of ABC transporters*. Planta, 2002. **216**(1): p. 95-106.

218. Toussaint, F., et al., *Purification and biochemical characterization of NpABCG5/NpPDR5, a plant pleiotropic drug resistance transporter expressed in Nicotiana tabacum BY-2 suspension cells*. Biochem J, 2017. **474**(10): p. 1689-1703.
219. Yang, H. and A.S. Murphy, *Functional expression and characterization of Arabidopsis ABCB, AUX 1 and PIN auxin transporters in Schizosaccharomyces pombe*. Plant J, 2009. **59**(1): p. 179-91.
220. Geisler, M., et al., *Cellular efflux of auxin catalyzed by the Arabidopsis MDR/PGP transporter AtPGP1*. Plant J, 2005. **44**(2): p. 179-94.
221. Lee, E.K., et al., *Binding of sulfonyleurea by AtMRP5, an Arabidopsis multidrug resistance-related protein that functions in salt tolerance*. Plant Physiol, 2004. **134**(1): p. 528-38.
222. Shitan, N., et al., *Involvement of CjMDR1, a plant multidrug-resistance-type ATP-binding cassette protein, in alkaloid transport in Coptis japonica*. Proc Natl Acad Sci U S A, 2003. **100**(2): p. 751-6.
223. Xu, D., et al., *Functional Expression and Characterization of Plant ABC Transporters in Xenopus laevis Oocytes for Transport Engineering Purposes*. Methods Enzymol, 2016. **576**: p. 207-24.
224. Sami, M., et al., *Hop-resistant Lactobacillus brevis contains a novel plasmid harboring a multidrug resistance-like gene*. Journal of Fermentation and Bioengineering, 1997. **84**(1): p. 1-6.
225. Stindt, J., et al., *Heterologous Overexpression and Mutagenesis of the Human Bile Salt Export Pump (ABCB11) Using DREAM (Directed REcombination-Assisted Mutagenesis)*. Plos One, 2011. **6**(5).
226. Ellinger, P., et al., *Detergent screening and purification of the human liver ABC transporters BSEP (ABCB11) and MDR3 (ABCB4) expressed in the yeast Pichia pastoris*. PLoS One, 2013. **8**(4): p. e60620.
227. Byrne, J.A., et al., *Missense mutations and single nucleotide polymorphisms in ABCB11 impair bile salt export pump processing and function or disrupt pre-messenger RNA splicing*. Hepatology, 2009. **49**(2): p. 553-67.
228. Noe, J., B. Stieger, and P.J. Meier, *Functional expression of the canalicular bile salt export pump of human liver*. Gastroenterology, 2002. **123**(5): p. 1659-66.
229. Tschopp, J.F., et al., *Expression of the lacZ gene from two methanol-regulated promoters in Pichia pastoris*. Nucleic Acids Res, 1987. **15**(9): p. 3859-76.
230. Chloupkova, M., et al., *Expression of 25 human ABC transporters in the yeast Pichia pastoris and characterization of the purified ABCC3 ATPase activity*. Biochemistry, 2007. **46**(27): p. 7992-8003.
231. Beaudet, L., I.L. Urbatsch, and P. Gros, *High-level expression of mouse Mdr3 P-glycoprotein in yeast Picia pastoris and characterization of ATPase activity*. Abc Transporters: Biochemical, Cellular, and Molecular Aspects, 1998. **292**: p. 397-413.
232. Infed, N., et al., *Influence of detergents on the activity of the ABC transporter LmrA*. Biochim Biophys Acta, 2011. **1808**(9): p. 2313-21.
233. Morita, M., et al., *ATP-binding and -hydrolysis activities of ALDP (ABCD1) and ALDRP (ABCD2), human peroxisomal ABC proteins, overexpressed in Sf21 cells*. Biol Pharm Bull, 2006. **29**(9): p. 1836-42.
234. Nyathi, Y., et al., *The Arabidopsis peroxisomal ABC transporter, comatose, complements the Saccharomyces cerevisiae pxa1 pxa2Delta mutant for metabolism of long-chain fatty acids and exhibits fatty acyl-CoA-stimulated ATPase activity*. J Biol Chem, 2010. **285**(39): p. 29892-902.

235. Barberon, M., et al., *Adaptation of Root Function by Nutrient-Induced Plasticity of Endodermal Differentiation*. Cell, 2016. **164**(3): p. 447-59.
236. Krishnamurthy, P., et al., *Root apoplastic barriers block Na<sup>+</sup> transport to shoots in rice (Oryza sativa L.)*. J Exp Bot, 2011. **62**(12): p. 4215-28.
237. Tylova, E., et al., *Casparian bands and suberin lamellae in exodermis of lateral roots: an important trait of roots system response to abiotic stress factors*. Ann Bot, 2017. **120**(1): p. 71-85.
238. Herget, M., et al., *Purification and reconstitution of the antigen transport complex TAP: a prerequisite for determination of peptide stoichiometry and ATP hydrolysis*. J Biol Chem, 2009. **284**(49): p. 33740-9.
239. Decottignies, A., et al., *Solubilization and characterization of the overexpressed PDR5 multidrug resistance nucleotide triphosphatase of yeast*. J Biol Chem, 1994. **269**(17): p. 12797-803.
240. Kaur, H., et al., *Coupled ATPase-adenylate kinase activity in ABC transporters*. Nat Commun, 2016. **7**: p. 13864.
241. Zhou, S.F., *Structure, function and regulation of P-glycoprotein and its clinical relevance in drug disposition*. Xenobiotica, 2008. **38**(7-8): p. 802-32.
242. Beisson, F., et al., *The acyltransferase GPAT5 is required for the synthesis of suberin in seed coat and root of Arabidopsis*. Plant Cell, 2007. **19**(1): p. 351-68.
243. Hofer, R., et al., *The Arabidopsis cytochrome P450 CYP86A1 encodes a fatty acid omega-hydroxylase involved in suberin monomer biosynthesis*. J Exp Bot, 2008. **59**(9): p. 2347-60.
244. Li, Q., et al., *Transporter-Mediated Nuclear Entry of Jasmonoyl-Isoleucine Is Essential for Jasmonate Signaling*. Mol Plant, 2017. **10**(5): p. 695-708.
245. Franke, R.M., I., *Biosynthesis of Suberin Polyesters*. The Arabidopsis book, 2013. **11**.
246. Saitou, N. and M. Nei, *The neighbor-joining method: a new method for reconstructing phylogenetic trees*. Mol Biol Evol, 1987. **4**(4): p. 406-25.
247. Zuckerkandl, E. and L. Pauling, *Evolutionary divergence and convergence in proteins*. Academic Press, New York, 1965: p. 97-166.
248. Kumar, S., G. Stecher, and K. Tamura, *MEGA7: Molecular Evolutionary Genetics Analysis Version 7.0 for Bigger Datasets*. Mol Biol Evol, 2016. **33**(7): p. 1870-4.
249. van Staden, C.J., et al., *Membrane vesicle ABC transporter assays for drug safety assessment*. Curr Protoc Toxicol, 2012. **Chapter 23**: p. Unit 23 5.
250. Krumpochova, P., et al., *Transportomics: screening for substrates of ABC transporters in body fluids using vesicular transport assays*. FASEB J, 2012. **26**(2): p. 738-47.
251. Egner, R., et al., *Genetic separation of FK506 susceptibility and drug transport in the yeast Pdr5 ATP-binding cassette multidrug resistance transporter*. Mol Biol Cell, 1998. **9**(2): p. 523-43.
252. Meyers, S., et al., *Interaction of the yeast pleiotropic drug resistance genes PDR1 and PDR5*. Curr Genet, 1992. **21**(6): p. 431-6.
253. Golin, J., et al., *Studies with novel Pdr5p substrates demonstrate a strong size dependence for xenobiotic efflux*. J Biol Chem, 2003. **278**(8): p. 5963-9.
254. Rogers, B., et al., *The pleiotropic drug ABC transporters from Saccharomyces cerevisiae*. J Mol Microbiol Biotechnol, 2001. **3**(2): p. 207-14.
255. Kolaczowski, M., et al., *Anticancer drugs, ionophoric peptides, and steroids as substrates of the yeast multidrug transporter Pdr5p*. J Biol Chem, 1996. **271**(49): p. 31543-8.

## 6. Curriculum vitae

### **Personal Data**

Name	Kalpana Shanmugarajah
Date of birth	30 January 1986
Place of birth	Berlin

### **Research Experience**

since May 2013	Ph.D. student at the Institute of Biochemistry with Prof. Dr. Lutz Schmitt, Heinrich-Heine-University Düsseldorf
Jan 2011– Apr 2011	Research studies for diploma thesis in the lab of Prof. Dr. Rolf Wagner, Institute of Physical Biology, Molecular Biology of Bacteria, Heinrich-Heine-University, Düsseldorf
Jan 2011– Feb 2011	Research internship in the lab of Prof. Dr. Rolf Wagner, Institute of Physical Biology, Molecular Biology of Bacteria, Heinrich-Heine-University, Düsseldorf

### **Academic Education**

Sep 2006 – Jan 2012	Diploma in Biology Heinrich-Heine-University Düsseldorf Institute of Physical Biology, Molecular Biology of Bacteria Prof. Dr. Rolf Wagner Construction and functional analysis of <i>rsd</i> and <i>ssrS</i> mutations in <i>Escherichia coli</i>
---------------------	--

### **School Education**

Aug 1998 – May 2005	Secondary school Schiller-Gymnasium Berlin Degree: Abitur
---------------------	---

Aug 1992 – Jul 1998	Elementary school Reinhold-Otto-Grundschule Berlin Trift-Grundschule Berlin
---------------------	---

### **Memberships**

since May 2013	Member at the Interdisciplinary Graduate and Research Academy (iGRAD) Heinrich-Heine-University Düsseldorf
----------------	---

since May 2013	Member at the Cluster of Excellence on Plant Sciences (CEPLAS) graduate school Heinrich-Heine-University Düsseldorf
----------------	--

### **Attended Conferences and Meetings**

Oct 2017	CEPLAS Symposium and Young Researcher Retreat 2017 in Cologne Poster: <i>In vitro</i> characterization of ABCG1 from <i>Arabidopsis thaliana</i>
May 2016	CEPLAS Symposium 2016 in Düsseldorf Poster: <i>In vitro</i> characterization of ABCG1 and ABCG30 from <i>Arabidopsis thaliana</i>
Jan 2016	Gordon Research Conference on Plant Volatiles in Ventura, USA Poster: <i>In vitro</i> characterization of ABCG transporters from <i>Arabidopsis thaliana</i>
May 2015	CEPLAS Symposium 2015 in Cologne Poster: <i>In vitro</i> characterization of ABCG transporters from <i>Arabidopsis thaliana</i>
Sep 2014	11th Horizons in Molecular Biology Symposium in Göttingen Poster: <i>In vitro</i> characterization of selected plant ABC

	transporters
Sep 2014	CEPLAS Young Researchers Retreat 2014 in Bad Honnef Poster: <i>In vitro</i> characterization of ABC transporters from <i>Arabidopsis thaliana</i>
May 2014	CEPLAS Symposium 2014 in Düsseldorf Poster: <i>In vitro</i> characterization of selected plant ABC transporters
Nov 2013	CEPLAS Young Researchers Retreat 2013 in Bielefeld

### **List of Publications**

Gräfe, K.<sup>¶</sup>, **Shanmugarajah, K.<sup>¶</sup>**, Zobel, T., Weidtkamp-Peters, S., Kleinschrodt, D., Smits, S. H. J., Schmitt, L. (2018). Cloning and expression of selected ABC transporters from the *Arabidopsis thaliana* ABCG family in *Pichia pastoris*. Plos One (submitted).

<sup>¶</sup> equally contributed

**Shanmugarajah, K.**, Kleinschrodt, D., Smits, S. H. J., Schmitt, L. (2018). Detergent screening and purification of AtABCG30 expressed in *Pichia pastoris*. In preparation.

**Shanmugarajah, K.**, Linka, N., Gräfe, K., Smits, S. H. J., Weber, A. P. M., Zeier, J., Schmitt, L. (2018). ABCG1 is involved in suberin barrier formation in *Arabidopsis thaliana*. In preparation.

**Shanmugarajah, K.**, Gräfe, K., Metzger, S., Smits, S. H. J., Schmitt, L. (2018). Proof-of-principle of a mass spectrometry-based vesicular transport assay for identification of plant ABCG transporters substrates. In preparation.

## 7. Acknowledgments

An dieser Stelle möchte ich mich als erstes bei meinem Doktorvater Prof. Dr. Lutz Schmitt bedanken. Vielen Dank dafür, dass ich dieses vielseitige Projekt unter deiner Betreuung bearbeiten durfte. Ich danke dir für die stetige Unterstützung über die letzten Jahre, die vielen Ideen, Denkanstöße aber auch deinen Optimismus, der es ermöglicht hat die unterschiedlichen Facetten dieses Projekt zu erforschen. Lutz, danke dass du mir diese schöne und lehrreiche Zeit ermöglicht hast!

Als nächstes möchte ich mich bei Dr. Sander Smits bedanken. Sander, dir möchte ich vor allem für deine Hilfsbereitschaft und für das Zuhören bei allen Problemen, sei es wissenschaftlicher oder auch privater Sorgen herzlichst danken. Vielen Dank dafür, dass ich immer auf deine Hilfe zählen konnte. Ich danke dir auch, für die vielen kritischen Fragen, Ideen aber auch motivierenden Gespräche und die Betreuung über die letzten Jahre!

Mein weiterer Dank gilt PD. Dr. Ulrich Schulte. Vielen Dank, für deine herzliche Art und die vielen interessanten Fragen während der Seminare.

Ich bedanke mich bei Prof. Dr. Karl-Erich Jaeger für die Übernahme des Korreferats. Ich danke ihm auch für das Interesse an meiner Arbeit und die vielen netten Diskussionen bei unseren TAC Meetings.

Ich danke Frau Mathilde Blum für das sorgfältige Organisieren und die Verwaltung. Ohne Sie hätte ich manche Rechnungen sicherlich in den Untiefen meines Schreibtisches vergessen. Ich wünsche Ihnen nun einen schönen Ruhestand!

Dr. Diana Kleinschrodt möchte ich für die Einarbeitung in das Projekt und auch die Betreuung über die ersten Jahre meiner Doktorarbeit danken. Vielen Dank für deine Unterstützung, Anregungen und tollen Klonierungsstrategien. Danke, dass ich mich immer bei dir ausheulen konnte, wenn ich wieder mal frustriert war. Egal ob das Klonieren oder die Testexpression zum X-ten Mal nicht geklappt oder ob ich einfach generell ausgelaugt war. Danke dafür, dass du mich über die gesamte Doktorarbeitszeit unterstützt hast!

Ich danke Martina, Silke und Iris, dafür dass ihr euch so fleißig um alle Bestellungen und die Labororganisation gekümmert habt. Ich danke Iris für die vielen Klonierungstips und auch fleißige Klonieren unzähliger Konstrukte. Vielen Dank an Martina für Ihre ruhige,



ausgeglichene Art und die vielen netten Unterhaltungen. Ich danke Silke, meiner Büroplatznachbarin für die vielen netten Gespräche über Beruf, Leben usw. Es hat wirklich Spaß gemacht das Büro mit dir zu teilen ☺

I would like to thank the former plant ladies Sakshi and Katharina. Thank you ladies, for the countless and refreshing tea breaks, lunch breaks, balcony sessions, dinners and all the funny and also serious chats.

Sakshi, I thank you for being such a supportive and good friend. Thank you so much for encouraging me and pushing me when I was frustrated. Thank you for the support, care and all the fun in the lab, as well as after work. I will never forget the great time we shared during the last years, and I hope that we will always stay in touch. Sakshi, thank you that I could continuously ask you questions and count on your advice, even when you were far away on another continent ;-)

Katharina, bei dir weiß ich gar nicht wo ich anfangen soll: geteiltes Projekt, geteilte Aufgaben im Institut, gemeinsame Konferenzbesuche, .... Ich danke dir für diese tolle gemeinsame Zeit und dafür, dass ich immer auf deine Unterstützung zählen konnte! Auch wenn wir anfangs mit unseren Pflanzen-ABC Transportern wie Paradiesvögel unter den anderen dastanden, war es toll, dass wir zu zweit waren und uns gegenseitig unterstützen konnten. Vielen Dank für deine vielen motivierenden Gespräche, deine Ideen und auch die zahlreichen lustigen Momente.

Als nächstes möchte ich dem MDR Team danken.

Ich danke Manuel und Katja für die geduldige Einarbeitung und Beantwortung aller Pdr5 Fragen. Danke an Manuel für die vielen Ideen und kritischen Fragen bei den Meetings. Katja, danke ich für ihre stets freundliche Art und ihre Hilfsbereitschaft. Auf deine Hilfe konnte ich immer zählen, ob Wagenbau, im Labor oder selbst wenn der Fermenter mal wieder mal versucht in die Luft zu gehen ;-)

Ich wünsche euch beiden noch viel Erfolg auf den letzten Metern!

Tim und Martin, unseren neuen Pichia-Experten wünsche ich viel Erfolg mit dem MDR Projekt. Tim, seit deiner Zeit als Masterstudent bei Sakshi, bringst du einen mit deinen Sprüchen und auch deinen leicht tollpatschigen Aktionen immer wieder zum Lachen. Vielen Dank für die lustigen Momente und deine Hilfsbereitschaft! Martin, danke für die netten Unterhaltungen und deine Unterstützung. Ein großes Dankeschön dafür, dass du dich um den Fermenter kümmerst ☺

Ich möchte mich auch bei den Nisin-Experten für ihre Unterstützung und Hilfsbereitschaft bedanken.

Ich danke Marcel vor allem für die Einarbeitung an der Äkta während meiner ersten

Proteinreinigungen, seine Ratschläge und netten Unterhaltungen. Außerdem danke ich ihm für das geduldige Ausmerzen der Dinge, die ich das ein oder andere Mal an der Äkta verursacht habe. Jens, dir danke ich dafür, dass du jeden im Labor mit deiner außerordentlichen Hilfsbereitschaft unterstützt! Vielen Dank für deine offene Art und deinen Humor, der den Laboralltag lustiger gemacht hat.

Ich danke Julia dafür, dass sie durch ihre fröhliche Art etwas mehr Leben in lab 22 gebracht hat. Danke für deine Unterstützung und die vielen netten und lustigen Gespräche!

Rebecca, dir möchte ich für deine Hilfsbereitschaft, egal ob privat oder im Labor danken. Danke dafür, dass du meist gerade dann ins Labor oder Büro hereinspaziert bist, wenn ich jemanden zum Reden brauchte. Vielen Dank für deine Unterstützung und auch die vielen schönen Momente!

An dieser Stelle möchte ich auch dem Hly-Team meinen Dank aussprechen. Vor allem danke ich Tobias dafür, dass er sein Wissen über Native Pages mit mir geteilt hat und Kerstin für die Diskussionen und Ideen zum Thema Aufreinigung und ATPasen. Ich danke auch, dem auch künstlerisch begabten Duo des Instituts, Olivia und Isabell für die vielen netten und lustigen Momente. Zohreh, I wish you all the best for your project!

Ich möchte auch Jun.-Prof. Dr. Alexej Kedrov und seinen Mitarbeitern Athanasios, Maryna und Michael danken.

Ich danke Dr. Sabine Metzger, Dr. Nicole Linka, Prof. Dr. Jürgen Zeier und Prof. Dr. Andreas Weber für die Kooperation. Mein besonderer Dank gilt zum einen Prof. Dr. Jürgen Zeier für die Einarbeitung und dafür, dass er mir das Durchführen der Experimente in seinem Labor ermöglicht hat. Ich danke auch seinen Mitarbeitern Karin Kiefer und Michael Hartmann für ihre Hilfsbereitschaft. Ein großes Dankeschön geht auch an Dr. Nicole Linka und Lennart Charton für die geduldige Einarbeitung in die Pflanzenwelt.

Dr. Stefanie-Weidtkamp-Peters und Dr. Thomas Zobel danke ich für die Einarbeitung am Mikroskop und die zahlreichen Stunden, die wir gemeinsam vor dem Fluoreszenzmikroskop verbracht haben. Es hat viel Spaß gemacht!

Ich bedanke mich bei CEPLAS für die finanzielle Unterstützung und die Ausbildung im Rahmen des CEPLAS Graduate School Programms.

Ich danke auch meinen CEPLAS Mitstreiterinnen Sarah Kranz und Ziba Ajami für die schöne gemeinsame Zeit bei allen CEPLAS Events, inklusive lustiger Zug-oder Autofahrten. I would like to express my special gratitude to Ziba for her support especially during the last couple of

months. Thank you for the nice coffee sessions, dinners and trips.

Mein weiterer Dank gilt den ehemaligen Mitarbeitern Marianne, Philipp, Jan, Zainab, Nacera, Susanne, Sabrina, Rakesh, Miro, Ricarda, André, Christian, Hilke, Josè, Jan-Peter, Michael, Sandra, Sven und Eleanor. Ein besonderes Dankeschön geht an Philipp und Marianne für die Einarbeitung und auch Jan für die Beantwortung aller Pichia-relevanten Fragen. Ich danke auch Michael für seine offene Art, seine weisen Ratschläge und die vielen lustigen Momente. I would also like to thank Zainab and Eleanor, for all the fun we had at and after work.

Zum Schluss möchte ich mich auch bei meiner Familie bedanken. Ich danke meinen Geschwistern Sagevan und Howshiga, dafür dass sie mich so großartig über die letzten Jahre unterstützt haben. Ich danke meiner lieben Mutter für Ihre Fürsorge, Geduld und ihre unendliche Unterstützung. Ohne euch hätte ich es sicherlich nicht soweit geschafft. Danke, dass ihr immer für mich da wart!

## 8. Declaration

Ich versichere an Eides Statt, dass die vorliegende Dissertation von mir selbständig und ohne unzulässige fremde Hilfe unter Beachtung der „Grundsätze zur Sicherung guter wissenschaftlicher Praxis an der Heinrich-Heine-Universität Düsseldorf“ erstellt worden ist. Die Dissertation wurde in der vorgelegten oder in ähnlicher Form noch bei keiner anderen Institution eingereicht. Ich habe bisher keine erfolglosen Promotionsversuche unternommen.

Düsseldorf, den

---

Kalpana Shanmugarajah